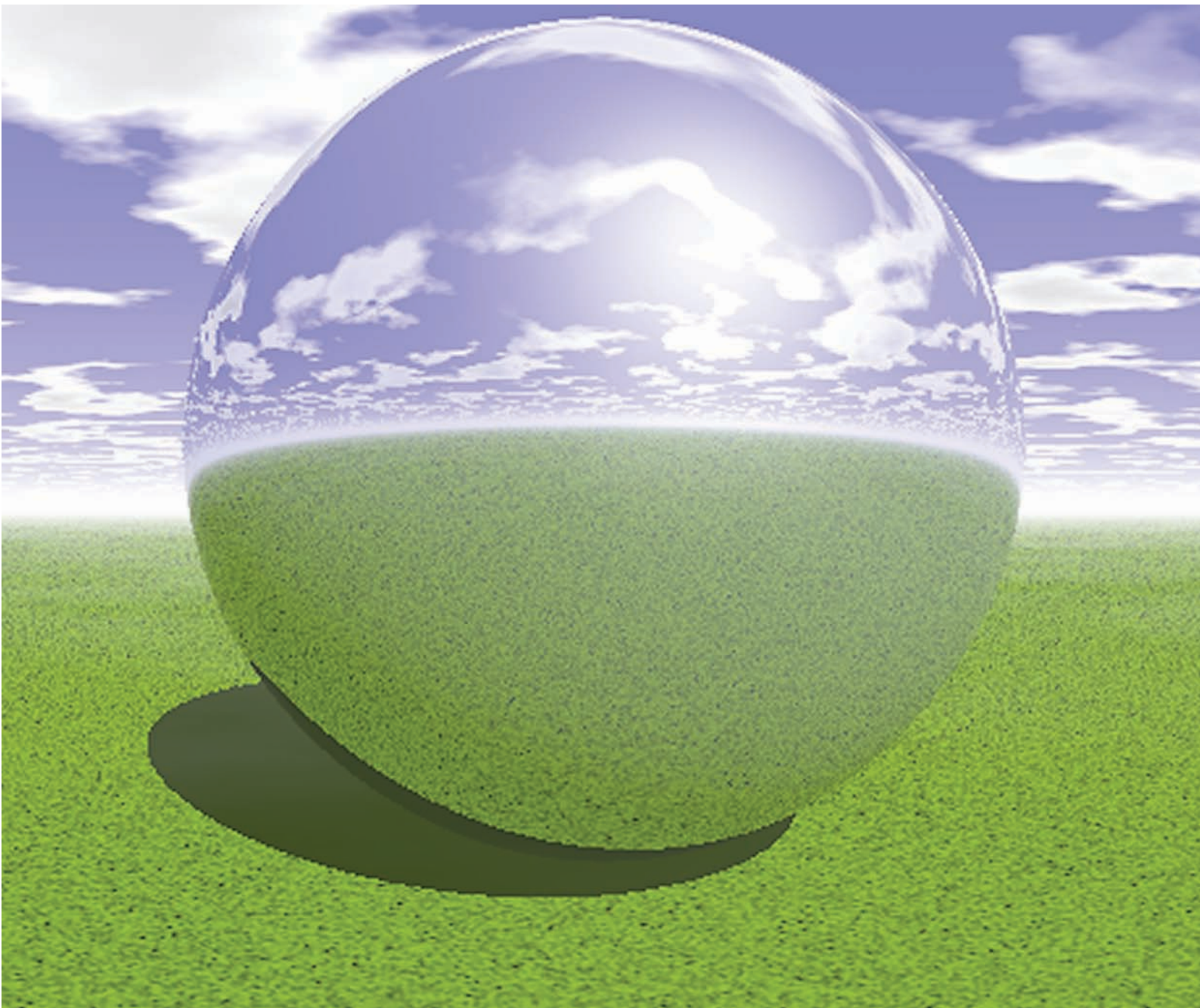


Green Chemistry

Cutting-edge research for a greener sustainable future

www.rsc.org/greenchem

Volume 9 | Number 4 | April 2007 | Pages 285–400



ISSN 1463-9262

Zhang *et al.*
Recent developments in microwave-assisted polymerization

Mack and Shumba
Rate enhancement of the Morita–Baylis–Hillman reaction

Carril *et al.*
A highly advantageous metal-free approach to diaryl disulfides in water

Gallezot
Process options for converting renewable feedstocks to bioproducts

RSC Publishing



1463-9262(2007)9:4;1-8

3rd International Conference on Green and Sustainable Chemistry



Delft University of Technology

**1-5 July 2007
Delft
The Netherlands**

Call for Abstracts

Full information and submission:
<http://www.greenchem2007.tudelft.nl>

Scope of the conference

The aim of the conference is to stimulate interactions and exchange of ideas between academia and industry and researchers in the various disciplines that underly the subject of green and sustainable chemistry. The scientific program will reflect this interdisciplinary nature of the subject and emphasize recent advances in relevant areas. In particular, sessions will be devoted to the following topics:

- Heterogeneous and homogeneous catalysis
- Biocatalysis/industrial biotechnology
- Multicatalytic cascade processes
- Alternative solvents/non-conventional reaction media
- Alternatives for toxic/hazardous reagents
- Integration of conversion and separation steps/new reactor technologies
- Renewable raw materials, biofuels and the biorefinery
- Sustainable energy
- Design of safer, environmentally friendly products
- Life cycle assessment and sustainability
- Metrics of green chemistry and sustainability
- Industrial ecology

Confirmed Invited Speakers

PLENARY:

Matthias Beller, Univ. Rostock (Germany)
Robert H. Grubbs, California Inst. of Technology (USA)
Shu Kobayashi, The Univ. of Tokyo (Japan)
Michael Braungart, Univ. Lüneburg/EPEA Hamburg (Germany) and MBDC (USA)

INVITED:

Peter Dunn, Pfizer (UK)
Jan van der Eijk, Shell (The Netherlands)
John Grate, Codexis (USA)
Richard Henderson, GSK (UK)
Istvan Horvath, Eotvos Univ. (Hungary)
Graham Hutchings, Cardiff Univ. (UK)
Takao Ikariya, Tokyo Inst. of Technology (Japan)
Andreas Kicherer, BASF (Germany)
Michel Philippe, l'Oréal (France)
Martyn Poliakoff, Univ. Nottingham (UK)
Jaap C. Schouten, Eindhoven Univ. of Technology (The Netherlands)
Peter Wasserscheid, Univ. Erlangen-Nürnberg (Germany)
Xumu Zhang, Pennsylvania State Univ. (USA)

Organizing Committee

Roger Sheldon (Chairman)
Isabel Arends – Herman van Bekkum - Ulf Hanefeld – Saul Lemkowitz - Cor Peters - Fred van Rantwijk - Adrie Straathof – Luuk van der Wielen - Jenny Boks - Mieke van der Kooij – Rob van der Lans - Elly Muilman - Ank Voskuil

Symposium Secretariat

GSC-3 Secretariat
Biocatalysis and Organic Chemistry
Julianalaan 136
2628 BL Delft
The Netherlands
T: +31 15 278 2683
F: +31 15 278 1415
E: greenchem2007-bt@tudelft.nl

Green Chemistry

Cutting-edge research for a greener sustainable future

www.rsc.org/greenchem

RSC Publishing is a not-for-profit publisher and a division of the Royal Society of Chemistry. Any surplus made is used to support charitable activities aimed at advancing the chemical sciences. Full details are available from www.rsc.org

IN THIS ISSUE

ISSN 1463-9262 CODEN GRCHFJ 9(4) 285-400 (2007)



Cover

Through the use of high speed ball milling, various solvent-less chemical reactions are possible. Image reproduced with permission from James Mack from *Green Chem.*, 2007, 9(4), 328.

CHEMICAL TECHNOLOGY

T25

Chemical Technology highlights the latest applications and technological aspects of research across the chemical sciences.

Chemical Technology

April 2007/Volume 4/Issue 4

www.rsc.org/chemicaltechnology

PERSPECTIVE

295

Process options for converting renewable feedstocks to bioproducts

Pierre Gallezot

The relative advantages of different process options to convert renewables to bioproducts are considered. Stress is laid on one-pot processes and new value chains adapted to biomass composition.



EDITORIAL STAFF

Editor

Sarah Ruthven

Publishing assistant

Emma Hacking

Team leader, serials production

Stephen Wilkes

Technical editor

Edward Morgan

Administration coordinator

Sonya Spring

Editorial secretaries

Donna Fordham, Jill Segev, Julie Thompson

Publisher

Emma Wilson

Green Chemistry (print: ISSN 1463-9262; electronic: ISSN 1463-9270) is published 12 times a year by the Royal Society of Chemistry, Thomas Graham House, Science Park, Milton Road, Cambridge, UK CB4 0WF.

All orders, with cheques made payable to the Royal Society of Chemistry, should be sent to RSC Distribution Services, c/o Portland Customer Services, Commerce Way, Colchester, Essex, UK CO2 8HP. Tel +44 (0) 1206 226050; E-mail sales@rscdistribution.org

2007 Annual (print + electronic) subscription price: £902; US\$1705. 2007 Annual (electronic) subscription price: £812; US\$1534. Customers in Canada will be subject to a surcharge to cover GST. Customers in the EU subscribing to the electronic version only will be charged VAT.

If you take an institutional subscription to any RSC journal you are entitled to free, site-wide web access to that journal. You can arrange access via Internet Protocol (IP) address at www.rsc.org/ip. Customers should make payments by cheque in sterling payable on a UK clearing bank or in US dollars payable on a US clearing bank. Periodicals postage paid at Rahway, NJ, USA and at additional mailing offices. Airfreight and mailing in the USA by Mercury Airfreight International Ltd., 365 Blair Road, Avenel, NJ 07001, USA.

US Postmaster: send address changes to Green Chemistry, c/o Mercury Airfreight International Ltd., 365 Blair Road, Avenel, NJ 07001. All despatches outside the UK by Consolidated Airfreight.

PRINTED IN THE UK

Advertisement sales: Tel +44 (0) 1223 432246; Fax +44 (0) 1223 426017; E-mail advertising@rsc.org

Green Chemistry

Cutting-edge research for a greener sustainable future

www.rsc.org/greenchem

Green Chemistry focuses on cutting-edge research that attempts to reduce the environmental impact of the chemical enterprise by developing a technology base that is inherently non-toxic to living things and the environment.

EDITORIAL BOARD

Chair

Professor Martyn Poliakoff
Nottingham, UK

Scientific Editor

Professor Walter Leitner
RWTH-Aachen, Germany

Associate Editors

Professor C. J. Li
McGill University, Canada
Professor Kyoko Nozaki
Kyoto University, Japan

Members

Professor Paul Anastas
Yale University, USA
Professor Joan Brennecke
University of Notre Dame, USA
Professor Mike Green
Sasol, South Africa
Professor Buxing Han
Chinese Academy of Sciences,
China
Professor Roshan Jachuck
Clarkson University, USA

Dr Alexei Lapkin
Bath University, UK
Dr Janet Scott
Unilever, UK
Professor Tom Welton
Imperial College, UK

INTERNATIONAL ADVISORY EDITORIAL BOARD

James Clark, York, UK
Avelino Corma, Universidad
Politécnica de Valencia, Spain
Mark Harmer, DuPont Central
R&D, USA
Herbert Hugl, Lanxess Fine
Chemicals, Germany
Makato Misono, Kogakuin
University, Japan
Colin Raston,
University of Western Australia,
Australia

Robin D. Rogers, Centre for Green
Manufacturing, USA
Kenneth Seddon, Queen's
University, Belfast, UK
Roger Sheldon, Delft University of
Technology, The Netherlands
Gary Sheldrake, Queen's
University, Belfast, UK
Pietro Tundo, Università ca
Foscari di Venezia, Italy

INFORMATION FOR AUTHORS

Full details of how to submit material for publication in Green Chemistry are given in the Instructions for Authors (available from <http://www.rsc.org/authors>). Submissions should be sent via ReSource: <http://www.rsc.org/resource>.

Authors may reproduce/republish portions of their published contribution without seeking permission from the RSC, provided that any such republication is accompanied by an acknowledgement in the form: (Original citation) – Reproduced by permission of the Royal Society of Chemistry.

© The Royal Society of Chemistry 2007. Apart from fair dealing for the purposes of research or private study for non-commercial purposes, or criticism or review, as permitted under the Copyright, Designs and Patents Act 1988 and the Copyright and Related Rights Regulations 2003, this publication may only be reproduced, stored or transmitted, in any form or by any means, with the prior permission in writing of the Publishers or in the case of reprographic reproduction in accordance with the terms of licences issued by the Copyright Licensing Agency in the UK. US copyright law is applicable to users in the USA.

The Royal Society of Chemistry takes reasonable care in the preparation of this publication but does not accept liability for the consequences of any errors or omissions.

Ⓢ The paper used in this publication meets the requirements of ANSI/NISO Z39.48-1992 (Permanence of Paper).

Royal Society of Chemistry: Registered Charity No. 207890

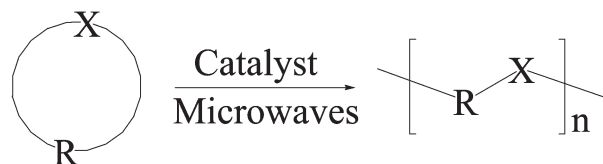
CRITICAL REVIEW

303

Recent developments in microwave-assisted polymerization with a focus on ring-opening polymerization

Chao Zhang, Liqiong Liao and Shaoqin (Sarah) Gong*

Recent developments in the field of microwave-assisted polymerization are presented in this review. Emphasis is addressed on microwave-assisted ring-opening polymerization; microwave-assisted step-growth polymerization and free radical polymerization are also briefly discussed.



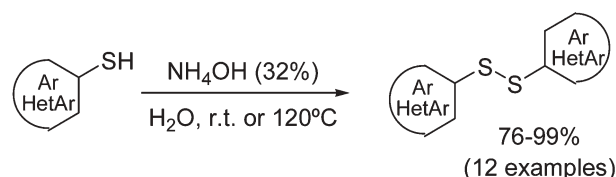
COMMUNICATIONS

315

A highly advantageous metal-free approach to diaryl disulfides in water

Mónica Carril, Raul SanMartin,* Esther Domínguez* and Imanol Tellitu

A novel green-chemical protocol for the synthesis of diaryl disulfides, based on a metal-free oxidation of thiol derivatives under mild basic conditions in aqueous media, is presented.

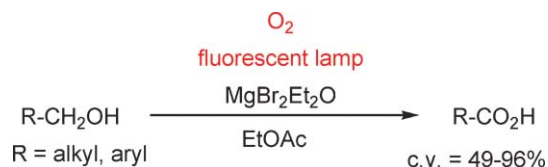


318

Aerobic oxidation of alcohols under visible light irradiation of fluorescent lamp

Shin-ichi Hirashima and Akichika Itoh*

A catalytic amount of magnesium bromide diethyl etherate enables us to carry out the aerobic photo-oxidation of alcohols under irradiation of VIS from a general-purpose fluorescent lamp.

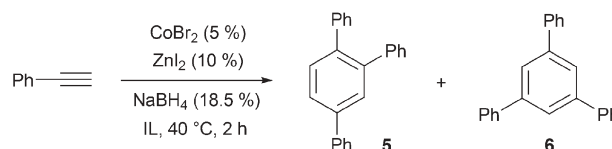


321

Task-specific ionic liquids as reaction media for the cobalt-catalysed cyclotrimerisation reaction of arylethyne

Marco Lombardo, Filippo Pasi, Claudio Trombini,* Kenneth R. Seddon* and William R. Pitner

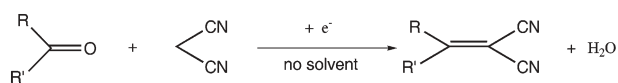
The use of nitrile-functionalised ionic liquids as solvents for cobalt-catalysed cyclotrimerisation reactions of monosubstituted aromatic alkynes is reported; the nitrile functionality stabilises the transient cobalt(I) catalytic species and ensures good conversions.



IL = [bmim][NTf₂]: Y = 35 %, **5** / **6** = 85 : 15
 IL = [(mCN)mim][NTf₂]: Y = 95 %, **5** / **6** = 95 : 5
 IL = [(mCN)edma][NTf₂]: Y = 85 %, **5** / **6** = 95 : 5

COMMUNICATIONS

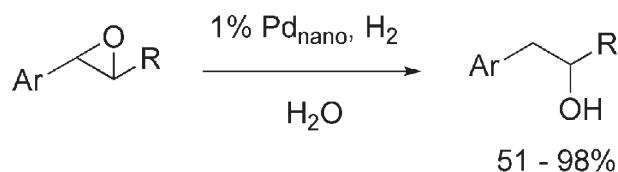
323

**Electrochemically induced Knoevenagel condensation in solvent- and supporting electrolyte-free conditions**

Marta Feroci,* Monica Orsini, Laura Palombi and Achille Inesi*

Solvent- and supporting electrolyte-free electrochemically induced Knoevenagel condensation of malononitrile with aldehydes or ketones, at 40 °C, yields ylidenemalononitriles in high yields.

326

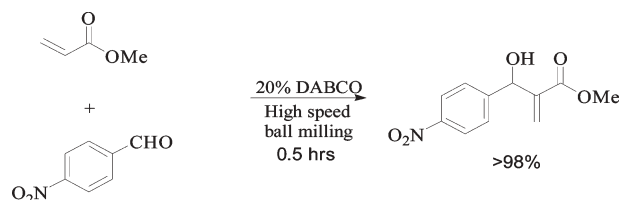
**Palladium nanoparticles-catalyzed regio- and chemoselective hydrogenolysis of benzylic epoxides in water**

Emilie Thiery, Jean Le Bras* and Jacques Muzart

Hydrogenolysis of various benzylic epoxides was achieved in water to give alcohols in 51–98% yield using recyclable Pd nanoparticles as catalyst.

PAPERS

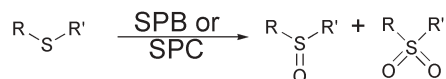
328

**Rate enhancement of the Morita–Baylis–Hillman reaction through mechanochemistry**

James Mack* and Maxwell Shumba

Baylis–Hillman products were produced in >98% yield in as little as 0.5 hours by solvent-free mechanochemistry. This represents one of the fastest methods of Baylis–Hillman reactions under neat conditions.

331

**Green and chemoselective oxidation of sulfides with sodium perborate and sodium percarbonate: nucleophilic and electrophilic character of the oxidation system**

M. Victoria Gómez, Rubén Caballero, Ester Vázquez,* Andrés Moreno, Antonio de la Hoz* and Ángel Díaz-Ortiz

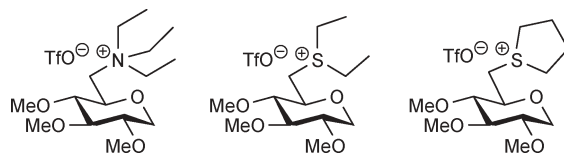
The use of SPB and SPC as cheap, non-toxic, stable and easily handled oxidants in an efficient, clean and safe method for the selective oxidation of sulfides to sulfoxides or sulfones.

337

Glucose-derived ionic liquids: exploring low-cost sources for novel chiral solvents

Laura Poletti,* Cinzia Chiappe, Luigi Lay, Daniela Pieraccini, Laura Polito and Giovanni Russo

Three sugar-derived ionic liquids were synthesized and fully characterized in their physico-chemical properties, including their ion-pairing ability.

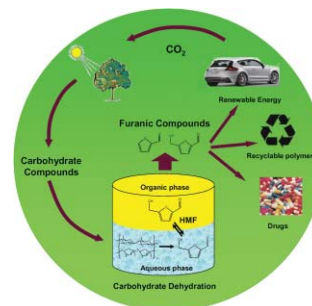


342

Production of 5-hydroxymethylfurfural and furfural by dehydration of biomass-derived mono- and poly-saccharides

Juben N. Chheda, Yuriy Román-Leshkov and James A. Dumesic*

We present a biphasic system for acid-catalyzed dehydration of various biomass-derived carbohydrates to form furan derivatives, which have potential to be sustainable substitutes for petroleum-based building blocks used in production of fuels, polymers and drugs.

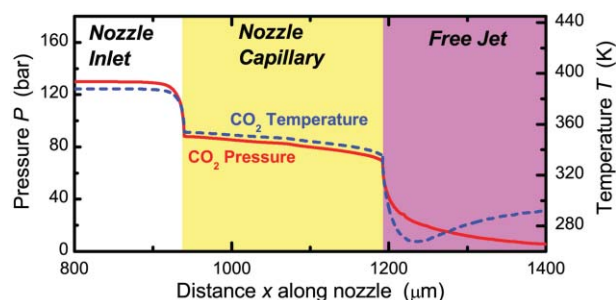


351

On-line *in-situ* characterization of CO₂ RESS processes for benzoic acid, cholesterol and aspirin

Jeremy J. Harrison, Changyoul Lee, Thomas Lenzer* and Kawon Oum*

The influence of temperature, pressure, nozzle distance and co-solvent amount on CO₂ RESS, producing different organic nanoparticles, is studied using laser scattering techniques to determine the particle size and distribution.



357

Synthesis of bi- and tricyclic β-lactam libraries in aqueous medium

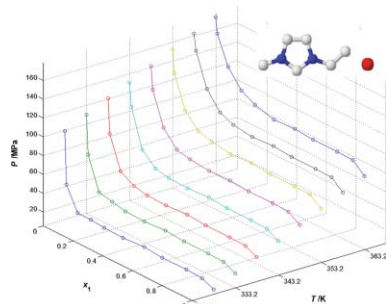
Iván Kanizsai, Szilvia Gyónfalvi, Zsolt Szakonyi, Reijo Sillanpää and Ferenc Fülöp*

A modified Ugi reaction in aqueous medium was used to construct β-lactam libraries.



$R^1 = \text{Et, } t\text{Bu, Ph, C}_6\text{H}_4\text{OMe}(p)$; $R^2 = \text{cyclohexyl or } tert\text{-butyl}$;
diastereomeric ratios from 60:40 up to 100:0; yields from 35% up to 95%.

361

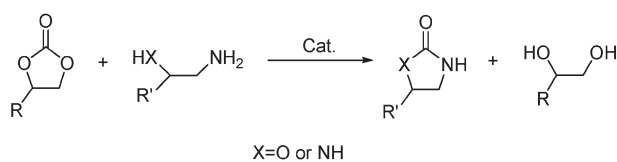


Influence of high pressure on solubility of ionic liquids: experimental data and correlation

Urszula Domańska* and Piotr Morawski

The solid–liquid phase equilibrium of systems {[EMIM][TOS] (1) + cyclohexane, or benzene (2)} and of {[MMIM][CH₃SO₄] (1) + hexan-1-ol (2)} have been measured under high pressure for the technological use. The Yang model was used for the correlation of the experimental data at high pressure (100–900 MPa).

369

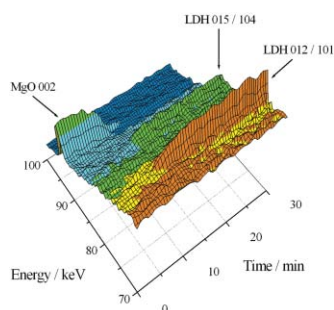


A method for the synthesis of 2-oxazolidinones and 2-imidazolidinones from five-membered cyclic carbonates and β -aminoalcohols or 1,2-diamines

Lin-fei Xiao, Li-wen Xu and Chun-gu Xia*

The first, highly efficient synthesis of 2-oxazolidinones from five-membered cyclic carbonates and β -aminoalcohols or 1,2-diamines, which gave excellent yields, are described. The effects of temperature, reaction time, solvent and the amount of catalyst were investigated.

373

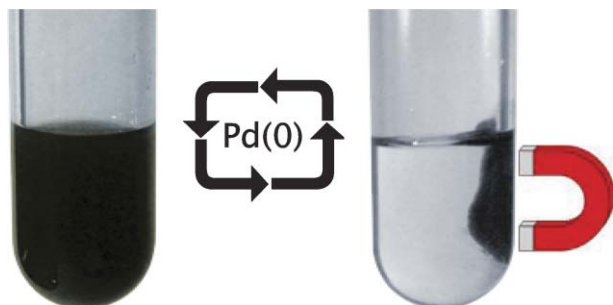


A synchrotron radiation study of the hydrothermal synthesis of layered double hydroxides from MgO and Al₂O₃ slurries

Sharon Mitchell, Timothy Biswick, William Jones,* Gareth Williams and Dermot O'Hare

We report an *in situ* synchrotron study of the formation of layered double hydroxides from the reaction of MgO and Al₂O₃ slurries at 100, 150, 180 and 240 °C. LDH formation was monitored, and no long-lasting intermediate phases were observed.

379



Superparamagnetic nanoparticle-supported palladium: a highly stable magnetically recoverable and reusable catalyst for hydrogenation reactions

Liane M. Rossi,* Fernanda P. Silva, Lucas L. R. Vono, Pedro K. Kiyohara, Evandro L. Duarte, Rosangela Itri, Richard Landers and Giovanna Machado

Magnetic separation is very promising to greatly improve separability and recycling of homogeneous and nanocluster catalysts. We here describe a new catalyst and an efficient recycling process for hydrogenation reactions.

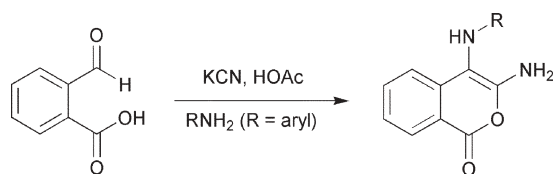
PAPERS

386

A HCN-based reaction under microreactor conditions: industrially feasible and continuous synthesis of 3,4-diamino-1*H*-isochromen-1-ones

Davy R. J. Acke and Christian V. Stevens*

A safe reaction setup, based on microreactor technology, was created to produce 3,4-diamino-1*H*-isochromen-1-ones. The release of the hazardous HCN gas was avoided during the process.

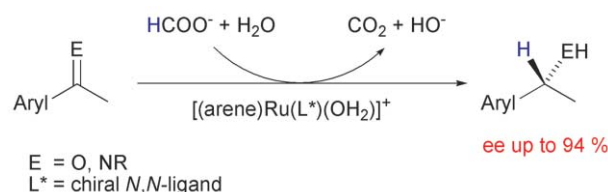


391

Water-soluble arene ruthenium catalysts containing sulfonated diamine ligands for asymmetric transfer hydrogenation of α -aryl ketones and imines in aqueous solution

Jérôme Canivet and Georg Süß-Fink*

A new family of cationic arene ruthenium complexes containing chiral *N,N*-chelating ligands is presented. The air-stable and water-soluble tetrafluoroborate salts catalyse the enantioselective transfer hydrogenation of prochiral ketones and imines in water as solvent.



AUTHOR INDEX

Acke, Davy R. J., 386
Biswick, Timothy, 373
Caballero, Rubén, 331
Canivet, Jérôme, 391
Carril, Mónica, 315
Chheda, Juben N., 342
Chiappe, Cinzia, 337
de la Hoz, Antonio, 331
Díaz-Ortiz, Ángel, 331
Domańska, Urszula, 361
Domínguez, Esther, 315
Duarte, Evandro L., 379
Dumesic, James A., 342
Feroci, Marta, 323
Fülöp, Ferenc, 357
Gallezot, Pierre, 295
Gómez, M. Victoria, 331
Gong, Shaoqin (Sarah), 303


Györfalvi, Szilvia, 357
Harrison, Jeremy J., 351
Hirashima, Shin-ichi, 318
Inesi, Achille, 323
Itoh, Akichika, 318
Itri, Rosangela, 379
Jones, William, 373
Kanizsai, Iván, 357
Kiyohara, Pedro K., 379
Landers, Richard, 379
Lay, Luigi, 337
Le Bras, Jean, 326
Lee, Changyoul, 351
Lenzer, Thomas, 351
Liao, Liqiong, 303
Lombardo, Marco, 321
Machado, Giovanna, 379
Mack, James, 328

Mitchell, Sharon, 373
Morawski, Piotr, 361
Moreno, Andrés, 331
Muzart, Jacques, 326
O'Hare, Dermot, 373
Orsini, Monica, 323
Oum, Kawon, 351
Palombi, Laura, 323
Pasi, Filippo, 321
Pieraccini, Daniela, 337
Pitner, William R., 321
Poletti, Laura, 337
Polito, Laura, 337
Román-Leshkov, Yuriy, 342
Rossi, Liane M., 379
Russo, Giovanni, 337
SanMartin, Raul, 315
Seddon, Kenneth R., 321

Shumba, Maxwell, 328
Sillanpää, Reijo, 357
Silva, Fernanda P., 379
Stevens, Christian V., 386
Süß-Fink, Georg, 391
Szakonyi, Zolt, 357
Tellitu, Imanol, 315
Thiery, Emilie, 326
Trombini, Claudio, 321
Vázquez, Ester, 331
Vono, Lucas L. R., 379
Williams, Gareth, 373
Xia, Chun-gu, 369
Xiao, Lin-fei, 369
Xu, Li-wen, 369
Zhang, Chao, 303

FREE E-MAIL ALERTS AND RSS FEEDS


Contents lists in advance of publication are available on the web *via* www.rsc.org/greenchem - or take advantage of our free e-mail alerting service (www.rsc.org/ej_alert) to receive notification each time a new list becomes available.

 Try our RSS feeds for up-to-the-minute news of the latest research. By setting up RSS feeds, preferably using feed reader software, you can be alerted to the latest Advance Articles published on the RSC web site. Visit www.rsc.org/publishing/technology/rss.asp for details.

ADVANCE ARTICLES AND ELECTRONIC JOURNAL

Free site-wide access to Advance Articles and the electronic form of this journal is provided with a full-rate institutional subscription. See www.rsc.org/ejs for more information.

* Indicates the author for correspondence: see article for details.

 Electronic supplementary information (ESI) is available *via* the online article (see <http://www.rsc.org/esi> for general information about ESI).

CALL FOR PAPERS

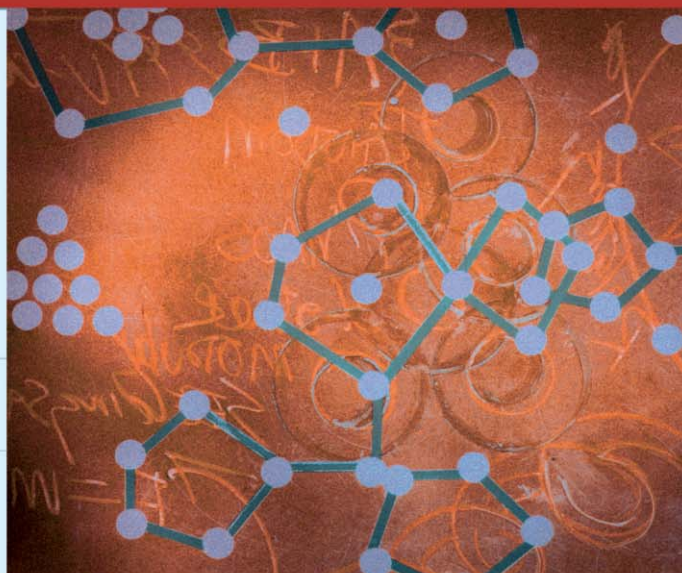
Abstracts due February 28, 2007

11th Annual Green Chemistry & Engineering Conference

› *From Small Steps to Giant Leaps —
Breakthrough Innovations for Sustainability*

June 25–28, 2007

WASHINGTON, DC



Submit Your Abstract Now...

Abstracts for both oral and poster presentations are now being accepted. The deadline is February 28, 2007. To learn more, and submit your abstract, please visit:

www.GCandE.org



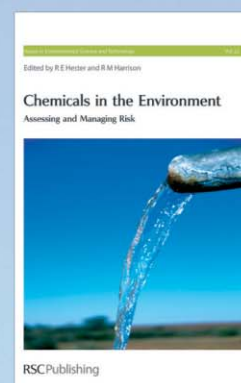
Chemicals in the Environment Assessing and Managing Risk

By R M Harrison

Chemicals in the Environment addresses important environmental issues relating to all aspects of risk management and regulation including;

- Current legislation on risk management of chemical products
- Scientific and technical issues
- Evaluating the risk of chemicals to humans and the environment
- Issues on evaluating metals in the environment
- Modelling the behaviour of organic chemicals

Ideal for industry, academia and government organisations -particularly those in environmental chemistry sectors.



Hardcover | 2006 | xvi + 158 pages | £45.00 | RSC member price £29.25 | ISBN-10: 0 85404 206 7 | ISBN-13: 978 0 85404 206 7

Registered Charity No. 207890

RSCPublishing

www.rsc.org/books/2067

Process options for converting renewable feedstocks to bioproducts

Pierre Gallezot

Received 24th October 2006, Accepted 20th December 2006

First published as an Advance Article on the web 16th January 2007

DOI: 10.1039/b615413a

This paper discusses the relative advantages of different process options to convert renewable feedstocks (carbohydrates, vegetable oils, terpenes and lignocellulosic materials) into valuable chemicals and polymers. Three process options are considered: (1) *via* degraded molecules, (2) *via* platform molecules, (3) *via* one-pot processes. These routes can all be integrated in a biorefinery scheme which maximises the value derived from biomass. These process options are illustrated by selected examples underlining the green chemistry value of process options 2 and 3. Stress is laid on new value chains adapted to biomass composition and on the use of recyclable heterogeneous catalysts that lead to waste minimisation and decrease the processing cost of renewables.

1 Introduction

The use of biomass for the production of energy, chemicals and materials is one of the key issues of sustainable development. Indeed, bio-based resources are renewable and CO₂ neutral in contrast with fossil fuels. Furthermore, due to the rapid increase of the oil price in 2005–2006 we face a new situation where the market price of crude is higher than that of biomass-derived pure molecules such as sucrose or glucose. The cost of platform molecules derived from carbohydrates or vegetable oils is fairly stable compared to that of fossil fuels and even tends to decrease steadily with time. The SusChem organisation in Europe has published its Implementation Action Plan¹ advocating the use of renewables as alternative feedstocks for fuel and chemical production.

As far as bioproducts are concerned there are additional benefits to using renewable feedstocks. Thus, the molecules extracted from bio-based resources are already functionalised so that the synthesis of chemicals may require a lower number of steps than from alkanes, thereby decreasing the overall waste generated. Also, bio-based products may have unique properties compared to hydrocarbon-derived products, for instance biodegradability and biocompatibility. Biomass processing by clean catalytic routes minimising synthesis steps fulfils several principles of green chemistry at the same time.² On a mere economical ground, products issued from biomass have a potential market differentiation and their marketing is made easier because of their “natural” or “bio” label.

There is a severe competition for the production of food/feed, bio-products (chemical and polymers) and transportation biofuels (bioethanol and biodiesel) from agricultural crops. Conventional crops based on cereals and seed oils could only be a partial answer to the fuel issue because of the huge needs at stake. To meet biofuel and chemicals demands in a more substantial way, it is recommended¹ that agricultural wastes are processed, new crops grown on marginal land, and

fast-growing vegetative biomass (grass, wood, stems, leaves, *etc.*) consisting of cellulose and ligno-cellulose rather than using seeds (cereals and vegetable oils).

Various hurdles may hamper the development of renewables for bio-product production. The main issue is the high cost involved in processing renewable feedstock to chemicals. Processes employed for the synthesis of chemicals from fossil fuels improved continuously during more than a century resulting in a very high degree of technical and cost optimisation. In contrast, processes to derive chemicals from biomass are comparatively in infancy and their cost weighs heavily on the market price of bioproducts. Accordingly, extensive research and development efforts in biotechnology, chemistry and engineering are required to reduce processing cost. As outlined in the SusChem Implementation Action Plan¹ a prerequisite for expending the use of biomass-derived feedstocks is the development of alternative value chains. This can be achieved by designing processing routes and catalytic systems different from those employed from hydrocarbons and adapted to the specific molecular structure of biomolecules. Whatever the route considered, it is mandatory to assess, by life cycle analysis, the sustainability of processes starting from renewable feedstocks, and to assess the benefits of employing biomass rather than fossil fuels to prepare a given chemical. Socio-economic life cycle assessment, rather than simple conventional LCA, should be performed to assess the societal impact of intensive agricultural activities covering large land areas, increasing the water stress and impairing biodiversity.

The present paper will focus on process options that could be integrated in a biorefinery scheme to help to produce bioproducts at a more competitive market price contributing to waste minimisation. The biorefinery concept has been developed early in food and paper industries, and is now going to be applied for the production of energy, chemicals and materials from renewable feedstocks.^{1,3,4} The underlying idea is to maximise the value derived from biomass by producing energy and multiple products *via* well integrated processes, valorising co-products and by-products and optimising the

Institut de recherches sur la catalyse et l'environnement de Lyon, 2 avenue Albert Einstein, Villeurbanne Cedex, 69626, France.
E-mail: pierre.gallezot@ircelyon.univ-lyon1.fr

inputs (feedstock supply, water management) and outputs (energy and product recovery, treatment of waste). Part of the biomass is converted to fuels by gasification (syngas and hydrogen), pyrolysis (bio-oil), and fermentation (biogas), while the other part is converted, by successive operations involving hydrolysis, fermentation and chemo-catalytic routes, to well-identified platform molecules that can be employed as building blocks in the synthesis of chemicals and polymeric materials. However, in contrast with traditional refineries, the economy of biorefineries will have to support the cost of transporting low energy density raw materials across long distances, and life cycle analysis should integrate the environmental impact of transportation.

Large biorefineries for carbohydrate processing to bioproducts are currently operating in the USA (e.g., Cargill biorefinery at Blair, Nebraska) and in Europe (e.g., Roquette bio-hub at Lestrem, France). Similarly, the production of oleochemicals and biofuels can be integrated in biorefineries using vegetable oils as the main feedstock and using platform fatty acid esters, fatty alcohols and glycerol as platform molecules.

2 Process options for biomass conversion to bioproducts

Within the biorefinery framework several processing options of renewables feedstocks can potentially be employed to produce bioproducts. The three main options discussed in this paper are given in the scheme of Fig. 1. They will be illustrated by selected examples and their respective advantages and limitations will be discussed in the following sections.

2.1 From biomass to products *via* degraded molecules

Biomass derivatives can potentially be converted to synthesis gas by adapting well known steam or autothermal reforming processes leading to syngas. Syngas is then converted, by Fischer–Tropsch synthesis, to hydrocarbons, which are subsequently converted to chemicals by usual synthesis routes

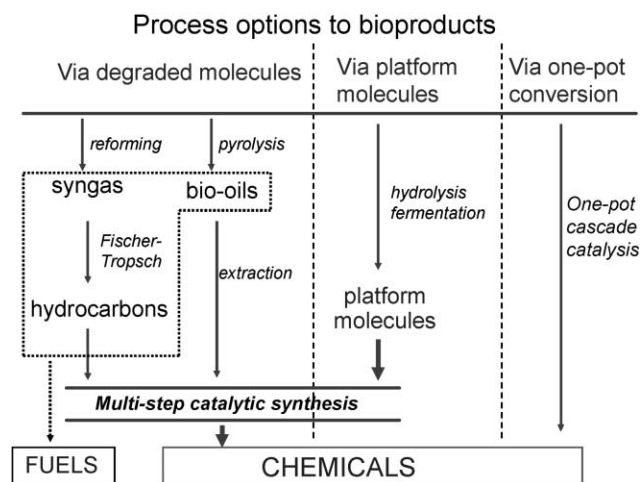


Fig. 1 Process options to bioproducts from carbohydrates or ligno-cellulosic materials integrated in a biorefinery scheme (simplified).

developed for petroleum feedstock. This approach has been little developed, particularly for the production chemicals. The overall sustainability and economy of the value chain—biomass to chemicals by gasification—is doubtful because it involves a succession of energy-demanding, high temperature reactions yielding hydrocarbons with different chain lengths which must be separated, and only a fraction of them can be used for the synthesis of intermediates by dehydrogenation or oxidation reactions. At the least, sustainability of this approach must be validated by life cycle analysis. A more appealing route consists of performing aqueous phase reforming of biomass directly yielding alkanes. Thus, water solution of ethylene glycol, glycerol and sugar-derived polyols were converted to hydrogen and alkanes conversion at 550 K under 15–50 bar pressure.^{5,6} Selectivities to H₂, CO₂ and alkanes were tuned with different bifunctional metal catalysts. Higher alkanes, with the number of carbon atoms ranging from C₇ to C₁₅, were obtained in several steps involving acid catalysed dehydration followed by base-catalysed aldol condensation, and the resulting products were dehydrated and hydrogenated to liquid alkanes over bifunctional catalysts in a four-phase reactor.⁷ Although the aim of these studies was to produce transportation fuels, the organic products formed during the dehydration step could be valuable starting material for chemical synthesis. However, reforming of renewables should be conducted with organic wastes or vegetative biomass rather than with high priced molecules such as sugar polyols obtained from cereals.

Another approach to produce chemicals *via* degraded molecules is the fast pyrolysis of biomass at high temperatures in the absence of oxygen, which results in gas, tar and up to 80 wt% of a liquid phase, so-called bio-oil, which is a mixture of hundreds molecules. Some of the compounds produced by pyrolysis were identified as fragments of the basic components of biomass, *viz.* lignin, cellulose and hemicellulose. The bio-oil composition depends upon the nature of starting materials and process conditions.^{8,9} Some valuable compounds present in bio-oils, particularly phenolic compounds issued from the degradation of lignin, can potentially be recovered. Thus, furfural and furfuryl alcohol can be recovered in amounts up to 30 wt% and 12–30%, respectively. Also, phenol–formaldehyde resins have been prepared from bio-oils containing a high fraction of phenolic compounds.^{10,11} Although bio-oils are primarily of interest for fuel production, their use as a source of chemicals may become attractive in the future. However, the sustainability and green character of biomass to gas or biomass to liquid processes is questionable and should be validated by life cycle analysis.

2.2 From biomass to products *via* platform molecules

2.2.1 Identification of main platform molecules. As far as carbohydrates are concerned a number of platform molecules are already well identified and currently employed to synthesize speciality and fine chemicals. Monosaccharides, such as glucose and fructose, and disaccharides, such as sucrose, that are easily obtained with great purity from various carbohydrate-containing crops, are well known platform molecules in sugar chemistry. Lactose, with a production of 6×10^5 t y⁻¹,

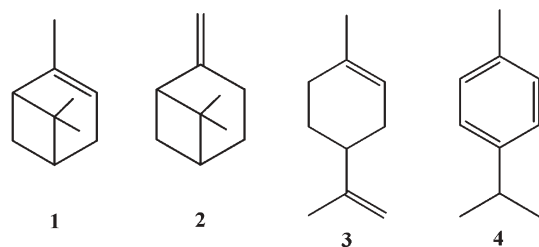
is also a useful platform molecule obtained from the milk industry. Most of the other platform molecules are obtained by fermentation from glucose or other carbohydrates using continuously improved processes with new genetically modified bacteria or yeasts.¹² The followings biomass-derived platform molecules are potentially useful building blocks for chemical synthesis: *aspartic acid*, *1,4-diacids (succinic, fumaric and malic)*, *ethanol*, *glutamic acid*, *glucaric acid*, *2,5-hydroxymethylfurfural*, *2,5-furandicarboxylic acid*, *3-hydroxypropionic acid*, *2-hydroxypropionic acid*, *itaconic acid*, *levulinic acid*, *1,3-propanediol*. This list includes the top platform molecules identified by the US Department of Energy.¹³ In the future the challenge will be to produce fermentable sugars from cellulose and hemicelluloses, which are available in huge amounts from vegetative biomass.

Vegetable oils or triglycerides obtained from the seeds of various plants are the source of a wide variety of fatty acid esters and derivatives (fatty acids and alcohols) with different molecular structures (chain length, number and position of C=C bonds), that can be used as platform molecules, as well as glycerol, which is a co-product of triglycerides transesterification.

The three main platform molecules employed in terpene chemistry are α -pinene and β -pinene, which are extracted from turpentine oil ($350\,000\text{ t y}^{-1}$), a co-product of paper pulp industry, and limonene extracted from citrus oil ($30\,000\text{ t y}^{-1}$).

2.2.2 Catalytic conversion of platform molecules. Conversion of platform molecules by catalytic routes involving one or more steps is currently used to synthesize a wide variety of specialties and fine chemicals. The present trend is to develop heterogeneous processes, allowing an easy recovery of the catalyst or continuous operation in fixed-bed reactors. This is illustrated in the following examples.

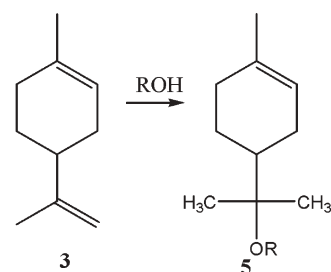
Terpenes. Terpenes (α -pinene **1**, β -pinene **2**, and limonene **3**) are employed in the synthesis of flavours and fragrances (F&F), although these compounds are often more easily obtained by catalytic routes from hydrocarbons.



p-Cymene **4**, a precursor of *p*-cresol and various F&Fs, was obtained by dehydrogenation of α -pinene at $300\text{ }^\circ\text{C}$ in a continuous fixed-bed flow reactor in the presence of $0.5\text{ wt}\%$ Pd/SiO₂.¹⁴ Under similar conditions, but starting from limonene, *p*-cymene was obtained with a 97% yield, and the catalytic activity was stable for 500 h on stream.¹⁵

The liquid phase alkoxylation of limonene **3** with C₁–C₄ alcohols to 1-methyl-4-[α -alkoxy-isopropyl]-1-cyclohexene **5** was carried out both in batch and continuous fixed-bed reactor at $60\text{ }^\circ\text{C}$ on various acidic catalysts.¹⁶ The best yields

were obtained in batch (85%) or continuous reactor (81%) using a beta-type zeolite with SiO₂/Al₂O₃ = 25.



Carbohydrates. Sucrose (total production $130 \times 10^6\text{ t y}^{-1}$) and starch ($40 \times 10^6\text{ t y}^{-1}$ used in industry), are two major sources of glucose and fructose. The catalytic conversion of sugars has been reviewed by van Bekkum and Besemer¹⁷ and by Lichtenthaler and Peters.¹⁸ The hydrogenation of $40\text{ wt}\%$ water solution of glucose was performed in trickle-bed reactor on 1.8% Ru/C catalysts.¹⁹ The catalyst was highly stable, since after 596 h on stream the selectivity to sorbitol at total glucose conversion was 99.3% . The oxidation of glucose to gluconic acid was achieved quantitatively on PtBi/C catalysts (yield $>99\%$); the catalysts was recycled many times with negligible loss of activity and selectivity.²⁰

There is a great interest to convert C₆ molecules available in large supply from biomass into C₅ and C₄ polyols that find many applications in food and non-food products. Thus, glucose can be converted to arabinol by an oxidative decarboxylation to arabinonic acid, which is subsequently hydrogenated to arabitol. The main pitfall is to avoid dehydroxylation reactions leading to deoxy-products not compatible with purity specifications required for arabitol. Aqueous solutions ($20\text{ wt}\%$) of arabinonic acid were hydrogenated on Ru-catalysts in a batch reactor.²¹ By adding 260 ppm of anthraquinone-2-sulfonate (A2S) with respect to arabinonic acid, the yield of deoxy-products decreased from 4.2 to 1.6%. A2S acted as permanent surface modifier since the catalyst was recycled with the same selectivity without further addition of A2S. The highest selectivity to arabitol was 98.9% at 98% conversion with a reaction rate of $73\text{ mmol h}^{-1}\text{ g}_{\text{Ru}}^{-1}$ at $80\text{ }^\circ\text{C}$.

Abbadi *et al.*²² have studied the oxidation of lactose, a co-product of milk industry, on PtBi/C catalyst at pH 7. Lactobionate was formed transiently and subsequently converted to 2-keto-lactobionate with a final yield of *ca.* 80% . Starting from lactobionate, without pH control, 2-keto-lactobionate was obtained with a 95% selectivity, but the oxidation reaction stopped at 50% conversion due to the poisoning of Pt–Bi/C catalysts.

Lactic (2-hydroxypropionic) acid obtained by fermentation of glucose and polysaccharides is the starting material employed by NatureWorks (Cargill/Dow LLC) to produce polylactide (PLA) a biodegradable or recyclable polymer with a potential production of $140\,000\text{ t y}^{-1}$.²³ Other potentially useful reactions from lactic acid were reviewed by Datta and Henry.²⁴ 3-Hydroxypropionic acid, obtained by fermentation of glucose, could also be a good candidate to produce various

chemicals by catalytic routes.²⁵ Research and development is actively conducted at DuPont Co. to employ levulinic acid derived from cellulose for the synthesis of pyrrolidones (solvents and surfactants), α -methylene- γ -valerolactone (monomer for the preparation of polymers similar to polymethylmethacrylate), and levulinic acid esters (fuel additives).²⁶

The catalytic routes to obtain chemicals and polymers from furan derivatives have been reviewed by Moreau *et al.*²⁷ The main catalytic routes are given in Fig. 2. From fructose the first transformation step is a dehydration to 5-hydroxymethylfurfural (HMF). Fructose dehydration at 165 °C was performed in the presence of dealuminated mordenite (Si/Al = 11) with a selectivity of 92% at 76% fructose conversion.²⁸ Starting from inulin hydrolysates, the selectivity to HMF went up to 97% at 54% conversion.²⁹ The hydrogenation of HMF in the presence of metal catalysts leads to quantitative amounts of 2,5-bishydroxymethylfuran used in the manufacture of polyurethanes, or 2,5-bishydroxymethyltetrahydrofuran, which can be used in the preparation of polyesters.³⁰ The oxidation of HMF is used to prepare 5-formyl-2-furancarboxylic acid, and 2,5-furandicarboxylic acid, a potential substitute of terephthalic acid. Oxidation by air on platinum catalysts leads quantitatively to the diacid.³¹ The oxidation of HMF to dialdehyde was achieved at 90 °C with air as the oxidizing agent in the presence of V₂O₅/TiO₂ catalysts, with a selectivity up to 95% at 90% conversion.³²

Furfural is obtained industrially (200 000 t y⁻¹) by dehydration of pentoses produced from hemicelluloses. Furfurylic alcohol is obtained by selective hydrogenation of the C=O bond of furfural, avoiding the hydrogenation of the furan ring. Liquid phase hydrogenation at 80 °C in ethanol on Raney nickel modified by heteropolyacid salts resulted in a 98% yield to furfurylic alcohol.³³

Fatty acid esters and fatty alcohols. Fatty acid ester of glycerol are efficient surfactants obtained either by transesterification of triglycerides with glycerol (glycerolysis) or by esterification of fatty acids with glycerol. The challenge in both cases is to selectively obtain glycerol monoesters that are non-ionic surfactants with a good hydrophilic/hydrophobic balance. Glycerolysis reactions have been conducted on basic oxides to replace liquid bases. Thus, glycerolysis of rapeseed oil on MgO catalysts gave a 63% yield to monoglyceride.³⁴ The synthesis of glycerol monoesters by esterification of fatty acids with glycerol was achieved with various acidic solids as substitutes for sulfuric acid.^{35–42} Fatty acid esters of sugars are also very important biodegradable and biocompatible surfactants that are prepared either by transesterification of

methyl ester with sugar on basic catalysts or by esterification of fatty acids with sugar on acidic catalysts. Liquid acids and bases have been replaced by enzymatic catalysis with lipase giving a higher yield to monoester,^{43,44} but solid catalysts have not been used extensively so far.

Alkylglucosides are a class of valuable commercial surfactants, particularly for cosmetics applications, because of their bio-compatibility. They are obtained by acetalisation of carbohydrates with fatty alcohols in the presence of acid catalysts. Zeolites and MCM-41 have been used as acidic catalysts to achieve glucose acetalisation with alcohols of different chain lengths.^{45,46} It was shown that shape selectivity effects decrease the amount of oligomers formed and that activity and selectivity can be controlled with the Si/Al ratio.

Fatty acid esters are suitable to manufacture biodegradable lubricants, but their resistance to oxidation and tribological properties need to be improved by epoxidation of the C=C bonds, followed by alcoholysis of the epoxide. The epoxidation of fatty acid methyl esters (FAME) is traditionally conducted in strong acidic media, but acidic solids are good substitutes to achieve a green process. Thus, the epoxidation of a mixture of FAME from sunflower oil was achieved with *tert*-butylhydroperoxide (TBHP) at 363 K in the presence of Ti-MCM-41 catalysts, yielding 85% of mono-epoxy compounds.⁴⁷ In the same way, Rios *et al.*⁴⁸ used different Ti-MCM-41 materials with pore diameters ranging from 1.9 to 4.1 nm and amorphous Ti/SiO₂ catalysts with different Ti-dispersion to perform methyl oleate epoxidation with TBHP at 70 °C. Selectivities higher than 95% were obtained whatever the structure of the supporting material, provided titanium was well dispersed. The alcoholysis of epoxidized FAME was studied on acidic resins of various structure and acid strength.^{49,50} The addition of methanol on epoxidized methyl oleate at 60 °C in the presence of Nafion entrapped in silica (SAC13) or of Amberlyst15, a sulfonated styrene-divinylbenzene copolymer, resulted in a selectivity higher than 98% at total conversion.

Catalytic reactions involving C=C bonds are widely used for the conversion of unsaturated fatty compounds to prepare useful monomers for polymer synthesis. Catalytic C–C coupling reactions of unsaturated fatty compounds have been reviewed by Biermann and Metzger.⁵¹ Metathesis reactions involving unsaturated fatty compounds to prepare ω -unsaturated fatty acid esters were applied by Warwel *et al.*⁵² The ethenolysis of methyl oleate catalysed by ruthenium carbenes developed by Grubb yields 1-decene and methyl-9-decenoate which can be very useful to prepare monomers for polyolefins, polyesters, polyethers and polyamides such as Nylon 10.

Glycerol. Besson and Gallezot⁵³ have shown that valuable oxygenates (Fig. 3) can be obtained by oxidation with air of aqueous solutions of glycerol in the presence of carbon-supported platinum and palladium catalysts.

The selectivity can be tuned by promotion of the noble metals with bismuth or by operating under controlled pH. Thus, Garcia *et al.*⁵⁴ found that the oxidation of glycerol at basic pH on palladium and platinum catalysts yielded 70% glycerate. Glyceric acid oxidation on 5% Pt–1.9% Bi/C catalyst yielded 74% hydroxyppyruvic at 80% conversion at acidic pH

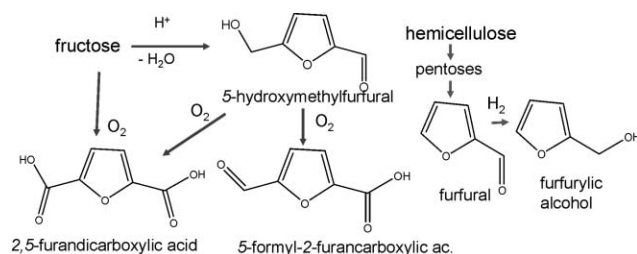


Fig. 2 Catalytic reactions involving furan derivatives.

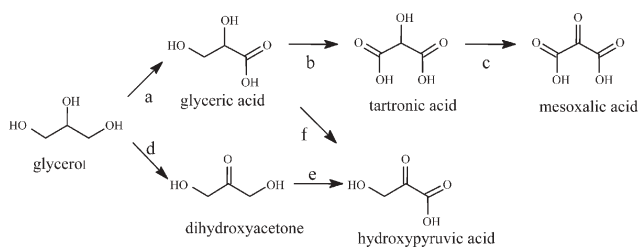


Fig. 3 Products obtained by air oxidation of glycerol (Ref. 53).

(3–4), but on the same catalyst under basic conditions (pH 10–11) an 83% yield to tartronate was obtained at 85% conversion.⁵⁵ Abbadi and van Bekkum⁵⁶ obtained a 93% selectivity to hydroxypyruvic acid at 95% conversion of glyceric acid on 5% Bi–5% Pt/C catalyst without pH regulation. More recently the oxidation of glycerol was conducted in the presence of gold catalysts in basic medium.^{57–59} The selectivity was shown to depend critically upon the size of gold particles.⁵⁹

Polyglycerols obtained by dehydration of glycerol are employed as surfactants, lubricants, cosmetic and food additives. Zeolites have been used to take advantage of the shape selectivity effect to minimize oligomer formation.^{60,61} A fair compromise between activity and selectivity was obtained by J. M. Clacens *et al.*⁶² using caesium-impregnated mesoporous MCM-41. Acrolein was obtained with a 38% yield by glycerol dehydration at 360 °C, 25 MPa in the presence of zinc sulfate.⁶³

Glycerol can be selectively dehydroxylated either to 1,2-propanediol (1,2-PDO), a chemical that can advantageously replace ethylene glycol as anti-freezing agent, or to 1,3-propanediol (1,3-PDO), which, copolymerized with terephthalic acid, give polyesters with unique mechanical properties. 1,3-PDO is currently produced by catalytic routes from ethylene oxide (Shell route) or acrolein (Degussa-DuPont route). The microbial production of 1,3-PDO is under development by DuPont-Genencor to produce 1,3-PDO from glucose.⁶⁴ Chaminand *et al.*⁶⁵ studied the hydrogenolysis of aqueous solutions of glycerol at 180 °C under 80 bar H₂-pressure in the presence of supported metal catalysts, in an attempt to selectively produce 1,2- and 1,3-PDO. The best selectivity (100%) to 1,2-PDO was obtained by hydrogenolysis of water solution of glycerol in the presence of CuO/ZnO catalysts. The best selectivity to 1,3-PDO (1,3-PDO/1,2-PDO = 2) was obtained in sulfolane with rhodium catalysts promoted with tungstic acid. Hydrogenolysis of glycerol to 1,2-PDO was also conducted on Ru/C catalysts in the presence of Amberlyst resin.⁶⁶ Dehydration of glycerol was performed in the presence of various metallic catalysts to obtain acetol with a 90% selectivity in a single stage reactive distillation.⁶⁷ Acetol can then be readily hydrogenated to form 1,2-PDO.

2.3 Biomass to products via one-pot reactions

The processing cost to convert biomass to valuable products and the amount of waste can be greatly reduced under the following process conditions: (i) multistep reactions to targeted molecules carried out by cascade catalysis without intermediate product recovery. (ii) One-step conversion to a mixture of products that can be used as such for the further synthesis of end-products.

2.3.1 One-pot reaction with cascade catalysis. There are several examples of one pot reactions on bifunctional catalysts. Thus, using a bifunctional Ru/HY catalyst, water solutions of corn starch (25 wt%) were hydrolysed on acidic sites of the Y-type zeolite and glucose formed transiently was hydrogenated on ruthenium to a mixture of sorbitol (96%), mannitol (1%), and xylitol (2%).⁶⁸ Similarly a one-pot process for hydrolysis and hydrogenation of inulin to sorbitol and mannitol was achieved with Ru/C catalysts, where the carbon support has been preoxidized to generate acidic sites.⁶⁹ Ribeiro and Schuchardt⁷⁰ succeeded in converting fructose to 2,5-furandicarboxylic acid with 99% selectivity at 72% conversion in a one-pot reaction over a bifunctional acidic and redox catalyst consisting of cobalt acetylacetonate encapsulated in sol-gel silica.

Cascade catalysis without recovery of intermediate products may involve more than two steps involving enzymatic, homogeneous, and heterogeneous catalysis. Several examples of this approach were given by Schoevaart and Kieboom.^{71,72}

2.3.2 One pot conversion to a mixture of products. In the food industry there is usually no requirement to prepare specific molecules from agroresources, but rather a mixture of either triglycerides or carbohydrates. This could well be extended to prepare commodities such as paints, paper, construction materials *etc.* The three following examples taken from two successful European projects conducted at IRC with industrial partners illustrate this innovative approach, consisting of one-pot catalytic conversion of biomass minimizing cost and wastes.

Conversion of sugars to polyols. In the framework of the European program STARPOL,⁷³ starch hydrolysates were converted, by combined hydrolysis–hydrogenation in a reactor loaded with Ru/HY catalysts, to sorbitol (Fig. 4). Then in a second reactor, sorbitol was converted either by dehydroxylation to C₄–C₆ products⁷⁴ or by dehydration to cyclic polyols, depending upon reaction conditions.⁷⁴ Copper-based catalysts, which have a low activity for hydrogenolysis of C–C bonds, were employed to treat 20 wt% aqueous sorbitol solutions in the temperature range 180–240 °C. Reactions carried out in the presence of 33% CuO–65% ZnO catalyst at 180 °C under

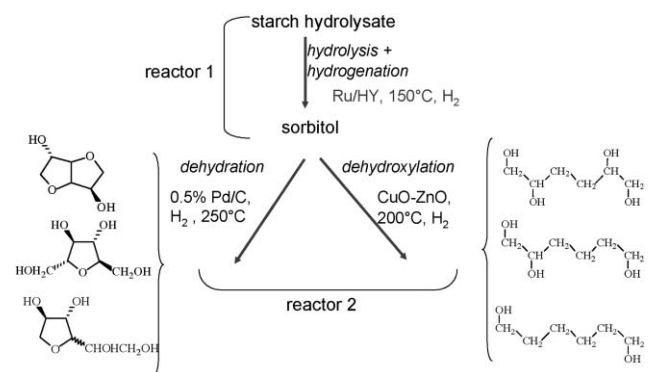


Fig. 4 Preparation of polyols (left field: cyclic ethers; right field: dehydroxyhexitols) from starch hydrolysates via a two step process in successive reactors.

H₂-pressure yielded 73% C₄⁺ polyols, and more specifically, 63% deoxyhexitols. Dehydration of water solution of sorbitol, acidified with propionic acid that can be recovered by distillation at the end of reaction, was carried out at 250 °C under 80 bar of hydrogen pressure in the presence of 0.5% Pd/C catalyst (Fig. 4). The reaction yielded cyclic ethers with the following selectivity at 90% conversion: 37.5% of isosorbide, 37.5% of 2,5-anhydromannitol, and 25% of 1,4-anhydrosorbitol.⁷⁵ The mixtures of polyols obtained by dehydroxylation or dehydration were successfully employed to synthesize alkyl resins to make decorative paints meeting all the specifications of commercial ones.⁷³

Oxidation of starch and other polysaccharides. There is a challenge to convert polysaccharide polymers such as starch or cellulose into valuable end-products *via* one-pot processes. This is difficult to achieve because these natural polymers are insoluble and partially crystallised and heterogeneous catalysts cannot be employed with solid substrates. Hydrophilic starch, obtained by partial oxidation, is used in paper and textile industries, and can be potentially applied in a variety of applications, *e.g.*, for the preparation of paints, cosmetics, and super-absorbents. The oxidation occurs at the C₆ primary hydroxyl group or at the vicinal diols on C₂ and C₃, involving a cleavage of the C₂–C₃ bond to give carbonyl and carboxyl functions.

Several transition metal catalysts based on Fe, Cu or W salts have been proposed to activate H₂O₂, but the concentration of metal ions was quite high and they were retained by carboxyl functions in the modified starch.⁷⁶ In the framework of the HYDROSTAR project,⁷⁷ native starch was oxidised with H₂O₂ in the presence of soluble organometallic complexes to meet specific hydrophilic/hydrophobic properties needed for end-products for paper, paint and cosmetic industries.^{78–80} Water soluble, iron tetrasulphophthalocyanine (FePcS) complex, which is cheap and available at industrial scale, was a very active and selective catalyst for the oxidation reaction. Starches from different origin (potatoes, rice, wheat, corn) were oxidized by H₂O₂ following two operating modes, *viz.*: oxidation in aqueous suspension and oxidation by incipient wetness.

The oxidation of starch in aqueous suspension with H₂O₂ in the presence of iron phthalocyanine gives both carboxylic and carbonyl groups (Table 1). The best yields were obtained with a molar ratio 12900/1 (0.0078 mol%), but the oxidation was still quite efficient with 0.0039 mol% of catalyst (25800/1 anhydro-glucose unit (AGU)/catalyst ratio). The oxidized starch had almost the same final Fe-content as the initial potato starch. Still, the efficiency of this method in view of

scaling up was limited by comparatively low activity and product isolation problems.

The oxidation of native starch by the incipient wetness method was achieved by adding a small volume of water containing the dissolved catalysts to starch powder under continuous mixing, followed by addition of hydrogen peroxide to the impregnated solid under mixing. With a substrate/catalyst ratio of only 25800/1, the oxidation yielded 1.5 carboxyl and 5.6 carbonyl functions per 100 AGU. The process was applied, with success, to the oxidation of starches of different physical and chemical properties (amylose/amylopectin ratio, granule size, temperature of gelatinisation) obtained from different crops (potato, wheat, rice, corn). It was further extended to cellulose, inulin and guar gum, giving a high degree of substitution (*e.g.*, up to DS_{COOH} = 26.5 and DS_{CHO} = 11.6 for cellulose).

This catalytic system was very flexible because, by simple modification of the reaction conditions, it was possible to prepare oxidized polymers with the desired level of carboxyl and carbonyl functions. No waste was formed because the process did not involve any acids, bases or buffer solutions. The incipient wetness process is very easy to scale up. Hydrophilic starch was prepared in batches of 150 L and incorporated successfully in paint formulations. Good results were also obtained with *in vitro* and *in vivo* tests for cosmetic formulation. Interestingly, this is a rather unique example of heterogeneous catalytic process involving a soluble catalyst and a solid substrate.

Modification of starch and other saccharides by hydrophobic chain grafting. A new route to prepare hydrophobic starch consisting of grafting octadienyl chains by butadiene telomerisation has been investigated.^{78,81–83} The reaction was catalysed by hydrosoluble palladium-catalytic systems prepared from palladium diacetate and trisodium tris(*m*-sulphonatophenyl)phosphine (TPPTS). The reaction was first conducted with success on sucrose.⁸¹ The degree of substitution (DS) was controlled by the reaction time. Thus, under standard conditions (0.05% Pd(OAc)₂–TPPTS, NaOH (1N)–iPrOH (5/1), 50 °C) the DS was 0.5 and 5 after 14 and 64 h reaction time, respectively. Telomerisation reaction was also conducted with success on other soluble carbohydrates such as fructose, maltose, sorbitol and β-cyclodextrin.

The transposition of this reaction to starch^{80,82} was challenging because this substrate is insoluble in water at room temperature and gelatinizes at temperatures higher than *ca.* 70 °C. The degree of substitution (DS) should be kept low enough because modified starch should not be too hydrophobic, and for obvious economical reason the catalyst/starch ratio should be kept low. Fig. 5 shows that the DS depends upon the amount of catalyst and temperature. Modified starch with DS = 0.06 obtained with 0.03% palladium at 50 °C meets specification for use as thickener for decorative paints. No palladium was detected in the modified polymer when the reaction was conducted in the presence of 0.05% palladium.

The etherified starch was further transformed by hydrogenation of the double bonds to yield the corresponding linear octyl groups using [RhCl(TPPTS)₃] catalyst soluble in EtOH/H₂O mixtures. Complete hydrogenation was obtained at 40 °C

Table 1 Oxidation of starch in aqueous suspension with H₂O₂ in the presence of iron phthalocyanine. Effect of substrate/catalyst ratio

AGU/Fe	DS _{COOH} ^a	DS _{C=O} ^a
25800 : 1	0.70	3.20
12900 : 1	2.00	10.40
6450 : 1	2.00	9.00

^a Degree of substitution expressed per 100 anhydroglucose units (AGU). ^b Reaction conditions: 58 °C; pH: 7; reaction time: 7 h; molar ratio H₂O₂ : AGU = 1 : 2.1.

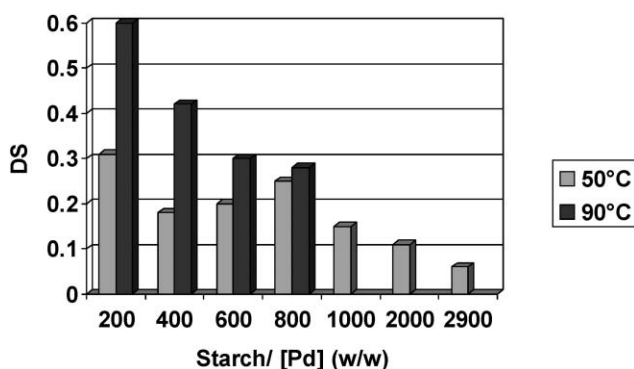


Fig. 5 Modification of starch by butadiene telomerisation. Influence of the catalyst mass and temperature on the degree of substitution (DS).

under 30 bar of H_2 after 12 h using 0.8 wt% Rh-catalyst.⁸³ Further catalytic transformations of the grafted starch, such as double bonds oxidation and olefin metathesis, could possibly be used to modify starch properties to meet specific applications.

3 Concluding remarks

So far bioproducts are derived mainly from vegetables oils and carbohydrates. These raw materials are issued from grains harvested primarily for food and feed and their productivity is low per area of cultivated land. In contrast, the non-grain portion of biomass, *i.e.* agricultural wastes (cobs, stalk, stovers) and vegetative biomass (trees, leaves, *etc.*) are hardly used in spite of their much larger availability. The development of an extended use of cellulosic and lignocellulosic materials for producing cost competitive bio-products must await progresses in depolymerisation processes relying on improved biotechnologies. Encouraging results were obtained on sugar recovery from hemicellulose and cellulose by combined pre-treatment and enzymatic hydrolysis operations applied to corn stover.⁸⁴

Although the market price of renewable feedstocks is now comparable to that of fossil fuels, their processing cost is much higher. Synthesis routes from hydrocarbons have been improved for more than a century, whereas biomass processing is comparatively in infancy. Alternative value chains have to be developed to decrease the cost and to increase the quality of end-products, because even if they may prefer bio-based products, consumers do not want to pay more and have lower quality products. Life cycle analysis, taking into account economic and societal issues due to the increased occupation of land, have to be performed to validate biomass processing options and justify the use of biomass in place of fossil feedstocks.

In view of the diversity and complexity of renewable feedstocks and of the potentially very high number of bio-products at stake, integrated eco-efficient processes should be conducted in biorefineries. The biorefinery framework maximises the value derived from biomass feedstocks by producing multiple products, valorising by-products and co-products, balancing energy production *vs.* energy consumption, and optimising inputs and outputs, including waste treatment.

Within the biorefinery scheme we have identified three process options to produce chemicals by catalytic routes, *viz.*:

1. The degradation of biomass by gasification or pyrolysis leading to syngas and bio-oils, respectively. This approach provides primarily fuels rather than starting materials for bio-product synthesis. However, this is a possible route to bioproducts, provided life cycle analysis demonstrates its validity in terms of economy and ecology. Partial catalytic degradation of biomass, such as that obtained in aqueous phase reforming, brings new opportunities.

2. The catalytic conversion of platform molecules produced by bioconversion of renewables to bioproducts. This is already the basis of many industrial processes leading to important tonnages of chemicals and polymers from carbohydrates and triglycerides and fine chemicals from terpenes. This approach needs to be extended, and process efficiency in terms of waste minimisation should be strengthened by designing more active and selective catalysts.

3. New synthesis routes based on one-pot reactions have to be developed for a drastic reduction of processing costs. Pure isolated products can be obtained by cascade catalysis involving two or more steps. A much larger gain in process economy and waste minimisation should be obtained if a mixture of products suitable for a particular application, *e.g.*, in paper, paint, construction materials and cosmetic industries, can be prepared in one pot process starting from raw materials such as starch, cellulose and triglycerides. Examples have been given in this chapter of the direct transformation of starch to a mixture of products that can be used as such to manufacture end-products.

To meet the challenge posed by the future increasing use of renewables, a large integrated research effort in chemistry, biochemistry, and genetics, as well as in chemical and biochemical engineering, will be required both in industrial and academic research centres. Whatever the process options chosen, catalysis in all its forms will have a major role to play. At present only a comparatively limited number of researchers from academia are working in the synthesis of biomass-derived chemicals and materials by catalytic green routes. In view of the importance of environmental and economic challenges to meet in the future, the workforce in academia should be strengthened to develop formation and research in this area.

References

- 1 <http://www.suschem.org/media.php?mId=4727>.
- 2 P. T. Anastas and J. C. Warner, *Green Chemistry: Theory and Practice*, Oxford University Press, New York, 1998, p. 30.
- 3 <http://www.eere.energy.gov/biomass/>.
- 4 J. J. Bozell, in *Feedstocks for the Future*, ed. J. J. Bozell and M. K. Patel, ACS Symposium Ser. 921, Oxford University Press, 2006, p. 1.
- 5 R. R. Davda, J. W. Shabaker, G. W. Huber, R. D. Cortright and J. A. Dumesic, *Appl. Catal., B*, 2005, **56**, 171.
- 6 G. W. Huber, R. D. Cortright and J. A. Dumesic, *Angew. Chem.*, 2004, **43**, 1549.
- 7 G. W. Huber, J. N. Cheda, C. J. Barrett and J. A. Dumesic, *Science*, 2005, **308**, 1446.
- 8 A. V. Bridgwater and G. V. C. Peacocke, *Renewable Sustainable Energy Rev.*, 2000, **4**, 1.
- 9 D. Mohan, C. U. Pittman, Jr. and P. H. Steele, *Energy Fuels*, 2006, **20**, 848.
- 10 H. Pakdel and C. Roy, *Bioresour. Technol.*, 1996, **58**, 83.

- 11 C. Amen-Chen, B. Riedl and C. Roy, *Holzforchung*, 2002, **56**, 281.
- 12 Th. Wilke and K. D. Vorlop, *Appl. Microbiol. Biotechnol.*, 2004, **66**, 131.
- 13 T. Werpy and G. Petersen, DOE/GO-102004-1992, August 1, 2004.
- 14 D. M. Roberge, D. Buhl, J. P. M. Niederer and W. F. Hölderich, *Appl. Catal., A.*, 2001, **215**, 111.
- 15 D. Buhl, D. M. Roberge and W. F. Hölderich, *Appl. Catal., A.*, 1999, **188**, 287.
- 16 K. Hensen, C. Mahaim and W. F. Hölderich, *Appl. Catal., A.*, 1997, **149**, 311.
- 17 H. van Bekkum and A. C. Besemer, *Chem. Sustainable Dev.*, 2003, **11**, 11.
- 18 F. W. Lichtenthaler and S. Peters, *C. R. Chim.*, 2004, **7**, 65.
- 19 N. Nicolaus, P. Gallezot and A. Perrard, *J. Catal.*, 1998, **180**, 51.
- 20 M. Besson, F. Lahmer, P. Gallezot, P. Fuertes and G. Flèche, *J. Catal.*, 1995, **152**, 116.
- 21 L. Fabre, P. Gallezot and A. Perrard, *J. Catal.*, 2002, **208**, 247.
- 22 A. Abbadi, K. F. Gotlieb, J. B. M. Meirberg and H. Van Bekkum, *Appl. Catal., A.*, 1997, **156**, 105.
- 23 P. R. Gruber, *Proceedings of the 2nd International Conference on Green and Sustainable Chemistry*, Washington DC, June 20–24, 2005, paper 149.
- 24 R. Datta and M. Henry, *J. Chem. Technol. Biotechnol.*, 2006, **81**, 1119.
- 25 D. C. Cameron, NSF workshop, June 23–24, Washington, 2005 http://www.cbe.iastate.edu/nsfbioren/presentations/Cameron_Cargill.pdf.
- 26 L. Manzer, in *Feedstocks for the Future*, ed. J. J. Bozell and M. K. Patel, ACS Symposium Ser. 921, Oxford University Press, 2006, p. 40.
- 27 C. Moreau, M. Belgacem and A. Gandini, *Top. Catal.*, 2004, **27**, 11.
- 28 C. Moreau, R. Durand, S. Razigade, J. Duhamet, P. Faugeras, P. Rivalier, P. Ros and G. Avignon, *Appl. Catal., A.*, 1996, **145**, 211.
- 29 C. Moreau, R. Durand, C. Pourcheron and S. Razigade, *Ind. Crops Prod.*, 1994, **3**, 85.
- 30 V. Schiavo, G. Descotes and J. Mentech, *Bull. Soc. Chim. Fr.*, 1991, **128**, 704.
- 31 P. Vinke, H. E. van Dam and H. van Bekkum, *Stud. Surf. Sci. Catal.*, 1990, **55**, 147.
- 32 C. Moreau, R. Durand, C. Pourcheron and D. Tichit, *Stud. Surf. Sci. Catal.*, 1997, **108**, 399.
- 33 B. J. Liu, L. H. Lu, B. C. Wang, T. X. Cai and K. Iwatani, *Appl. Catal., A.*, 1998, **171**, 117.
- 34 A. Corma, S. Iborra, S. Miquel and J. Primo, *J. Catal.*, 1998, **173**, 315.
- 35 H. E. Hoydonckx, D. E. De Vos, S. A. Chavan and P. A. Jacobs, *Top. Catal.*, 2003, **27**, 83.
- 36 M. S. Machado, J. Perez-Pariente, E. Sastre, D. Cardoso and A. M. de Guerenú, *Appl. Catal., A.*, 2000, **203**, 321.
- 37 N. Sanchez, M. Martinez and J. Aracil, *Ind. Eng. Chem. Res.*, 1997, **36**, 1529.
- 38 S. Abro, Y. Pouilloux and J. Barrault, Heterogeneous Catalysis and Fine Chemicals IV, *Stud. Surf. Sci. Catal.*, 1997, **108**, 539.
- 39 Y. Pouilloux, S. Abro, C. Vanhove and J. Barrault, *J. Mol. Catal. A: Chem.*, 1999, **149**, 243.
- 40 W. D. Bossaert, D. E. De Vos, W. Van Rhijn, J. Bullen, P. J. Grobet and P. A. Jacobs, *J. Catal.*, 1999, **182**, 156.
- 41 I. Diaz, C. Marquez-Alvarez, F. Mohino, J. Perez-Pariente and E. Sastre, *J. Catal.*, 2000, **193**, 295.
- 42 I. Diaz, F. Mohino, J. Perez-Pariente and E. Sastre, *Appl. Catal., A.*, 2003, **242**, 161.
- 43 A. T. J. W. de Goede, M. van Oosterom, M. P. J. van Deurzen, R. A. Sheldon, H. van Bekkum and F. van Rantwijk, *Biocatalysis*, 1994, **9**, 145.
- 44 R. T. Otto, H. Scheib, U. T. Bornscheuer, J. Pleiss, C. Syldatk and R. D. Schmid, *J. Mol. Catal. B: Enzym.*, 2000, **8**, 201.
- 45 M. A. Cambor, A. Corma, S. Iborra, S. Miquel, J. Primo and S. Valencia, *J. Catal.*, 1997, **172**, 76.
- 46 M. J. Climent, A. Corma, S. Iborra, J. Miquel, S. Primo and F. Rey, *J. Catal.*, 1999, **183**, 76.
- 47 M. Guidotti, N. Ravasio, R. Psaro, E. Gianotti, L. Marchese and S. Coluccia, *Green Chem.*, 2003, **5**, 421.
- 48 L. A. Rios, P. Weckes, H. Schuster and W. F. Hölderich, *J. Catal.*, 2005, **232**, 19.
- 49 L. A. Rios, P. P. Weckes, H. Schuster and W. F. Hölderich, *Appl. Catal., A.*, 2005, **284**, 155.
- 50 W. F. Hölderich, L. A. Rios, P. P. Werke and H. Schuster, *J. Synth. Lubr.*, 2004, **20**, 289.
- 51 U. Biermann and J. Metzger, *Top. Catal.*, 2004, **27**, 119.
- 52 S. Warwel, P. Bavaj, M. Rüschen, Klaas and B. Wolff, in *Perspektiven nachwachsender Rohstoffe in der Chemie*, VCH, Weinheim, 1996, 119.
- 53 M. Besson and P. Gallezot, *Catal. Today*, 2000, **57**, 127.
- 54 R. Garcia, M. Besson and P. Gallezot, *Appl. Catal., A.*, 1995, **127**, 165.
- 55 P. Fordham, M. Besson and P. Gallezot, *Appl. Catal., A.*, 1995, **133**, L179.
- 56 A. Abbadi and H. Van Bekkum, *Appl. Catal., A.*, 1996, **148**, 113.
- 57 S. Carrettin, P. McMorn, P. Johnston, K. Griffin and G. J. Hutchings, *Chem. Commun.*, 2002, 696.
- 58 S. Carrettin, P. McMorn, P. Johnston, K. Griffin, C. Kiely, G. A. Attard and G. J. Hutchings, *Top. Catal.*, 2003, **27**, 131.
- 59 S. Demirel-Gülen, M. Lucas and P. Claus, *Catal. Today*, 2005, **102**, 166.
- 60 Henkel, *US Pat* 5349094, 1992.
- 61 Unichema, *US Pat* 5635588, 1997.
- 62 J. M. Clacens, Y. Pouilloux and J. Barrault, *Appl. Catal., A.*, 2002, **227**, 181.
- 63 L. Ott, M. Bicker and H. Vogel, *Green Chem.*, 2006, **8**, 214.
- 64 G. M. White, B. Bulthuis, D. E. Trimbur and A. A. Gatenby, *World Pat.* WO 99 10356, 1999.
- 65 J. Chaminand, L. Djakovitch, P. Gallezot, P. Marion, C. Pinel and C. Rosier, *Green Chem.*, 2004, **6**, 359.
- 66 T. Miyazawa, Y. Kusunoki, K. Knimori and K. Tomishige, *J. Catal.*, 2006, **240**, 213.
- 67 C. W. Chiu, M. A. Dasari, G. J. Suppes and W. R. Sutterlin, *AIChE J.*, 2006, **52**, 3543.
- 68 P. A. Jacobs and H. Hinnekens, (Synfina-Oleofina), *Eur. Pat.*, EP 0 329 923, 1989.
- 69 A. W. Heinen, J. A. Peter and H. van Bekkum, *Carbohydr. Res.*, 2001, **330**, 381.
- 70 M. L. Ribeiro and U. Schuchardt, *Catal. Commun.*, 2003, **4**, 83.
- 71 A. Bruggink, R. Schoevaart and T. Kieboom, *Org. Process Res. Dev.*, 2003, 622.
- 72 R. Schoevaart and T. Kieboom, *Top. Catal.*, 2004, **27**, 3.
- 73 STARPOL project (EC contract FAIR CT95-0837).
- 74 B. Blanc, A. Bourrel, P. Gallezot, T. Haas and P. Taylor, *Green Chem.*, 2000, 89.
- 75 T. Haas, O. Burkhardt, M. Morawietz, A. Vanheertum and A. Bourrel, (Degussa), *Ger. Pat.* DE 19749202, 1999.
- 76 P. Parovuori, A. Hamunen, P. Forssell, K. Autio and K. Poutanen, *Starch/Stärke*, 1995, **47**, 19.
- 77 HYDROSTAR (EC contract GRD1-1999-10200).
- 78 A. Sorokin, S. Kachkarova-Sorokina, C. Donzé, C. Pinel and P. Gallezot, *Top. Catal.*, 2004, **27**, 67.
- 79 A. Sorokin, S. Sorokina and P. Gallezot, *Chem. Commun.*, 2004, 2844.
- 80 A. Sorokin, S. Kachkarova-Sorokina and P. Gallezot, *World Pat.* WO2004/007560 A1, 2004.
- 81 V. Desvergnès-Breuil, C. Pinel and P. Gallezot, *Green Chem.*, 2001, **3**, 175.
- 82 C. Donzé, C. Pinel, P. Gallezot and P. Taylor, *Adv. Synth. Catal.*, 2002, **344**, 906.
- 83 C. Pinel, C. Donzé and P. Gallezot, *Catal. Commun.*, 2003, **4**, 465.
- 84 C. E. Wyman, B. E. Dale, R. T. Elander, M. Holtzapple, M. R. Ladisch and Y. Y. Lee, *Bioresour. Technol.*, 2005, **96**, 1959.

Recent developments in microwave-assisted polymerization with a focus on ring-opening polymerization

Chao Zhang, Liqiong Liao and Shaoqin (Sarah) Gong*

Received 22nd June 2006, Accepted 3rd January 2007

First published as an Advance Article on the web 22nd January 2007

DOI: 10.1039/b608891k

Due to its advantages of direct heating, high temperature homogeneity, reaction rate enhancement, as well as energy savings, microwave-assisted polymerization has become a fast-growing field of polymer research. This paper reviews microwave-assisted polymerization, with an emphasis on the microwave-assisted ring-opening polymerization, covering both homopolymerization and copolymerization of the cyclic monomers. The advantages of microwave-assisted ring-opening polymerization over conventional polymerization are discussed briefly.

Introduction

Microwaves are electromagnetic radiation with frequencies between 300 GHz and 300 MHz (with a wavelength in the range of 1 mm to 1 m). Most commercial microwave ovens produce a microwave wavelength of 12.25 cm, which corresponds to a frequency of 2.45 GHz. Microwaves have been used widely in heating materials for industrial and domestic purposes. As an environmentally benign process, microwave irradiation offers several advantages over conventional heating, such as instantaneous and rapid bulk heating, direct heating, high temperature homogeneity, selective heating (with material that can strongly absorb microwaves in a less polar reaction medium) and energy savings. Over the last decade, microwave irradiation has developed into a highly useful technique and provides an effective alternative energy source for chemical reactions and processes.¹

The unique advantages of microwave-assisted chemistry have triggered an almost exponential increase of publications.² Many chemical reactions undergo an increase/improvement in reaction rate, yield and selectivity under microwave irradiation compared with conventional heating. Microwave irradiation has also been widely used in polymerizations (including polycondensation, free and controlled radical polymerization and ring-opening polymerization) and polymer processing (e.g., polymer modification, curing processes and preparation of dental materials).²

Several review papers² have been published recently on microwave-assisted polymer synthesis and processing; thus, this paper focuses on the new developments in microwave-assisted ring-opening polymerization in recent years. Other types of polymerization, such as step-growth polymerization and free radical polymerization, are briefly discussed.

1. Step-growth polymerization

Extensive research has been conducted in the field of microwave-assisted step-growth polymerization, including

microwave-assisted synthesis of various polyamides, polyimides, poly(amide-imide)s, polyesters and poly(ether-ester)s by means of polycondensation and polyaddition.

Zoldakova and co-workers³ studied microwave-assisted thermal polycondensation of aspartic acid in propylene carbonate solvent. Polysuccinimide, the polycondensation product, was hydrolyzed to obtain linear poly(aspartic acid). A polymeric biocomposite also was synthesized under microwave irradiation by copolymerization of the poly(aspartic acid) with 4-*O*-glucuronoxylan or carboxymethyl-cellulose (CM-cellulose).

Using a mono-mode microwave oven, Loupy and coworkers⁴ synthesized new aromatic polyamides by the microwave-assisted polycondensation of an optically active isosorbide-derived diamine with different diacyl chlorides in the presence of a small amount of *N*-methylpyrrolidinone. Polymers with inherent viscosities between 0.22 and 0.73 dL g⁻¹ were obtained, corresponding to a molecular molar mass (MW) of up to 140 000 g mol⁻¹. Lower MW polymers were obtained with inherent viscosities in the range of 0.04–0.36 dL g⁻¹ by means of interfacial polymerization or the Higashi method. Differential scanning calorimetry measurements clearly demonstrated that polymers with high thermal stability (mp 180–300 °C) were synthesized.

Polyimides have excellent mechanical and heat/chemical resistant properties. Imai *et al.*⁵ studied the solution polycondensation of aliphatic diamines with pyromellitic acid or its diethyl ester in a domestic microwave oven, using various solvents with high boiling points and high dielectric constants. A small amount of polar solvent, such as 1,3-dimethyl-2-imidazolidone, was found to enhance the absorption of microwave irradiation. Recently, Lu *et al.*⁶ investigated the synthesis of polyimide with a p- π conjugated main chain by polycondensation of benzoguanamine (BGA) and pyromellitic dianhydride (PMDA) in a domestic microwave oven. After the polycondensation, the resulting BGA-PMDA polyimide was coordinated with Eu³⁺ in the solid state under microwave irradiation. The effects of microwave irradiation at different power levels and irradiation time were studied.

Mallakpour and co-workers⁷ have synthesized numerous poly(amide-imide)s from various amino acid derivatives and

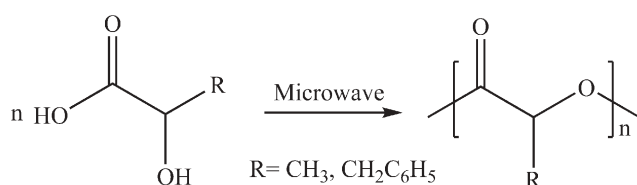
Department of Mechanical Engineering, University of Wisconsin-Milwaukee, 3200 North Cramer Street, Milwaukee, WI, 53211, USA. E-mail: sgong@uwm.edu; Fax: +1 414 229 6958; Tel: +1 414 229 5946

aromatic diamines in a domestic microwave oven. One of the most interesting works by Mallakpour and co-workers is the combined application of microwave irradiation and ionic liquids in the synthesis of poly(amide-imide)s. Ionic liquids, which are comprised entirely of ions, are non-volatile and non-flammable organic salts. They can be heated rapidly at rates exceeding $10\text{ }^{\circ}\text{C s}^{-1}$ under microwave irradiation by an ionic conduction mechanism. A small amount of ionic liquid has been proved to have a dramatic effect on the heating characteristics of solvents under microwave irradiation. Mallakpour and co-workers reported the microwave-assisted polycondensation of *N,N'*-(4,4'-hexafluoroisopropylidene-diphthaloyl)-bis-L-methionine and various aromatic diamines using 1,3-substituted imidazolium bromide/chloride ionic liquids as a solvent and a catalyst in conjunction with triphenylphosphite. Poly(amide-imide)s with high MWs were synthesized rapidly using this microwave-assisted polycondensation method in the presence of ionic liquids.

Faghihi *et al.*⁸ studied the polycondensation of *N,N'*-(3,3'-diphenylphenylphosphine oxide)-bistrimellitimide diacid chloride with hydantoin derivatives or aromatic diamines in a domestic microwave oven. New types of flame-retardant poly(amide-imide)s with high inherent viscosities were synthesized. Compared with the solution polycondensation method under conventional heating, the microwave-assisted polycondensations proceeded rapidly and were completed in approximately 7–12 min.

In contrast with polyamides and polyimides, fewer reports can be found on the microwave-assisted synthesis of polyesters by means of step-growth polymerization. Zsuga *et al.*⁹ studied the polycondensation of D,L-lactic acid in a domestic microwave oven (Scheme 1), and oligomers with number-average molecular molar masses (M_n) ranging from 500 to 2000 g mol^{-1} and yields ranging from 63.2% to 96.2% were prepared in 30 min. In comparison with the reactions conducted in an oil bath at similar conditions, microwave irradiation facilitated the polycondensation of D,L-lactic acid. Interestingly, prolonged microwave irradiation could lead to the formation of cyclic oligomers, which were confirmed by matrix-assisted laser-desorption ionization time-of-flight mass spectrometry (MALDI-TOF MS).

The polycondensation of L-2-hydroxy-3-phenyl-propanoic acid, one aromatic group substituted L-lactic acid, was studied under atmospheric pressure by Liu and co-workers¹⁰ using a domestic microwave oven (Scheme 1). Under microwave irradiation power ranging from 340 to 510 W, poly(L-2-hydroxy-3-phenyl-propanoic acid)s were synthesized with weight-average molecular molar masses (M_w) ranging from 1800 to 5300 g mol^{-1} and yields ranging from 9% to 22% in



Scheme 1 Microwave-assisted synthesis of poly(α -hydroxyalkanoate)s by polycondensation

2.5 h; however, it took up to 96 h to obtain similar results using the conventional melting polycondensation method.

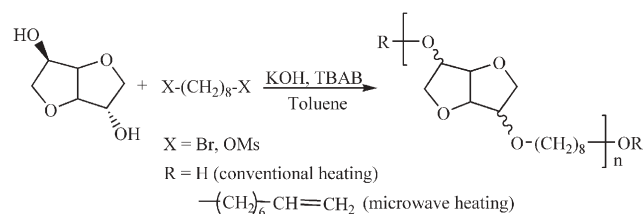
Hurduc *et al.*¹¹ investigated the microwave-assisted synthesis of polyethers. Polyethers were synthesized by polycondensation of 3,3-bis(chloromethyl)oxetane and various bisphenol derivatives, catalyzed by tetrabutylammonium bromide (a phase transfer catalyst), under 60 W microwave irradiation (frequency 2.75 GHz) in a microwave generator. The authors found that microwave irradiation did not have a significant influence on the MW and structure of the polymers except for the shortened reaction time.

Loupy and co-workers¹² recently reported the synthesis of polyesters and poly(ether-ester)s from isosorbide. Polycondensations of aliphatic diols of isosorbide and 1,8-dimesyloctane or other aliphatic dibromo and disulfonated alkylating agents were performed under phase-transfer catalytic conditions in a mono-mode microwave oven (Scheme 2). Reactions were comparatively performed in an oil bath under similar conditions to check the non-thermal microwave effects. The resulting polyethers were characterized by MALDI-TOF MS, and it was found that polymers synthesized under microwave heating had higher MWs and were terminated with ethylenic end groups, while polymers synthesized under conventional heating had lower MWs and were terminated with hydroxyl groups.

2. Radical polymerization

Recent progress in microwave-assisted free radical polymerization, including the classical free radical polymerizations, (mini)emulsion polymerizations, and controlled free radical polymerizations are summarized in this section.

Greiner *et al.*¹³ reported the radical homopolymerizations of styrene (St) and its copolymerizations with methyl methacrylate (MMA) in a CEM Discover mono-mode microwave oven, as well as in a conventional oil bath. The reactions were performed in solvents such as toluene and *N,N'*-dimethylformamide (DMF) using tert-butyl perbenzoate (tBPB), dibenzoyl peroxide (DBPO), di-tert-peroxide (DtBP), dicumylperoxide (DCP), and lauryl peroxide (LP) as the initiators. Compared with the conventional heating, only the homopolymerization of St under microwave irradiation in DMF with DtBP showed significantly enhanced St conversion, whereas other initiators resulted in no increase or only a slight increase of St conversion under microwave irradiation. Since DMF has higher microwave energy absorption than toluene, both the microwave-assisted homopolymerizations and copolymerizations showed increased monomer conversions in



Scheme 2 Efficient microwave synthesis of polyethers from isosorbide.

DMF compared with that under conventional heating. Significantly higher monomer conversions were observed under otherwise comparable conditions in the copolymerization of St with MMA in DMF.

Ritter and co-workers¹⁴ reported the synthesis of N-substituted maleimides, and investigated their free radical polymerization using 2,2'-azoisobutyronitrile (AIBN) as the initiator in a mono-mode microwave oven. Good yields and shortened reaction times were achieved.

Holtze *et al.*¹⁵ studied the microwave-assisted miniemulsion polymerization of St using a pulsed microwave (duration of 9–12 s) at 1000 W. By combining the advantages of the confinement of the polymerization inside nano-reactors during hetero-phase polymerization with the very rapid and efficient microwave heating, short microwave pulses (about 10 s) and longer intervals of cooling (at least 15 min) can be programmed and applied to the reaction. Under optimized conditions, polymer radicals could survive the heating pulse and grow during the cooling period to give polymers with an MW as high as 10^7 g mol⁻¹ and a conversion up to 40% after the first pulse cycle. Besides the ultra-rapid heating by the microwaves, the surviving radical effect is purely thermal in nature and can be explained by the elemental reactions of radical hetero-phase polymerizations.

Zhu *et al.*¹⁶ studied the nitroxide-mediated free-radical miniemulsion polymerization of St in a CEM Discover mono-mode microwave oven at 135 °C; potassium persulfate was used as an initiator in conjunction with 4-hydroxyl-2,2,6,6-tetramethyl-1-piperidinyloxy (OH-TEMPO). The polymerizations proceeded in a controlled manner yielding polymers whose MW increased linearly with increasing conversion. The resulting latexes were colloidally stable. The polymerization behavior under microwave and conventional heating, as well as the MW of the polymers and the Z-average size of the latex particles formed under both heating conditions, were compared. The M_n of polymers obtained under microwave irradiation were close to the theoretical value, while the M_n of polymers obtained under conventional heating were much higher than the theoretical value. The polydispersity indices (PDIs) of latex particles obtained under microwave irradiation were lower than those obtained under conventional heating. Microwave irradiation increased the decomposition rate of the initiator and decreased the particle sizes, resulting in the increase of polymerization rate of St.

Aldana-Garcia¹⁷ studied the microwave-assisted emulsion polymerization of St, and modeled the polymerizations under both microwave and conventional heating using the Predici simulation package of CiT. Microwave activated initiation was modeled as adding a second conventional free-radical chemical initiator, whose concentration is determined by the intensity of microwave irradiation, and its “decomposition” kinetic rate constant is related to the ratio of monomer concentration to the rate of absorbed microwave irradiation. The modeling predictions of conversion and polymer MW for both microwave and conventional heating systems agree well with the experimental data reported in the literature.

Zhu and co-workers¹⁸ have studied various atom transfer radical polymerizations (ATRPs) under microwave irradiation. They recently reported the ATRP of St and butylmethacrylate

(BMA) under mono-mode microwave irradiation. Both microwave-assisted ATRPs (*i.e.*, St and BMA) showed increased polymerization rates in comparison with ATRP conducted under similar conventional conditions. Similarly, Schubert *et al.*¹⁹ investigated the controlled polymerizations of both MMA by ATRP and methyl acrylate (MA) by a nitroxide-mediated process under microwave irradiation. Narrower MW distribution was achieved under microwave irradiation. Microwave heating at higher temperatures resulted in a higher probability of chain termination reactions for both types of monomers.

3. Ring-opening polymerization

Ring-opening polymerization (ROP) is a type of polymerization in which a cyclic monomer yields a monomeric unit that is either acyclic or contains fewer cycles than the monomer. As one type of chain polymerization, ROP consists of a sequence of initiation, propagation, and termination.²⁰ ROP plays an important role in academic research and industrial production. A wide variety of cyclic monomers have been successfully polymerized by the ROP, such as cyclic ethers, acetals, amides, esters and siloxanes. Compared with polymerizations of monomers containing a carbon–carbon double bond (such as vinyl), the chain propagation rate constants for ROP are several orders of magnitude lower.²⁰ Completion of the ROP of cyclic monomers is slower than that of the polymerization of monomers containing a carbon–carbon double bond.²⁰ This section presents a detailed review of microwave-assisted ring-opening polymerization (MROP). According to the architectures of polymers obtained from MROP, the content is divided into two general parts in terms of homopolymerization and copolymerization.

3.1 Microwave-assisted ring-opening homopolymerization (MROHP)

The term homopolymerization often is used to distinguish the polymerization of a single monomer from the copolymerization process. In the MROHP, microwave irradiation is used in the living cationic ring-opening homopolymerization (LROHP) of 2-oxazolines and coordination ring-opening homopolymerization (CROHP) of cyclic lactones, lactides, lactam and carbonates.

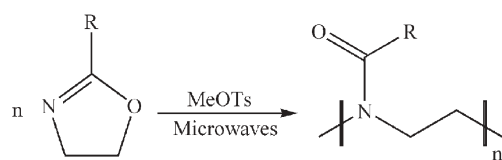
3.1.1. Microwave-assisted living cationic ring-opening homopolymerization (MLROHP). Over the past decade, living polymerization techniques have attracted much attention for providing simple and robust routes to the synthesis of polymers with predetermined MW, low PDI, specific functionalities and various architectures. According to the reaction mechanism, living polymerization can be classified into two categories: (1) living radical polymerization; and (2) living cationic ring-opening polymerization. Living radical polymerization has been studied intensively under microwave irradiation,²¹ exhibiting advantages such as increased reaction rates and improved polymer properties. MLROHP using 2-oxazolines as monomers was reported recently.²²

Poly(2-oxazolines) have attracted much interest due to the biological activity displayed by many molecules possessing this

core structure, which can provide applications in micelle catalysis, drug delivery and hydrogels. The strong interest generated for this class of molecules has led to the development of numerous synthetic strategies for their preparation. The LROHP of 2-oxazolines is a slow process with a reaction time ranging from hours to days; thus, a reduced reaction time is important to achieve widespread industrial applications. MLROHPs of 2-methyl-2-oxazoline (MeOx), 2-ethyl-2-oxazoline (EtOx), 2-nonyl-2-oxazoline (NonOx), 2-phenyl-2-oxazoline (PhOx) and soy based 2-oxazoline were investigated and the polymerization time had been reduced to only a few minutes (Scheme 3).

Schubert^{22c} and co-workers reported the methyl tosylate (TsOMe) initiated MLROHP of EtOx, which is the first example in this area. The reaction was carried out in an Emrys Liberator single-mode microwave oven. The kinetic curves on the cationic ring-opening polymerization of EtOx were investigated under both conventional and microwave conditions. For the conventional method, polymerization was carried out at approximately 80 °C in acetonitrile and the reaction took six hours. Under microwave irradiation, the reaction mixtures were heated directly, quickly and homogeneously; cationic ring-opening polymerization of EtOx could be performed either in bulk or with a drastically reduced amount of solvent with minimum side reactions. The temperatures of the polymerizations in bulk under microwave irradiation reached 200 °C without being limited to the boiling point of acetonitrile (82 °C) by conventional heating. The living nature of the microwave-assisted polymerization was observed in the temperature range between 80 and 180 °C, and polymers were obtained with a narrow MW distribution (PDI < 1.2). The kinetics of the TsOMe initiated polymerization of EtOx showed that the reaction rate increased with temperature. Consequently, the reaction at 190 °C under microwave irradiation was completed in one minute and was 350 times faster than that by conventional heating at 80 °C. The activation energy for the microwave-assisted polymerization of EtOx was 73.4 kJ mol⁻¹, which was in good agreement with previously reported values (68.7 to 80.0 kJ mol⁻¹) for similar systems by the conventional method.

Since many reactions were improved under microwave irradiation, the mechanisms of the acceleration had been a matter of debate over the existence of the thermal effect and specific/non-thermal effect.²³ The thermal effect, which is related to the fast increase of temperatures when polar groups are irradiated by microwaves, can be estimated easily by temperature measurements. The non-thermal effect was classified as the direct interaction of the electric field with specific



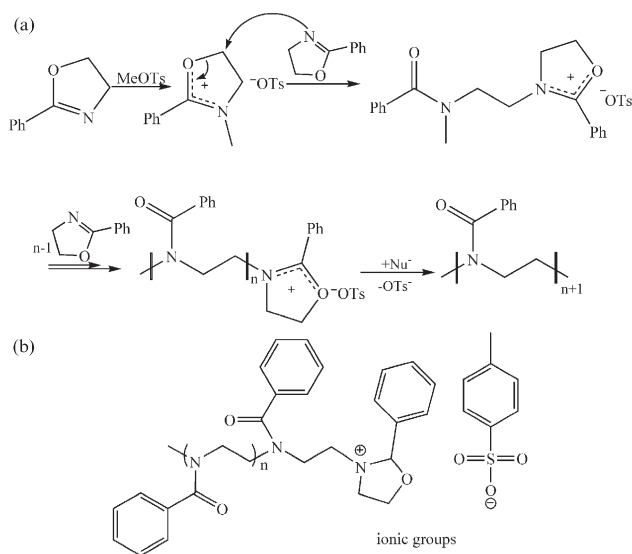
R = ethyl, nonyl, phenyl, soyalkyl

Scheme 3 Cationic ring-opening polymerization of 2-oxazolines under microwave irradiation.

reaction molecules and can be evaluated from the changes in the pre-exponential factor A (representative of the probability of molecular impacts) or the activation energy (entropy term) in the Arrhenius equation.²⁴ It is difficult to make direct comparisons between the microwave method and the conventional method because of the inaccuracy of temperature measurement in the microwave field and the difficulty in reproducing the reaction by the conventional heating method. In the microwave-assisted polymerization of EtOx^{22c} mentioned above, the reaction rate acceleration in the range from 110 to 190 °C was calculated from the Arrhenius equation (rate acceleration factor 54), and complied perfectly with that observed from the reaction (60 min → 1 min, rate acceleration factor 60), suggesting that the improvement of the reaction rate enhancement was caused purely by the thermal effect.

Contradictory arguments about the thermal and non-thermal microwave effects in the MLROHP of PhOx were reported.^{22d,22e} Sinnwell *et al.*^{22d} claimed the existence of the non-thermal effect. The reaction was performed in a CEM-Discover monomode microwave oven under an inert argon atmosphere; a fiber optical sensor was equipped to measure the polymerization temperature. Four systems were used in the LROHP of PhOx: (1) a conventional heating closed system (CCS); (2) a conventional heating open system (COS); (3) a microwave irradiation closed system (MCS); and (4) a microwave irradiation open system (MOS). In the closed system (CS), the monomer and TsOMe were dissolved in acetonitrile and the reaction temperature was approximately 125 °C. In the open system (OS), butyronitrile was used as solvent and the temperature of the reaction medium was approximately 123 °C. In all four systems, the linear plots of $\ln([M_0]/[M_t])$ (where $[M_0]$ is the initial monomer concentration and $[M_t]$ is the concentration of monomer after time, t) against time showed that the reaction rate follows the first-order kinetics. MLROHP showed a great enhancement in reaction rates compared with the thermal LROHP. Both MCS (under a superheated condition) and MOS (under a reflux condition) showed nearly the same enhancement of the reaction rate over CCS and COS, respectively. The same enhancement of the reaction rate was explained by the strong microwave effect that took place mainly in the active growing polymer (Scheme 4a), which was composed of a tosylate counterion of the active oxazolinium end group (Scheme 4b). In the case of the active oxazoline polymer, the microwave radiation was absorbed mainly by the growing, high polar end group. This corresponded to the part of the molecule where the activation energy is required to propagate the polymer chain. To investigate further, the author measured the increase in temperature of the reaction mixtures with various monomer-to-initiator ratios corresponding to a variable ratio of ionic species. The temperature increased with the amount of the initiator, and the final temperature of the pure solvent (80 °C) is considerably lower, which is in accordance with the low dielectric loss of acetonitrile. This interesting behavior indicates that there is a strong microwave effect that mainly takes place at the ionic oxazolinium species.

However, Schubert's group attributed the acceleration of the LROHP of PhOx under microwave irradiation only to the temperature effects.^{22e} In their work, LROHP of PhOx was



Scheme 4 Mechanism of the cationic ring-opening polymerization of 2-phenyl-2-oxazoline using (a) methyl tosylate and (b) active oxazoline polymer.

investigated in three systems: (1) MCS (in butyronitrile); (2) automated CCS (under pressure, in acetonitrile); and (3) automated COS (under reflux, in butyronitrile). Both pressure polymerizations in acetonitrile and reflux polymerization in butyronitrile revealed similar polymerization rates under microwave irradiation and conventional heating. The first-order kinetic plots of the three systems and good correspondence in the gel permeation chromatography (GPC) traces of the polymerization mixtures demonstrated the absence of the non-thermal microwave effects.

Based on the above results, a detailed study on the kinetics and the livingness of the LROHP were performed on a series of linear 2-oxazolines, including MeOx, EtOx, NonOx and PhOx in acetonitrile at high temperatures of up to 200 °C under microwave irradiation.^{22a} The reaction rates of MLROHP were enhanced significantly by factors of up to 400 times of that of the conventional LROHP. The first-order kinetics of the monomer consumption and the livingness of the polymerization were maintained in MLROHP at temperatures ranging from 80–200 °C (Figure 1). The activation energies for the MLROHP of the four 2-oxazolines were determined from the corresponding Arrhenius plots and were found to fall in the range of the values obtained with conventional heating. A comparison of the four activation energies showed that MeOx, EtOx and NonOx had similar activation energies, while that of PhOx is significantly higher because of the +M stabilization effect of the propagating species.

Soy based 2-oxazoline (SoyOx) monomer,²⁵ which is prepared from a sustainable biomass resource—soybean, contains unsaturated groups that can provide cross-links for the resulting polymers. TsOMe initiated LROHP of the SoyOx also was carried out under microwave irradiation in bulk or in acetonitrile (Scheme 5). The polymerization was completed in 15 min when it was heated up to 140 °C in acetonitrile and presented the living characteristics as the other four kinds of 2-oxazoline. These investigations on MLROHP of

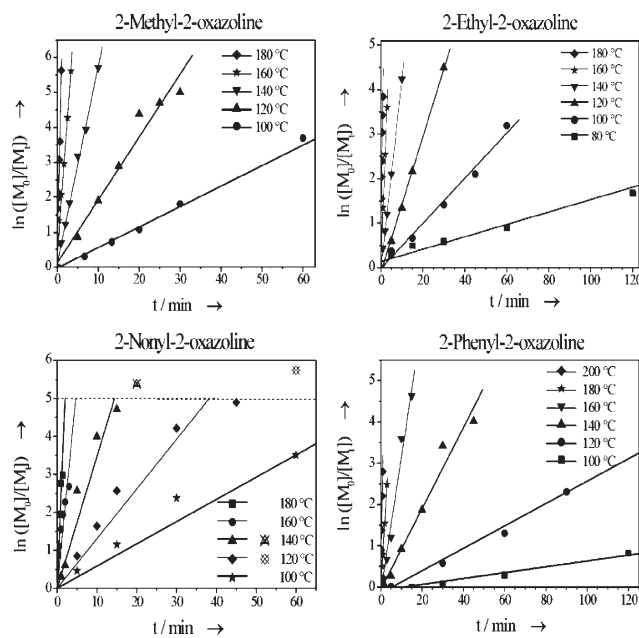
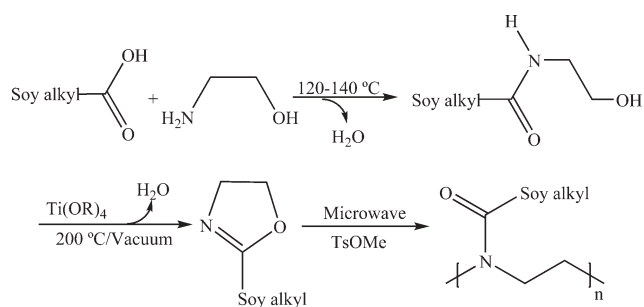


Fig. 1 Kinetics of the different congeners of the 2-oxazolines, plotted against time ($[monomer]/[initiator] = 60$).

2-oxazolines conducted by Schubert and co-workers showed that only temperature effects were responsible for the tremendous increase in 2-oxazoline polymerization rate (*i.e.*, the non-thermal microwave effect was not discernible).

During the polymer synthesis process, various reaction conditions, such as monomers, catalysts, reaction times and temperatures, had to be optimized to obtain well-defined polymers, which is a very time-consuming process. High-throughput methods represent a very promising approach by which different parameters can be screened simultaneously or in a fast serial mode and the results can be compared easily, thereby leading to new structure–property relationships.²⁶ Hoogenboom *et al.*²⁷ reported a microwave-assisted high-throughput method for LROHP of 2-oxazolines. The system included a single-mode microwave synthesizer and high-throughput workflow (high-throughput screening with peripheral characterization equipment) (Figure 2). MLROHP of NonOx at 140 °C was carried out in solvent, and kinetic investigations in dichloromethane revealed a living mechanism. Polymerizations under microwave irradiation proceeded significantly faster than conventionally heated polymerizations (at ambient pressure) because they combined the advantages of



Scheme 5 Synthesis of the soy based 2-oxazoline monomer SoyOx.

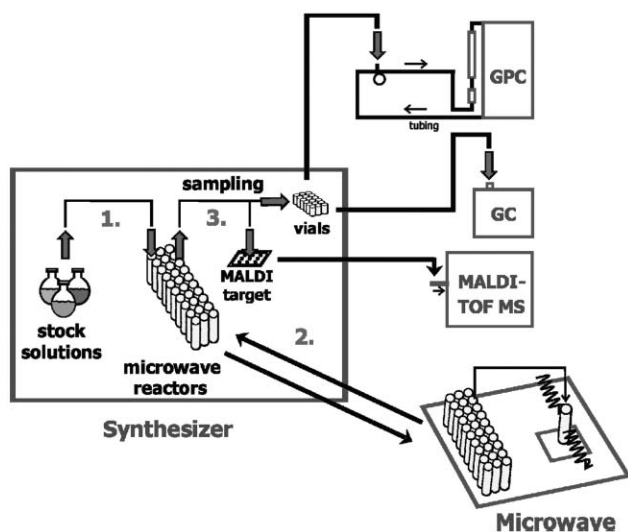


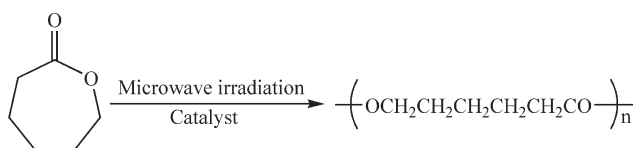
Fig. 2 Microwave high-throughput workflow.

both microwave-assisted polymer synthesis and high-throughput polymer synthesis.

3.1.2. Microwave coordination ring-opening homopolymerization. Aliphatic polyester is one of the most important classes of biodegradable polymers due to its excellent biodegradability and biocompatibility. Aliphatic polyesters are synthesized mainly by ROHP of aliphatic lactones, lactides and cyclic carbonates.

The first microwave coordination ring-opening polymerization (MCROHP) of lactone was reported in 1996,²⁸ when Albert and co-workers first disclosed titanium tetrabutylate catalyzed MCROHP of ϵ -caprolactone (CL) under microwave irradiation. They also compared MCROHP of CL under microwave irradiation and conventional thermal methods in terms of MW, conversion and reaction kinetics. A pulsed microwave was used to control the reaction temperatures. The reactions were carried out at 180 °C with different monomer/catalyst molar ratios. The results showed that the conversion and M_n were similar for both processes and no significant difference was found between the kinetics of the two methods.

Fang and Scola²⁹ applied variable frequency (2.4–7.0 GHz) microwave irradiation in the CROHP of CL to gain optimum processing control (Scheme 6). CL can absorb microwave energy effectively; therefore, the polymerization mixture can be heated easily to induce chemical reaction during the microwave processing. Under 70–100 W of microwave irradiation, the temperatures of the reaction mixtures could reach 150–200 °C, and poly(ϵ -caprolactone) (PCL) with a M_w of 9900–86 000 g mol⁻¹ was obtained after 2 h of irradiation.



Scheme 6 Polymerization of ϵ -caprolactone under microwave irradiation.

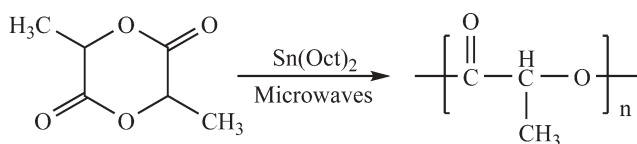
Compared with commercial products produced by the conventional heating process, microwave-produced PCL had equivalent glass transition temperature (T_g), melting temperature (T_m) and thermal stability. The characterization results revealed that high quality PCL could be prepared by microwave irradiation within 2 h, versus more than 12 h by the commercial thermal process.

Liu and Liao³⁰ reported the CROHP of CL that was conducted in a domestic microwave oven at a frequency of 2.45 GHz. The CROHP of CL was carried out effectively with constant microwave powers of 170, 340, 510, and 680 W. The temperatures of the polymerization ranged from 80 to 210 °C. PCL with a M_w of 124 000 g mol⁻¹ and a yield of 90% was obtained at 680 W for 30 min using 0.1% (mol/mol) stannous octanoate (Sn(Oct)₂) as a catalyst. When the polymerization was catalyzed by 1% (wt/wt) zinc powder, the M_w of PCL was 92 300 g mol⁻¹ after the reaction mixture was irradiated at 680 W for 270 min.

Heating characteristics of the CROHP of CL under microwave irradiation also were studied.^{30d} Liu and Liao found that the reaction temperature of CL was self-regulated to an equilibrium temperature under microwave irradiation. For example, at 680 W of microwave irradiation, the temperature of CL (10 g) increased rapidly from 20 to 355 °C during the first 10 min and then fluctuated slightly around 360 °C during the next 20 min. An exothermic peak was observed from the thermogram of MCROHP of CL with Sn(Oct)₂ as a catalyst. When a mixture of 10 g of CL with 0.1% (mol/mol) Sn(Oct)₂ was irradiated at 680 W, an exothermic peak appeared between 2 min and 5 min with a maximum temperature of 343 °C at 3 min. During this period of time (2–5 min), the MCROHP of CL was very fast, resulting in PCL with an M_w of 123 000 g mol⁻¹ and yield of 95%. The author concluded that the thermal effect of microwave energy on the CL monomer and the reaction mixture was dependent on the power levels of microwaves and the mass scale of materials.

Sivalingam and Madras³¹ studied the kinetics of MCROHP of CL in bulk at 350 W with different cycle-heating periods (30–50 s). They set up two models for both thermal and microwave heating processes. The MW distributions, which were measured by GPC, were determined as a function of reaction time. Because the temperature of the system continuously varied with the reaction time, a model was proposed based on continuous distribution kinetics with time/temperature-dependent rate coefficients. Experiments were conducted under thermal heating to quantify the effect of the microwave on polymerization. The polymerization also was investigated with thermal and microwave heating in the presence of a zinc catalyst. The activation energies determined from temperature-dependent rate coefficients for pure thermal heating, thermally aided catalytic polymerization, and microwave-aided catalytic polymerization were 24.3, 13.4, and 5.7 kcal mol⁻¹, respectively. This indicates that microwaves increase the polymerization rate by lowering the activation energy.

Sinnwell and co-workers³² studied the direct synthesis of methacrylate PCL macromonomers. The MCROHP of CL in the presence of methacrylic acid or acrylic acid yields radical polymerizable polyester macromonomers. Studies showed fast



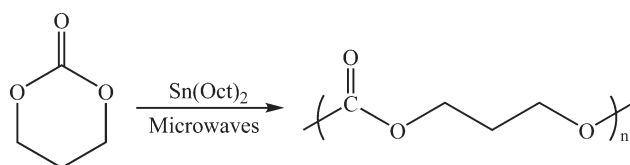
Scheme 7 Microwave-assisted ring-opening polymerization of lactide.

access to defined unsaturated macromonomers from unpurified educts. The process has the advantages of requiring only one step and providing high functionality. Investigation of the thermal properties shows that the melting point of the macromonomers was adjustable between 46 and 51 °C.

Poly(lactide/poly(lactic acid) (PLA) is one of the most important biodegradable polyesters because it can be derived from naturally renewable biomass such as corn. As a biobased, biodegradable polyester, the synthesis of PLA has attracted much more interest. Most of the commercial PLA is produced by CROHP of lactide (LA), which is a time-consuming process. Liu and co-workers³³ first reported the MCROHP of D,L-lactide (D,L-LA) (Scheme 7). Poly(D,L-lactide) (PDLA) with a M_w of 4×10^5 g mol⁻¹ and a yield over 90% was produced in 10 min by the CROHP of D,L-LA under 255 W microwave irradiation. Degradation of PDLA was also induced by microwaves with a power level over 340 W. The MW of PDLA was dependent upon the competition between the polymerization of D,L-LA and the degradation of the resulting polymer. Wang and co-workers³⁴ investigated the MCROHP of D,L-LA under atmospheric conditions with carborundum as a heating assistant material. The effects of the heating medium, monomer purity, catalyst concentration, microwave irradiation time and vacuum level were discussed. PDLA with a viscosity-average molar mass (M_η) over 250 000 g mol⁻¹ and a yield over 85% was obtained.

Several groups also studied MCROHP of L-lactide (L-LA). McCarthy and co-workers³⁵ presented some preliminary results of MCROHP of L-LA. Liu and Zhang³⁶ conducted a more detailed study on the MCROHP of L-LA. The heating characteristics of L-LA, Poly(L-lactide) (PLLA) and L-LA/Sn(Oct)₂ mixture under 2.45 GHz microwave irradiation were investigated. It was observed that the temperatures of the three systems increased rapidly and were self-regulated to an equilibrated temperature. As expected, the microwave power level had a significant influence on the equilibrium temperatures—a higher level of microwave power induced a higher equilibrium temperature. Exothermal peaks in the temperature–time curves were observed for L-LA/Sn(Oct)₂ mixtures when the irradiation power was above 170 W. The CROHP of L-LA proceeded quickly under microwave irradiation, with a simultaneous degradation of the resulting PLLA. The MW of PLLA depended on the competition between the polymerization of L-LA and the degradation of the resulting polymer, which was greatly influenced by the microwave power level. PLLA with a MW of 10^5 g mol⁻¹ was obtained when the MCROHP of L-LA was carried out under 170 W microwave irradiation for 10 min.

Besides CL and LA, Liu and co-workers³⁷ also investigated the CROHP of an aliphatic cyclic carbonate monomer, trimethylene carbonate (TMC), under microwave irradiation



Scheme 8 Microwave-assisted ring-opening polymerization of trimethylene carbonate.

(Scheme 8). High MW poly(trimethylene carbonate) (PTMC) ($M_w = 10^5$ g mol⁻¹) was obtained when the MCROHP of TMC was carried out with microwave forward energy at 255 W for 20 min. Compared with CROHP in an oil bath at the same temperature, MCROHP of TMC showed a slower reaction rate but a higher MW, indicating more serious degradation under the conventional heating method.

3.1.3 Other types of ring-opening homopolymerization. The application of biodegradable polyesters in the biomedical field requires the material to be highly safe for the living body. PCL usually is synthesized by CROHP of CL with Sn(Oct)₂ as a catalyst, which has been approved by FDA as a food additive. However, Sn(Oct)₂ contains the organic tin element, which leads to potential toxicity problems for biomedical applications.³⁸ Therefore, there is an increased interest in using a non-toxic or non-metallic catalyst/initiator during the polymerization. Liu and co-workers³⁹ reported carboxylic acid catalyzed MCROHP of CL. Benzoic acid and chlorinated acetic acids were studied in the metal-free reaction. The product was characterized as PCL by proton nuclear magnetic resonance spectroscopy, Fourier transform infra-red spectroscopy, ultra-violet spectroscopy, and GPC. For a mixture of CL and benzoic acid with a molar ratio of 25/1, the M_w and PDI of the PCL synthesized by microwave irradiation at 680 W for 4 h were 44 800 g mol⁻¹ and 1.6, respectively. Starting from the same mixtures, the M_w and PDI of the PCL synthesized by conventional heating at 210 °C for 4 h were 12 100 g mol⁻¹ and 4.2, respectively. Clearly, the polymerization improved significantly under microwave irradiation both in terms of MW and PDI. Degradation of the resultant PCL was observed during microwave polymerization processes in the presence of chlorinated acetic acids, which caused a reduction in MW of PCL.

The effect of microwave energy on the chain propagation of benzoic acid-initiated MCROHP of CL also was investigated.⁴⁰ The molar ratios of CL to benzoic acid used were 5, 15 and 25. The mixtures of CL–benzoic acid were heated under microwave irradiation, and the temperature was self-regulated to an equilibrated temperature between 204 and 240 °C, with microwave power ranging from 340 to 680 W. The polymer chain propagated rapidly between 160 and 230 °C, and the rate of propagation increased with higher temperatures within this temperature range. Degradation of the resultant PCL occurred when the temperature was above 230 °C. The results suggested that under microwave irradiation, the propagation of PCL chains was enhanced significantly but the formation of growing centers at the beginning stage of the polymerization was greatly inhibited (Table 1). With this metal-free method, PCL with a MW over 4×10^4 g mol⁻¹ was prepared.

Table 1 Results of ring-opening polymerization of ϵ -caprolactone ($M/I = 5$)

Experiment ^a	Time/ min	$M_n/g \text{ mol}^{-1}$	Monomer conversion (%)	N_t/N_m	$M_{n(m)}/$ $M_{n(t)}$
1 ^t	30	1500	92.1	19.0	6.6
2 ^m		9900	32.0		
3 ^t	60	1700	99.0	6.8	6.5
4 ^m		11 100	95.0		
5 ^t	100	2300	99.0	6.7	6.4
6 ^m		14700	94.9		

^a t: Thermal polymerization at 210 °C, m: microwave-assisted polymerization at 680 W.

Liu and co-workers⁴¹ studied acid-initiated MCROHP of CL and its application in the preparation of a drug controlled-release system. The effects of microwave power, irradiation time, CL/acid molar ratio, and acidity of acid on the polymerization were investigated. Both the polymerization rate and the MW of polymers obtained were enhanced in comparison with the conventional thermal method. PCL with an M_w higher than 12 000 $g \text{ mol}^{-1}$ and a PDI below 1.6 was synthesized in the presence of maleic acid, succinic acid and adipic acid. MCROHP also was carried out when the CL monomer was mixed with a certain amount of ibuprofen (IBU), from which the IBU-PCL controlled-release system was prepared directly. Neither ibuprofen particles nor microphase separation were observed from the surface of the ibuprofen-PCL controlled-release system by scanning electron microscopy. The sustained release of IBU from the system was observed from 12 h to 9 days with an increasing IBU loading level from 5 to 20 wt% (Figure 3). This appeared to be a promising method to prepare drug controlled-release systems.

Since lanthanide compounds are efficient catalysts for ROP of cyclic esters and also lack toxicity,⁴² MCROHP of CL using early lanthanide halides as catalysts was investigated.⁴³ Two types of microwave ovens, a monomodal reactor (Synthwave S402, Prolabo) and a multimode microwave oven, were used for MCROHP of CL. Hydrated lanthanide halide catalyzed MCROHP of CL is a very easy and efficient method to obtain

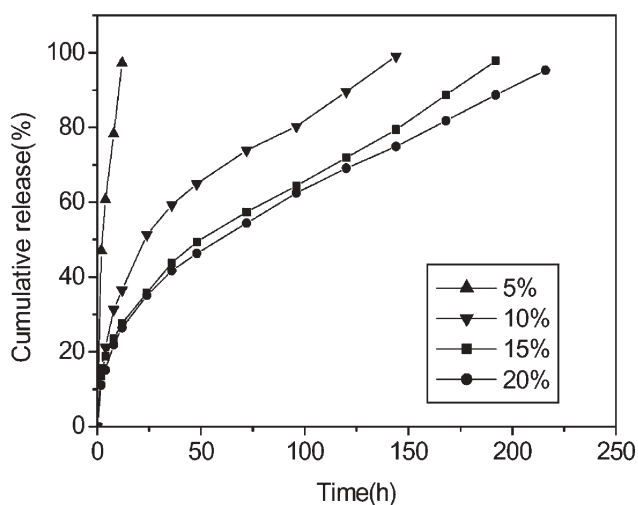
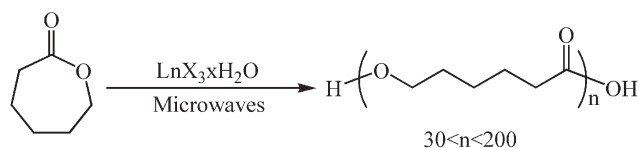


Fig. 3 *In vitro* release of ibuprofen from PCL-ibuprofen system prepared by microwave irradiation.



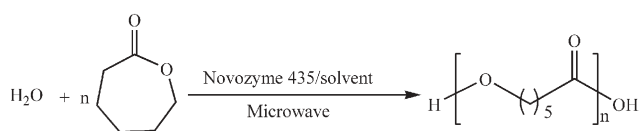
Scheme 9 Microwave ring-opening polymerization of ϵ -caprolactone using lanthanide halides as catalyst.

macro-monomers with controlled MWs in the range of 3000–5000 $g \text{ mol}^{-1}$, which can be used as starting materials for functionalization and copolymerization reactions (Scheme 9). Differential scanning calorimetry and thermal gravity analyses were performed to study the thermal properties of the polymers produced by MCROHP and conventional CROHP. The results revealed no significant difference between the polymers.

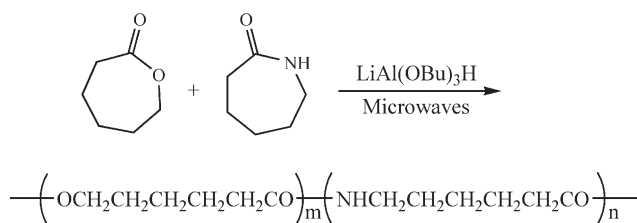
Ritter and co-workers⁴⁴ reported the microwave-assisted Novozyme 435-catalyzed CROHP of CL in organic solvents. (Scheme 10). Since the Novozyme 435-catalyzed ROP strongly depends on the temperature and the polarity of the medium, five solvents with varying polarity and boiling points, tetrahydrofuran, dioxane, toluene, benzene and diethyl ether, were chosen for this study. No polymerization was observed using the two polar solvents tetrahydrofuran and dioxane. Using less polar solvents such as toluene, benzene and diethyl ether could lead to the enzymatic polymerization of CL, although the M_w is only up to several thousands (5800 $g \text{ mol}^{-1}$, in diethyl ether). The authors discovered the unexpected accelerating and decelerating effects of the microwave upon the ROP in different solvents. They found that in boiling benzene and toluene, the polymerization rate under microwave irradiation was significantly lower than that conducted in a conventional oil bath, but monomer conversion accelerated when using boiling diethyl ether as solvent. It was concluded that the enzyme-catalyzed CROHP of CL was influenced significantly by the microwave irradiation.

Schubert *et al.*^{22g} have studied the microwave-assisted cationic ring-opening polymerization of EtOx in different ionic liquids as reaction media and the polymerization was completed in one minute. Based on the solubility difference between polymer and ionic liquid, polymer can be isolated by simple water extraction, which is considered a convenient and “environmentally friendly” process, while the ionic liquid can be efficiently recovered from water, thereby completely avoiding the use of volatile organic compounds during the purification step.

More recently, Liao and Gong *et al.*⁴⁵ investigated the microwave-assisted ring-opening polymerization of CL in the presence of 1-butyl-3-methylimidazolium tetrafluoroborate ionic liquid. Using zinc oxide as the catalyst, PCL with a M_w



Scheme 10 Reactivity of the microwave-assisted ring-opening polymerization of ϵ -caprolactone compared with conventional thermal heating in different solvents.



Scheme 11 Microwave-assisted ring-opening copolymerization of ϵ -caprolactone and ϵ -caprolactam.

of 28 500 g mol⁻¹ could be obtained in 30 min in a domestic microwave oven (85 W) by adding 30 wt% ionic liquid to the reaction mixture. Temperature profiles of the reaction mixtures revealed that the addition of ionic liquid drastically changed the temperature of the reaction.

3.2. Microwave-assisted ring-opening copolymerization

Copolymerization is the simultaneous polymerization of two or more types of monomers and it is a useful method to obtain polymers with adjustable properties. In ring-opening copolymerizations (ROCP), microwaves have been introduced to prepare random copolymers and block copolymers. The following section of this paper discusses two kinds of copolymers (copolymers based on lactones and 2-oxazolines, respectively) synthesized by microwave-assisted ring-opening copolymerization (MROCP).

3.2.1. Microwave-assisted ring-opening copolymerization of lactones/lactides. While PCL is one of the most widely used biodegradable polyesters, copolymers of PCL have attracted much attention due to their adjustable properties. Anionic-catalyzed ring-opening copolymerization (AROCP) of ϵ -caprolactam and CL was conducted using a Lambda LT502XB variable frequency microwave furnace (Scheme 11).⁴⁶ The microwave frequency used in the reactions is 4.69 GHz with a bandwidth of 1.0 GHz and a sweep rate of 0.5 s. The reaction was programmed to a set temperature, which was controlled by a pulsed power on/off system. Dielectric properties of ϵ -caprolactam and CL measured in the microwave region ranging from 0.4 to 3.0 GHz showed that both monomers exhibited effective absorption of microwave energy. After a 30 min reaction, poly(amide ester) with a yield of 70% and M_w of 22 000 g mol⁻¹ was obtained.

Compared with conventional AROCP, microwave-assisted anionic ring-opening copolymerization was more effective for the preparation of a higher yield, higher amide content, and

higher T_g poly(amide-ester) with an equivalent MW (Table 2). The higher yield under microwave irradiation suggested that microwave energy provides a more efficient synthetic route as a consequence of the direct interaction between microwaves and the molecular dipole moments of the reactants; however, it is difficult to measure accurately the temperature in the bulk of the reaction mixture. A higher amide/ester ratio in MROCP synthesized copolymers was obtained. This phenomenon suggested that microwave energy was more efficiently absorbed by caprolactam than CL, thus providing greater reactivity of caprolactam during MROCP. As a result of the higher amide/ester ratio, MROCP produced copolymers exhibited a higher T_g .

Liu⁴⁷ and co-workers reported the microwave-assisted graft ring-opening copolymerization (MGROP) of CL onto chitosan. The MGROP was carried out by a protection-graft-deprotection procedure, with phthaloylchitosan as the precursor, and Sn(Oct)₂ as the catalyst (Scheme 12). After being irradiated at 450 W for 15 min, a high grafting percentage of 232% was achieved. The graft of CL onto chitosan was greatly accelerated and enhanced under microwave irradiation.

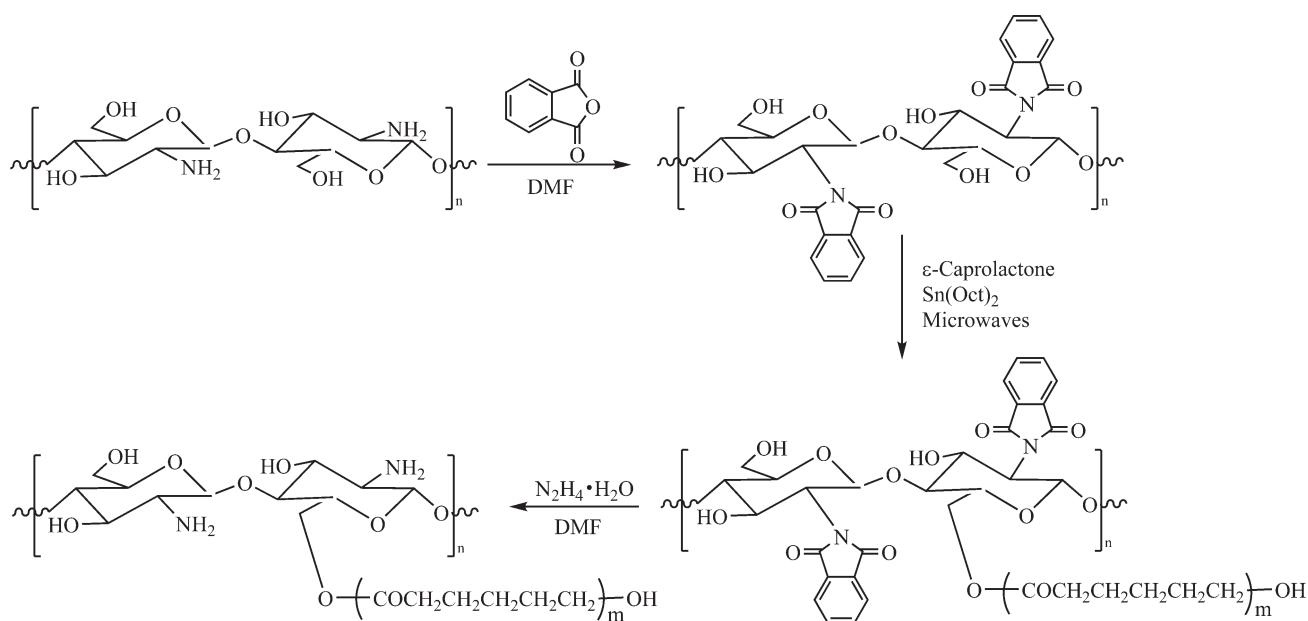
Block copolymers with hydrophilic and hydrophobic segments can aggregate into micelles in an aqueous solution, giving them a wide range of applications in micellar catalysts, drug delivery vehicles and tissue engineering scaffolds. The microwave method also has proved useful for the preparation of amphiphilic ABA triblock copolymers containing PCL and poly(ethylene glycol) (PEG) segments. Poly(ϵ -caprolactone-co-PEG-co- ϵ -caprolactone) (PCL-PEG-PCL) with an M_n over 20 000 g mol⁻¹ was synthesized by PEG initiated MROCP of CL in a domestic microwave oven.⁴⁸ The M_n and composition of the resulting triblock copolymers can be controlled by varying the amount and the length of the PEG segment. Another ABA block copolymer has also been synthesized using either PEG or water-soluble N-terminal functionalized CL as the central hydrophilic portion and peptide sequences of non-polar residues as the flanking hydrophobic segments.⁴⁹

Gong *et al.*⁵⁰ recently reported the microwave-assisted synthesis of triblock copolymers of L-lactide with PEG (PLLA-PEG-PLLA) in a CEM Discover mono-mode microwave oven. Poly(L-lactide)-co-poly(ethylene glycol)-co-poly(L-lactide) triblock copolymer with a M_n of 28 230 g mol⁻¹ and an L-lactide conversion of 92.4% could be synthesized after the L-lactide-PEG2000 reaction mixture was irradiated for 3 min at 100 °C. Compared with the polymerizations conducted under similar conventional conditions, the microwave-assisted synthesis of PLLA-PEG-PLLA triblock copolymers was much faster and resulted in higher MW products.

Table 2 Comparison of microwave energy and thermal energy in copolymerization reactions (160 °C, 0.5 h)^a

Sample	TH-PAE 1%	TH-PAE 2%	TH-PAE 3%	MW-PAE 1%	MW-PAE 2%	MW-PAE 3%
Ester/amide feed ratio	1 : 2	1 : 2	1 : 2	1 : 2	1 : 2	1 : 2
Ester/amide found ratio	1 : 0.61	1 : 1.19	1 : 1.29	1 : 1.08	1 : 1.36	1 : 2.00
Yield (%)	51.2	52.7	57	61.9	70.1	78.2
T_g (meas.)	-25.0	-18.5	-14.5	-14	-7.5	6.0
M_w /g mol ⁻¹	25 400	19 800	17 100	22 000	21 300	16 200
M_w/M_n	1.4	1.5	1.6	2.1	2.0	1.5

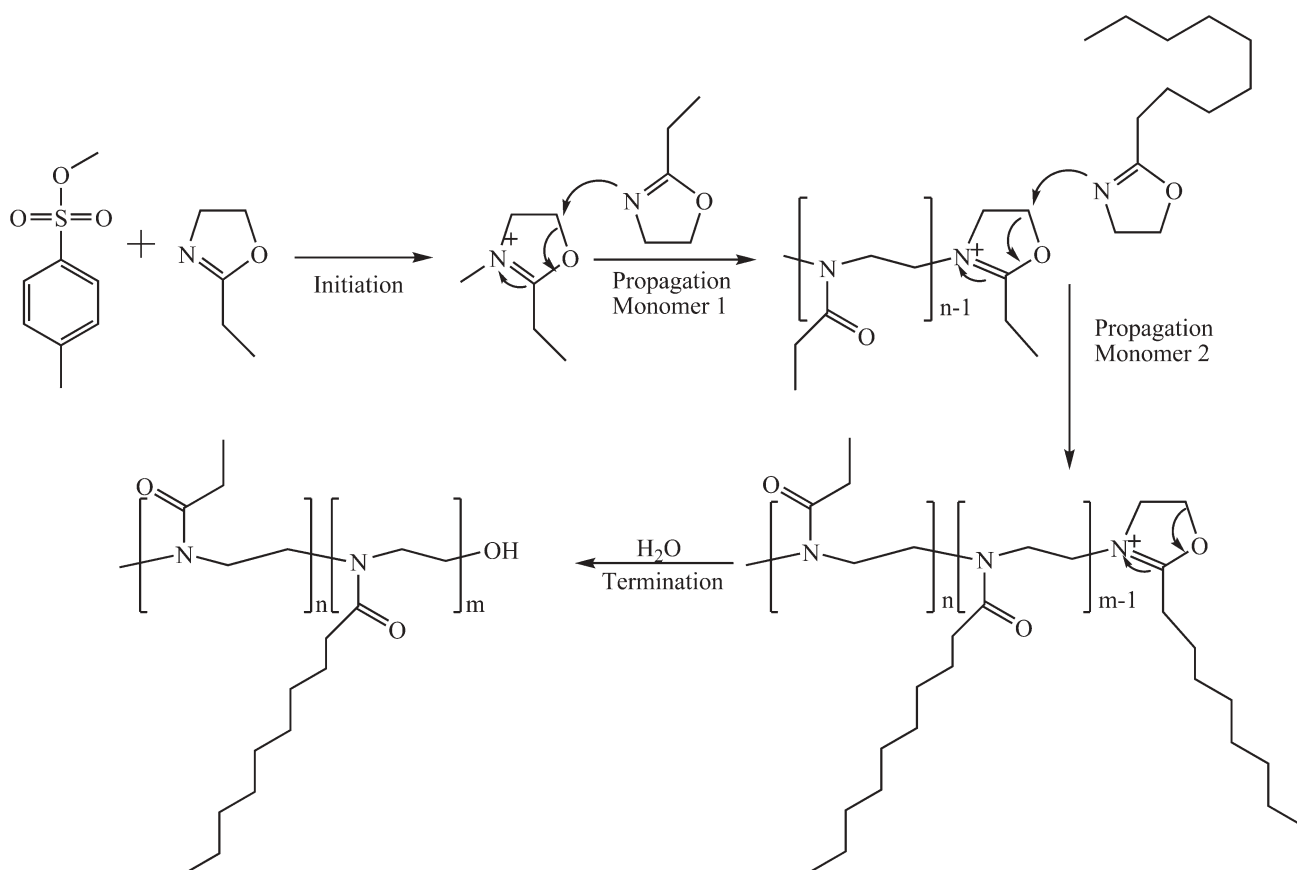
^a PAE-poly(ϵ -caprolactam-co- ϵ -caprolactone); TH-thermal process; MW-microwave process; 1%, 2%, 3%-catalyst level.



Scheme 12 Microwave graft copolymerization of ϵ -caprolactone and chitosan.

3.2.2. Microwave-assisted ring-opening copolymerization of 2-oxazolines. Tunable properties of poly(2-oxazoline) copolymers, which have become the focus of many investigations, can be achieved by selecting an appropriately substituted

monomer. For example, amphiphilic block co-poly(2-oxazoline)s can be obtained by a combination of a hydrophilic block poly(2-ethyl-2-oxazoline) and a hydrophobic block poly(2-nonyl-2-oxazoline). Similar to their LROHP, the living



Scheme 13 Mechanism for the stepwise preparation of the et50-non50 block copolymer from the cationic ring-opening polymerization of 2-ethyl- and 2-nonyl-2-oxazoline, initiated by methyl tosylate.

ring-opening copolymerization (LROCP) of 2-oxazolines also took hours or days to be completed. Schubert *et al.*⁵¹ expanded the LROHP of 2-oxazolines to the LROCP in preparation of block co-poly(2-oxazolines), using four monomers: MeOx, EtOx, NonOx and PhOx (Scheme 13).

This LROCP was initiated by TsOMe and performed in acetonitrile at 140 °C in a single-mode microwave reactor.^{51b} A total number of 100 (50 + 50) monomer units were incorporated into the polymer chains, resulting in a library of four chain-extended homo- and 12 diblock co-poly(2-oxazoline)s with narrow distributions (PDI < 1.30). The polymerization kinetics of LROCP of 2-oxazolines in acetonitrile was investigated under different pressures. In addition, a series of block copolymers was synthesized in an automated parallel synthesis robot by this pressure polymerization method. These studies indicated that the microwave copolymerization of 2-oxazolines was an efficient method for preparing copolymers in batch.

Besides the copolymers containing CL or 2-oxazolines, MROCP of ethylene isophthalate cyclic dimer (EI c-2mer) and bis(2-hydroxyethyl) terephthalate (BHET) in bulk was also reported.⁵² Poly(ethylene terephthalate-co-isophthalate) with $M_w > 20\,000\text{ g mol}^{-1}$ was obtained, and the polymerization mechanisms were investigated by the MALDI-TOF MS. The results showed that the reaction involved three stages. In the first stage, the homopolymerization of BHET proceeded with the copolymerization simultaneously; in the second stage, reactive end-groups of poly(ethylene terephthalate) or BHET attacked the EI c-2mer and gradually produced an EI-terminated copolymer; in the third stage, the propagation reactions composed of three types of elementary reaction routes took place.

In summary, microwave irradiation is a fast and effective method for copolymer synthesis. Compared with the conventional method, the microwave can not only reduce the reaction time, it also can yield copolymers with improved properties.

Concluding remarks of microwave-assisted ring-opening polymerization

During the past decade, significant progress has been made in the field of microwave-assisted polymer synthesis, including step-growth polymerization, free radical polymerization and microwave-assisted ring-opening polymerization. However, there are still many issues that are far from being elucidated, such as the so-called non-thermal effect. Many researchers now believe that there is no general non-thermal effect, and attribute the so-called non-thermal effect to inaccurate temperature measurement.^{1a,53} More studies in this challenging field are required to further understand the mechanism and kinetics of microwave-assisted polymerization.

Despite the conflicts about the non-thermal effects, interest in microwave-assisted polymerization is increasing quickly because of its unique advantage of rate enhancement over the conventional heating method. For the ring-opening polymerization of cyclic monomers under microwave irradiation, the enhancement of reaction rate and product yield, as well as polymer property improvement, have become the most promising features of this technology.

References

- (a) D. Adam, *Nature*, 2003, **421**, 571–572; (b) C. O.Kappe, *Angew. Chem., Int. Ed.*, 2004, **43**, 6250–6284.
- (a) D. Bogdal, P. Penczek, J. Pielichowski and A. Prociak, *Adv. Polym. Sci.*, 2003, **163**, 193–263; (b) F. Wiesbrock, R. Hoogenboom and U. S. Schubert, *Macromol. Rapid Commun.*, 2004, **25**, 1739–1764; (c) L. Zong, S. Zhou, N. Sgriccia, M. C. Hawley and L. C. Kempel, *J. Microwave Power and Electromagnetic Energy*, 2003, **38**, 49–74.
- A. Zoldakova, V. Tomanova, K. Pielichowski, J. Polaczek and J. Pielichowski, *Modern Polymeric Materials for Environmental Applications, 2nd International Seminar*, Krakow, Poland, March 23–25, 2006, 205.
- A. A. Caouthar, A. Loupy, M. Bortolussi, J.-C. Blais, L. Dubreucq and A. Meddour, *J. Polym. Sci., Part A: Polym. Chem.*, 2005, **43**(24), 6480–6491.
- (a) S. Watanabe, K. Hayama and Y. Imai, *Makromol. Chem., Rapid Commun.*, 1993, **14**, 481–184; (b) Y. Imai, *Polym. Prepr. (Am. Chem. Soc., Div. Polym. Chem.)*, 1995, **36**, 735–736; (c) Y. Imai, N. Hisashi, S. Watanabe and K. Masaki, *Polym. J. (Tokyo)*, 1996, **28**, 256–260.
- Y. Xue, W. Dai and J. Lu, *Chem. J. Internet*, 2005, **7**(5), 38, <http://www.chemistrymag.org/cji/2005/075038pe.htm>.
- (a) S. Mallakpour and E. Kowsari, *J. Appl. Polym. Sci.*, 2006, **99**(3), 1038–1044; (b) S. Mallakpour and E. Kowsari, *Polym. Eng. Sci.*, 2006, **46**(4), 558–565; (c) S. Mallakpour and E. Kowsari, *Polym. Adv. Technol.*, 2005, **16**(10), 732–737; (d) S. Mallakpour and E. Kowsari, *Polym. Adv. Technol.*, 2005, **16**(6), 466–472; (e) S. Mallakpour and E. Kowsari, *J. Appl. Polym. Sci.*, 2005, **96**(2), 435–442; (f) S. Mallakpour and E. Kowsari, *Polym. Bull. (Heidelberg, Ger.)*, 2005, **53**(3), 169–180.
- (a) K. Faghihi, *J. Appl. Polym. Sci.*, 2006, **102**(5), 5062–5071; (b) K. Faghihi and K. Zamani, *J. Appl. Polym. Sci.*, 2006, **101**(6), 4263–4269.
- S. Keki, I. Bodnar, J. Borda, G. Deak and M. Zsuga, *Macromol. Rapid Commun.*, 2001, **22**(13), 1063–1065.
- L. Liu, L. Liao, C. Zhang, F. He and R. Zhuo, *Chin. Chem. Lett.*, 2001, **12**(9), 761–762.
- N. Hurduc, D. Abdelyah, J.-M. Buisine and P. Decock, *Eur. Polym. J.*, 1997, **33**, 187–190.
- (a) S. Chatti, M. Bortolussi, A. Loupy, J. C. Blais and D. Bogdal, *Eur. Polym. J.*, 2002, **38**, 1851–1861; (b) S. Chatti, M. Bortolussi, D. Bogdal, J. C. Blais and A. Loupy, *Eur. Polym. J.*, 2006, **42**, 410–424.
- H. Stange, M. Ishaque, N. Niessner, M. Pepers and A. Greiner, *Macromol. Rapid Commun.*, 2006, **27**(2), 156–161.
- (a) E. Bezdushna and H. Ritter, *Macromol. Rapid Commun.*, 2005, **26**(13), 1087–1092; (b) P. Eckstein and H. Ritter, *Des. Monomers Polym.*, 2005, **8**(6), 601–607.
- C. Holtze, M. Antonietti and K. Tauer, *Macromolecules*, 2006, **39**(17), 5720–5728.
- J. Li, X. Zhu, J. Zhu and Z. Cheng, *Radiat. Phys. Chem.*, 2007, **76**(1), 23–26.
- M. Aldana-Garcia, J. Palacios and E. Vivaldo-Lima, *J. Macromol. Sci., Pure Appl. Chem.*, 2005, **A42**(9), 1207–1225.
- (a) W. Xu, N. Zhou, X. Zhu and Z. Cheng, *Huaxue Yanjiu Yu Yingyong*, 2005, **17**(2), 223–225; (b) Z. Cheng, X. Zhu, N. Zhou, J. Zhu and Z. Zhang, *Radiat. Phys. Chem.*, 2005, **72**(6), 695–701.
- R. Hoogenboom, F. Wiesbrock, M. A. M. Leenen, H. Zhang and U. S. Schubert, *Polym. Prepr. (Am. Chem. Soc., Div. Polym. Chem.)*, 2005, **46**(2), 293–294.
- G. Odian, *Principles of Polymerization*, John Wiley & Sons, Inc., 4th edn, 2004, p. 544.
- (a) D. D. Wisnoski, W. H. Leister, K. A. Strauss, Z. Zhao and C. W. Lindsley, *Tetrahedron Lett.*, 2003, **44**(23), 4321–4325; (b) G. Chen, X. Zhu, Z. Cheng, J. Lu and J. Chen, *Polym. Int.*, 2004, **53**(4), 357–363; (c) H. Zhang and U. S. Schubert, *Macromol. Rapid Commun.*, 2004, **25**(13), 1225–1230; (d) W. Xu, X. Zhu, Z. Cheng, G. Chen and J. Lu, *Eur. Polym. J.*, 2003, **39**(7), 1349–1353.
- (a) F. Wiesbrock, R. Hoogenboom, M. A. M. Leenen, M. A. R. Meier and U. S. Schubert, *Macromolecules*, 2005, **38**(12), 5025–5034; (b) R. Hoogenboom, M. W. M. Fijten, H. M. L. Thijs, B. M. Van Lankvelt and U. S. Schubert, *Desgn. Monom. and Polym.*, 2005, **8**(6), 659–671; (c) F. Wiesbrock, R. Hoogenboom, C. H. Abeln and U. S. Schubert, *Macromol. Rapid Commun.*, 2004,

- 25(22), 1895–1899; (d) S. Sinnwell and H. Ritter, *Macromol. Rapid Commun.*, 2005, **26**(3), 160–163; (e) R. Hoogenboom, M. A. M. Leenen, F. Wiesbrock and U. S. Schubert, *Macromol. Rapid Commun.*, 2005, **26**(22), 1773–1778; (f) C. Guerrero-Sanchez, R. Hoogenboom and U. S. Schubert, *Abstr. Pap.*, 231st ACS National Meeting, Atlanta, GA, USA, March 26–30, 2006, IEC-123; (g) C. Guerrero-Sanchez, R. Hoogenboom and U. S. Schubert, *Chem. Commun.*, 2006, **36**, 3797; (h) M. Nuchter, U. Muller, B. Ondruschka, A. Tied and W. Lautenschlager, *Chem. Eng. Technol.*, 2003, **26**, 1207–1216.
- 23 (a) N. Kuhnert, *Angew. Chem., Int. Ed.*, 2002, **41**, 1863–1866; (b) C. R. Strauss, *Angew. Chem., Int. Ed.*, 2002, **41**(19), 3589–3590.
- 24 L. Perreux and A. Loupy, *Tetrahedron*, 2001, **57**, 9199–9223.
- 25 (a) R. Hoogenboom, F. Wiesbrock and U. S. Schubert, *Abstracts of Papers, 230th ACS National Meeting*, Washington, DC, United States, Aug. 28–Sept. 1, 2005, PMSE-516; (b) R. Hoogenboom, F. Wiesbrock and U. S. Schubert, *PMSE Prepr.*, 2005, **93**, 894–895.
- 26 (a) S. Schmatloch, H. Bach, R. A. T. M. van Benthem and U. S. Schubert, *Macromol. Rapid Commun.*, 2004, **25**, 95–107; (b) S. Schmatloch and U. S. Schubert, *Macromol. Rapid Commun.*, 2004, **25**, 69–76; (c) N. Adams and U. S. Schubert, *Macromol. Rapid Commun.*, 2004, **25**, 48–58; (d) M. A. R. Meier, R. Hoogenboom and U. S. Schubert, *Macromol. Rapid Commun.*, 2004, **25**, 21–23; (e) H. Zhang, R. Hoogenboom, M. A. R. Meier and U. S. Schubert, *Meas. Sci. Technol.*, 2005, **16**, 203–211; (f) M. A. R. Meier and U. S. Schubert, *Rev. Sci. Instrum.*, 2005, **76**, 062211; (g) R. Hoogenboom and U. S. Schubert, *Rev. Sci. Instrum.*, 2005, **76**, 062202; (h) R. Hoogenboom, *Expanding the Polymer Science Toolbox: High-throughput Experimentation, Microwave Irradiation and Grid-like Metal Complexes*, Technische Universiteit, Eindhoven, 2005, p. 3.
- 27 R. Hoogenboom, F. Wiesbrock, M. A. M. Leenen, M. A. R. Meier and U. S. Schubert, *J. Comb. Chem.*, 2005, **7**(1), 10–13.
- 28 P. Albert, H. Warth, R. Muehlhaupt and R. Janda, *Macromol. Chem. Phys.*, 1996, **197**(5), 1633–1641.
- 29 (a) X. M. Fang, S. J. Huang and D. A. Scola, *Polym. Mater. Sci. Eng.*, 1998, **79**, 518–519; (b) X. M. Fang, S. J. Huang and D. A. Scola, *Book of Abstracts, 216th ACS National Meeting*, 1998, PMSE-279; (c) X. M. Fang, C. D. Simone, E. Vaccaro, S. J. Huang and D. A. Scola, *J. Polym. Sci., Part A: Polym. Chem.*, 2002, **40**(14), 2264–2275.
- 30 (a) L. Q. Liao, L. J. Liu, C. Zhang, F. He, R. X. Zhuo and K. Wan, *J. Polym. Sci., Part A: Polym. Chem.*, 2002, **40**(11), 1749–1755; (b) L. Q. Liao, L. J. Liu, C. Zhang and R. X. Zhuo, *Polym. Prepr. (Am. Chem. Soc., Div. Polym. Chem.)*, 2003, **44**(1), 864–865; (c) L. Q. Liao, L. J. Liu, C. Zhang and R. X. Zhuo, *Abstr. Pap.*, 225th ACS National Meeting, New Orleans, LA, United States, March 23–27, 2003, POLY-220; (d) L. Q. Liao, L. J. Liu, C. Zhang, F. He and R. X. Zhuo, *J. Appl. Polym. Sci.*, 2003, **90**(10), 2657–2664.
- 31 G. Sivalingam, N. Agarwal and G. Madras, *J. Appl. Polym. Sci.*, 2004, **91**(3), 1450–1456.
- 32 S. Sinnwell, A. M. Schmidt and H. Ritter, *J. Macromol. Sci., Pure and Appl. Chem.*, 2006, **43**(3), 469–476.
- 33 (a) L. J. Liu, C. Zhang, L. Q. Liao, X. L. Wang and R. X. Zhuo, *Chin. Chem. Lett.*, 2001, **12**(8), 663–664; (b) C. Zhang, L. J. Liu and L. Q. Liao, *Macromol. Rapid Commun.*, 2004, **25**(15), 1402–1405.
- 34 K. Zhang, P. Wang, W. K. Li and J. Shu, *Gaofenzi Cailiao Kexue Yu Gongcheng*, 2004, **20**(3), 46–48.
- 35 (a) B. Koroskenyi and S. P. McCarthy, *J. Polym. Environ.*, 2002, **10**(3), 93; (b) S. P. McCarthy and B. Koroskenyi, *PMSE Prepr.*, 2002, **86**, 350–351.
- 36 (a) C. Zhang, *MSc Thesis*, Wuhan University, 2002; (b) C. Zhang, L. Q. Liao and L. J. Liu, 39th IUPAC World Polymer Congress (Macro2002), July 7–12, 2002, Beijing, China, 9e-1P-19, 64; (c) C. Zhang, L. Q. Liao and L. J. Liu, 2003, *National Conference on Polymers (Polymer 2003)*, October 9–14, 2003, Hangzhou, China, E5-6; (d) C. Zhang, *PhD Thesis*, Wuhan University, 2005.
- 37 C. Zhang, L. J. Liu, L. Q. Liao and R. X. Zhuo, *Polym. Prepr. (Am. Chem. Soc., Div. Polym. Chem.)*, 2003, **44**(1), 874–875.
- 38 (a) H. R. Kricheldorf, I. Kreiser-Saunders and D.-O. Damrau, *Macromol. Symp.*, 2000, **159**, 247–258; (b) M. C. Tanzi, P. Verderio, M. G. Lampugnani, M. Resnati, E. Dejana and E. Sturani, *J. Mater. Sci.: Mater. Med.*, 1994, **5**(6–7), 393–396.
- 39 (a) Z. J. Yu, L. J. Liu and R. X. Zhuo, *J. Polym. Sci., Part A: Polym. Chem.*, 2003, **41**(1), 13–21; (b) Z. J. Yu, L. J. Liu, Y. Song and R. X. Zhuo, *Abstr. Pap.*, 225th ACS National Meeting, New Orleans, LA, USA, March 23–27, 2003, POLY-222; (c) Z. J. Yu, L. J. Liu, Y. Song and R. X. Zhuo, *Polym. Prepr. (Am. Chem. Soc., Div. Polym. Chem.)*, 2003, **44**(1), 868–869.
- 40 Z. J. Yu and L. J. Liu, *Eur. Polym. J.*, 2004, **40**(9), 2213–2220.
- 41 (a) Y. Song, L. J. Weng, X. C. Liu and R. X. Zhuo, *J. Biomater. Sci., Polym. Ed.*, 2003, **14**(3), 241–253; (b) Y. Song, L. J. Liu, Z. J. Yu, X. C. Weng and R. X. Zhuo, *Abstr. Pap.*, 225th ACS National Meeting, New Orleans, LA, USA, March 23–27, 2003, POLY-259; (c) Y. Song, L. J. Liu, Z. J. Yu, X. C. Weng and R. X. Zhuo, *Polym. Prepr. (Am. Chem. Soc., Div. Polym. Chem.)*, 2003, **44**(1), 936–937; (d) Y. Song, L. J. Liu and R. X. Zhuo, *Chin. Chem. Lett.*, 2003, **14**(1), 32–34.
- 42 (a) S. Aime, M. Botta, M. Fasano and E. Terreno, *Chem. Soc. Rev.*, 1998, **27**, 19–29; (b) K. H. Thompson and C. Orvig, *Science*, 2003, **300**, 936–939.
- 43 D. Barbier-Baudry, C. H. Brachais, A. Cretu, A. Loupy and D. Stuerge, *Macromol. Rapid Commun.*, 2002, **23**(3), 200–204.
- 44 P. Kerep and H. Ritter, *Macromol. Rapid Commun.*, 2006, **27**, 707–710.
- 45 L. Liao, L. Liu, C. Zhang and S. Gong, *Macromol. Rapid Commun.*, 2006, **27**, 2060.
- 46 X. M. Fang, R. Hutcheon and D. A. Scola, *J. Polym. Sci., Part A: Polym. Chem.*, 2000, **38**(8), 1379–1390.
- 47 L. Liu, Y. Li, Y. Fang and L. X. Chen, *Carbohydr. Polym.*, 2005, **60**(3), 351–356.
- 48 Yu Zhaoju and Liu Lijian, *J. Biomater. Sci., Polym. Ed.*, 2005, **16**(8), 957–971.
- 49 M. B. Anzovino, K. E. Rutledge, M. A. Baron and S. L. Goh, *Abstr. Pap.*, 231st ACS National Meeting, Atlanta, GA, United States, March 26–30, 2006, POLY-202.
- 50 C. Zhang, L. Liao and S. Gong, *Macromol. Rapid Commun.*, DOI: 10.1002/marc.200600709.
- 51 (a) R. Hoogenboom, F. Wiesbrock, M. A. M. Leenen and U. S. Schubert, *PMSE Prepr.*, 2005, **93**, 814–815; (b) F. Wiesbrock, R. Hoogenboom, M. Leenen, S. F. G. M. Van Nispen, M. Van der Loop, C. H. Abeln, A. M. J. Van den Berg and U. S. Schubert, *Macromolecules*, 2005, **38**(19), 7957–7966; (c) R. Hoogenboom, M. W. M. Fijten, R. M. Paulus, H. M. L. Thijs, S. Hoepfener, G. Kickelbick and U. S. Schubert, *Polymer*, 2006, **47**(1), 75–84.
- 52 R. Nagahata, J. Sugiyama, S. Velmathi, Y. Nakao, M. Goto and K. Takeuchi, *Polym. J. (Tokyo)*, 2004, **36**(6), 483–488.
- 53 Committee on microwave processing of materials: an emerging industrial technology, National Materials Advisory Board, *Microwave Processing of Materials*, National Academy Press, Washington D. C., 1994.

A highly advantageous metal-free approach to diaryl disulfides in water†

Mónica Carril, Raul SanMartin,* Esther Domínguez* and Imanol Tellitu

Received 9th October 2006, Accepted 5th January 2007

First published as an Advance Article on the web 11th January 2007

DOI: 10.1039/b614623f

A novel green-chemical protocol for the synthesis of diaryl disulfides, based on a metal-free oxidation of thiol derivatives under mild basic conditions in aqueous media, is presented.

Disulfide bond formation is a relevant transformation in many biological processes, since it is responsible for the construction of the secondary and tertiary structures in proteins. In addition, diaryl disulfide derivatives have often been employed as key intermediates in the synthesis of bio-active molecules due to the reversibility of S–S bond formation, which allows them to participate in different exchange¹ and addition reactions.² Furthermore, this type of linkage is also of high practical value in industry. For instance, polysulfide bonds are present in well-known useful polymers such as rubber, and compounds containing the disulfide moiety have proved suitable for the design of rechargeable lithium batteries.³

The most commonly employed methodology for the synthesis of diaryl disulfides involves oxidation of the corresponding thiols by means of a diverse array of metal-containing oxidants in the presence of a base. Though efficient, these methods generally imply the use of expensive and sometimes harmful metallic reagents (rhodium is often used for this transformation), long reaction times, difficult isolation of the so-obtained disulfides and, in some cases, they involve overoxidation of the final product.⁴

Given their valuable role as versatile building-blocks and their industrial applications, the development of a green-chemical protocol for the synthesis of disulfides is rather desirable. Indeed, nowadays the design of sustainable protocols to feature common but useful transformations with important applications in industry is considered of high practical value. In this context, the use of a benign solvent such as water is of great interest due to its non-toxicity, low cost, safe-handling, non-flammability and easy isolation of final products. Hence we present a metal-free synthesis of diaryl disulfides starting from the corresponding thiol derivative featured in a basic aqueous medium.

First of all, to optimise the process we stirred commercially available thiophenol **1a** in water in the presence of a diverse array of organic and inorganic bases, as shown in Table 1. Interestingly, it was observed that some of the commonly-used water-soluble bases were mostly inadequate, delivering the target compound **2a** in low yield (Table 1, entries 5–7) and that the counteraction of

such bases seemed to have a role. Indeed, the use of Na₂CO₃ provided diphenyl disulfide **2a** in 64% yield (Table 1, entry 6), whereas the result obtained using K₂CO₃ was not even quantified due to the low conversion observed for the starting thiophenol.

Surprisingly, organic insoluble bases such as either TMEDA or DMAP furnished the target compound in good yield (Table 1, entries 1–3). The better results obtained when using TMEDA or DMAP compared to those obtained with water-soluble bases, may suggest that the nature of the base is more determinant than the homogeneity of the system and that the presence of nitrogen atoms in such bases is highly convenient for the success of the target reaction. In this context, the simplest nitrogen-containing base is ammonia, and its use furnished the target compound **2a** in excellent yield, with no variation observed at different temperatures (Table 1, entries 8 and 9). On the contrary, the rest of the tested bases provided the best results at 120 °C, and lower temperatures resulted in much lower conversion of thiophenol **1a**.

In order to determine the scope of the designed protocol, a number of commercially available thiophenol derivatives **1** were reacted under optimised reaction conditions (Table 2).⁵ The methodology proved suitable rendering the corresponding disulfides **2** in good to excellent yields (76–99%), although the conversion for some of the thiol substrates **1** was not complete at room temperature and for those cases the reaction was carried out at 120 °C (Table 2, entries 2–4, 6–9 and 12). In addition, the isolation of the products was remarkably simple. Indeed, the solid products, stable under the reaction conditions and in air, were filtrated directly from the crude mixture and the liquid products were extracted and did not require further purification, eliminating

Table 1 Selected assays for base and temperature screening

$\text{Ph-SH} \xrightarrow{\text{base, H}_2\text{O, T (}^\circ\text{C)}} \text{Ph-S-S-Ph}$				
1a		2a		
Entry	Base ^a	T/°C	t/h	2a (%) ^b
1	TMEDA	120	2	81
2	TMEDA	80	4	72
3	DMAP	120	2	85
4	TEA	120	2	61
5	NaOH	120	8	31
6	Na ₂ CO ₃	120	4	64
7	NaO ^t Bu	120	4	45
8 ^c	NH ₄ OH	120	2	97
9 ^c	NH ₄ OH	Room temp.	2	97
10	—	120	4	— ^d

^a The reactions were performed starting from 0.94 mmol of **1a** and using 1–1.25 equiv. of base. ^b Isolated yields. ^c 0.15 ml of a 32% aqueous solution of NH₃ was used. ^d **2a** was not detected in the reaction mixture.

Kimika Organikoa II Saila, Zientzia eta Teknologia Fakultatea, Euskal Herriko Unibertsitatea, P.O. Box 644, 48080, Bilbao, Spain.
E-mail: raul.sanmartin@ehu.es; Fax: +34 946012748;
Tel: +34 94 946015435

† Electronic supplementary information (ESI) available: Experimental procedures and NMR spectra for new compounds. See DOI: 10.1039/b614623f

Table 2 Synthesis of disulfides **2**

Entry	2 (%) ^a
1	2a (97) ^b
2	2b (85) ^c
3	2c R = OMe (11) ^b
4	2d R = Cl (6) ^b
5	2e R = NO ₂ (86) ^c
6	2f R = Me (8) ^b
7	(46) ^d (95) ^c
8	2g R = OMe (93) ^c
	2h R = Me (99) ^c
9	2i (98) ^c
10	2j (76) ^b
11	2k (83) ^b
12	2l (88) ^f

^a Isolated yield. ^b Room temperature, 2 h. ^c 120 °C, 4 h. ^d 80 °C, 2 h. ^e Room temperature, 4 h. ^f 120 °C, 7 h.

thereby the solvent and silica waste derived from standard chromatographic isolation techniques.⁶

It must be pointed out that the reaction outcome was not affected by the electronic nature of the substituents present in the aryl rings of substrates **1**. Thus, our protocol displayed a high degree of generality delivering in excellent yields disulfides containing both electron-poor (Table 2, entries 4 and 5) and electron-rich aromatic rings (Table 2, entries 2 and 3, 6–10), as well as pyridine derivatives (Table 2, 11–12). Moreover, the presented

methodology was not limited by the steric hindrance derived from the presence of *ortho*-substituents to the thiol functionality in substrate **1** (Table 2, entries 9–10) and proved suitable for the synthesis of disulfides containing a free amine moiety (Table 2, entry 10).

In reference to the mechanism, we propose that the oxygen naturally dissolved in the water used as the solvent to effect the presented transformation is responsible for the oxidation of the thiol derivatives **1**. In order to prove this hypothesis, we carried out two experiments. In the first one, the reaction of thiophenol **1a** in the presence of ammonia was performed under argon and with degassed water. The result for this experiment was the recovery of unreacted starting material without even a trace of target disulfide. In the second one, the same reaction was performed under argon but using water without previous degassing. Conversely, in this case, disulfide **2a** was obtained in 95% yield, suggesting that the oxygen already present in water is sufficient to effect the oxidation without needing an external supply of oxygen. Such oxygen may allow the formation of thiyl radicals, which have been previously proposed as intermediates in the oxidation of thiols, though the pathway of this reaction remains obscure and dependent on the oxidant employed in each case.⁷

To sum up, we have designed a green-chemical protocol for the synthesis of diaryl disulfides in good to excellent yields. The use of simple inexpensive materials, such as thiols, air, ammonia and water, together with mild reaction conditions and the easy isolation of final products by either filtration or extraction from the crude mixtures, render the presented methodology highly practical and appealing for its application in industrial processes. Moreover, this novel methodology avoids the use of toxic metallic salts and employs, instead, a common and readily-available oxidant such as the oxygen already dissolved in water.‡

Acknowledgements

This research was supported by the University of the Basque Country (Project UPV 41.310-13656) and the Spanish Ministry of Education and Science (MEC CTQ2004-03706/BQU). M. C. thanks the Ministry of Education and Science (MEC) for a predoctoral scholarship.

Notes and references

‡ Synthesis of **2a**, typical procedure: A Schlenk flask was charged with thiophenol (0.1 ml, 0.94 mmol), a 32% aqueous solution of NH₃ (0.15 ml) and water (6 ml). The Schlenk was sealed and the mixture was stirred at room temperature for 2 h. The crude mixture was filtered to afford disulfide **2a** (99.7 mg, 97%) as a white solid.

- 1 K. Tanaka and K. Ajiki, *Tetrahedron Lett.*, 2004, **45**, 5677.
- 2 (a) T. Kondo and T.-A. Mitsudo, *Chem. Rev.*, 2000, **100**, 3205; (b) S. Kumar and L. Engman, *J. Org. Chem.*, 2006, **71**, 5400.
- 3 T. Maddanimath, Y. B. Khollam, M. Aslam, I. S. Mulla and K. Vijayamohanam, *J. Power Sources*, 2003, **124**, 133.
- 4 For procedures using iron (III) salts, see: (a) N. Iranpoor and B. Zeynizadeh, *Synthesis*, 1999, 49; Cobalt (II) salts: (b) S. M. S. Chauhan, A. Kumar and K. A. Srinivas, *Chem. Commun.*, 2003, 2348; Chromium salts: (c) S. Patel and B. K. Mishra, *Tetrahedron Lett.*, 2004, **45**, 1371; Rhodium salts: (d) M. Arisawa, C. Sugata and M. Yamaguchi, *Tetrahedron Lett.*, 2005, **46**, 6097. For some protocols using non-metallic reagents, see: (e) M. M. Hashemi, H. Ghafuri and Z. Karimi-Jaberi, *J. Sulfur Chem.*, 2006, **27**, 165; (f) B. Karami, M. Montazerzohori and M. H. Habibi, *Molecules*, 2005, **10**, 1358.

- 5 Although a series of preliminary assays proved unsuccessful, the extension of this methodology to the synthesis of dialkyl disulfides is currently being investigated.
- 6 The major drawback of some of the protocols for the oxidation of thiols reported thus far is the troublesome purification of the obtained disulfides, especially when using metallic or halide reagents. See ref. 4.
- 7 Examples of aerobic oxidations of thiols are scarce in the literature and the reported examples require an external input of oxygen and, in some cases, even the presence of a metallic catalyst. See: (a) M. Kirihara, K. Okubo, T. Uchiyama, Y. Kato, Y. Ochiai, S. Matsushita, A. Hatano and K. Kanamorf, *Chem. Pharm. Bull.*, 2004, **52**, 625; (b) T. J. Wallace, A. Schriesheim and W. Bartok, *J. Org. Chem.*, 1963, **28**, 1311.

		<p>Comments received from just a few of the thousands of satisfied RSC authors and referees who have used ReSource - the online portal helping you through every step of the publication process.</p> <p>authors benefit from a user-friendly electronic submission process, manuscript tracking facilities, online proof collection, free pdf reprints, and can review all aspects of their publishing history</p> <p>referees can download articles, submit reports, monitor the outcome of reviewed manuscripts, and check and update their personal profile</p> <p>NEW!! We have added a number of enhancements to ReSource, to improve your publishing experience even further.</p> <p>New features include:</p> <ul style="list-style-type: none"> ● the facility for authors to save manuscript submissions at key stages in the process (handy for those juggling a hectic research schedule) ● checklists and support notes (with useful hints, tips and reminders) ● and a fresh new look (so that you can more easily see what you have done and need to do next) <p>Go online today and find out more.</p>
	<p>'I wish the others were as easy to use.'</p>	
<p>'ReSource is the best online submission system of any publisher.'</p>		

Registered Charity No. 207890

RSCPublishing

www.rsc.org/resource

Aerobic oxidation of alcohols under visible light irradiation of fluorescent lamp†

Shin-ichi Hirashima and Akichika Itoh*

Received 25th September 2006, Accepted 4th January 2007

First published as an Advance Article on the web 11th January 2007

DOI: 10.1039/b613931k

A catalytic amount of magnesium bromide diethyl etherate enables us to carry out the aerobic photo-oxidation of alcohols under irradiation of VIS from a general-purpose fluorescent lamp. Aliphatic primary alcohols, secondary alcohols and benzyl alcohols generally afforded the carboxylic acids directly in good to high yield. The bromine radical is thought to be generated in situ by continuous aerobic photo-oxidation of the bromo anion from $\text{MgBr}_2 \cdot \text{Et}_2\text{O}$, and to effect this oxidation reaction.

Oxidation is a most important transformation in organic synthesis; however, these reactions essentially involve the use of large quantities of heavy metals and complex organic compounds, which generate large amounts of waste, and are not at all environmentally benign.¹ On the other hand, recently, catalytic oxidation processes with hydrogen peroxide² or molecular oxygen,^{3,4} which generate little waste, have been reported by many researchers. In particular, molecular oxygen has received much attention as an ultimate oxidant, since it is photosynthesized by plants, produces little waste, is inexpensive and of larger atom efficiency than that of other oxidants. With this background in mind, we examined a new oxidation method with the catalysis of a bromo source and molecular oxygen, and, in the course of our study of photo-oxidation, we have found that alcohols were oxidized directly to the corresponding carboxylic acids in the presence of a catalytic amount of lithium bromide,⁵ *N*-bromosuccinimide,⁶ bromine or hydrobromic acid⁷ in oxygen atmosphere under ultraviolet ray (UV) irradiation by a high-pressure mercury lamp.⁸ Although this reaction has the advantages of both inexpensive acquisition of safe reagents and easy work-up, UV, which is irradiated by an expensive high-pressure mercury lamp and has harmful effect on the human body, is needed to proceed. On the other hand, we also found that alcohols were oxidized with a combination of sodium bromide and Amberlyst 15 under solar radiation, which is clean and infinite energy; however, the results are not steady due to the reaction being dependent on the weather. As mentioned above, this reaction becomes safe, economical and steady, and the equipment is more easily installed, if visible light (VIS) from a fluorescent lamp is applicable instead of the high-pressure mercury lamp; however, unfortunately, in our study, only a trace amount of the oxidative product was obtained with the bromo sources mentioned above under irradiation of VIS by a

general-purpose fluorescent lamp. This is the driving force of our continued wide-ranging studies on this oxidation with a new bromo source, which is safe and easily separable from the reaction mixture by extraction, and we have found that magnesium bromide diethyl etherate ($\text{MgBr}_2 \cdot \text{Et}_2\text{O}$) is suitable for this purpose.⁹ The effective use of VIS is a most important research topic at this time of hoped-for development of new energy conversion and energy-using technology, and our new oxidation method is interesting since there have been no reports about application of photo-oxidation with VIS by a general-purpose fluorescent lamp to fine chemistry. We now report our detailed study for visible light oxidation of alcohols with molecular oxygen in the presence of a catalytic amount of $\text{MgBr}_2 \cdot \text{Et}_2\text{O}$.

Table 1 shows the results of our study of reaction conditions for the aerobic oxidation conducted with 1-dodecanol (**1**, 0.3 mmol) as a test substrate in the presence of additives in typical solvents, equipped with an oxygen balloon. Among the solvents examined, only ethyl acetate was found to be effective. Regarding the additives examined, anhydrous calcium bromide (CaBr_2) and $\text{MgBr}_2 \cdot \text{Et}_2\text{O}$ were found to afford similar results; however, we exclusively used $\text{MgBr}_2 \cdot \text{Et}_2\text{O}$ since anhydrous CaBr_2 is more expensive than $\text{MgBr}_2 \cdot \text{Et}_2\text{O}$.

Table 2 shows the results for oxidation of several substrates under the reaction conditions mentioned above. Aliphatic primary alcohols generally afforded the corresponding carboxylic acids in

Table 1 Study of reaction conditions for the photo-oxidation of 1-dodecanol (**1**)^a

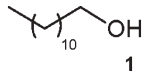
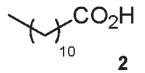
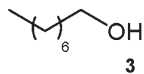
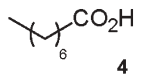
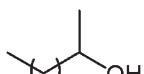
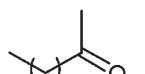
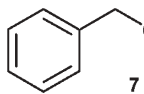
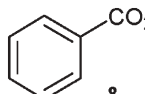
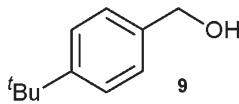
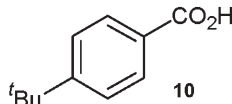
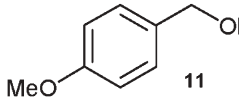
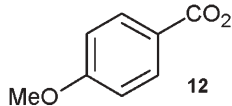
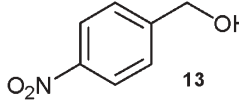
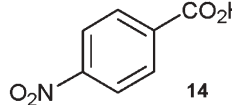
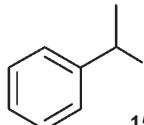
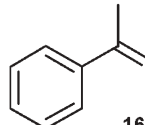
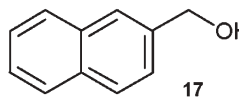
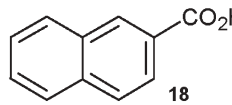
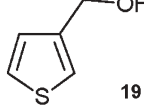
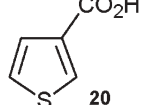
Entry	Additive	Solvent	Yield of 2 (%) ^b
1	$\text{MgBr}_2 \cdot \text{Et}_2\text{O}$	Hexane	trace
2	$\text{MgBr}_2 \cdot \text{Et}_2\text{O}$	Acetone	0
3	$\text{MgBr}_2 \cdot \text{Et}_2\text{O}$	MeCN	0
4	$\text{MgBr}_2 \cdot \text{Et}_2\text{O}$	Et_2O	0
5	$\text{MgBr}_2 \cdot \text{Et}_2\text{O}$	H_2O	0
6	$\text{MgBr}_2 \cdot \text{Et}_2\text{O}$	EtOAc	84
7	CaBr_2	EtOAc	87
8	SrBr_2	EtOAc	49
9	CoBr_2	EtOAc	83
10	NiBr_2	EtOAc	68
11	LaBr_3	EtOAc	77
12	SmBr_3	EtOAc	65

^a A solution of alcohol (0.3 mmol), additive (0.2 equiv.) in dry solvent (5 mL) in a Pyrex tube was irradiated with a fluorescent lamp (22 W × 4) for 10 h. ^b All yields are for pure, isolated products.

Gifu Pharmaceutical University, 5-6-1 Mitahora-higashi, Gifu, 502-8585, Japan. E-mail: itoha@gifu-pu.ac.jp

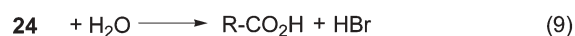
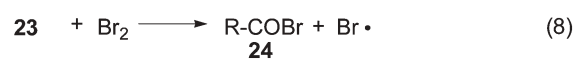
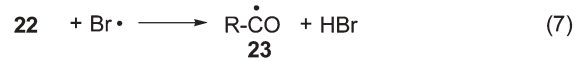
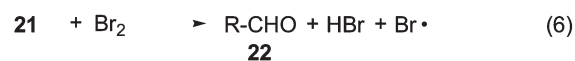
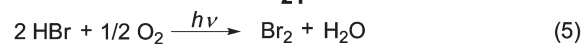
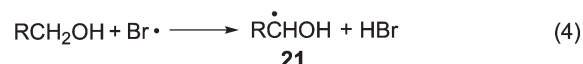
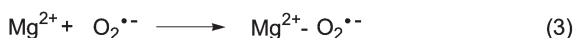
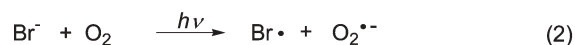
† Electronic supplementary information (ESI) available: Experimental details, results of optimization experiments and spectral distribution of fluorescent lamp used. See DOI: 10.1039/b613931k

Table 2 Aerobic photo-oxidation with fluorescent lamp^a

Entry	Substrate	O ₂ -balloon, fluorescent lamp MgBr ₂ ·Et ₂ O (0.2 equiv.) EtOAc (5 ml), 10 h		Yield (%) ^b
		Substrate (0.3 mmol)	Product	
1			(84)	
2			(64)	
3			(49) ^c	
4			(96)	
5			(89)	
6			(93)	
7			(89)	
8			(60) ^c	
9			(92)	
10			(81)	

^a A typical procedure follows: a solution of alcohol (0.3 mmol), MgBr₂·Et₂O (0.2 equiv.) in dry ethyl acetate (5 mL) in a Pyrex tube was irradiated with fluorescent lamp (22 W × 4) for the indicated time. ^b All yields are for pure, isolated products. ^c The product was to some extent volatile.

good yield; however, secondary alcohols were found to give the corresponding carbonyl compounds in modest yield (entries 1–3). Benzyl alcohols were also found to give the corresponding benzoic acids in high yield (entries 4–9). Furthermore, 3-thiophenemethanol (**19**), which is a heterocyclic substrate, afforded 3-thiophenecarboxylic acid (**20**) in 81% yield (entry 10); however, unfortunately, 3-pyridinemethanol was intact under the conditions.

**Scheme 1** Plausible path of the aerobic photo-oxidation of alcohols.

In order to examine the mechanism of this reaction, at first, 4-*tert*-butylbenzaldehyde, which is presumed to be an intermediate, was subjected to similar aerobic photo-oxidation conditions, and **10** was obtained in 83% yield. Thus, this reaction is thought to proceed through the aldehyde as an intermediate. Also, lowering of the yield (23%) under the condition whereby **1** was reacted under irradiation for 5 h with a fluorescent lamp and then reacted in the dark for 5 h, shows the necessity of continuous irradiation to complete this oxidation, and this reaction does not involve an auto-oxidation path. Also, this reaction includes bromine formation because of the yellow color of the reaction mixture. We present in Scheme 1 what we assume is a plausible path of this oxidation, which is postulated by considering all of the results mentioned above, and the necessity of a catalytic amount of MgBr₂·Et₂O and of molecular oxygen in this reaction. The radical species **21** is thought to be generated by abstraction of a hydrogen radical with a bromine radical, formed by continuous aerobic photo-oxidation of the bromo anion from MgBr₂·Et₂O (equations 1–4). Although the reason for non-requirement of UV is not clear yet, both the low ionic dissociation energy of MgBr₂·Et₂O and the solvation effect of ethyl acetate to the corresponding counter cation by the oxygen atom are thought to be suitable for liberating the “naked” bromo anion. Furthermore, Mg²⁺ is thought to stabilize O₂^{•-}, which is generated by electron transfer from the bromo anion under photo-irradiation, by formation of their 1 : 1 complex (equation 3).¹⁰ Due to all of these reasons, the bromine radical is generated comparatively easily even under irradiation of VIS. Bromine, then, was formed by aerobic photo-oxidation of hydrogen bromide, which is generated in equation 4 (equation 5). Aldehyde **22** was afforded by abstraction of a hydrogen radical with bromine (equation 6), and the regenerated bromine radical abstracted a hydrogen radical from **22** to give radical species **23**, which was transformed to acyl bromide **24** (equations 7 and 8).⁷ The carboxylic acid was formed by reaction with water, generated in equation 5 (equation 9). An equivalent of water, not an excess amount of water, is necessary for this reaction since the yield of **2** decreased a little (72%) when another 1 equiv. of water (to **1**) was added in the reaction mixture

and only a trace amount of **2** was obtained in the presence of an activated molecular sieve 4A as a desiccant.

In conclusion, we have found a useful method for aerobic oxidation of alcohols directly to the corresponding carboxylic acid in the presence of a catalytic amount of $\text{MgBr}_2 \cdot \text{Et}_2\text{O}$ under visible light irradiated from a general-purpose fluorescent lamp. This new form of oxidation reaction is interesting in keeping with the notion of green chemistry due to non-use of heavy metals and halogenated solvents, waste reduction, use of molecular oxygen and safe reagents.

Notes and references

- 1 R. C. Larock, *Comprehensive Organic Transformations: A Guide to Functional Group Preparations*, Wiley-VCH, New York, 1999.
- 2 For recent examples of oxidation of alcohols with hydrogen peroxide, see: R. Noyori, K. Aoki and K. Sato, *Chem. Commun.*, 2003, 1977; Y. Usui, K. Sato and M. Tanaka, *Angew. Chem., Int. Ed.*, 2003, **42**, 5623; Y. Usui and K. Sato, *Green Chem.*, 2003, **5**, 373.
- 3 For recent examples of oxidation of alcohols to the corresponding carboxylic acids with molecular oxygen, see: P. J. Figiel, J. M. Sobczak and J. J. Ziolkowski, *Chem. Commun.*, 2004, 244; K. Ebitani, H.-B. Ji, T. Mizugaki and K. Kaneda, *J. Mol. Catal. A: Chem.*, 2004, **212**, 161; X. Baucherel, L. Gonsalvi, I. W. C. E. Arends, S. Ellwood and R. A. Sheldon, *Adv. Synth. Catal.*, 2004, **346**, 286; Y. Matsumura, Y. Yamamoto, N. Moriyama, S. Furukubo, F. Iwasaki and O. Onomura, *Tetrahedron Lett.*, 2004, **45**, 8221; Y. Uozumi and R. Nakao, *Angew. Chem., Int. Ed.*, 2003, **42**, 194; H. Ji, T. Mizugaki, K. Ebitani and K. Kaneda, *Tetrahedron Lett.*, 2002, **43**, 7179; H.-R. Bjorsvik, L. Liguori and J. A. V. Merinero, *J. Org. Chem.*, 2002, **67**, 7493; S. R. Cicco, M. Latronico, P. Mastrorilli, G. P. Suranna and C. F. Nobile, *J. Mol. Catal. A: Chem.*, 2001, **165**, 135; G. Jenzer, M. S. Schneider, R. Wandeler, T. Mallat and A. Baiker, *J. Catal.*, 2001, **199**, 141; Y. Ishii, S. Sakaguchi and T. Iwahama, *Adv. Synth. Catal.*, 2001, **343**, 393 and references therein.
- 4 For recent examples of oxidation of alcohols to the corresponding aldehydes with molecular oxygen, see: K. Ohkubo, K. Suga and S. Fukuzumi, *Chem. Commun.*, 2006, 2018; B. Guan, D. Xing, G. Cai, X. Wan, N. Yu, Z. Fang, L. Yang and Z. Shi, *J. Am. Chem. Soc.*, 2005, **127**, 18004; R. Mu, Z. Liu, Z. Yang, Z. Liu, L. Wu and Z.-L. Liu, *Adv. Synth. Catal.*, 2005, **347**, 1333; M. J. Schultz, S. S. Hamilton, D. R. Jensen and M. S. Sigman, *J. Org. Chem.*, 2005, **70**, 3343; R. Liu, X. Liang, C. Dong and X. Hu, *J. Am. Chem. Soc.*, 2004, **126**, 4112; K. Mori, T. Hara, T. Mizugaki, K. Ebitani and K. Kaneda, *J. Am. Chem. Soc.*, 2004, **126**, 10657; I. E. Marko, A. Gautier, R. Dumeunier, K. Doda, F. Philippart, S. M. Brown and C. J. Urch, *Angew. Chem., Int. Ed.*, 2004, **43**, 1588; S. S. Stahl, *Angew. Chem., Int. Ed.*, 2004, **43**, 3400 and references cited therein; T. Iwasawa, M. Tokunaga, Y. Obora and Y. Tsuji, *J. Am. Chem. Soc.*, 2004, **126**, 6554; D. R. Jensen, M. J. Schultz, J. A. Mueller and M. S. Sigman, *Angew. Chem., Int. Ed.*, 2003, **42**, 3810.
- 5 A. Itoh, S. Hashimoto and Y. Masaki, *Synlett*, 2005, 2639.
- 6 K. Kuwabara and A. Itoh, *Synthesis*, 2006, 1949.
- 7 S.-I. Hirashima, S. Hashimoto, Y. Masaki and A. Itoh, *Tetrahedron*, 2006, **62**, 7887.
- 8 For oxidation of alcohols to esters in the presence of Br_2 with molecular oxygen, see: F. Minisci, O. Porta, F. Recupero, C. Punta, C. Gambarotti, M. Pierini and L. Galimberti, *Synlett*, 2004, 2203.
- 9 Selective oxidation of *p*-xylene to *p*-tolualdehyde with molecular oxygen was reported: K. Ohkubo, K. Suga, K. Morikawa and S. Fukuzumi, *J. Am. Chem. Soc.*, 2003, **125**, 12850; K. Ohkubo and S. Fukuzumi, *Org. Lett.*, 2000, **2**, 3647.
- 10 S. Fukuzumi and K. Ohkubo, *Chem.-Eur. J.*, 2000, **6**, 4532.

Task-specific ionic liquids as reaction media for the cobalt-catalysed cyclotrimerisation reaction of arylethynes†

Marco Lombardo,^a Filippo Pasi,^a Claudio Trombini,^{*a} Kenneth R. Seddon^{*b} and William R. Pitner^c

Received 10th November 2006, Accepted 8th January 2007

First published as an Advance Article on the web 16th January 2007

DOI: 10.1039/b616427g

The use of nitrile-functionalised ionic liquids as solvents for cobalt-catalysed cyclotrimerisation reactions of monosubstituted aromatic alkynes is reported; the nitrile functionality stabilises the transient cobalt(I) catalytic species and ensures good conversions.

Over the past five years, various types of functionalised ionic liquids (ILs) (often categorised as task-specific ionic liquids¹) have been designed and synthesised for specific purposes such as catalysis,² stereo-controlled synthesis,³ and extractive chemistry.⁴ A common design theme is the incorporation of additional functionality through a side-chain appended to the cation. Ionic liquids have been designed to stabilise catalytic species, a recent example being cations bearing nitrile functional groups **1–4** (Fig. 1), which were used as ligands for palladium in Suzuki and Stille coupling reactions.⁵

In this paper, we describe the use of two nitrile-functionalised cations, 1-(cyanomethyl)-3-methylimidazolium [(mCN)mim]⁺ (**2a**) and (cyanomethyl)ethyltrimethylammonium [(mCN)edma]⁺ (**4**), in combination with the bistriflamide anion ([N(SO₂CF₃)₂]⁻; [NTf₂]⁻), as reaction media for the *in situ* production of cobalt(I) catalysts able to promote the cyclotrimerisation reaction of arylethynes (Scheme 1).

In the last decade, several authors exploited *in situ* generated cobalt(I) species for metal-catalysed [4 + 2 + 2] and [2 + 2 + 2] cycloadditions.^{6–8} The generation of cobalt(I) species involves treatment of a cobalt(II) salt with a variety of reducing agents, *i.e.* zinc metal, Na[BH₄] and Zn[BH₄]₂, ZnEt₂, or AlEt₂Cl. However,

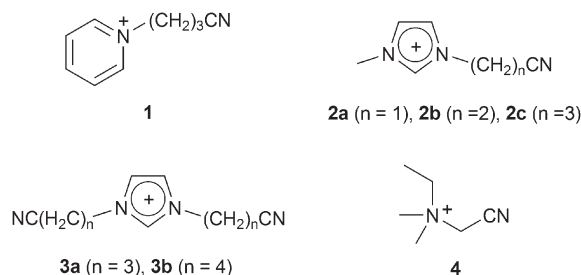


Fig. 1 Nitrile-functionalised cations **1–4**.

^aDipartimento di Chimica "G. Ciamician", University of Bologna, via Selmi 2, Bologna, 40126, Italy. E-mail: claudio.trombini@unibo.it; Fax: +39 051 2099456; Tel: +39 051 2099513

^bThe Quill Centre, The Queen's University of Belfast, Stranmillis Road, Belfast, UK BT9 5AG. E-mail: k.seddon@qub.ac.uk

^cMerck KGaA, S&T Ionic Liquids, Frankfurter Strasse 250, Darmstadt, 64271, Germany. E-mail: william-robert.pitner@merck.de

† Electronic supplementary information (ESI) available: Preparation of ILs **2a** and **4**, detailed experimental procedure and spectroscopic data of cycloadducts. See DOI: 10.1039/b616427g

the presence of both a ligand (*e.g.* a diphosphine, or a diimine) and of a Lewis acid (typically ZnI₂) is necessary for the formation of an effective catalyst. For example, one of the best catalytic systems for the [4 + 2 + 2] cycloaddition of norbornadienes and butadiene was obtained by reacting CoI₂/dppe/Zn⁰/ZnI₂ in a 1 : 1 : 1 : 3 ratio in CH₂Cl₂,⁷ while the reduction of the CoBr₂-glyoxal dicyclohexylimine complex/ZnI₂ system with zinc metal in a 1 : 2 : 2 ratio in anhydrous CH₃CN was developed by Hilt⁸ as one of the most efficient cyclotrimerisation protocols for alkynes.

The attraction of the nitrile-functionalised ionic liquids was the possibility that the cyano group might stabilise the transient cobalt(I) catalytic species, as CH₃CN is known to do.⁹ In particular, this study was centred on the use of [(mCN)mim][NTf₂] and [(mCN)edma][NTf₂] for two reasons: (i) the easy access to structures **2a** and **4** by S_N2-type reactions using the highly reactive 2-chloroethanenitrile, and (ii) the effect of the bistriflamide anion on minimising the ionic liquid solubility both in water and in hexane, a helpful property in terms of workup optimisation.

The catalyst was prepared by reducing a CoBr₂/ZnI₂ (1 : 2) solution in [(mCN)mim][NTf₂] or in [(mCN)edma][NTf₂] with Na[BH₄], ZnEt₂, or with zinc powder.¹⁰ A few representative cyclotrimerisation reactions of arylethynes are collected in Table 1. The best reaction conditions, in terms of yield and regioselectivity (**5** : **6**),¹¹ were those involving the use of Na[BH₄]¹² in [(mCN)mim][NTf₂]. Much less effective than [(mCN)mim][NTf₂] and [(mCN)edma][NTf₂] was [bmim][NTf₂] (run 1), while the beneficial catalyst-stabilisation effect of the nitrile group in [(mCN)mim][NTf₂] was still efficiently exerted in a 2 : 1 mixture (v/v) of [bmim][NTf₂] and [(mCN)mim][NTf₂] (run 4). Just slightly less effective and less regioselective was the use of ZnEt₂, even though the colour change indicated that reduction of the initial cobalt(II) salt was faster than in the case of Na[BH₄]. Reaction temperature (40 °C) and alkyne concentration (1 M) corresponded to the lowest temperature and the highest molarity allowing an efficient stirring, even when product formation thickens the reaction mixture.¹³ 5% of cobalt(II) was chosen in analogy to the reaction reported by Hilt,⁸ the reaction system closest to our protocol. Of course, a consistently higher conversion was achieved using 10% cobalt(II) and a 0.5 M alkyne solution in [(mCN)mim][NTf₂] (*cf.* run 10). The order of addition of reagents was also important. In

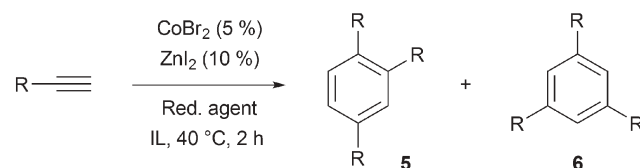


Table 1 Cyclotrimerisation of monosubstituted conjugated alkynes, carried out at 40 °C in 2 cm³ of ionic liquid, using 2 mmol of alkyne^a

Run	Alkyne	Ionic liquid	Reducing agent ^b	5 + 6 Yield (%) ^c	5/6 ^d
1	Phenylethyne	[bmim][NTf ₂]	Na[BH ₄]	35	85 : 15
2	Phenylethyne	[(mCN)mim][NTf ₂]	Na[BH ₄]	95	95 : 5
3	Phenylethyne	[(mCN)edma][NTf ₂]	Na[BH ₄]	85	95 : 5
4	Phenylethyne	[bmim][NTf ₂] + [(mCN)mim][NTf ₂] (1 : 2 v/v)	Na[BH ₄]	78	85 : 15
5	Phenylethyne	[(mCN)mim][NTf ₂]	Zinc powder	60	85 : 15
6	Phenylethyne	[(mCN)mim][NTf ₂]	ZnEt ₂	80	85 : 15
7 ^e	Phenylethyne	[(mCN)mim][NTf ₂]	ZnEt ₂	40	85 : 15
8	Phenylethyne	[(mCN)edma][NTf ₂]	ZnEt ₂	75	85 : 15
9	2-Naphthylethyne	[(mCN)mim][NTf ₂]	ZnEt ₂	72	30 : 70
10 ^f	2-Naphthylethyne	[(mCN)edma][NTf ₂]	Na[BH ₄]	90	30 : 70
11	4-Methoxyphenylethyne	[(mCN)mim][NTf ₂]	Na[BH ₄]	65	83 : 17
12	4-Methylphenylethyne	[(mCN)mim][NTf ₂]	Na[BH ₄]	60	85 : 15
13	4-Fluorophenylethyne	[(mCN)mim][NTf ₂]	Na[BH ₄]	55	70 : 30
14	Propynoic acid, ethyl ester	[(mCN)mim][NTf ₂]	Na[BH ₄]	33	85 : 15
15 ^g	Propynoic acid, ethyl ester	[(mCN)mim][NTf ₂]	Na[BH ₄]	55	82 : 18

^a CoBr₂ and ZnI₂ were used in 5 and 10% molar amounts, respectively, with respect to the starting alkyne. ^b The reducing agent was used in 15% molar amount with respect to the alkyne. ^c Yields refer to the isolated mixture of **5** and **6**, purified by flash-chromatography. ^d Ratio determined by GC or HPLC analysis or by integral ratios in the NMR spectra. ^e Reaction carried out in the absence of ZnI₂. ^f CoBr₂ and ZnI₂ were used in 10 and 20% molar amount, respectively. ^g Reaction carried out at 70 °C.

particular, the reducing agent must be added as the last reactant. An inversion of the order of addition of Na[BH₄] and the alkyne was, indeed, detrimental to the final yield, which rapidly declined as the time elapsed between Na[BH₄] and the alkyne addition increased.¹⁴ We believe that the alkyne contributes to stabilise the catalytically-active cobalt(I) species; the consequence is that as the alkyne concentration decreases, the catalyst concentration drops off, too. Unfortunately, this low catalyst stability makes recyclability impossible. When a reaction analogous to run 2 was worked-up by extraction with hexane, and the ionic liquid phase was charged again with the alkyne, no reaction took place. However, the addition of further Na[BH₄] restarted a catalytic cycle, even though product recovery was only a half of the first cycle. We believe that cobalt(I) is, in part, oxidised by dioxygen to cobalt(II) during work-up, regenerating a cobalt(II) species, which was able to sustain again the cycloaddition reaction.

To compare the performance of Na[BH₄] in ILs and in molecular solvents, run 2 was replicated in THF and CH₃CN. Adducts **5** + **6** were recovered in 25 and 50% yield, respectively, thus suggesting a positive effect of the coulombic environment associated with the IL on the CoBr₂/ZnI₂/Na[BH₄]-catalysed cyclotrimerisation reaction.

In conclusion, a cyclotrimerisation protocol of arylolefines has been developed using task-specific ionic liquids [(mCN)mim][NTf₂] and [(mCN)edma][NTf₂], easily accessible on the 100 g scale. The role of the appended cyano group in stabilising the cobalt(I) catalyst is essential to ensure good results.

Notes and references

- A. E. Visser, R. P. Swatloski, W. M. Reichert, R. Mayton, S. Sheff, A. Wierzbicki, J. H. Davis, Jr. and R. D. Rogers, *Chem. Commun.*, 2001, 135; S.-G. Lee, *Chem. Commun.*, 2006, 1049; Z. Fei, T. J. Geldbach, D. Zhao and P. J. Dyson, *Chem.-Eur. J.*, 2006, **12**, 2122; J. H. Davis, Jr., *Chem. Lett.*, 2004, **33**, 1072.
- H. Xing, T. Wang, Z. Zhou and Y. Dai, *Ind. Eng. Chem. Res.*, 2005, **44**, 4147; X.-E. Wu, L. Ma, M.-X. Ding and L.-X. Gao, *Synlett*, 2005, 607; T. J. Geldbach and P. J. Dyson, *J. Am. Chem. Soc.*, 2004, **126**, 8114; J. C. Xiao, B. Twamly and J. M. Shreeve, *Org. Lett.*, 2004, **6**, 3845; C. Baleizão, B. Gigante, H. Garcia and A. Corma, *Tetrahedron Lett.*, 2003, **44**, 6813; A. C. Cole, J. L. Jensen, I. Ntai, K. L. T. Tran, K. J. Weaver, D. C. Forbes and J. H. Davis, *J. Am. Chem. Soc.*, 2002, **124**, 5962.
- G.-H. Tao, L. He, N. Sun and Y. Kou, *Chem. Commun.*, 2005, 3562; B. Pégot, G. Vo-Thanh, D. Gori and A. Loupy, *Tetrahedron Lett.*, 2004, **45**, 6425; P. Wasserscheid, A. Bösmann and C. Bolm, *Chem. Commun.*, 2002, 200.
- H. Hakkou, J. J. V. Eynde, J. Hamelin and J. P. Bazureau, *Synthesis*, 2004, 1793; A. E. Visser, R. P. Swatloski, W. M. Reichert, R. Mayton, S. Sheff, A. Wierzbicki, J. H. Davis, Jr. and R. D. Rogers, *Environ. Sci. Technol.*, 2002, **36**, 2523; A. E. Visser, R. P. Swatloski, W. M. Reichert, R. Mayton, S. Sheff, A. Wierzbicki, J. H. Davis, Jr. and R. D. Rogers, *Chem. Commun.*, 2001, 135.
- C. Chiappe, D. Pieraccini, D. Zhao, Z. Fei and P. J. Dyson, *Adv. Synth. Catal.*, 2006, **348**, 68; D. Zhao, Z. Fei, T. J. Geldbach, R. Scopelliti and P. J. Dyson, *J. Am. Chem. Soc.*, 2004, **126**, 15876; D. Zhao, Z. Fei, R. Scopelliti and P. J. Dyson, *Inorg. Chem.*, 2004, **43**, 2197.
- M. Lautens, W. Tam, J. C. Lautens, L. G. Edwards, C. M. Crudden and A. C. Smith, *J. Am. Chem. Soc.*, 1995, **117**, 6863.
- B. Ma and J. K. Snyder, *Organometallics*, 2002, **21**, 4688.
- G. Hilt, W. Hess, T. Vogler and C. Hengst, *J. Organomet. Chem.*, 2005, **690**, 5170 and references therein.
- The beneficial role of ethanenitrile in the chemical formation, and in the electrogeneration, of cobalt(I) has been demonstrated in a series of recent papers: I. Kazmierski, C. Gosmini, J.-M. Paris and J. Périchon, *Synlett*, 2006, 881; M. Amatore, C. Gosmini and J. Périchon, *Eur. J. Org. Chem.*, 2005, 989; L. Polleux, E. Labbe, O. Buriez and J. Périchon, *Chem.-Eur. J.*, 2005, **11**, 4678.
- Zinc powder was less effective as a reducing agent (run 5) due to the very slow diffusion of fine metal particles (–100 mesh) into the IL phase, made difficult by the high air-liquid surface tension.
- The generally observed preference for the 1,2,4-adduct **5** (ref. 8) was reversed in the case of 2-naphthylethyne as a likely consequence of steric repulsion between naphthyl groups.
- We did not investigate if Na[BH₄] reacts with **2a** in a way similar to that reported for 1,3-bis(mesityl)imidazolium chloride, forming an imidazol-2-ylidene borane complex. See: T. Ramnial, H. Jong, I. D. McKenzie, M. Jennings and J. A. C. Clyburne, *Chem. Commun.*, 2003, 1722. Several scenarios are however plausible: (i) reduction of cobalt(II) is faster than the formation of an imidazol-2-ylidene borane complex; (ii) an imidazol-2-ylidene is formed which then binds to cobalt acting as a supplementary ligand; (iii) the imidazol-2-ylidene borane complex is formed, acting as the true reducing agent of cobalt(II).
- Viscosity η of **2a** decreases from 455 at 20 °C to 119 mPa s at 40 °C; for **4**, η is 916 at 20 °C and 227 mPa s at 40 °C.
- When phenylethyne was added 15 min after the addition of Na[BH₄] using [(mCN)mim][NTf₂] as solvent, cyclotrimers **5** and **6** were isolated in an overall 38% yield. A similar effect was observed in CH₃CN using both zinc powder and Na[BH₄] as reducing agents, but with less dramatic consequences. When phenylethyne was added 15 min after the reducing agent in CH₃CN at 20 °C, the yield of **5** + **6** were 84 and 35%, using zinc powder and Na[BH₄], respectively. When the reducing agent was added last, as usual, 95 and 50% of cyclotrimers were isolated. In all these experiments the **5** : **6** ratio was 95 : 5.

Electrochemically induced Knoevenagel condensation in solvent- and supporting electrolyte-free conditions

Marta Feroci,*^a Monica Orsini,^a Laura Palombi^b and Achille Inesi*^a

Received 4th October 2006, Accepted 22nd January 2007

First published as an Advance Article on the web 29th January 2007

DOI: 10.1039/b614483g

Solvent- and supporting electrolyte-free electrochemically induced Knoevenagel condensation of malononitrile with aldehydes or ketones, at 40 °C, yields ylidenemalononitriles in high yields.

Introduction

The Knoevenagel condensation is a well known organic reaction leading to the formation of a new C–C bond. It is the base-catalysed reaction between an aldehyde or ketone and an active methylene compound (*e.g.*, malononitrile, nitromethane, *etc.*) with elimination of water.¹ When the active methylene compound used is malononitrile, ylidenemalononitriles are obtained (see scheme in Table 1). These compounds are of growing interest due to their use in the synthesis of fine chemicals, in agriculture, medicine and as precursors of heterocycles with biological activity.^{2,3} As an example, (4-methoxybenzylidene)malononitrile, also known as Tyrphostin 1, is an EGFR (epidermal growth factor receptor) tyrosine kinase inhibitor.⁴

Many efforts have been made to obtain these useful intermediates minimizing the environmental impact, avoiding the use of solvents, catalysts, *etc.* Recently, for the Knoevenagel reaction between aldehydes and malononitrile, water and ionic liquids have been used as solvent at room temperature. The reaction has also been carried out without solvent but at high temperature.⁵ In all cases, the yields in Knoevenagel products were high.

Electrochemistry can be considered a green methodology in organic synthesis, due to its non-polluting reagent, the electron.

The solvent-supporting electrolyte system constitutes the medium in which electrochemical reactions take place. The need for using only solvents with particular characteristics (suitable potential range, high dielectric constant, *etc.*) and the use of large amounts of supporting electrolyte are two important restrictions that, under some circumstances, can render the electrochemical methodology of synthesis not competitive with classical organic synthesis. In this communication, concerning the electrochemically induced Knoevenagel condensation, a considerable effort to minimize these restrictions has been made. In fact, the presence of both solvent and supporting electrolyte has been avoided completely (method A) or, otherwise, a catalytic amount of supporting electrolyte (released from a gel) has been used (method B).

Results and discussion

The cathodic reduction of some organic compounds leads to the formation of intermediates that can behave as bases (electro-generated bases (EGBs)), nucleophiles or both.⁶ It is thus possible, in principle, to perform any reaction that needs a base by generating the base electrochemically. Usually these EGBs are produced by reduction of compounds purposely added to the reaction mixture. In some cases, one of the reagents can behave also as a precursor of the base, but then part of this reagent is lost in the acid–base reaction. If the reaction is base-catalysed, there is little or no loss of reagent.

As the Knoevenagel condensation falls within this kind of reaction, we thought of using malononitrile both as reagent and as probase. We therefore performed the electrolyses at a temperature at which malononitrile is liquid (40 °C) avoiding the use of solvent. Moreover, the supporting electrolyte was eliminated and the electrolyses were performed (method A) simply with a mixture of the two reagents (malononitrile and carbonyl compound, 10 mmol each) by immersing two pieces of platinum and applying a constant current of 5 to 10 mA (galvanostatic conditions), depending on the nature of the carbonyl compound. Only a catalytic amount of electricity was necessary. The electrolyses were stopped after 2 hours. The yields of isolated products and the corresponding Faradays per mol needed are reported in Table 1. The yields of ylidenemalononitriles **3** are very high when starting from aldehydes (except for entry 7), while less brilliant results are obtained with ketones. In fact, along with good yields obtained with cyclohexanones (56–86%), very poor yields are obtained with 2-heptanone (entry 1) and cyclopentanone (entry 5). In order to enhance these yields, we have used an alternative electrochemical method (method B).⁷ In this case, a divided cell was used and a gel containing the supporting electrolyte ensured the electrical connection between anolite and catholite. All the other conditions were the same as method A. Using this methodology, very high yields are obtained, both with aldehydes and with ketones, and surely this electrochemical method can be competitive with the reported chemical reactions (see Table 1, literature data).

It is noteworthy that all these reactions were performed in gram quantities, as one of the difficulties in organic electrochemistry is indeed the scale up. Moreover, using this methodology it was possible to obtain nearly two grams of Tyrphostin 1 (entry 7), a quite expensive biological active compound.

Conclusions

We have developed an environmentally friendly methodology for the synthesis of ylidenemalononitriles, by simply adding two

^aDept. ICMMPM, Univerity "La Sapienza", via Castro Laurenziano, 7, Rome, I-00161, Italy. E-mail: marta.feroci@uniroma1.it;

achille.inesi@uniroma1.it; Fax: 39 06 49766749; Tel: 39 0649766563

^bDept. of Chemistry, University of Salerno, via Salvatore Allende, Baronissi (Salerno), I-84081, Italy

Table 1 Electrochemically induced syntheses of ylidenemalononitrile

Entry	1	Electrochemical method A		Electrochemical method B		Literature data 3 (%) ^c
		F per mol ^a	3 (%) ^b	F per mol ^a	3 (%) ^b	
1		0.007	18	0.030	96	61 ^d
2		0.016	86	0.008	100	82 ^e
3		0.020	56	0.013	98	73 ^e
4		0.007	76	0.004	93	95 ^f
5		0.026	12	0.013	97	91 ^g
6		0.008	93	0.005	98	92 ^h
7		0.040	28	0.010	100	90 ⁱ
8		0.010	90	0.006	99	94 ⁱ
9		0.030	100	0.005	100	93 ⁱ
10		0.030	75	0.003	100	98 ⁱ

^a Faradays per mol of malononitrile supplied to the electrodes. ^b Yields of isolated **3** in the electrochemically induced reactions. ^c Yields of isolated **3** reported in the literature. ^d Ref. 8a (benzene, NH₄OAc, reflux). ^e Ref. 8b (water, β-alanine, reflux). ^f Ref. 8c (toluene, mesoporous material, 50 °C). ^g Ref. 8d (water, Ru catalyst, rt). ^h Ref. 8e (*i*-PrOH, Ti(O-*i*-Pr)₄, 20 °C). ⁱ Ref. 5a (water, 65 °C). ^j Ref. 8f (EtOH, piperidine, reflux).

platinum electrodes to a mixture of malononitrile and an aldehyde or ketone, kept at 40 °C, and applying a constant current in the absence of any solvent or supporting electrolyte, in a undivided or divided cell. The yields are high and the products are obtained in gram quantities.

Experimental

Method A

In a three-neck cell, equipped with a platinum spiral cathode (apparent area 0.8 cm²), a platinum spiral anode (apparent area 0.8 cm²) and a gas inlet–outlet (N₂), kept at 40 °C, malononitrile (10 mmol) and a carbonyl compound (10 mmol) were added. A constant current electrolysis was performed (typical current: 10–5 mA) for 2 hours (the number of F per mol passed through the cell in each experiment is reported in Table 1). The applied potential was switched off and the mixture was kept at 40 °C for 10 h. Usual workup gave the products described in Table 1, whose spectral data were consistent with the reported ones.

Method B

The electrolyses were the same, except for the cell, in this case a divided one with a G3-glass diaphragm filled with an agar gel containing tetraethylammonium hexafluorophosphate was used.⁷ The presence of the diaphragm, while permitting a noticeable increase of the yields (method B vs. method A), does not cause further difficulty in isolation and purification of the products. In fact, after mechanical removal of the anodic compartment and of the solid electrode, the catholite (which remains in the cell) was worked up according to simple and green methodologies: the products were purified by crystallization from EtOH (entry 8) or vacuum distillation (entries 1 and 3–6). Moreover, in four cases (entries 2, 7, 9, 10) method B permits ylidenemalononitriles to be obtained in quantitative yields; consequently, in these cases, any procedure for purification is avoided.

Acknowledgements

This work was supported by research grants from MIUR (Prin 2004) and CNR, Roma, Italy.

Notes and references

- (a) G. Jones, *Org. React.*, 1967, **15**, 204; (b) R. L. Reeves, in *The Chemistry of the Carbonyl Group*, ed. S. Patai, Interscience, New York, 1966, 593.
- F. Freeman, *Chem. Rev.*, 1980, **80**, 329.
- L. F. Tietze, *Chem. Rev.*, 1996, **96**, 115.
- A. Gazit, P. Yaish, C. Gilon and A. Levitzki, *J. Med. Chem.*, 1989, **32**, 2344.
- (a) F. Bigi, M. L. Conforti, R. Maggi, A. Piccinni and G. Sartori, *Green Chem.*, 2000, **2**, 101; (b) R. V. Hangarge, S. A. Sonwane, D. V. Jarikote and M. S. Shingare, *Green Chem.*, 2001, **3**, 310; (c) M. L. Deb and P. J. Bhuyan, *Tetrahedron Lett.*, 2005, **45**, 6453; (d) F. A. Khan, J. Dash, R. Satapathy and S. K. Upadhyay, *Tetrahedron Lett.*, 2004, **45**, 3055; (e) G. Kaupp, M. R. Naimi-Jamal and L. Schmeyers, *Tetrahedron*, 2003, **59**, 3753.
- J. H. P. Utley and M. Folmer Nielsen, in *Organic Electrochemistry*, ed. H. Lund and O. Hammerich, Marcel Dekker, New York, 2001, pp. 1227–1257 and references cited therein.
- L. Palombi, M. Feroci, M. Orsini and A. Inesi, *Chem. Commun.*, 2004, 1846.
- (a) H. Hart and Y. C. Kim, *J. Org. Chem.*, 1966, **31**, 2784; (b) T. Hayamizu, H. Maeda and K. Mizuno, *J. Org. Chem.*, 2004, **69**, 4997; (c) B. M. Choudary, M. Lakshmi Kantam, P. Sreekanth, T. Bandopadhyay, F. Figueras and A. Tuel, *J. Mol. Catal. A: Chem.*, 1999, **142**, 361; (d) K. Mori, T. Hara, T. Mizugaki, K. Ebitani and K. Kaneda, *J. Am. Chem. Soc.*, 2003, **125**, 11460; (e) K. Yamashita, T. Tanaka and M. Hayashi, *Tetrahedron*, 2005, **61**, 7981; (f) L. C. W. Chang, J. K. von Frijtag Drabbe Künzel, T. Mulder-Krieger, R. F. Spanjersberg, S. F. Roerink, G. van der Hout, M. W. Beukers, J. Brussee and A. P. Ijzerman, *J. Med. Chem.*, 2005, **48**, 2045.

Find a SOLUTION

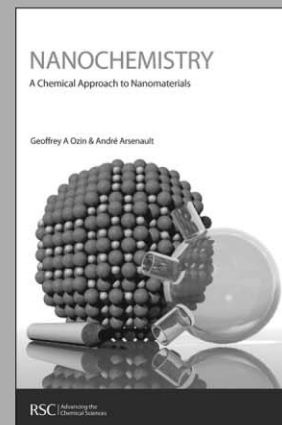
... with books from the RSC

Choose from exciting textbooks, research level books or reference books in a wide range of subject areas, including:

- Biological science
- Food and nutrition
- Materials and nanoscience
- Analytical and environmental sciences
- Organic, inorganic and physical chemistry

Look out for 3 new series coming soon ...

- RSC Nanoscience & Nanotechnology Series
- Issues in Toxicology
- RSC Biomolecular Sciences Series



RSC | Advancing the
Chemical Sciences

www.rsc.org/books

Palladium nanoparticles-catalyzed regio- and chemoselective hydrogenolysis of benzylic epoxides in water

Emilie Thiery, Jean Le Bras* and Jacques Muzart

Received 10th November 2006, Accepted 18th January 2007

First published as an Advance Article on the web 29th January 2007

DOI: 10.1039/b616486b

Hydrogenolysis of various benzylic epoxides was achieved in water to give alcohols in 51–98% yield using recyclable Pd nanoparticles as catalyst.

Hydrogenolysis of epoxides is a useful transformation in organic synthesis.¹ Stoichiometric metal hydrides or dissolving metals are common reagents for this reductive cleavage reaction.² However, heterogeneous catalytic systems have gained interest since they offer several advantages such as easy separation, low waste and low cost. Pd/C is probably the most famous catalyst, but one drawback is the further hydrogenolysis of the resulting C–O bond.³ Efforts were directed toward improving the chemoselectivity and regioselectivity. Sajiki and Hirota have used a carbon-supported Pd–ethylenediamine complex, as a catalyst in alcoholic solvents, for the reductive ring-opening of terminal epoxides into secondary alcohols with high yields and selectivities, although solvolysis of benzylic epoxides was observed.⁴ Hydrogenation with Pd/C/HCO₂H/R₃N exhibited better selectivity than conventional Pd/C/H₂,⁵ but the procedure generates inorganic waste. Nevertheless, palladium nanoparticles encapsulated in polyurea in association with HCO₂H/Et₃N have been recently used as a recyclable catalyst for hydrogenolysis of benzylic epoxides in ethyl acetate.⁶

Increasing environmental awareness and economic reasons has led to consider the use of unusual solvents.⁷ For example, water is an attractive alternative to traditional organic solvents because it is inexpensive, non-flammable, non-toxic and environmentally sustainable. Hydrogenolysis of epoxides with hydrogen in water, would lead to a particularly green process. However, the reductive cleavage of epoxides sensitive to solvolysis, such as benzylic epoxides,⁴ could be problematic.

During the last decade, transition metal nanoparticles have been revealed as efficient catalysts in various media.⁸ Interest in hydrogenations involving metal nanoparticles in aqueous solvents has progressed,⁹ but remains to be developed. Recently we described a mild and selective hydrogenation method of carbon–carbon double bonds using recyclable palladium nanoparticles in an ionic liquid.¹⁰ The particles, namely Pd_{OAc,N}, were easily prepared from a mixture of *n*-Bu₄NBr, *n*-Bu₃N and Pd(OAc)₂. We report here application of Pd_{OAc,N} for the hydrogenolysis of benzylic epoxides.

Hydrogenolysis of styrene oxide was studied in different media, at room temperature under a hydrogen atmosphere and 1% of

Table 1 Hydrogenolysis of styrene oxide in various media^a

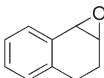
Entry	Solvent	Conversion (%)	Yield (%) ^b
1	MeOH	100	88
2	EtOAc	0	0
3	MeCN	77	34
4	[bmim][PF ₆]	55	16
5	H ₂ O	100	97

^a Styrene oxide (1 mmol), Pd_{OAc,N} (0.01 mmol), solvent (2 mL), H₂ (gas bag), 20 h. ^b Isolated yield

Pd_{OAc,N} (Table 1). In MeOH, the reaction reached completion after 20 h to give the corresponding primary alcohol in 88% isolated yield (Entry 1), illustrating a clear advantage over Pd/C³ and Pd/C(en)⁴ in terms of selectivity. The use of other organic solvents or an ionic liquid was not beneficial to the process (Entries 2–4), and, surprisingly, water was found to be the best medium, providing an excellent yield of the alcohol (Entry 5). It is worth noting that hydrolysis of the epoxide or further hydrogenolysis of the alcoholic C–O bond was not observed under our experimental conditions (Entry 5).

A variety of other benzylic epoxides were then subjected to hydrogenolysis in water at room temperature (Table 2). 2-Methyl-3-phenyloxirane, ethyl 3-phenyloxirane-2-carboxylate

Table 2 Hydrogenolysis of benzylic epoxides in water^a

Entry	Ar	R	Time/h	Yield (%) ^b
1	C ₆ H ₅	CH ₃	20	81
2	C ₆ H ₅	CO ₂ Et	20	80
3			20	74
4 ^c	C ₆ H ₅	C ₆ H ₅	20	92
5 ^d	C ₆ H ₅	C ₆ H ₅	15	98
6	<i>p</i> -ClC ₆ H ₄	H	20	51 ^e
7	<i>m</i> -ClC ₆ H ₄	H	20	82
8 ^d	C ₆ H ₅	CO ₂ CH ₂ C ₆ H ₅	21	84

^a Epoxide (1 mmol), Pd_{OAc,N} (0.01 mmol), water (2 mL), H₂ (gas bag), rt, conversion 100%. ^b Isolated yield. ^c Reaction performed with MeCN (1 mL) as co-solvent. ^d Reaction performed at 80 °C. ^e 1-(4-chlorophenyl)ethane-1,2-diol was also isolated in 25% yield.

Unité Mixte de Recherche "Réactions Sélectives et Applications", Boîte 44, CNRS-Université de Reims Champagne-Ardenne, BP 1039, Reims cedex 2, 51687, France. E-mail: jean.lebras@univ-reims.fr; Fax: +33 3 26 91 31 66

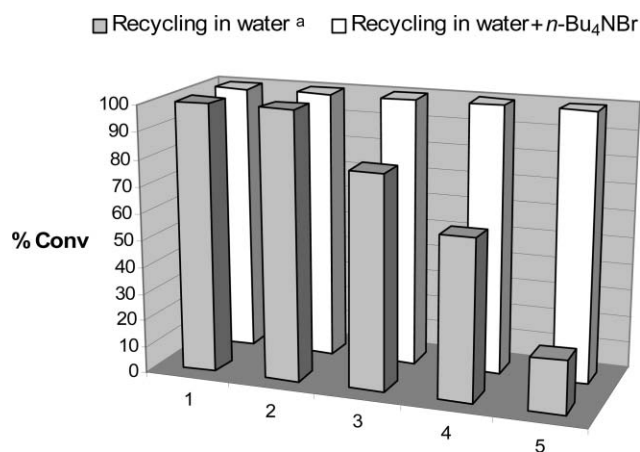


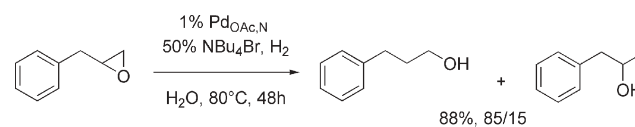
Fig. 1 Recycling experiments. Styrene oxide (1 mmol), *n*-Bu₄NBr (0 or 0.5 mmol), Pd_{OAc}N (0.01 mmol), water (2 mL), H₂ (gas bag). After the first cycle, 2-phenylethanol was extracted with Et₂O (5 × 4 mL) and a new batch of styrene oxide (1 mmol) was added to the aqueous phase. (a) Hydrolysis was observed in cycles n° 3 (18%), 4 (20%) and 5 (11%).

and dihydronaphthalene oxide were hydrogenolyzed efficiently to homobenzyl alcohols (Entries 1–3). Stilbene oxide was reluctant to react, since this compound is a solid and interaction with the catalyst was probably prevented. The use of MeCN as co-solvent at room temperature (Entry 4), or performing the reaction at 80 °C (Entry 5), afforded the corresponding alcohol in high yield. Chemoselective hydrogenolysis between epoxides and a benzylic group or chloro-substituted aryl was then attempted. Fair yield was obtained from 2-(4-chlorophenyl)oxirane (Entry 6), while 2-(3-chlorophenyl)oxirane and benzyl 3-phenyloxirane-2-carboxylate were hydrogenolyzed in good yields (Entries 7–8). These last results are, to the best of our knowledge, unprecedented examples of chemoselective hydrogenolysis of epoxides in water.

We have observed that dispersion of the nanoparticles in a water–oil system led to the formation of “black aqueous droplets” in which palladium is probably adsorbed on the surface. This led us to perform recycling experiments. Styrene oxide was selected as the substrate. The first two cycles showed total conversion and afforded 2-phenylethanol in high yields (97% for each cycle), however, conversion dropped progressively after the 3rd cycle and solvolysis was also observed (Fig. 1). We suspect that *n*-Bu₄NBr could be progressively solubilized in water, damaging the structure of the nanoparticles. Experiments were then performed with *n*-Bu₄NBr as additive (0.5 equiv.). To our delight, under such conditions, no loss of activity was observed over 5 cycles (Fig. 1) and 2-phenylethanol was respectively isolated in 97, 97, 88, 97 and 88% yield.

To further expand the scope of our catalytic system, we turned our attention to epoxyalkanes. The hydrogenolysis of 2-benzyl-oxirane was not efficient in only water, while quantitative conversion was observed at 80 °C in the presence of *n*-Bu₄NBr as additive. In contrast to other palladium catalysts, including nanoparticles,^{4–6} the regioselectivity was in favour of the primary alcohol,¹¹ suggesting that further development of this catalytic system could lead, in connections with constant progress in

epoxidations of terminal olefins,¹² to a new green alternative for the preparation of primary alcohols.



In conclusion, easily obtained recyclable palladium nanoparticles led to regioselective hydrogenolysis of benzylic epoxides in water. Further exploration of this catalytic system will be reported.

Notes and references

- For recent references, see: N. M. Williamson and A. D. Ward, *Tetrahedron*, 2005, **61**, 155–165; R. Löser, M. Chlupacova, A. Marecek, V. Opletalova and M. Gütschow, *Helv. Chim. Acta*, 2004, **87**, 2597–2601; M. Ito, M. Hirakawa, A. Osaku and T. Ikariya, *Organometallics*, 2003, **22**, 4190–4192; T. Hamada and Y. Kobayashi, *Tetrahedron Lett.*, 2003, **44**, 4347–4350; M. R. Paleo, N. Aurrecoechea, K.-Y. Jung and H. Rapoport, *J. Org. Chem.*, 2003, **68**, 130–138.
- R. C. Larock, *Comprehensive Organic Transformations*, VCH, New York, 1989, p. 505.
- For benzylic epoxides, see: S. Mitsui, S. Imaizumi, M. Hisashige and Y. Sugi, *Tetrahedron*, 1973, **29**, 4093–4097. For aliphatic epoxides, see: G. C. Accrombessi, P. Geneste, J.-L. Olivé and A. A. Pavia, *J. Org. Chem.*, 1980, **45**, 4139–4143.
- H. Sajiki, K. Hattori and K. Hirota, *Chem. Commun.*, 1999, 1041–1042.
- P. S. Dragovich, T. J. Prins and R. Zhou, *J. Org. Chem.*, 1995, **60**, 4922–4924; J. P. Verghere, A. Sudalai and S. Iyer, *Synth. Commun.*, 1995, **25**, 2267–2273.
- S. V. Ley, C. Mitchell, D. Pears, C. Ramarao, J.-Q. Yu and W. Zhou, *Org. Lett.*, 2003, **5**, 4665–4668.
- C.-J. Li and L. Chen, *Chem. Soc. Rev.*, 2006, **35**, 68–82; C.-J. Li, *Chem. Rev.*, 2005, **105**, 3095–3165; U. M. Lindström, *Chem. Rev.*, 2002, **102**, 2751–2772.
- Selected reviews: D. Astruc, F. Lu and J. R. Aranzas, *Angew. Chem., Int. Ed.*, 2005, **44**, 7852–7872; M. T. Reetz and J. G. de Vries, *Chem. Commun.*, 2004, 1559–1563; M. Moreno-Mañas and R. Pleixats, *Acc. Chem. Res.*, 2003, **36**, 638–643; M. Králik and A. Biffis, *J. Mol. Catal. A: Chem.*, 2001, **177**, 113–138; R. M. Crooks, M. Zhao, L. Sun, V. Chechik and L. K. Yeung, *Acc. Chem. Res.*, 2001, **34**, 181–190; J. D. Aiken, III and R. G. Finke, *J. Mol. Catal. A: Chem.*, 1999, **145**, 1–44.
- S. C. Mhadgut, K. Palaniappan, M. Thimmaiah, S. A. Hackney, B. Török and J. Liu, *Chem. Commun.*, 2005, 3207–3209; M. Krämer, N. Pérignon, R. Haag, J.-D. Marty, R. Thomann, N. Lauth-de Viguier and C. Mingotaud, *Macromolecules*, 2005, **38**, 8308–8315; R. Nakao, H. Rhee and Y. Uozumi, *Org. Lett.*, 2005, **7**, 163–165; V. Mévellec, A. Roucoux, E. Ramirez, K. Philippot and B. Chaudret, *Adv. Synth. Catal.*, 2004, **346**, 72–76; B. Yoon, H. Kim and C. M. Wai, *Chem. Commun.*, 2003, 1040–1041; J.-L. Pellegatta, C. Blandy, V. Collière, R. Choukroun, B. Chaudret, P. Cheng and K. Philippot, *J. Mol. Catal. A: Chem.*, 2002, **178**, 55–61; A. Borsla, A. M. Wilhelm and H. Delmas, *Catal. Today*, 2001, **66**, 389–395; J. Schulz, A. Roucoux and H. Patin, *Chem.–Eur. J.*, 2000, **6**, 618–624; J. Alvarez, J. Liu, E. Román and A. E. Kaifer, *Chem. Commun.*, 2000, 1151–1152.
- J. Le Bras, D. K. Mukherjee, S. González, M. Tristany, B. Ganchegui, M. Moreno-Mañas, R. Pleixats, F. Héning and J. Muzart, *New J. Chem.*, 2004, **28**, 1550–1553.
- The differences in selectivities observed between our system and the polyurea-microencapsulated Pd(0) nanoparticles,⁶ could be attributed to the nature of the stabilizing agent used in the preparation of the nanoparticles or in the catalytic reaction.
- M. Colladon, A. Scarso, P. Sgarbossa, R. A. Michelin and G. Strukul, *J. Am. Chem. Soc.*, 2006, **128**, 14006–14007; R. Noyori, M. Aoki and K. Sato, *Chem. Commun.*, 2003, 1977–1986; B. S. Lane and K. Burgess, *Chem. Rev.*, 2003, **103**, 2457–2473; G. Dubois, A. Murphy and T. D. P. Stack, *Org. Lett.*, 2003, **5**, 2469–2472; M. C. White, A. G. Doyle and E. N. Jacobsen, *J. Am. Chem. Soc.*, 2001, **123**, 7194–7195.

Rate enhancement of the Morita–Baylis–Hillman reaction through mechanochemistry†

James Mack* and Maxwell Shumba

Received 7th September 2006, Accepted 18th December 2006

First published as an Advance Article on the web 5th January 2007

DOI: 10.1039/b612983h

Through the novel technique of high speed ball milling we were able to generate Baylis–Hillman products in as little as 0.5 hours. This represents one of the fastest methods of Baylis–Hillman reactions under neat conditions. Upon analysis of various catalysts we found 1,4-diazabicyclo[2.2.2]octane to be the catalyst that led to the highest product yields in the shortest reaction time.

Introduction

Chemistry is essential to the continued technological advancement of our society. Due to the global interest in the reduction of chemical waste, various regulations and stipulations have been placed on the chemical industry; specifically in the area of waste minimization. These restrictions have caused scientists to explore more environmentally benign methods to carry out reactions. Environmental concerns about solvent-based chemistry have stimulated a renewed interest in the study of chemical reactions under solvent-free conditions. Although, much of the research conducted in this area has been performed by the use of mortar and pestle,^{1,2} high speed ball milling (HSBM) is an alternative solvent-free method that has started to gain attention. In the HSBM method, a ball bearing is placed inside a vessel that is shaken at high speeds.³ The high speed attained by the ball-bearing has enough force to make an amorphous mixture of the reagents that facilitates chemical reactions. This method has been studied in metal alloying and for the generation of inorganic salts; however, few organic reactions have been studied by this process.⁴ We look to further examine the nuances of this solvent-free technique as it pertains to various organic reactions. The focus of this paper is our results of ball milling on the Baylis–Hillman (BH) reaction, also known as the Morita–Baylis–Hillman reaction.

The BH reaction,⁵ patented in 1972, produces a product that has been a key derivative to various pharmaceutical compounds.⁶ This atom-economical reaction typically uses an electron deficient olefin, a tertiary amine catalyst and an electrophile, usually an aldehyde, to produce a multifunctional product. One of the main drawbacks of this powerful reaction is its slow rate.⁷ The BH reaction has been shown typically to take days to weeks to produce adequate product yields. Various physical, chemical and mechanistic studies^{8,9} have been explored in attempts to increase the rate of this important reaction. We chose to study it under solvent-free HSBM conditions.

University of Cincinnati, Cincinnati, OH, USA.

E-mail: james.mack@uc.edu; Fax: +1 513 9239; Tel: +1 513 9249

† Electronic supplementary information (ESI) available: Spectroscopic data of Baylis–Hillman products, experimental preparation and design of reaction vials. See DOI: 10.1039/b612983h

Results and discussion

Our initial investigations have focused on the use of methyl acrylate and 20% 1,4-diazabicyclo[2.2.2]octane (DABCO) catalyst along with different *p*-substituted aryl aldehydes (Scheme 1). The reactions were conducted in a custom made 0.5 × 2.0 inch screw-capped stainless steel vial and milled with a Spexcertiprep mixer/mill 5000 M for various times with a 0.125 inch stainless steel ball-bearing. At the conclusion of the reaction, standard work-up procedures¹⁰ were followed and products isolated. ¹H NMR, ¹³C NMR, GC-MS were obtained on the products and compared to literature values. The results are summarized in Table 1.

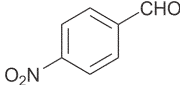
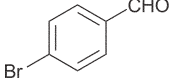
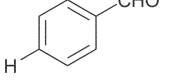
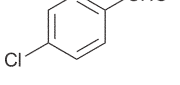
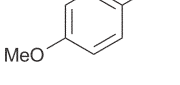
We have found a significant rate enhancement of the BH reaction by ball milling. Previous reports have shown the solvent-less BH reaction of *p*-nitrobenzaldehyde and methyl acrylate with DABCO catalyst can take between 3–4 days and provide yields between 70–87%;¹¹ by HSBM we are able to produce >98% yield in as little as 0.5 hours. This represents one of the fastest rates of this reaction under neat conditions.

Various catalysts have been studied in solution to determine their effect on the rate of the BH reaction; we have likewise examined a range of catalysts to determine which is most effective under HSBM conditions. Using *p*-nitrobenzaldehyde and methyl acrylate along with 20% catalyst over a period of 0.5 hours we analyzed several catalysts. The results are summarized in Table 2. According to our results, DABCO was consistently found to be the catalyst that led to the highest yield in the shortest time. DABCO was also observed to be the best catalyst for all the *p*-substituted aryl aldehydes we tested. We are currently investigating other catalysts reported in the literature for the BH reaction to determine their effect under HSBM conditions.



Scheme 1

Table 1 Reactions of *p*-substituted aryl aldehydes with methyl acrylate using 20% DABCO catalyst by high speed ball milling^a

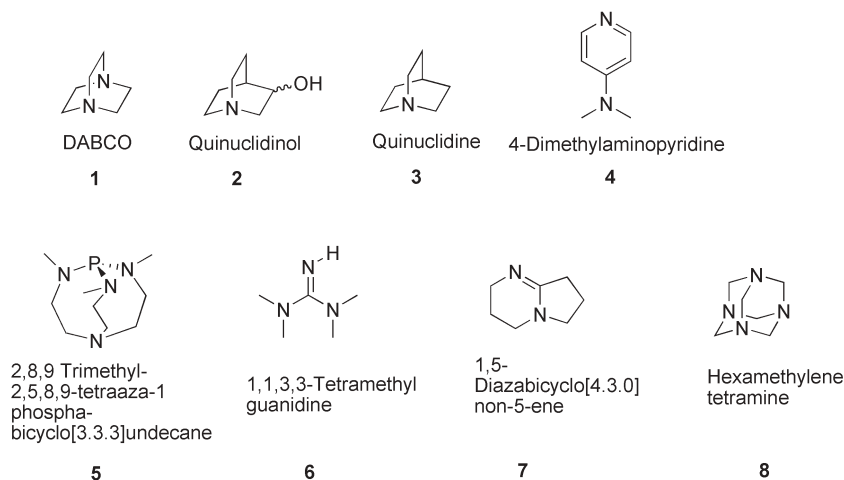
Entry	Aryl aldehyde	Time/h	Yield (%) ^b
1		0.5	>98
2		9	97
3		39	96
4		21	54
5		45	28

^a Typical reaction used 5 mmol of methyl acrylate, 5 mmol of aryl aldehyde and 1 mmol DABCO. ^b All yields reported as isolated yields.

Table 2 Reactions of *p*-nitrobenzaldehyde with methyl acrylate in the presence of various catalysts^a

Entry	Catalyst ^b	Time/h	Yield (%) ^c
1	DABCO	0.5	>98
2	Quinuclidinol	0.5	89
3	Quinuclidine	0.5	86
4	4-Dimethylaminopyridine	0.5	80
5	2,8,9-Trimethyl-2,5,8,9-tetraaza-1-phospha-bicyclo[3.3.3]undecane	0.5	69
6	1,1,3,3-Tetramethylguanidine	0.5	52
7	1,5-Diazabicyclo[4.3.0]non-5-ene	0.5	45
8	Hexamethylenetetramine	0.5	8.2

^a All reactions were run with 5 mmol of methyl acrylate and 5 mmol of *p*-nitrobenzaldehyde along with 1 mmol catalyst. ^b Other catalysts tested were triphenylphosphine, imidazole, and Na₂S, all of which gave less than 5% product over a 0.5 hour period. ^c All yields reported are isolated yields. ^d Structures of catalysts are provided in Chart 1.

**Chart 1**

Conclusions

In conclusion, we report a significant rate enhancement of the BH reaction by ball-milling. Further investigations are on going as to the rate enhancement of the BH reaction with other electrophiles, namely ketones and amides. We are also investigating the ability to incorporate enantioselectivity using this method, a pursuit that has been very challenging in solution. Ball milling is a process that can have a large impact on the field of organic synthesis. We are looking to demonstrate a firm understanding of the guiding principles of HSBM. With a firm understanding we will be able to utilize this process better and adapt it to various other organic reactions creating more general environmentally friendlier reactions.

Experimental

¹H NMR spectra were recorded on a Bruker Avance 400 spectrometer. Deuterated NMR solvents were obtained from Cambridge Isotope Laboratories, Inc., Andover, MA, USA and used without further purification. Methyl acrylate, *p*-nitrobenzaldehyde, *p*-bromobenzaldehyde, *p*-chlorobenzaldehyde, anisaldehyde, benzaldehyde, diazabicyclo[2.2.2]octane, quinuclidine, tetramethylguanidine, quinuclidinol, 4-dimethylaminopyridine, 1,5-diazabicyclo[4.3.0]non-5-ene, hexamethylenetetramine, triphenylphosphine, imidazole and sodium sulfide were purchased from Acros Organics and used without further purification. 2,8,9-Trimethyl-2,5,8,9-tetraaza-1-phospha-bicyclo[3.3.3]undecane was purchased from Aldrich Chemical Company and used without further purification. Ball milling was carried out in an 8000 M SpexCertiprep Mixer/Mill. Separation was done using an Isco Combiflash Companion column system.

Typical procedure

Methyl acrylate (0.43 g, 5 mmol), *p*-nitrobenzaldehyde (0.76 g, 5 mmol) and DABCO (0.11 g, 1 mmol) were added to a custom-made 2.0 inch by 0.5 inch screw capped stainless steel vial, along with a 0.125 inch stainless steel ball bearing. The vial was placed in an 8000 M Spex Certiprep mixer/mill and

the contents were ball milled for 0.5 h. The resulting mixture was dissolved in CH₂Cl₂ (10 mL) and extracted with 10% HCl (3 × 10 mL). The combined organic layers were dried over anhydrous MgSO₄, and the solvent was evaporated under reduced pressure. The resulting yellow mixture was purified by column chromatography over silica gel (1 : 1 CH₂Cl₂–ethyl acetate) to afford 2-Hydroxy-(4-nitro-phenyl)-methyl]-acrylic acid methyl ester in 98% yield.

Acknowledgements

We thank the National Science Foundation (CHE-0548150) and the URC at the University of Cincinnati for financial support of this research.

References

- (a) K. Tanaka, *Solvent-free Organic Synthesis*, Wiley-VCH, Cambridge, 2003.
- (a) K. Tanaka and F. Toda, *Chem. Rev.*, 2000, **100**, 1025–1074; (b) G. Rothenberg, A. P. Downie, C. L. Raston and J. L. Scott, *J. Am. Chem. Soc.*, 2001, **123**, 8701–8708.
- (a) C. Suryanarayana, *Prog. Mater. Sci.*, 2000, **46**, 1–184; (b) L. Takacs, *Prog. Mater. Sci.*, 2002, **47**, 355–414.
- (a) G. Kaupp, *Top. Curr. Chem.*, 2005, **254**, 95–183; (b) V. P. Balema, J. W. Wiench, M. Pruski and V. K. Pecharsky, *Chem. Commun.*, 2002, 724–725; (c) V. P. Balema, J. W. Wiench, M. Pruski and V. K. Pecharsky, *J. Am. Chem. Soc.*, 2002, **124**, 6244–6245; (d) K. Komatsu, G.-W. Wang, Y. Murata, T. Tanaka, K. Fujiwara, K. Yamamoto and M. Saunders, *J. Org. Chem.*, 1998, **63**, 9358–9366; (e) K. Komatsu, K. Fujiwara and Y. Murata, *Chem. Commun.*, 2000, 1583–1584; (f) K. Komatsu, K. Fujiwara, Y. Murata and T. Braun, *J. Chem. Soc., Perkin Trans. I*, 1999, 2963–2966; (g) K. Komatsu, Y. Murata, G.-W. Wang, T. Tanaka, N. Kato and K. Fujiwara, *Fullerene Sci. Technol.*, 1999, **7**, 609–620.
- (a) A. B. Baylis and M. E. D. Hillman, *German Pat.* 2155113, 1972; (b) A. B. Baylis and M. E. D. Hillman, *Chem. Abs.*, 1972, **77**, 34174q; (c) K. Morita, Z. Suzuki and H. Hirose, *Bull. Chem. Soc. Jpn.*, 1968, **41**, 2815.
- (a) S. Zhu, T. H. Hudson, D. E. Kyle and A. J. Lin, *J. Med. Chem.*, 2002, **45**, 3491–3496; (b) M. P. Feltrin and W. P. Almeida, *Synth. Commun.*, 2003, **33**, 1141–1146; (c) P. J. Dunn, M. L. Hughes, P. M. Searle and A. S. Wood, *Org. Process Res. Dev.*, 2003, **7**, 244–253.
- For comprehensive reviews see: (a) D. Basavaiah, A. J. Rao and T. Satyanarayana, *Chem. Rev.*, 2003, **103**, 811–891; (b) D. Basavaiah, P. D. Rao and R. S. Hyma, *Tetrahedron*, 1996, **52**, 8001–8062; (c) E. Ciganek, *Organic Reactions*, ed. L.A. Paquette, Wiley, New York, 1997, vol. 51, p. 201; (d) S. E. Drewes and G. H. P. Roos, *Tetrahedron*, 1988, **44**, 4653–4670.
- (a) K. E. Price, S. J. Broadwater, B. J. Walker and D. T. McQuade, *J. Org. Chem.*, 2005, **70**, 3980–3987; (b) K. E. Price, S. J. Broadwater, H. M. Jung and D. T. McQuade, *Org. Lett.*, 2005, **7**, 147–150; (c) V. K. Aggarwal, S. Y. Fulford and G. C. Lloyd-Jones, *Angew. Chem., Int. Ed.*, 2005, **44**, 1706–1708; (d) M. E. Krafft, T. F. N. Haxell, K. A. Seibert and K. A. Abboud, *J. Am. Chem. Soc.*, 2006, **128**, 4174–4175.
- (a) Y. Fort, M. C. Berthe and P. Caubere, *Tetrahedron*, 1992, **48**, 6371–6384; (b) T. Kataoka, H. Kinoshita, T. Iwama, S. I. Tsujiyama, T. Iwamura, S. I. Watanabe, O. Muraoka and G. Tanabe, *Tetrahedron*, 2000, **56**, 4725–4731; (c) L. S. Santos, C. H. Pavam, W. P. Almeida, F. Coelho and M. N. Eberlin, *Angew. Chem., Int. Ed.*, 2004, **43**, 4330–4333; (d) M. Shi, C.-Q. Li and J.-K. Jiang, *Tetrahedron*, 2003, **59**, 1181–1189.
- At the conclusion of ball milling, the crude product was dissolved in a minimal amount of methylene chloride and subjected to a 10% HCl wash. The organic layer was removed under reduced pressure and prepared for chromatography. Additional details can be obtained in the ESI†.
- (a) R. Galeazzi, G. Martelli, G. Mobbili, M. Orena and S. Rinaldi, *Org. Lett.*, 2004, **6**, 2571–2574; (b) D. Nilov, R. Racker and O. Reiser, *Synthesis*, 2002, 2232–2242.

Green and chemoselective oxidation of sulfides with sodium perborate and sodium percarbonate: nucleophilic and electrophilic character of the oxidation system

M. Victoria Gómez, Rubén Caballero, Ester Vázquez,* Andrés Moreno, Antonio de la Hoz* and Ángel Díaz-Ortiz

Received 12th October 2006, Accepted 19th December 2006

First published as an Advance Article on the web 10th January 2007

DOI: 10.1039/b614847f

An efficient, chemoselective and environmentally friendly procedure for the oxidation of sulfides is described. Reactions are carried out using sodium perborate or sodium percarbonate as the oxidant, solvent-free conditions or water as the reaction medium and microwave irradiation or conventional heating as the energy source. A comparative study concerning the effect of the oxidant and reaction conditions on yield and chemoselectivity (sulfoxide vs. sulfone) has been carried out. In the solid phase, the nature of the solid support or catalyst has a more marked influence than the oxidant on the electrophilic and nucleophilic character of the oxidation.

Introduction

In recent years a great deal of effort has been focused on the field of green chemistry in adopting methods and processes that reduce the use of toxic chemicals, produce smaller amounts of by-products and have lower energy consumption. As part of this “green” concept, toxic and/or flammable organic solvents are replaced by alternative non-toxic and non-flammable media or the reactions are carried out without the use of any solvent, and the classical sources of heating are often replaced by microwave heating.¹ In this context, many efforts have been made to use aqueous media² or a supported reagent in so-called solvent-free conditions.³ Among alternative green solvents, water has been the solvent of choice for a variety of transformations. It is known to be one of the best green solvents and is also a microwave-absorbing medium.

Oxidation processes have received considerable attention, especially in the search for efficient, selective and environmentally friendly oxidants.⁴ Extremely high selectivity can be achieved for some functional group oxidations,⁵ but for most transformations and for large scale applications the ultimate objective of cheap and safe oxidation under catalytic conditions have not been achieved.

Although oxidation reactions under microwave irradiation have been considered to a lesser extent, due to unsafe and uncontrollable experimental conditions, several examples of oxidation processes using reactants absorbed on inorganic supports have recently been published.⁶

Sulfoxides have fascinated organic chemists for a long time owing to the reactivity of this functional group for transformations into a variety of organo sulfur compounds. These transformations are useful for the synthesis of drugs and sulfur-substituted natural products. Despite the myriad of oxidants capable of converting sulfides to the corresponding

sulfoxides, most reagents require careful control of the reaction conditions, including the quantity of oxidants, to minimize the formation of sulfones as side products. Stoichiometric oxidation can be accomplished with reagents like HNO₃, KMnO₄, MnO₂ and *m*-CPBA, but cleaner methods based on catalytically promoted oxidation using aqueous hydrogen peroxide are preferred.

On the other hand, the oxidation of sulfides to sulfones is a well established procedure. The transformation, however, requires either lengthy treatment with oxidants that contain polluting heavy metals, such as KMnO₄ and osmium tetroxide/N-oxides, or the use of various peroxides, including dimethyldioxirane. In addition, the reactions may require many hours and high temperatures.

Hydrogen peroxide is a cheap and environmentally friendly oxidant.⁷ However, it is quite a weak oxidizing agent that often requires specific activation toward the functional group to be transformed⁸ and, in addition, the use, storage and transportation of its concentrated solutions is not desirable for safety reasons. Sodium perborate (SPB) and sodium percarbonate (SPC) represent good alternatives to the use of hydrogen peroxide, and their versatility in functional group oxidations has been highlighted in different reviews.⁹ SPC and SPB represent two of the most powerful, yet underused, oxidants available.

SPB and SPC are solid peroxygen compounds that are cheap, non-toxic, stable and easily handled. They are large-scale industrial chemicals, primarily used in detergents as bleaching and antiseptic agents.¹⁰ SPC and SPB are particularly advantageous owing to their ease of handling and storage. Although SPB and SPC are completely different, they have often been employed for the same purpose and, to the best of our knowledge, a comparative study of the results has not been carried out with both oxidants in a given reaction.

For these reasons, and as a continuation of our studies into environmentally benign chemical processes, we report here the chemoselective oxidation of sulfides to sulfoxides or sulfones

Departamento de Química Orgánica, Facultad de Químicas, Universidad de Castilla-La Mancha, Campus Universitario, Ciudad Real, 13071, Spain. E-mail: Antonio.Hoz@uclm.es



using SPC or SPB in solvent-free conditions (with solid supports) or in aqueous media. Comparison of the two oxidants is made and the role of the different reaction conditions in the selectivity of the oxidation is discussed.

Although the chosen oxidants have similar names, their structures are quite different. SPB is a cyclic disubstituted peroxide while SPC is simply a peroxyhydrate. In water or in solvents with a significant aqueous component, both persalts function mainly as a convenient source of hydrogen peroxide but SPB can be activated towards nucleophilic oxidation through associated species, such as $[B(OH)_3OOH]^-$, while SPC forms the percarbonate species $[HOOC(O)O]^-$, which would be expected to behave as an electrophile (in contrast with SPB). Reactions in non-aqueous media are mostly carried out with carboxylic acids or anhydrides and the formation of the corresponding peracids may be the oxidising species in these kinds of reactions.^{9,11}

With the above considerations in mind, we decided to design an oxidation procedure using water as the solvent. We chose tetrahydrothiophene (**1**) as a sulfide model and the reactions were carried out with both oxidants (SPC and SPB) and under microwave irradiation or conventional heating in order to compare the different permutations of oxidants and heating methodologies (Scheme 1). The results of these experiments are shown in Table 1.

Results and discussion

Reaction conditions were optimized with SPB. The sulfide underwent oxidation to the corresponding sulfone in quantitative yield in 45 min under microwave irradiation (entry 3). Under these conditions the presence of sulfoxide was not observed. All attempts to reduce the reaction time by increasing the irradiation power (entry 2), temperature (entry 5) or by using a phase transfer catalyst (entry 6) were unsuccessful. Oxidation under conventional heating in comparable reaction

conditions (temperature and time) gave a slightly lower yield (entry 4).

A similar set of reactions was performed with SPC. In all cases the yields were lower and, moreover, conventional heating gave a significantly increased yield (entry 7 vs. entry 8). This different behaviour in comparison with SPB can be explained by the differences between the two oxidants in the liberation of H_2O_2 in aqueous solution. The structure of SPC shows that H_2O_2 is rather loosely bound and when liberated it is rather unstable.⁹

Stoichiometric oxidations have been carried out and are described in the literature.^{9,12} However, when the amount of SPB was reduced to 1.5 equivalents, the yield and selectivity were reduced (entry 9). In contrast, an excess of SPC did not improve yields or give better selectivities (entries 10 and 11).

From these results it can be concluded that *SPB favours the nucleophilic oxidation to give mainly the sulfone while SPC leads to the sulfoxide*—even when using a lower stoichiometric amount of SPB than required for the oxidation to the sulfone (entry 9).

The electrophilic behaviour of SPC seems to be less marked and this effect can be explained by the fact that the amount of hydrogen percarbonate (HCO_4^-) in solutions of SPC is lower than the amount of hydrogen perborate ($[B(OH)_3OOH]^-$) in solutions of SPB.^{12,13} As a consequence, in practice the aqueous chemistry of SPC deviates little from that of alkaline H_2O_2 .

We also focused on developing an oxidation procedure in solvent-free conditions: reactions in the absence of solvent were conducted by simply mixing the support, tetrahydrothiophene and the oxidant. The resulting mixtures were heated either conventionally or by microwave irradiation without the addition of any solvent during the reaction. Under these conditions it was possible to avoid the use of carboxylic acids or anhydrides, which are commonly used as solvents in the non-aqueous chemistry of SPB and SPC. These conditions also allowed the use of organic solvents to be reduced as much as possible, thereby extending the environmentally benign characteristics of these reactions. The effect of solid catalysts was also tested in order to improve the nucleophilic and electrophilic character of the oxidising agents.

In an effort to elucidate the role of the solid support we tried the oxidation with SPC using supports with different acidic and basic characteristics (Table 2). Reactions were performed

Table 1 Oxidation of THT **1** in aqueous media

Entry	Oxidant	1 : oxidant molar ratio	Conventional heating	Microwave irradiation	Yield (%)	1a : 1b RSOR : SO ₂ R
1	SPB	1 : 3		90 °C, 30 W, 25 min	88	6 : 94
2	SPB	1 : 3		90 °C, 150 W, 25 min	82	9 : 91
3	SPB	1 : 3		90 °C, 30 W, 45 min	99	0 : 100
4	SPB	1 : 3	90 °C, 45 min		90	0 : 100
5	SPB	1 : 3		130 °C, 15 min ^a	56	9 : 91
6	SPB	1 : 3		170 °C, 5 min ^{a,b}	75 ^c	38 : 62
7	SPC	1 : 1.5		90 °C, 30 W, 45 min	7	78 : 22
8	SPC	1 : 1.5	90 °C, 45 min		24	83 : 17
9	SPB	1 : 1.5		90 °C, 30 W, 45 min	70	22 : 78
10	SPC	1 : 3		90 °C, 30 W, 45 min	21	42 : 58
11	SPC	1 : 3	90 °C, 45 min		20	53 : 47

^a Reaction in a closed vessel with pressure control in a CEM DISCOVER microwave reactor. ^b Polyethylene glycol was used as a phase transfer agent. ^c Impure.

Table 2 Effect of the solid support or catalyst on the oxidation of THT **1** under solvent-free conditions^a

Entry	Support	Yield (%)	1a : 1b RSOR : RSO ₂ R
1	Silica gel	4	94 : 6
2	Montmorillonite KSF	15	68 : 32
3	Basic Alumina	8	27 : 73
4	Dowex	10	82 : 18
5	Amberlyst	5	100 : 0

^a Oxidant: SPC; THT : oxidant molar ratio, 1 : 1; temperature, 20 °C; time, 12 h under conventional heating.

at room temperature as higher temperatures favour the formation of the sulfone.

From the data in Table 2 it can be concluded that basic alumina is the best support for nucleophilic oxidations and the acidic solid Amberlyst is the best catalyst for electrophilic oxidations (entries 3 and 5).

Having identified these supports and catalyst, reactions were extended to include both oxidants (SPB and SPC) and conventional heating and microwave irradiation (Table 3). Conversions at room temperature were very low and so the reactions were performed at 60 °C.

Inspection of Table 3 reveals that the behaviour of both oxidants under these conditions differs from that in aqueous media; the nature of the solid support has a more marked influence than that of the oxidant. Indeed, it is now the acidic or basic character of the solid support or catalyst that plays the most important role in the selectivity of the oxidation. Amberlyst is able to liberate protons and favours electrophilic oxidations, *i.e.*, the formation of sulfoxide, while basic alumina increases the proportion of sulfone formed (entries 1, 2, 5 and 6). These results are in agreement with previous studies on nucleophilic and electrophilic oxidations with H₂O₂ in the presence of an acid or a base.¹⁴

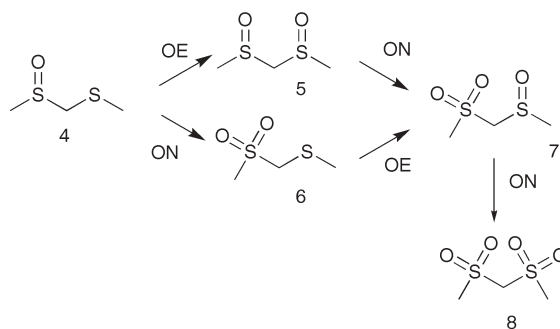
Moreover, *microwave irradiation increases the amount of sulfone*, which is consistent with the fact that the sulfoxide is more polar than the sulfide and, once formed, absorbs microwaves more efficiently and promotes the formation of the sulfone (entry 1 *vs.* 5). This behaviour can also be observed when water is used as the solvent (Table 1, entry 10 *vs.* 11).

SPC is the best oxidant in these solvent-free conditions, giving cleaner reactions and higher yields. Furthermore, when the reaction was performed with a stoichiometric amount of SPC and in the presence of Amberlyst resin, the yield obtained was

Table 3 Oxidation under solvent-free conditions

Entry	Oxidant	Support	1 : oxidant molar ratio	Conventional heating ^a	Microwave irradiation ^{b,c}	Yield (%)	1a : 1b RSOR : RSO ₂ R
1	SPC	Alumina	1 : 1		60 °C, 30 min	29	38 : 62
2	SPC	Amberlyst	1 : 1		60 °C, 30 min	29	91 : 9
3	SPB	Alumina	1 : 1		60 °C, 30 min	2	—
4	SPB	Amberlyst	1 : 1		60 °C, 30 min	30	94 : 6
5	SPC	Alumina	1 : 1	60 °C, 3 h		36	63 : 37
6	SPC	Amberlyst	1 : 1	60 °C, 3 h		47	82 : 18
7	SPB	Alumina	1 : 1	60 °C, 3 h		31	91 : 9
8	SPB	Amberlyst	1 : 1	60 °C, 3 h		50	94 : 6
9	SPC	Amberlyst	1 : 1.5	60 °C, 3 h		99	95 : 5

^a 10 mmol tetrahydrothiophene and 0.5 g support or catalyst. ^b 1 mmol tetrahydrothiophene and 0.05 g support or catalyst. ^c Power controlled by the microwave reactor.

**Scheme 2**

almost quantitative, with the sulfoxide obtained with a very high selectivity (entry 9).

It seems that the method is efficient, clean and safe for the selective oxidation of sulfides to sulfones (using SPB in water) and to sulfoxides (using SPC and acid catalysis, Amberlyst, in solvent-free conditions) when tetrahydrothiophene is used as the starting material. In an effort to obtain more general information about the electrophilic and nucleophilic character of our oxidation system, a more exhaustive study was carried out.

Having studied the useful application of SPB and SPC as oxidants for sulfides, it is important to consider a rational design of the catalyst for oxygen transfer reactions to ascertain whether the oxidant attacks the substrate in an electrophilic or nucleophilic way.¹⁵

This information about the nature of oxidant attack is defined as the electronic character of oxygen-transfer reactions. One of the most valuable probes for the electronic character was introduced by Adam and co-workers.¹⁶ The SSO molecule contains both a sulfide group ("S site") and a sulfoxide group ("SO site", Scheme 2).

Electrophilic oxidants preferentially attack the SSO molecule at the sulfide moiety, yielding dioxides (SOSO), whereas nucleophilic oxidants transform the sulfoxide moiety to the sulfone (SSO₂). Subsequent oxidation of SOSO and SSO₂ gives SOSO₂ in each case.

The reaction of an oxidant with SSO yields a mixture of oxidation products, the relative amounts of which allows the classification of the oxidant on the X_{so} scale:

$$X_{so} = \frac{\text{SOSO oxidation}}{\text{Total oxidation}} = \frac{y(\text{SSO}_2) + y(\text{SOSO}_2)}{y(\text{SOSO}) + y(\text{SSO}_2) + 2y(\text{SOSO}_2)}$$

Table 4 Nucleophilic and electrophilic character of the oxidation system

Entry	Oxidant	Support	4 : oxidant molar ratio	Conventional heating	mmol 4/g catalyst	Yield (%)	X _{so}
1	SPC	Amberlyst	1 : 1.5	60 °C, 3 h	5/0.25	30	0.18
2	SPB	Amberlyst	1 : 1.3	60 °C, 3 h	5/0.25	48	0.1
3	SPC	NaOH	1 : 1	60 °C, 3 h	1/2.5	10	1
4	SPC	—	1 : 1	60 °C, 3 h	1/—	<3	—
5	SPB	Alumina	1 : 1	60 °C, 3 h	1/2.5	37	0.58
6	SPB	Alumina ^a	1 : 1	60 °C, 3 h	1/2.5	52	0.36
7	SPC	Alumina	1 : 1.5	60 °C, 3 h	1/2.5	73	0.73
8	SPC	Alumina	1 : 1	60 °C, 30 min, MW	0.2/0.5	47	0.7
9	SPC	Silica	1 : 1.5	60 °C, 3 h	5/0.25	25	0.47
10	SPC	Silica	1 : 1	60 °C, 3 h	1/2.5	20	0.64
11	SPC	Silica	1 : 1	60 °C, 3 h	5/0.25	40	0.3

^a Inverse order of addition to alumina.

X_{so} = 0.0 represents complete electrophilic and X_{so} = 1.0 complete nucleophilic character for the oxygen-transfer system.

We describe below the oxidation of methyl(methylthio) methylsulfoxide to estimate the nucleophilic *versus* electrophilic nature of oxygen-transfer agents. Taking into account the results obtained in the oxidation of tetrahydrothiophene in the solid phase, it is also important to establish the influence of the catalyst and/or the mineral support in the chemoselectivity. For this reason, the reactions were carried out in the solid phase (solvent-free conditions) using Amberlyst or sodium hydroxide as catalyst and silica or alumina as mineral support.

As shown in Scheme 2 there are a variety of final products depending of the character of the oxidation that has taken place.

To start with, reactions with acidic and basic catalysts, Amberlyst and sodium hydroxide, are reported in Table 4. The X_{so} value again shows that the nature of the solid catalyst has a more marked influence than that of the oxidant (entry 1 *vs.* 2, Table 4). With sodium hydroxide, the X_{so} value is consistent with a nucleophilic oxidation (entry 3, Table 4). SPC and SPB both behave as a medium to transport hydrogen peroxide and require a catalyst for the hydrogen peroxide to be released (entry 4, Table 4). Thus, we can confirm the results obtained with tetrahydrothiophene.

Furthermore, alumina and silica have been used as basic and acidic supports (Table 4). These materials were employed by Kropp *et al.*¹⁷ for the oxidation of sulfide with *tert*-butyl hydroperoxide as the oxidant.

These studies afford insights into the mechanisms of surface-mediated processes. If we consider the mechanism proposed by Kropp *et al.*,¹⁶ oxidation to the sulfone would be expected on using alumina, with the order of addition to alumina being critical in the process. In this sense, on using silica, both types of oxidation would be expected.

The X_{so} values are consistent with a nucleophilic oxidation for both SPC and SPB (entry 5, 7 and 8, Table 4). The nature of the support once again has a more marked influence than that of the oxidants SPB and SPC. Basic alumina increases the proportion of sulfone. Confirmation that the order of addition to alumina is critical can be seen by the lower value of X_{so} when the order is changed (entry 6, Table 4). This is due to association of the oxidant with the Al⁺ sites, which blocks the Al⁺ sites from adsorption by the sulfoxide.

Silica is not a good support to mediate the oxidation of this compound (entries 9, 10 and 11). The use of this support in conjunction with SPB as the oxidant gives yields that are too low. On using SPC, the X_{so} value seems to depend on the amount of silica (entry 10 *vs.* 11). The X_{so} value can support both types of mechanism, as reported by Kropp.¹⁶

Given our knowledge on the nucleophilic and electrophilic character of our oxidation system, a general method for the selective oxidation of sulfides to sulfoxides and sulfones has been established; SPB in water for oxidation to sulfones and SPC/Amberlyst for oxidation to sulfoxides. It is possible to oxidise both aromatic and aliphatic sulfides (Scheme 3) with good yield and chemoselectivity (Table 5).

For aliphatic compounds, such as diethylsulfide, this oxidation system gives quantitative yields in the vast majority of cases with a very high selectivity to the sulfoxide and the sulfone, depending on the reaction conditions (entries 1 and 2, Table 5). SPB/water is the best combination to form the sulfone, while SPC/amberlyst is a very good system for the formation of sulfoxides.

The oxidation of aromatic compounds (entries 5, 6 and 7, Table 5) to give good yields and high selectivities is also possible.

The results obtained with sulfide **10** show that the presence of an additional functional group on the molecule can be tolerated (entry 4, Table 5).

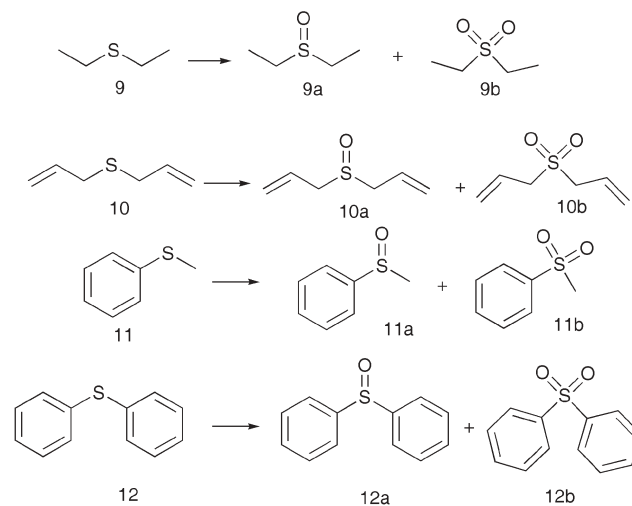
**Scheme 3**

Table 5 Chemoselective oxidation of sulfides 9–12

Entry	Sulfide	Oxidant/support or H ₂ O	mmol sulfide/g support or ml H ₂ O	Sulfide : oxidant molar ratio	Conventional heating	Yield (%)	RSOR : RSO ₂ R
1	9	SPB/H ₂ O	10/10	1 : 3	90 °C, 45 min	81	9 : 91
2	9	SPC/Amberlyst	10/0.5	1 : 1.5	60 °C, 6 h	92	92 : 8
3	10	SPB/H ₂ O	10/10	1 : 3	90 °C, 45 min	39	8 : 92
4	10	SPC/Amberlyst	10/2.5	1 : 1.5	60 °C, 1.5 h	83	100 : 0
5	11	SPB/H ₂ O	10/10	1 : 3	90 °C, 45 min, 30 W ^a	78	4 : 96
6	11	SPC/Amberlyst	5/2.5	1 : 1.5	60 °C, 5 h	96	98 : 2
7	12	SPC/Amberlyst	5/2.5	1 : 1.5	60 °C, 3 h	40	93 : 7

^a The energy source is microwaves, although the use of ultrasound gives a quantitative yield.

Conclusion

In summary, we have developed an efficient, clean and safe method for the selective oxidation of sulfides to sulfones (*using SPB as the oxidant, water as a solvent and heating under microwave irradiation*) or sulfoxides (*using SPC as the oxidant, Amberlyst as a support, solvent free conditions and conventional heating*). A comparative study of SPB and SPC has been performed, and revealed that these oxidants behave differently. SPB is more effective under aqueous conditions and SPC is preferred for solvent-free reactions. Moreover, in general it can be said that SPB can be used for nucleophilic oxidations and SPC for electrophilic ones. When the reaction is carried out in solid phase, the influence of the support or catalyst is more marked than that of the oxidant. Finally, the heating methodology also plays a significant role in the selectivity, with microwave irradiation favouring oxidation to the sulfone and conventional heating to the sulfoxide.

This procedure offers three major advantages: (i) control over the degree of oxidation of products, *i.e.*, the method allows high purity sulfoxides or sulfones to be obtained by varying the conditions; (ii) excellent chemoselectivity of these complexes toward the sulfur group of substituted sulfides and sulfoxides containing other functional groups susceptible to oxidation; (iii) the method conforms to several of the guiding principles of green chemistry proposed by Anastas and Warner.¹⁸ In this sense, this method is efficient for the selective oxidation of both aliphatic and aromatic sulfides.

Experimental

General methods

¹H-NMR spectra were recorded at 499.772 MHz on an Inova-500 spectrometer with tetramethylsilane (TMS) as an internal reference and were run in deuterated chloroform solutions. Microwave irradiations were conducted in a focused microwave reactor: PROLABO MAXIDIGEST MX350, modified with a mechanical stirrer and an infrared pyrometer, with power and temperature controlled by computer using the software MPX-2 from PACAM Electrónica, or a CEM DISCOVER, with infrared pyrometer and pressure control system and stirring and air-cooling option. All solvents and reagents were purchased from commercial sources and used without further purification. The mixtures of oxidation products obtained were clean in all cases, in that they contained the sulfoxide and/or sulfone only. Furthermore, the spectroscopic data are consistent with those found in the literature.¹⁹

Reactions in water

The appropriate sulfide (20 mmol), water (20 ml) and finely ground SPC or SPB were added to a reaction vessel equipped with a reflux condenser. The reaction mixture was heated in an oil bath or irradiated in the Prolabo microwave reactor under the conditions given in Table 1. The mixture was cooled to room temperature and extracted with diethyl ether (3 × 20 ml). The organic solution was dried over magnesium sulfate. The solvent and unreacted reagents were removed *in vacuo* and the residue was weighed and analyzed by ¹H-NMR spectroscopy.

Reactions in solvent-free conditions

The appropriate amounts of sulfide, support or catalyst and oxidant are shown in the corresponding tables.

(a) Conventional heating

To the solid support and the finely ground oxidant (SPC or SPB as appropriate) was added the appropriate sulfide. The mixture was heated in a screw-cap sealed reaction vessel in an aluminum block at the temperature and for the time indicated in the different tables. The reaction mixture was allowed to cool to room temperature. The products were isolated by extraction with methanol (60 ml). Solvent and unreacted reagent were removed *in vacuo* and the residue was weighed and analyzed by ¹H-NMR spectroscopy.

(b) Microwave Irradiation

The solid support and the finely ground oxidant (SPC or SPB as appropriate) were added to a 10 ml vessel. The corresponding sulfide was added and the vessel was closed with a septum and irradiated in a DISCOVER reactor at 60 °C for 30 min. The mixture was allowed to cool to room temperature and CDCl₃ (2 ml) was added. The solid was filtered off and the crude mixture was analyzed by ¹H-NMR spectroscopy.

Synthesis of methyl(methylthio)methylsulfoxide (4)

To Amberlyst (2.5 g) and the finely ground oxidant SPC (15 mmol, 2.35 g) was added bismethylthiomethane (10 mmol, 1.02 ml). The mixture was heated in a screw-cap sealed reaction vessel in an aluminum block at 60 °C for 5 h. The reaction mixture was allowed to cool to room temperature. The products were isolated by extraction with methanol (60 ml). Solvent and unreacted reagents were removed *in vacuo*. The product was purified by column chromatography

using hexane : ethyl acetate (1 : 1). A colourless liquid was obtained in 45% yield.

Acknowledgements

Financial Support from the DGICYT of Spain through project CTQ2004-01177/BQU and from the Consejería de Ciencia y Tecnología JCCM through project PAI-02-019 is gratefully acknowledged. We also thank the Ministerio de Educación y Ciencia for a predoctoral grant for M. Victoria Gómez.

References

- 1 D. Adam, *Nature*, 2003, **421**, 571; C. O. Kappe, *Angew. Chem., Int. Ed.*, 2004, **43**, 6250; A. Díaz-Ortiz, A. de la Hoz and A. Moreno, *Chem. Soc. Rev.*, 2005, **34**, 164; *Microwave-Assisted Organic Synthesis*, ed. P. Lidström and J. P. Tierney, Blackwell Scientific, 2005; C. O. Kappe and A. Stadler, *Microwaves in Organic and Medicinal Chemistry*, in *Methods and Principles in Medicinal Chemistry*, ed. R. Mannhold, H. Kubinyi and G. Folkers, Wiley, Weinheim, 2005, vol. 25; *Microwaves in Organic Synthesis*, ed. A. Loupy, Wiley-VCH, 2nd edn, 2006.
- 2 C.-J. Li, *Chem. Rev.*, 1993, **93**, 2023; C.-J. Li, *Chem. Rev.*, 2005, **105**, 3095.
- 3 P. Laszlo, *Preparative Chemistry using Supported Reagents*, Academic Press, New York, 1987; Y. Izumi, K. Urabe and M. Onaka, *Zeolite, Clay and Heteropolyacids in Organic Chemistry*, Kodansha-VCH, Tokyo-Weinheim, 1992; K. Smith, *Solid Supports and Catalysts in Organic Synthesis*, Ellis Horwood, London, 1992.
- 4 See for example: K. Sato, M. Aoki and R. Noyori, *Science*, 1998, **281**, 1646; K. Sato, M. Aoki, J. Tagaki and R. Noyori, *J. Am. Chem. Soc.*, 1997, **119**, 1886; A. Corma and H. García, *Chem. Rev.*, 2002, **102**, 3837; R. S. Varma, *Tetrahedron*, 2002, **58**, 1235.
- 5 See S. V. Ley, J. Norman, W. P. Griffith and S. P. Mardesden, *Synthesis*, 1994, 639.
- 6 R. S. Varma and R. Dahiya, *Tetrahedron Lett.*, 1997, **38**, 2043; R. S. Varma, R. K. Saini and H. M. Meshram, *Tetrahedron Lett.*, 1997, **38**, 6525; R. S. Varma, R. K. Saini and R. Dahiya, *Tetrahedron Lett.*, 1997, **38**, 7823; R. S. Varma and R. K. Saini, *Tetrahedron Lett.*, 1998, **39**, 1481; R. S. Varma, R. K. Saini and R. Dahiya, *J. Chem. Res.*, 1998, S120; R. S. Varma and R. Dahiya, *Synth. Commun.*, 1998, **28**, 4087; R. S. Varma and K. P. Naicker, *Org. Lett.*, 1999, **1**, 189; D. Bogdal and M. Lukasiewicz, *Synlett*, 2000, 143; A. Sharifi, F. Mohsenzadeh, M. M. Mojtahedi, M. R. Saidi and S. Balalaie, *Synth. Commun.*, 2001, **31**, 431.
- 7 R. A. Sheldon, *Green Chem.*, 2000, **1**, G1; P. T. Anastas, L. B. Bartlett, M. M. Kirchhoff and T. C. Williamson, *Catal. Today*, 2000, **55**, 11.
- 8 See for example: U. R. Pillai, E. Sahle-Demessie and R. S. Varma, *Tetrahedron Lett.*, 2002, **43**, 2909.
- 9 J. Muzart, *Synthesis*, 1995, 1325; A. McKillop and W. R. Sanderson, *Tetrahedron*, 1995, **51**, 6145; A. McKillop and W. R. Sanderson, *J. Chem. Soc., Perkin Trans. 1*, 2000, 471.
- 10 T. K. Das, A. K. Mandavawalla and S. K. Datta, *Colourage*, 1983, **30**, 15; T. K. Das and A. K. Mandavawalla, *Chem. Abs.*, 1984, **101**, 8593v; P. Kuzel, T. Lieser and M. Dankowski, *Chim. Oggi*, 1986, 3(October), 60.
- 11 C. Karunakaran and R. Kamalam, *Eur. J. Org. Chem.*, 2000, 3261.
- 12 A. Sharifi, M. Bolourtchian and F. Mohsenzadeh, *J. Chem. Res.*, 1998, S668; G. Kabalka, P. P. Wadgaonkar and T. M. Shoup, *Organometallics*, 1990, **9**, 1316.
- 13 J. Flanagan, D. P. Jones, W. P. Griffith, A. C. Skapski and A. P. West, *J. Chem. Soc., Chem. Commun.*, 1986, 20.
- 14 A. Waldemar, W. Haas and B. B. Lohray, *J. Am. Chem. Soc.*, 1991, **113**, 6202.
- 15 D. V. Deubel and G. Frenking, *J. Am. Chem. Soc.*, 1999, **121**, 2021; D. V. Deubel, J. Sundermeyer and G. Frenking, *Inorg. Chem.*, 2000, **39**, 2314; D. V. Deubel, J. Sundermeyer and G. Frenking, *Org. Lett.*, 2001, **3**, 329.
- 16 W. Adam, W. Haas and G. Sieker, *J. Am. Chem. Soc.*, 1984, **106**, 5020; W. Adam, W. Haas and B. B. Lohray, *J. Am. Chem. Soc.*, 1991, **113**, 6203.
- 17 P. J. Kropp, G. W. Breton, J. D. Fields, J. C. Tung and B. R. Loomis, *J. Am. Chem. Soc.*, 2000, **122**, 4280.
- 18 P. T. Anastas and J. C. Warner, *Green Chemistry: Theory and Practice*, Oxford University Press, Oxford, 1998; P. T. Anastas and M. M. Kirchhoff, *Acc. Chem. Res.*, 2002, **35**, 686.
- 19 K. Orito, T. Hatakeyama, M. Takeo and H. Sugimoto, *Synthesis*, 1995, 1357; C. J. Pouchert and J. Behnke, *The Aldrich Library of ¹³C and ¹H FT NMR Spectra*, 1st edn, 1993, vol. 1. For oxidation products of ethylsulfide see: R. S. Reddy, J. S. Reddy, R. Kumar and P. Kumar, *J. Chem. Soc., Chem. Commun.*, 1992, 84. For oxidation products of methylphenylsulfide, diphenylsulfide and diallylsulfide see: M. Hirano, S. Yakabe, S. Itoh, J. H. Clark and T. Morimoto, *Synthesis*, 1997, 1161.

Glucose-derived ionic liquids: exploring low-cost sources for novel chiral solvents†

Laura Poletti,^{*a} Cinzia Chiappe,^b Luigi Lay,^a Daniela Pieraccini,^b Laura Polito^a and Giovanni Russo^a

Received 27th October 2006, Accepted 21st December 2006

First published as an Advance Article on the web 16th January 2007

DOI: 10.1039/b615650a

Novel sugar-based ionic liquids were easily synthesized starting from commercially available methyl-D-glucopyranoside, and they were fully characterized in their physico-chemical properties. They represent the first terms of a new class of chiral solvents from low-cost natural sources.

Introduction

The exploration of Chiral Ionic Liquids (CILs) has expanded exponentially over the past five years, and the increasing number of new CILs published so far, displaying either chiral anion or chiral cation, gives good reason for the recent reviews reporting their synthesis and applications.¹ CILs have been designed to act as stereoselective solvents in asymmetric synthesis,² as a chiral phase in gas chromatography,³ as shift reagents and chiral selectors in the determination of enantiomeric composition of pharmaceutical drugs.⁴ The synthesis of many CILs exploits the asymmetry already present in the chiral pool, especially in natural amino acids or α -hydroxy acids. However, although two papers reported the synthesis of ILs starting from fructose⁵ or from non-nutritive sweeteners,⁶ no ILs based on natural carbohydrates have been reported so far.

Carbohydrates are among the most abundant, low-cost natural sources of chiral material. Moreover, their manipulation has widely developed over more than one century, so that the protection and derivatization of natural monosaccharides can be easily performed through largely applied standard reactions.

These considerations prompted us to design the synthesis and characterization of carbohydrate-based ionic liquids as new chiral solvents. Owing to the presence of many hydroxy groups, these CILs are provided of high coordination ability that can be tuned by varying the electronic density of their oxygens through a proper protecting group pattern. Therefore, carbohydrate-based ILs could be used as coordinating solvents in stereoselective and/or metal-catalysed reactions and, in principle, they could be used as shift reagents.

We synthesized compounds 1–3 (Fig. 1) as the first carbohydrate-based ILs, starting from commercially available methyl- α -D-glucopyranoside. As these new CILs were supposed to act as solvents in organic reactions, they had to be stable in common reaction conditions. For this reason, the reactivity of the hydroxy groups was considerably lowered by

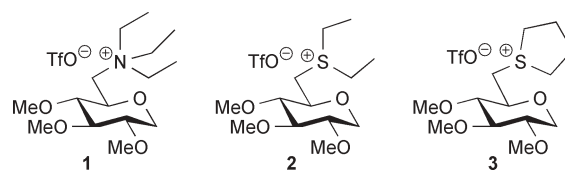


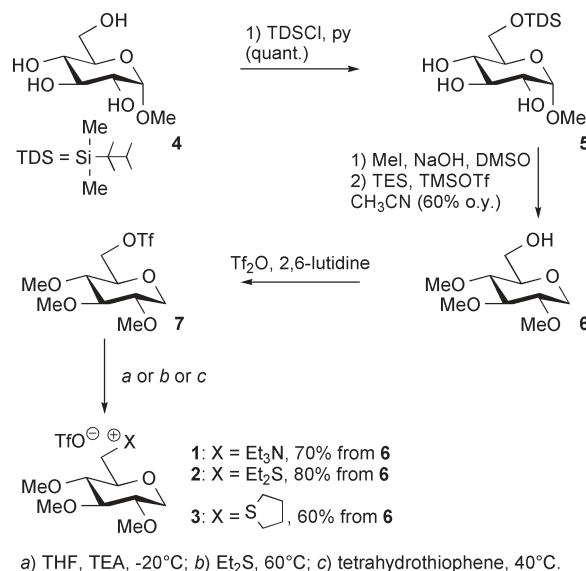
Fig. 1 Glucose-derived ILs.

protection as methyl ethers, and the labile anomeric acetal was reduced to an inert methylene group.

Results and discussion

Synthesis of carbohydrate-based ILs

ILs 1–3 were prepared following a common synthetic approach (Scheme 1). Commercially available methyl-D-glucopyranoside 4 was selectively protected at the primary position as thelyldimethylsilyl (TDS) ether to obtain intermediate 5 in quantitative yield. The secondary hydroxyls were then transformed into methyl ethers by reaction with methyl iodide and sodium hydroxide. The subsequent reduction of the anomeric position with triethyl silane (TES) and trimethylsilyl



a) THF, TEA, -20°C; b) Et₂S, 60°C; c) tetrahydrothiophene, 40°C.

Scheme 1 Synthesis of ILs 1–3.

^aDipartimento di Chimica Organica e Industriale, Via Venezian 21, 20133 Milano, Italy. E-mail: laura.poletti@unimi.it; Fax: +39 02 50314061; Tel: +39 02 50314063/5

^bDipartimento di Chimica Bioorganica e Biofarmacia, via Bonanno 33, 56126 Pisa, Italy. E-mail: cinziac@farm.unipi.it; Fax: +39 050 2219660; Tel: +39 050 2219669

† Electronic supplementary information (ESI) available: NMR spectra and TGA diagrams of compounds 1–3. See DOI: 10.1039/b615650a

trifluoromethanesulfonate (trimethylsilyltriflate, TMSOTf) led to the contemporary removal of the silyl ether at C-6 in 60% overall yield. The primary hydroxyl was then transformed into the corresponding triflate **7** by reaction with triflic anhydride.

Final ILs **1–3** were obtained by reaction of triflate **7** with triethylamine (TEA), diethyl sulfide and tetrahydrothiophene, respectively, in three different reaction conditions. While the reaction with triethylamine was performed at $-20\text{ }^{\circ}\text{C}$ by using THF as the solvent, reactions with diethyl sulfide and tetrahydrothiophene needed higher temperatures and ran smoothly in neat reagents. The new ILs were highly soluble in water and scarcely soluble in diethyl ether and methylene chloride, therefore their purification was achieved by extraction of the impurities with these two organic solvents from the aqueous phase. The obtained ILs were characterized in their physico-chemical properties.

Thermal analysis

The thermal data of ILs **1–3** arising from differential scanning calorimetry traces are summarized in Table 1. Samples **1** and **3** appeared as solids at rt, while compound **2** was a liquid with a viscosity comparable to that of [omim][PF₆]. Consequently, two different sequences were applied according to their physical state, the difference being represented by the starting and end point in each cycle: solid compounds were firstly heated from -50 to $200\text{ }^{\circ}\text{C}$ at a rate of $10\text{ }^{\circ}\text{C min}^{-1}$, quenched, held at $-50\text{ }^{\circ}\text{C}$ before heating again and finally cooled at the same rate. Liquid derivative **2** was heated starting from -150 to $50\text{ }^{\circ}\text{C}$, quenched, held at $50\text{ }^{\circ}\text{C}$ before heating again, and finally cooled to $-150\text{ }^{\circ}\text{C}$. Both compounds **1** and **3** showed sharp melting points, $>100\text{ }^{\circ}\text{C}$, even if a difference of $27.5\text{ }^{\circ}\text{C}$ may be appreciated on passing from the ammonium derivative **1** to the cyclic sulfonium **3**. Moreover, IL **3** displayed an exothermic crystallization at $52.6\text{ }^{\circ}\text{C}$, which could be detected only at the second heating cycle, that is after quenching the sample. No melting point was detected in the case of compound **2**, which is liquid even at a temperature well below rt. This compound tends to form a glass on cooling, at a temperature of $-53\text{ }^{\circ}\text{C}$. Therefore, it seems that low molecular, acyclic dialkyl sulfides are good candidates to obtain liquid solvents, at least for the triflate series, when derivatized with glucose nuclei.

Although differential scanning calorimetry traces of ionic liquids often evidences the presence of multiple phases, arising from rotational motions of one or both of the ionic counterparts, no solid–solid transition was detected in the case of glucose-derived ionic liquids.

Table 1 Physical properties of glucose-derived ionic liquids

Ionic liquid	T_g^a	T_m^b	T_x^c	T_{decomp}^d
1		137.5		300
2	-53			210
3		110	52.6	250

^a Glass transition temperature ($^{\circ}\text{C}$). ^b Melting point ($^{\circ}\text{C}$). ^c Temperature of crystallization ($^{\circ}\text{C}$). ^d Decomposition temperature ($^{\circ}\text{C}$).

Thermogravimetric analysis

The data arising from thermogravimetric analysis of ILs **1–3** are also collected in Table 1 and are expressed as thermal decomposition temperatures. The decomposition temperature, T_{decomp} , represents the temperature at which irreversible mass loss is detected. According to data reported in this study, glucose-derived ionic liquids having triflate as the anion are thermally stable from ambient temperature to at least $200\text{ }^{\circ}\text{C}$. An appreciable difference in thermal stability may be envisaged according to the structure of the cationic counterpart. Indeed, ammonium salts are, among those investigated, the most stable, with a decomposition temperature of $300\text{ }^{\circ}\text{C}$, followed by the tetrahydrothiophene derivative ($250\text{ }^{\circ}\text{C}$). Therefore, while diethyl sulfide ensures low melting salts, its nucleus displays a rather low thermal stability; on the other hand, the ammonium salt **1** is characterized by a good thermal stability but it is solid at temperatures well above $100\text{ }^{\circ}\text{C}$. Further investigations will be performed in order to assess the effect of the anionic counterpart on the thermal behaviour of glucose-derived ionic liquids.

ESI-MS analysis and ion-pairing

Electrospray ionization (ESI-MS)⁷ was applied to assess the intrinsic solvent-free strength of the ion-pairing in glucose-derived ionic liquids with respect to a classical imidazolium derivative shearing the same anion, [bmim][OTf]. A water–methanol mixture was used to dissolve the samples and two different temperatures were applied to the capillary. The extremely high difference in the mass of the investigated cations hampered the possibility of isolating the heterogeneous cluster [C₁][OTf][bmim] (where C₁ is a glucose-derived cation), thus preventing a direct evaluation of the anion–cation interaction by fragmentation of the latter, as reported for other imidazolium derivatives.⁸ However, it has recently been shown that an estimation of the ion-pairing strength might be obtained by a careful analysis of the shape of the full mass spectrum of the pure ionic liquids.⁹ Fig. 2 reports the relative abundance of the peaks observed when operating in positive

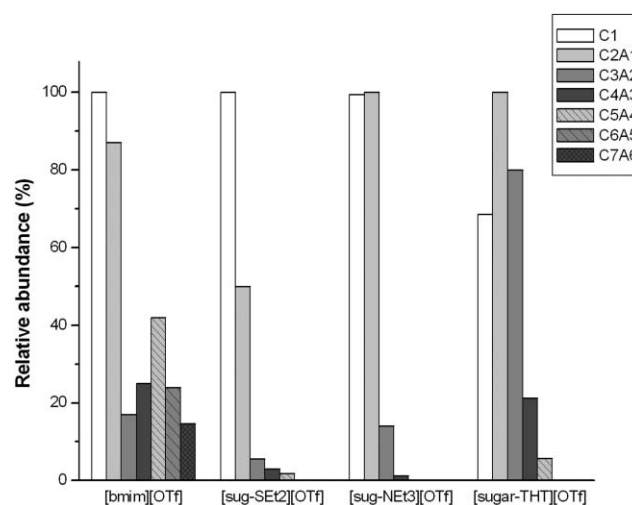


Fig. 2 Cluster distribution in full positive ESI-MS spectra of glucose-derived ILs and [bmim][OTf] at $150\text{ }^{\circ}\text{C}$.

mode in the ESI-MS spectra of the sugar-based ionic liquids **1–3** and [bmim][TfO].

Whereas the ESI-MS spectra of pure [bmim][OTf] and **3** ([sugar-THT][OTf]) are characterized by the presence of several intense peaks, ascribed to the free cation (C_1) and several clusters, those of **1** ([sugar-NEt₃][OTf]) and **2** ([sugar-SEt₂][OTf]) show only two main peaks, due to the free cation (the most intense) and the cluster of lower mass ($[C_2A_1]$).

Clearly, cations more loosely coordinated give an intense C_1 and possibly the first cluster (C_2A_1), whereas the stronger interacting species are preferentially present as high order clusters. On these bases, compounds **1** and **2** seem to possess a much lower ion-pairing with respect to the corresponding imidazolium triflate and compound **3** can be considered as an intermediate situation. It is also worth noting that the results of this kind of analysis seem not to be strongly related to the experimental conditions applied to the instruments, in particular to the temperature of the capillary, as almost similar results have been obtained at both 150 and 200 °C.

It has already been shown by several groups that the ability of the cationic and/or anionic moiety of ILs interacting with dissolved species, either as substrates, intermediates or catalysts, is a competitive process depending on the relative interactions which may take place inside the ionic medium itself and in particular on the strength of ion-pairing.^{9,10} On these bases, compounds **1** and **2** should be those having a cationic moiety more prone to interact with any catalyst dissolved in the IL. Research is still in progress to evaluate the truthfulness of this statement and to assess if the nature of the anion may exert any effect on the ion-pairing of glucose-derived ionic liquids.

Conclusions

Nature provides several opportunities for the preparation of new recyclable, biodegradable solvents displaying improved properties. Here, sugars have been used as safer, low-cost materials to synthesize the first terms of a novel, broad class of CILs through simple derivatization procedures.

The new CILs have been characterized and their thermal and ion-pairing behavior has been assessed with regard to their potential use as solvents for organic reactions. Two of them (compounds **1** and **2**) display a loose ion-pairing that makes them suitable for solvating reagents present in the solution.

Studies apt at assessing the influence of the carbohydrate skeleton of sugar-based CILs in the stereochemical course of organic reactions will be reported in due course.

Experimental

¹H NMR and ¹³C NMR spectra were recorded with a Bruker Avance 400 spectrometer at 298 K. When required for unambiguous characterization, COSY, TOCSY and HMQC spectra were also recorded. Optical rotations were measured at room temperature using a Perkin-Elmer 241 polarimeter. Elemental analyses were performed using a Carlo Erba 1108 elemental analyser.

Synthesis

Methyl 6-O-thexyldimethylsilyl- α -D-glucopyranoside 5. Methyl α -D-glucopyranoside **4** (30 g, 154 mmol) was dissolved in 100 mL of pyridine, then thexyldimethylchlorosilane (33 g, 185 mmol) and dimethylaminopyridine (150 mg, 1.23 mmol) were added. The reaction was stirred overnight at room temperature, then EtOAc was added and the solution was washed with a 3% v/v solution of H₂SO₄ (3 × 100 mL). The organic phase was dried (Na₂SO₄) and concentrated under reduced pressure. A short chromatography (95 : 5, EtOAc–MeOH) afforded compound **5** (51 g, quant.). ¹H NMR (300 MHz, CDCl₃): δ_H 4.70 (d, 1H, $J_{1,2} = 3.8$ Hz, H-1); 3.81–3.79 (m, 2H, H-6, H-6'); 3.72 (t, 1H, $J_{2,3} = J_{3,4} = 9.0$ Hz, H-3); 3.59–3.53 (m, 1H, H-5); 3.47 (dd, 1H, $J_{1,2} = 3.8$, $J_{2,3} = 9.0$ Hz, H-2); 3.42–3.36 (m, 4H, H-4, OMe); 1.61 (septuplet, 1H, $J = 6.8$ Hz, H_{tex}); 0.89–0.83 (m, 12H, CH_{3tex}); 0.11 (s, 6H, CH_{3tex}). $\alpha_D^{23} +78.0$ (c 1, CHCl₃). Found: C, 53.56; H, 9.63. C₁₅H₃₂O₆Si requires C, 53.54; H, 9.59%.

1,5-Anhydro-2,3,4-tri-O-methyl-D-glucitol 6. Compound **5** (22.8 g, 67.7 mmol) was dissolved in DMSO (120 mL) under N₂, then a 50% v/v solution of NaOH in water was added (30 mL), the mixture was vigorously stirred to form a gel-like solution and methyl iodide (43.2 g, 304 mmol) was added dropwise. The reaction was stirred overnight at room temperature, then it was poured into 100 mL of water and extracted with diethyl ether (3 × 100 mL). The organic phases were dried with Na₂SO₄, filtered and concentrated under reduced pressure. The crude compound was dissolved in CH₃CN under N₂. TMSOTf (74.5 g, 335 mmol) and triethylsilane (39 g, 335 mmol) were added and the reaction medium was stirred overnight. The reaction mixture was quenched with saturated NaHCO₃, and extracted with CH₂Cl₂ (5 × 100 mL). The organic solution was dried (Na₂SO₄) and concentrated under reduced pressure. The product was purified with flash chromatography (5 : 3, hexane–EtOAc) affording compound **6** (8.4 g, 60%). ¹H NMR (400 MHz, CDCl₃): δ_H 4.06 (dd, 1H, $J_{1,2} = 4.8$, $J_{1,1'} = 10.8$ Hz, H-1_{eq}); 3.85 (dd, 1H, $J_{6,5} = 2.5$, $J_{6,6'} = 11.6$ Hz, H-6); 3.68 (dd, 1H, $J_{6,5} = 4.6$, $J_{6,6'} = 11.6$ Hz, H-6'); 3.66 (s, 3H, OMe); 3.57 (s, 3H, OMe); 3.50 (s, 3H, OMe); 3.25–3.09 (m, 5H, H-1_{ax}, H-2, H-3, H-4, H-5). $\alpha_D^{23} +82.8$ (c 1, CHCl₃). C, 52.41; H, 8.80. C₉H₁₈O₅ requires C, 52.38; H, 8.85%.

1,5-Anhydro-2,3,4-tri-O-methyl-6-O-trifluoromethanesulfonyl-D-glucitol 7. 2,6-Lutidine (3.1 mL, 26 mmol) was dissolved in CH₂Cl₂ under N₂. The reaction was cooled to –20 °C and triflic anhydride (4.3 mL, 26 mmol) was added. The reaction was stirred for 5 min and then a solution of compound **6** (4.1 g, 20 mmol) in CH₂Cl₂ was added dropwise. After 5 min the reaction was warmed to 0 °C. After 1 h the reaction solution was poured into a mixture of ice and water (30 mL). The organic phase was separated and washed with cold water (3 × 20 mL). The organic phase was dried with Na₂SO₄ and concentrated under reduced pressure. The product was purified through a fast column of flash chromatography (8 : 2, hexane–EtOAc). The formation of the triflate was ascertained through the diagnostic ¹H NMR H-6 signals: 4.69 (dd, 1H,

$J_{6,5} = 2.0$, $J_{6,6'} = 10.6$ Hz, H-6); 4.62 (dd, 1H, $J_{6,5} = 2.0$, $J_{6,6'} = 10.6$ Hz, H-6). The product was used as such without further purification.

1,5-Anhydro-2,3,4-tri-*O*-methyl-D-glucitol-6-*O*-triethylammonium trifluoromethanesulfonate 1. Triflate derivative **7** (5.7 g, 20 mmol) was dissolved in 3 mL of THF under N_2 and cooled to -20 °C, then freshly distilled triethylamine (5.5 mL, 40 mmol) was added. The reaction was stirred overnight, then THF was evaporated under reduced pressure. The product was purified by dissolving the crude compound in distilled water and washing out the organic impurities extracting them with CH_2Cl_2 (3×10 mL), toluene (3×10 mL) and diethyl ether (3×10 mL). The aqueous phase was evaporated under reduced pressure affording ionic liquid **1** as a white solid (6.15 g, 70%). Compound **1** was decoloured by stirring it overnight with activated charcoal in water and filtering the solution over a neutral alumina column. 1H NMR (400 MHz, D_2O): δ_H 3.82 (br d, 1H, $J_{1,1'} = 7.1$ Hz, H-1_{eq}); 3.46, 3.44 (2 s, 6H, OMe); 3.46–3.40 (m, 1H, H-3); 3.30–3.19 (m, 9H, H-4, H-6, H-6', 3 CH_2N); 3.10–2.96 (m, 3H, H-1_{ax}, H-2, H-5); 1.15 (t, 9H, $J = 7.0$ Hz, 3 CH_3). ^{13}C NMR (100.58 MHz, D_2O): δ_C 120.70 (q, $J = 320.8$ Hz, CF_3); 87.4 (C-4); 80.0 (C-2); 79.2 (C-5); 73.2 (C-3); 66.7 (C-1); 58.0 (C-6); 53.6 (3 CH_2N); 7.62 (6 CH_3). $\alpha_D^{23} +29.6$ (c 1, D_2O). ES-MS: $ES^+ m/z$ 290.3 C_1^+ . $ES^- m/z$ 149.1 OTf.

1,5-Anhydro-2,3,4-tri-*O*-methyl-D-glucitol-6-*O*-diethylsulfonium trifluoromethanesulfonate 2. Triflate **7** (5.42 g, 19 mmol) was dissolved in diethyl sulfide (2.1 mL, 19 mmol) and the mixture was stirred for 3 h at 60 °C under N_2 . The mixture was then poured into distilled water and washed with diethyl ether (5×10 mL). The aqueous phase was evaporated under reduced pressure affording IL **2** as a viscous oil (6.5 g, 80%). Compound **2** was decoloured by stirring it overnight with activated charcoal in water and filtering the solution over a neutral alumina column. 1H NMR (400 MHz, D_2O): δ_H 4.05 (dd, 1H, $J_{1,2} = 5.0$, $J_{1,1'} = 11.2$ Hz, H-1_{eq}); 3.59 (dt, 1H, $J_{5,4} = J_{5,6} = 9.5$, $J_{5,6'} = 2.7$ Hz, H-5); 3.54–3.50 (m, 4H, H-6, OMe); 3.46 (s, 3H, OMe); 3.41 (dd, 1H, $J_{6,5} = 9.5$, $J_{6,6'} = 13.9$ Hz, H-6'); 3.35 (s, 3H, OMe); 3.31–3.21 (m, 6H, H-2, H-4, 2 CH_2S); 3.13–3.07 (m, 2H, H-1_{ax}, H-3); 1.32 (2t, 6H, CH_3). ^{13}C NMR (100.58 MHz, D_2O): δ_C 85.5 (C-4); 81.5 (C-3); 78.1 (C-2); 74.0 (C-5); 66.5 (C-1); 60.1, 59.8, 58.0 (3 OMe); 39.5 (C-6); 34.0, 33.5 (2 CH_2S); 7.7, 7.6 (2 CH_3). $\alpha_D^{23} +33.2$ (c 1, D_2O). ES-MS: $ES^+ m/z$ 277.1 C_1^+ . $ES^- m/z$ 149.0 OTf.

1,5-Anhydro-2,3,4-tri-*O*-methyl-D-glucitol-6-*O*-tetrahydrothiophenyl trifluoromethanesulfonate 3. Triflate **7** (5.42 g, 19 mmol) was dissolved in THF (3 mL) under N_2 , then tetrahydrothiophene (3.41 mL, 39 mmol) was added to the mixture and the temperature was set to 40 °C. The reaction was stirred overnight, then THF was evaporated under reduced pressure. The product was purified by crystallization (1 : 1, diethyl ether–EtOAc) affording ionic liquid **3** as a white solid (4.86 g, 60%). 1H NMR (400 MHz, D_2O): δ_H 4.12 (dd, 1H, $J_{5,5} = 4.9$, $J_{6,6'} = 11.2$ Hz, H-6); 3.66 (ddd, 1H, $J_{1,2} = 3.1$, $J_{1',2} = J_{2,3} = 9.5$ Hz, H-2); 3.61–3.33 (m, 7H, H-1_{ax}, H-1_{eq}, H-5, 2 SCH_2); 3.16 (dd, 1H, $J_{5,6} = J_{6,6'} = 11.2$ Hz, H-6'); 3.13

(dd, 1H, $J_{2,3} = J_{3,4} = 9.5$ Hz, H-3); 2.31–2.18 (m, 4H, CH_2-CH_2). ^{13}C NMR (100.58 MHz, D_2O): δ_C 86.4 (C-4); 82.5 (C-3); 79.1 (C-5); 75.6 (C-2); 67.5 (C-6); 61.0, 60.1, 59.0 (3 OMe); 45.7, 45.1 (2 SCH_2); 44.7 (C-1); 29.0 (CH_2-CH_2). $\alpha_D^{23} +22.0$ (c 1, D_2O). ES-MS: $ES^+ m/z$ 279.1 C_1^+ . $ES^- m/z$ 149.1 OTf.

DSC analysis

Melting points were determined using a Mettler differential scanning calorimeter. Each sample (*ca.* 10 mg) was analysed in a hermetically sealed aluminium pan. For each experiment, an empty hermetically sealed pan was referenced as the blank. A ramp temperature of 10 °C min^{-1} was employed over the range temperature of -50 to 200 °C for each warming and cooling cycle in the case of solid samples. A ramp temperature of 10 °C min^{-1} was instead employed over the range temperature of -150 to 50 °C for liquid compounds.

TGA analysis

Thermogravimetric analysis was performed with a Perkin Elmer TGA7 apparatus employing a ramp temperature of 10 °C min^{-1} from rt to 500 °C. All experiments were performed under a nitrogen atmosphere.

ESI-MS analysis

Full mass and collision-induced dissociation spectra of the investigated ILs dissolved in 80 : 20 H_2O –MeOH were acquired in both negative-ion and positive-ion mode using a Finnigan LCQ Advantage electrospray mass spectrometer equipped with an ion-trap analyzer. Instrumental parameters were tuned for each IL. The capillary voltage was set on 10.83 V, spray voltage of 3.44 kV, a capillary temperature from 150 to 280 °C was employed, mass scan range was from m/z 50 to 2000 amu, for a 30 000 ms scan time and N_2 was used as a sheath gas. Collision-induced dissociation mass spectra were obtained by applying normalized collision energies from 10 to 25% of the instrument maximum. The samples were injected into the spectrometer by a syringe pump at a constant flow rate of 20 μL min^{-1} .

Acknowledgements

We thank Dr Daggetti for recording ESI-MS spectra and Dr Rossetti for TGA analysis. We gratefully acknowledge MIUR (Ministero dell'Università e della Ricerca, COFIN 2004, protocol number 2004039212) and CNR (National Research Council) for financial support.

References

- 1 C. Baudequin, D. Brégeon, J. Levillain, F. Guillen, J.-C. Plaquevent and A.-C. Gaumont, *Tetrahedron: Asymmetry*, 2005, **16**, 3921; N. Jain, A. Kumar, S. Chauhan and S. M. S. Chauhan, *Tetrahedron*, 2005, **61**, 1015; J. Ding and D. W. Armstrong, *Chirality*, 2005, **17**, 281; C. Baudequin, J. Baudoux, J. Levillain, D. Cahard, A.-C. Gaumont and J.-C. Plaquevent, *Tetrahedron: Asymmetry*, 2003, **14**, 3081; S. T. Handy, *Chem.–Eur. J.*, 2003, **9**, 2938; P. Wasserscheid, A. Boesmann and C. Bolm, *Chem. Commun.*, 2002, 200; R. Gausephl, P. Buskens, J. Kleinen, A. Bruckmann, C. W. Lehmann, J. Klankermayer and W. Leitner, *Angew. Chem., Int. Ed.*, 2006, **45**, 3689.

- 2 J. Ding, V. Desikan, X. Han, T. L. Xiao, R. Ding, W. S. Jenks and D. W. Armstrong, *Org. Lett.*, 2005, **7**, 335; Z. Wang, Q. Wang, Y. Zhanga and W. Bao, *Tetrahedron Lett.*, 2005, **46**, 4657.
- 3 J. Ding, T. Welton and D. W. Armstrong, *Anal. Chem.*, 2004, **76**, 6819.
- 4 C. D. Tran, D. Oliveira and S. Yu, *Anal. Chem.*, 2006, **78**, 1349.
- 5 S. T. Handy, M. Okello and G. Dickenson, *Org. Lett.*, 2003, **5**, 2513.
- 6 E. B. Carter, S. L. Culver, P. A. Fox, R. D. Goode, I. Ntai, M. D. Tickell, R. K. Traylor, N. W. Hoffman, J. James and H. Davis, *Chem. Commun.*, 2004, 630.
- 7 P. J. Dyson, J. S. McIndoe and D. Zhao, *Chem. Commun.*, 2003, 508.
- 8 F. C. Gozzo, L. S. Santos, R. Augusti, C. S. Consorti, J. Dupont and M. N. Eberlin, *Chem.-Eur. J.*, 2004, **10**, 6187.
- 9 R. Bini, C. Chiappe, E. Marmugi and D. Pieraccini, *Chem. Commun.*, 2006, 897–899.
- 10 A. Aggarwal, L. Lancaster, A. R. Sethi and T. Welton, *Green Chem.*, 2002, **4**, 517; C. Chiappe, G. Imperato, E. Napolitano and D. Pieraccini, *Green Chem.*, 2004, **6**, 33–36.



Looking for that **special** chemical science research paper?

TRY this free news service:

Chemical Science

- highlights of newsworthy and significant advances in chemical science from across RSC journals
- free online access
- updated daily
- free access to the original research paper from every online article
- also available as a free print supplement in selected RSC journals.*

*A separately issued print subscription is also available.

Registered Charity Number: 207890

RSCPublishing

www.rsc.org/chemicalscience

22030682

Production of 5-hydroxymethylfurfural and furfural by dehydration of biomass-derived mono- and poly-saccharides†

Juben N. Chheda, Yuri Román-Leshkov and James A. Dumesic*

Received 10th August 2006, Accepted 21st December 2006

First published as an Advance Article on the web 17th January 2007

DOI: 10.1039/b611568c

Furan derivatives, such as 5-hydroxymethylfurfural (HMF) and furfural, obtained from renewable biomass-derived carbohydrates have potential to be sustainable substitutes for petroleum-based building blocks used in production of fine chemicals and plastics. We have studied the production of HMF and furfural by dehydration of fructose, glucose and xylose using a biphasic reactor system, comprised of reactive aqueous phase modified with DMSO, combined with an organic extracting phase consisting of a 7 : 3 (w/w) MIBK–2-butanol mixture or dichloromethane (DCM). Experiments with the MIBK–2-butanol mixture were conducted at a temperature of 443 K using mineral acid catalysts (HCl, H₂SO₄ and H₃PO₄) at a pH from 1.0 to 2.0, whereas experiments with DCM as the extracting solvent were conducted at 413 K and did not require the use of an acid catalyst. The modifiable nature of the biphasic system allowed us to identify preferred DMSO and pH levels for each sugar to maximize the HMF selectivity at high sugar conversions, leading to selectivities of 89%, 91%, and 53% for dehydration of fructose, xylose, and glucose, respectively. Using these reaction conditions for each monosaccharide unit, we can process the corresponding polysaccharides, such as sucrose (a disaccharide of glucose and fructose), inulin (a polyfructan), starch (a polyglucan), cellobiose (a glucose dimer) and xylan (a xylose polysaccharide), with equally good selectivities at high conversions. In addition, we show that the biphasic reactor system can process high feed concentrations (10 to 30 wt%) along with excellent recycling ability. By processing these highly functionalized polysaccharides, that are inexpensive and abundantly available, we eliminate the need to obtain simple carbohydrate molecules by acid hydrolysis as a separate processing step.

1. Introduction

Renewable biomass resources have the potential to serve as a sustainable supply of fuels and chemical intermediates (*e.g.* alcohols, aldehydes, acids).¹ The challenge for the effective utilization of these sustainable resources is to develop cost-effective processing methods to transform highly functionalized carbohydrate moieties into value-added chemicals. In this respect, furan derivatives, such as furfural and 5-hydroxymethylfurfural (HMF), can be produced from renewable biomass resources by acid-catalyzed dehydration of pentoses and hexoses, respectively. These compounds have the potential to be sustainable substitutes for building blocks derived from petrochemicals in the production of plastics and fine chemicals.² In the present work, we have identified preferred reaction conditions for the production of HMF and furfural in a biphasic reactor system for glucose, fructose and xylose monosaccharide units. Subsequently, we employed these reaction conditions to process the corresponding polysaccharides such as sucrose (a disaccharide of glucose and fructose), inulin (a polyfructan), starch (a polyglucan), cellobiose (a glucose dimer), and xylan (a xylose polysaccharide), with equally good

selectivities at high conversions. By processing polysaccharides that are inexpensive and abundantly available, we eliminate the need to obtain monosaccharides in a separate process, thereby moving the technology further toward practical application.

Following the production of HMF, this compound can be converted to 2,5-furandicarboxylic acid (FDCA) by selective oxidation, which can be used as a replacement for terephthalic acid in the production of polyesters (*e.g.* PET and PBT).³ Because HMF is not yet a high-volume chemical (in view of the current difficulties regarding its cost-effective production),^{4–6} the potential uses of HMF-derived compounds to produce polymers have not been studied in detail. Importantly, however, various research groups have, in fact, reported promising results in this direction.^{6,7} For example, reports have shown that polyesters formed from the combination of furanic diacid derivatives and aromatic moieties exhibit excellent thermal stability and resistance to atmospheric oxidation.^{7,8} Similarly, it has been suggested that thermally and mechanically stable polyesters can be obtained from the polymerization of 5-furanacrylic esters and also from furanic acid chlorides.^{7,9} Furanic polyamides prepared using furan dicarboxylic acid and aromatic diamines show decomposition and glass temperature profiles analogous to those of Kevlar[®].⁷ Thermoplastic elastomers and foams based on furanic polyurethanes are already used industrially in multiple applications. It has been reported that furanic polyesters, polyamides,

University of Wisconsin-Madison, Department of Chemical and Biological Engineering, Madison, 53706, WI, USA.

E-mail: dumesic@engr.wisc.edu; Fax: (+1) 608-262-5434

† Electronic supplementary information (ESI) available: Energy efficiency analysis. See DOI: 10.1039/b611568c

and polyurethanes show no difference in degradation when compared to that of the best aliphatic and aromatic counterparts.⁷ In addition, disubstituted furan derivatives obtained from HMF serve as an important component of pharmacologically active compounds associated with a wide spectrum of biological activities.⁶

Furfural is a key chemical for the commercial production of furan (through catalytic decarbonylation) and tetrahydrofuran (through hydrogenation), thereby providing a biomass-based alternative to petrochemical production of these compounds by dehydration of 1,4-butanediol.¹⁰ Furfural is primarily used in refining of lubricating oil, and in condensations with formaldehyde, phenol, acetone or urea to yield resins with excellent thermosetting properties and extreme physical strength.¹⁰ Methyl tetrahydrofuran (MeTHF) serves as a principal component for P-series fuel,¹¹ which is developed primarily from renewable resources. In addition, we have recently shown that HMF and furfural can serve as precursors for production of liquid alkanes (C₇–C₁₅) that serve as diesel fuel components.¹² Indeed, furan derivatives, such as HMF and furfural, obtained from renewable sources have been described in the literature as key compounds that bridge the gap between carbohydrate chemistry and petroleum-based industrial chemistry¹³ because of the wide range of chemical intermediates and end-products that can be produced from these compounds for use in the polymer, fuel, and pharmaceutical industries.

2. State of the art

The dehydration of hexoses to form HMF has been conducted in water,¹⁴ aprotic organic solvents (dimethylsulfoxide (DMSO)),¹⁵ and biphasic systems (water/methylisobutylketone (MIBK)),^{16,17} using catalysts such as organic acids (oxalic, maleic),¹⁸ inorganic acids (sulfuric, hydrochloric),¹⁸ salts (MgCl₂),¹⁹ organocatalysts (LaCl₃),²⁰ and solid acids (ion-exchange resin,¹⁶ VPO₄,²¹ zeolites¹⁷). However, all of these catalytic systems exhibit limitations. First, in pure water, dehydration of fructose is generally non-selective, leading to many byproducts besides HMF.¹⁴ Carlini *et al.* obtained high HMF selectivities (>80%) from fructose in water using various heterogeneous catalysts at low temperatures (*e.g.*, <370 K), but at low conversion (25–50%).^{21,22} Next, biphasic systems used for fructose dehydration, where a water-immiscible organic solvent is added to extract continuously the HMF from the aqueous phase, have shown poor partitioning of HMF into the organic phase, necessitating large amounts of solvent and hence large energy expenditures.^{16,17,23} Finally, as various researchers have shown, HMF can be produced in high yields (>90%) from fructose using pure high-boiling organic solvents, such as dimethylsulfoxide (DMSO), and mixtures of polyethyleneglycol (PEG) with water; however, this approach necessitates energy intensive isolation procedures.^{15,24–27}

Compared to fructose, glucose is the preferred feed source for the production of HMF, as it is more abundant and readily available. Previous work by various researchers has focused on fructose dehydration to HMF, because fructose dehydration to HMF has higher reaction rates and better selectivity when compared to using glucose as a feed molecule.⁴ In pure water,

glucose dehydration to HMF is non-selective (about 6%), leading to formation of insoluble humins.²⁸ Importantly, while it is possible to achieve high yields of HMF from fructose in DMSO, the yields of HMF from 3 wt% glucose solution are low (about 42%) in this high boiling-point solvent.²⁶ Recent advances by Bicker *et al.* in glucose dehydration have shown improved results (~48% HMF selectivity) in water-miscible solvent systems (*e.g.*, acetone–water),² but only using low initial carbohydrate concentrations (<3 wt%), which inevitably generate low HMF concentrations. Acid–base mixtures (*e.g.*, H₃PO₄–pyridinium) have been investigated with the purpose of increasing the HMF yields from glucose in a water–dioxane mixture; however, this system led to complicated product mixtures containing furans, pyrroles, and pyridines.⁴ Limited work on HMF production using polysaccharides such as inulin (a polyfructan) and sucrose (a dimer of glucose and fructose molecule) has been reported, and only the fructose part of the sucrose molecule is processed leaving behind unconverted glucose.²²

In addition to the use of glucose and fructose to make HMF, researchers have studied xylose as a feedstock for the production of furfural. The production of furfural requires raw materials rich in pentosan, such as corncobs, oat hulls, bagasse, and certain woods (like beech).²⁹ Most furfural production processes employ batch reactors using the Quaker Oats technology with yields less than 50%, requiring large amounts of steam (30 to 50 times the amount of furfural produced) and long reaction times.²⁹ Various researchers have studied the dehydration of xylose to furfural using acid catalysts, including mineral acids,³⁰ zeolites,³¹ acid-functionalized MCM materials,³² and heteropolyacids.³³ High yields of furfural, up to 75%, have been obtained with an MCM-41 catalyst modified with sulfonic acid groups in DMSO and water–toluene solvents, however at low initial concentrations of xylose (~3 wt%).³² Moreau, *et al.* conducted the dehydration reaction in a batch mode using H-faujasite and H-mordenite catalysts at 443 K and in a solvent mixture of water and MIBK or toluene (1 : 3 by vol.), and they achieved selectivities ranging from 70–96% (in toluene) and 50–60% (in MIBK), but at low xylose conversions.³¹

Although a wide variety of systems exist that use various combinations of solvents and catalysts to produce HMF and furfural from one of the multiple feedstocks, a single system capable of efficiently processing glucose, fructose, and xylose into HMF and furfural is still lacking. We recently developed a biphasic catalytic process for the selective dehydration of fructose to 5-hydroxymethylfurfural (HMF) using aqueous and organic phase modifiers that delivers HMF in a separation-friendly solvent.³⁴ Unfortunately, the specific reaction conditions that generate good HMF yields (>80%) from fructose achieve low yields from glucose (*e.g.*, 28%), providing further support for the well known behavior that keto-hexoses produce higher yields of HMF compared to aldo-hexoses.⁴ However, a strong incentive exists for the development of processes that utilize cheap and abundantly available glucose directly without requiring an additional step of glucose isomerization to fructose. Besides, isomerization of glucose to fructose also necessitates an additional acid hydrolysis step to obtain simple sugars from polysaccharide molecules. In this

work, we have improved the HMF selectivity from glucose dehydration using a biphasic system containing a reactive aqueous phase modified with DMSO. We further show that by fine-tuning the processing parameters for monosaccharides such as glucose, fructose and xylose, we can process various inexpensive and abundantly available polysaccharides such as inulin, starch, cellobiose, sucrose and xylan, in the same reactor system with equally good selectivities, thereby eliminating an additional acid hydrolysis step.

3. Experimental

3.1. Materials and experimental methods

All dehydration reactions were carried out in a two-phase batch reactor system containing a reactive aqueous layer (mixture of water–DMSO) and an extracting organic layer (mixture of MIBK–2-butanol or dichloromethane(DCM)). Aqueous- and organic-phase components including glucose, fructose, xylose, cellobiose, starch, xylan, sucrose, inulin, DMSO, MIBK, 2-butanol, DCM, and HCl were obtained from Sigma–Aldrich Corp. Dehydration experiments using 7 : 3 (w/w) MIBK : 2-butanol as the extracting phase were carried out in 10 ml (Alltech), thick-walled glass reactors heated in a temperature controlled oil bath placed on a magnetic stirrer (Table 2, runs 1–20). The temperature in the oil bath was measured by a K-type thermocouple (OMEGA), and series 16A temperature controller (Dwyer Instruments) coupled with a 150 W heating cartridge (McMaster Carr) controlled the temperature. In a typical experiment, 1.5 g of aqueous phase solution adjusted to a pH value using HCl acid catalyst and 3.0 g of organic phase solution were poured into the reactor. The reactor was placed in an oil bath at 443 K for the time specified in Table 2. The reaction was stopped by rapidly cooling the reactor in an ethylene glycol bath at 298 K. In a typical run with DCM as the extracting solvent (Table 2, runs 21–29), a Parr reactor (Model # 4749, size 23 ml) was filled with 7 g of the sugar aqueous solution and 7 g of DCM. The Parr reactor was then immersed in an oil bath at 413 K for time indicated in Table 2 (Runs 21–29). After reaction, the reactor was cooled to room temperature by flowing air.

3.2. Analysis

After each dehydration run (Table 2, runs 1–29), portions of the aqueous and organic phases were pipetted out and analyzed using HPLC analysis in a Waters 2690 system equipped with PDA 960 UV and RI 410 refractive index detectors. Sugar disappearance was monitored with an Aminex

HPX-87H column (Bio-Rad), using MilliQ water (pH = 2) as the mobile phase at a flow rate of 0.6 ml min⁻¹ and a column temperature of 303 K. HMF was quantified in the aqueous and organic phases with a Zorbax SB-C18 reverse phase column (Agilent), using a 2 : 8 v/v methanol : water (pH = 2) gradient at a flow rate of 0.7 ml min⁻¹ and a column temperature of 303 K using a UV detector (320 nm).

Sugar conversion and HMF selectivity were calculated from the aqueous and organic phase concentrations obtained from HPLC and the corresponding volume of each phase, as indicated in Table 1. Because the density of aqueous phase changes after addition of sugar, the volume occupied by the feed aqueous solution (V_{feed}) was measured using standard feedstock solutions (Table 1). In addition, after mixing the aqueous phase with the organic phase, some fraction of DMSO transfers to the organic phase, thereby changing the volumes of each phases to the values listed as V_{org} and V_{aq} . Thus, the volumes of the two phases were determined for each system using standard solutions. It was assumed that after the dehydration reaction the volume changes are negligible for the 10 wt% initial sugar concentration. The fraction of DMSO carried over to the organic phase was measured using HPLC analysis (Table 1).

3.3. Calculations

Sugar conversion and HMF selectivity were calculated as given below. Sugar concentration (micromoles per cm³) refers to the aqueous phase concentration because no sugar was present in the organic phase.

$$\text{Conversion} = \frac{[\text{Sugar}]_{\text{feed}} \times V_{\text{feed}} - [\text{Sugar}]_{\text{final}} \times V_{\text{aq}}}{[\text{Sugar}]_{\text{feed}} \times V_{\text{feed}}}$$

$$\text{Selectivity} = \frac{[\text{HMF}]_{\text{org}} \times V_{\text{org}} + [\text{HMF}]_{\text{aq}} \times V_{\text{aq}}}{[\text{Sugar}]_{\text{feed}} \times V_{\text{feed}} - [\text{Sugar}]_{\text{final}} \times V_{\text{aq}}}$$

4. Results and discussion

4.1. Reaction scheme

Fig. 1 depicts a generalized reaction scheme for production of HMF from polysaccharides containing hexose monomer units, involving a series of consecutive and parallel reactions starting with acid hydrolysis of polysaccharides to form monosaccharides. Glucose or fructose thus formed can be dehydrated in the presence of an acid catalyst to produce HMF *via* an open-chain or the cyclic furanose intermediate pathways.^{17,35} The reaction intermediates and the HMF product can further react

Table 1 Volumes (cm³) occupied by different reaction systems using standard glucose (G) feed solutions with HCl

Standard System	Volume of feed, V_{feed}	Volume of aqueous layer, V_{aq}	Volume of organic layer, V_{org}	DMSO in organic layer (wt%)
1 10% G 5:5 W:DMSO; 7:3 MIBK:2-butanol pH 1.0	4.5	3.9	12.9	5.1
2 10% G 5:5 W:DMSO; 7:3 MIBK:2-butanol pH 1.5	4.5	3.8	13.3	5.9
3 10% G 5:5 W:DMSO; 7:3 MIBK:2-butanol pH 2.0	4.5	3.8	13.3	5.9
4 10% G 4:6 W:DMSO; 7:3 MIBK:2-butanol pH 1.0	4.5	3.6	13.1	8.7
5 10% G 3:7 W:DMSO; DCM	4.4	3.6	4.6	20.0

^a V_{feed} corresponds to volume occupied by 5 g of feedstock solution. V_{aq} and V_{org} correspond to volume occupied by each phase after mixing 5 g of aqueous phase with 10 g of 7 : 3 (w/w) MIBK : 2-butanol organic solution (entries 1–4) and 5 g of DCM (entry 5).

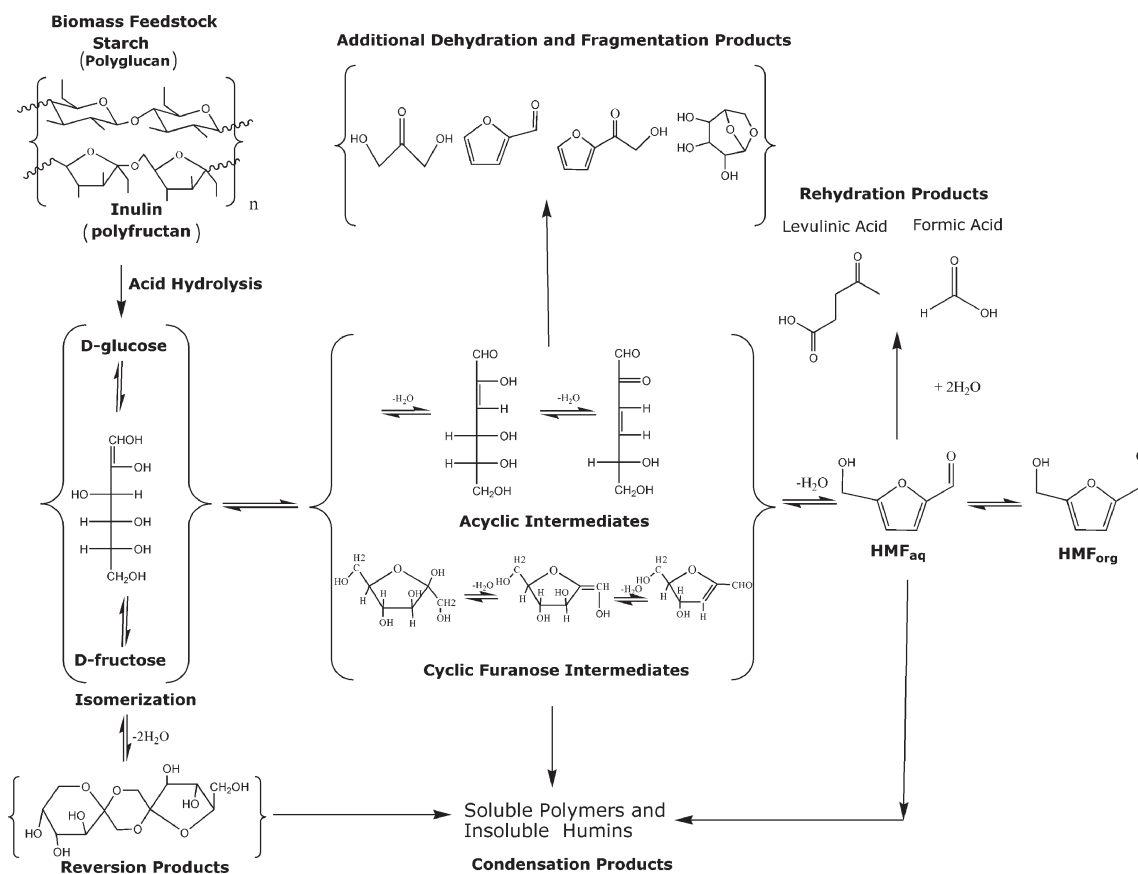


Fig. 1 Schematic representation of reaction pathways for acid-catalyzed hydrolysis and dehydration of polysaccharides (containing hexose monomer units) to 5-hydroxymethylfurfural (HMF) in a biphasic system. Structures in brackets correspond to representative species.

or degrade by processes such as isomerization, condensation, rehydration, reversion, fragmentation and/or additional dehydration reactions. Similarly, formation of furfural from xylose can proceed through two 1,2-eliminations and one 1,4-elimination of water or through a cyclic 2,5 anhydride intermediate.^{29,36}

4.2. Effect of extracting and aprotic organic solvent

We conducted dehydration experiments with glucose, the least reactive but most abundant monosaccharide, in the presence of HCl (pH 1.0) as catalyst, with the goal of maximizing HMF selectivity at 443 K under autonomous pressure. Fig. 2 shows the effects on the HMF selectivity of adding DMSO (60 wt%) and an extracting organic phase containing 7 : 3 (w/w) MIBK : 2-butanol. In pure water, the HMF selectivity from glucose (Table 2, run 1) was low (11%), and the reaction resulted in formation of insoluble byproducts. Adding an extracting solvent improves the selectivity to 28% (Table 2, run 3). The extracting solvent not only improves the selectivity by minimizing degradation reactions arising from extended HMF residence in the reactive aqueous phase, but it also achieves efficient recovery by extracting 82% of HMF in the organic layer for subsequent isolation. In parallel, adding DMSO to the aqueous reactive phase with no extracting solvent results in improved dehydration rates (about nine times) along with an increase in the selectivity to 26% (Table 2,

run 2). Importantly, adding DMSO along with an extracting solvent improves the rate of dehydration and increases the selectivity to 53% (Table 2, run 4). Thus, it can be seen that adding DMSO to water and using an efficient extracting phase not only improves the dehydration rates and HMF selectivity, but it also provides a system that allows simpler product purification.

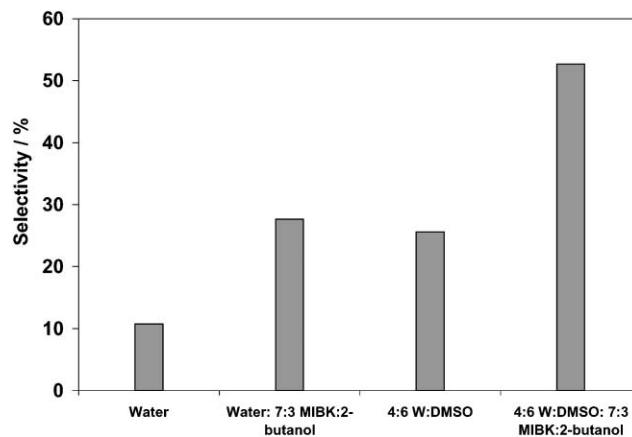


Fig. 2 Effect on HMF selectivity of adding an extracting organic solvent 7 : 3 (w/w) MIBK : 2-butanol and DMSO (60 wt%) to the aqueous phase for 10 wt% glucose dehydration at 443 K using HCl as catalyst at pH 1.0.

Table 2 Results for dehydration of various carbohydrates feedstock compounds. Runs 1–18 were carried out with 10 wt% initial concentration of carbohydrates using HCl as catalyst at 443 K. Runs 3–20 used 7 : 3 (w/w) MIBK : 2-butanol organic solvent in twice the amount by weight with respect to aqueous phase. Runs 21–29, except run 22, were carried out with 10 wt% initial concentration of carbohydrates without catalyst at 413 K using equal amount by weight of dichloromethane (DCM) as organic solvent. $R = [\text{HMF or Fur}]_{\text{org}}/[\text{HMF or Fur}]_{\text{aq}}$

Run #	Sugar	Aqueous phase composition	pH	Time/h:min	Conversion (%)	Selectivity (%)	HMF or Fur Organic Phase (%)	[HMF or Fur] _{org} /mg cc ⁻¹	[HMF or Fur] _{aq} /mg cc ⁻¹	R
No organic solvent										
1	Glucose	Water	1.0	0:45	20	11	—	—	1.5	—
2	Glucose	4:6 W:DMSO	1.0	0:10	41	26	—	—	8.3	—
Organic solvent: 7:3 (w/w) MIBK:2-butanol										
3	Glucose	Water	1.0	0:50	17	28	82	1.0	0.6	1.6
4	Glucose	4:6 W:DMSO	1.0	0:10	43	53	74	4.3	5.5	0.8
5	Fructose	5:5 W:DMSO	1.0	0:04	95	89	74	16.7	19.0	0.9
6	Fructose	5:5 W:DMSO	1.5	0:06	94	88	76	16.2	18.0	0.9
7	Fructose	5:5 W:DMSO	2.0	0:08	95	86	77	16.2	16.9	1.0
8	Glucose	5:5 W:DMSO	1.0	0:17	50	47	76	4.7	5.0	0.9
9	Glucose	5:5 W:DMSO	1.5	0:42	47	41	76	3.8	4.2	0.9
10	Glucose	5:5 W:DMSO	2.0	1:40	48	40	76	3.7	4.2	0.9
11	Xylose ^a	5:5 W:DMSO	1.0	0:12	71	91	91	14.1	4.7	3.0
12	Xylose ^a	5:5 W:DMSO	1.5	0:27	82	68	92	12.0	3.6	3.4
13	Xylose ^a	5:5 W:DMSO	2.0	0:55	53	54	92	6.2	2.0	3.1
14	Inulin	5:5 W:DMSO	1.5	0:05	98	77	76	16.3	18.0	0.9
15	Sucrose	4:6 W:DMSO	1.0	0:05	65	77	75	10.1	12.4	0.8
16	Starch	4:6 W:DMSO	1.0	0:11	61	43	74	5.5	6.9	0.8
17	Cellobiose	4:6 W:DMSO	1.0	0:10	52	52	74	5.6	7.0	0.8
18	Xylan ^a	5:5 W:DMSO	1.0	0:25	100	66	91	12.3	4.1	3.0
19	Glucose ^b	5:5 W:DMSO	1.5	1:00	48	34	77	3.2	3.5	0.9
20	Glucose ^b	5:5 W:DMSO	1.5	1:00	36	48	75	3.5	3.7	0.9
Organic solvent: dichloromethane (DCM)										
21	Fructose	3:7 W:DMSO	—	2:00	100	87	61	38.3	31.4	1.2
22	Fructose ^c	3:7 W:DMSO	—	4:30	100	78	62	105.0	81.1	1.3
23	Inulin	3:7 W:DMSO	—	2:30	100	70	62	34.4	27.4	1.3
24	Glucose	3:7 W:DMSO	—	4:30	62	48	63	13.6	10.0	1.3
25	Sucrose	3:7 W:DMSO	—	4:30	82	62	64	24.4	17.6	1.4
26	Starch	3:7 W:DMSO	—	11:00	91	40	65	18.9	12.9	1.4
27	Cellobiose	3:7 W:DMSO	—	9:30	85	45	68	20.6	12.5	1.6
28	Xylose ^a	3:7 W:DMSO	—	3:00	72	79	87	32.7	6.3	5.2
29	Xylan ^a	3:7 W:DMSO	—	3:00	100	76	85	36.2	8.4	4.3

^a Furfural selectivity from xylose or xylan feed. ^b Runs were carried out using H₂SO₄ (run 19) and H₃PO₄ (run 20) as catalyst. ^c Run 22 has initial concentration of 30 wt% fructose using equal amount by weight of dichloromethane (DCM) as organic solvent.

4.3. Effect of acidity (pH)

Fig. 3 shows the effect of pH on the selectivity for dehydration of fructose, glucose and xylose using HCl as the acid catalyst. These experiments were conducted in a 5 : 5 (w/w) W : DMSO mixture at 443 K using 7 : 3 (w/w) MIBK : 2-butanol as an extracting solvent. Fructose dehydration to HMF had the highest rates among the three sugars, with selectivities higher than 85% at high conversion (>90%) for all levels of acidity (Table 2, runs 5–7). Previous studies have shown that the reaction rates are first order with respect to fructose concentration.^{27,37} The highest selectivity achieved from glucose was 47% (pH 1.0), thus indicating the inherent difference in dehydration rates and selectivity of keto-hexoses and aldohexoses in a similar reacting environment (Table 2, runs 5 and 8). The low yields of HMF from glucose can be attributed to stable ring structures, thereby leading to a lower fraction of open chain forms in solution, and consequently lower rates of enolization, which determines the rate of HMF formation.⁴ In addition, glucose forms oligosaccharides, which contain reactive hydroxyl groups leading to higher rates of cross-polymerizations with reactive intermediates and HMF.⁴ For xylose dehydration to furfural, a significant increase in the

selectivity to a value of 91% is achieved by decreasing the pH to 1.0, with a 6-fold improvement in dehydration rate (Table 2,

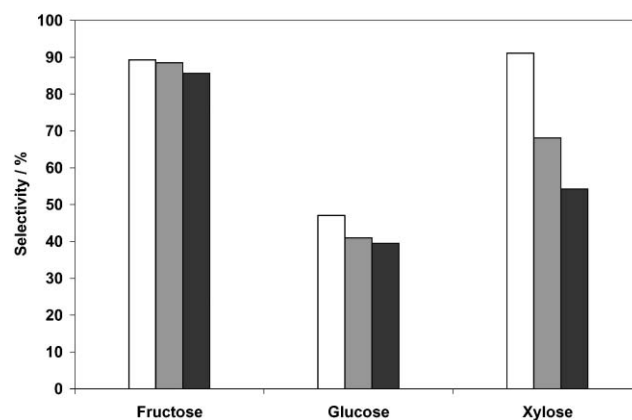


Fig. 3 Effect of pH on HMF selectivity from fructose and glucose, and furfural selectivity from xylose for dehydration of 10 wt% feed concentration of monosaccharides in 5 : 5 (w/w) W : DMSO aqueous mixture and 7 : 3 (w/w) MIBK : 2-butanol as organic phase at 443 K. White, grey, and black bars represent pH of 1.0, 1.5, and 2.0, respectively.

runs 11–13). Since furfural is less soluble in water, as compared to HMF, 91% of furfural is extracted into the organic phase, compared to a value of 75% for HMF (Table 2, runs 5, 8 and 11), thereby having higher efficiency for furfural production from xylose feedstock.

4.4. Effect of DMSO

The improved selectivities and dehydration rates observed in the presence of DMSO led us to study the effects of varying the DMSO level in the aqueous phase. Glucose dehydration was conducted at a constant pH, equal to 1.0, and 443 K in the presence of 7 : 3 (w/w) MIBK : 2-butanol as an extracting solvent. As seen in Fig. 4, adding DMSO to a level of 50 wt% improves the selectivity from 28% to 47%, with a further increase in selectivity to 53% for 60 wt% DMSO (Table 2, runs 3, 4 and 8). Earlier work has suggested that DMSO suppresses both the formation of condensation byproducts and the HMF rehydration by lowering the overall water concentration.^{4,27} Whereas the predominant form of hexoses in water is the β -pyranose structure, the furanose form is stabilized in DMSO and is favored at higher temperatures.³⁸ We suggest that this shift toward the furanose form upon adding DMSO or increasing the temperature is reflected in higher reactivities and selectivities toward production of HMF (see Fig. 1). However, it should be noted that increasing the DMSO content decreases the extracting power of solvent, as indicated by a decrease in the value of R (defined as ratio of HMF concentration in organic phase to HMF concentration in aqueous phase) from 1.58 to 0.78. In addition, in the case of 4 : 6 (w/w) W : DMSO a larger portion of DMSO is carried-over into the extracting solvent (8.7 wt% DMSO as detected by HPLC), compared to the case of 5 : 5 (w/w) W : DMSO (5 wt% DMSO as detected by HPLC), leading to a balance between selectivity improvement and added energy in further recovery of HMF upon addition of DMSO (see Table 1 and section 4.8).

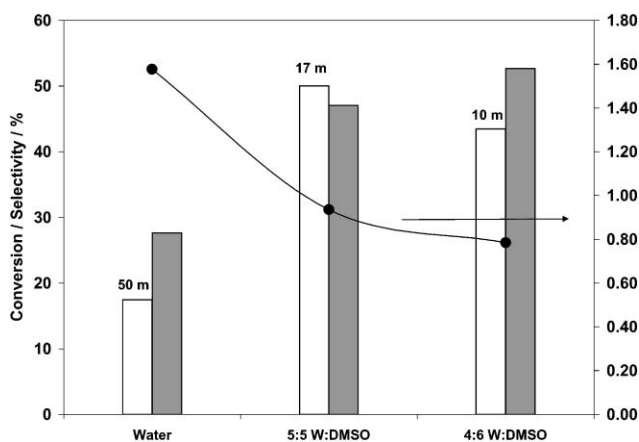


Fig. 4 Effect of DMSO content in (w/w) W : DMSO mixture on glucose conversion and HMF selectivity (left axis), and effect on extraction ratio R (right axis). $R = [\text{HMF or Fur}]_{\text{org}}/[\text{HMF or Fur}]_{\text{aq}}$. White and grey bars represent glucose conversion and HMF selectivity respectively. Reaction time (in minutes) is indicated above the conversion bars.

4.5. Processing of polysaccharide feed molecules

We subsequently studied the dehydration of various polysaccharide compounds at conditions optimized by adjusting pH and DMSO content for their monomer units. As seen in Fig. 5, dehydration of inulin, a fructose precursor obtained from chicory, gives a selectivity of 77% at high conversions in 5 : 5 (w/w) W : DMSO at pH 1.5, and this selectivity is consistent with the results obtained from fructose, assuming that some losses occur during the hydrolysis of the polyfructan to fructose. Similarly, reacting sucrose, a disaccharide having a unit of one fructose and one glucose monomer found in sugarcane or sugar beet, in 4 : 6 (w/w) W : DMSO at pH 1.0 achieves 77% selectivity at 65% sucrose conversion (Table 2, run 15). At these processing conditions, fructose would be completely converted and, assuming a glucose conversion of 30%, the expected selectivity to HMF from sucrose should be 81%. Thus, the conversion of sucrose follows the selectivity trends set by its monomer units, *i.e.*, fructose (89%) and glucose (53%). The conversion of cellobiose, a glucose dimer connected by β -1,4 glycosidic linkages obtained from partial hydrolysis of cellulose, gives similar selectivity for HMF (52%) as that of its monomer glucose unit. The conversion of soluble starch, a precursor for glucose containing α -1,4 glycosidic linkages and readily obtained from corn, rice *etc.*, gives a selectivity of 43% when processed at similar conditions. This value is lower than the value of 53% for glucose, suggesting that some loss of selectivity occurs during hydrolysis of the multiple glycosidic linkages in this polymer. Xylan (obtained from oat hulls), is a xylose polymer representative of

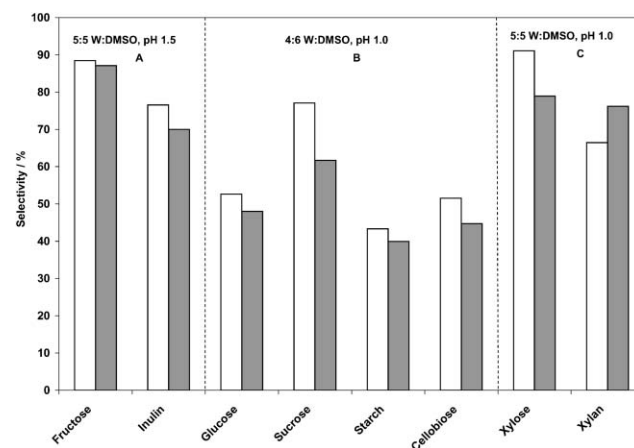


Fig. 5 HMF and furfural selectivities for processing biomass feedstocks at different conditions as separated by partitioning dotted lines. White bars represent the selectivity for dehydration in water–DMSO aqueous mixtures using HCl as catalyst and 7 : 3 (w/w) MIBK : 2-butanol as an extracting solvent at 443 K. First section (section A) represents HMF selectivity from fructose and inulin dehydration, in 5 : 5 (w/w) W : DMSO mixture at pH 1.5. Second section (section B) represents HMF selectivity from glucose, sucrose, starch and cellobiose dehydration, in 4 : 6 (w/w) W : DMSO mixture at pH 1.0. Third section (section C) represents furfural selectivity from xylose and xylan dehydration, in 5 : 5 (w/w) W : DMSO mixture at pH 1.0. Grey bars represent the selectivities in 3 : 7 (w/w) W : DMSO mixture and dichloromethane (DCM) as an extracting solvent at 413 K without catalyst.

hemi-cellulose, and the dehydration of this compound gave a selectivity of 66% at high conversions when subjected to the 5 : 5 (w/w) W : DMSO system and pH 1.0.

Even though fructose dehydration can be conducted with 20% DMSO to achieve 75% selectivity, as shown in our previous work,³⁴ under similar reaction conditions only the fructose fraction of sucrose would be converted, leaving the glucose molecules unreacted. However, in this system both monomers that constitute the sucrose molecule are converted to HMF by increasing the pH to 1.0 and DMSO content to 60%. In addition, this reaction system effectively processes polysaccharides such as starch or xylan, which have limited solubility in the aqueous phase. Indeed, solid biomass feeds (such as lignocelluloses) that are not completely soluble in any solvent, along with water-soluble carbohydrates, can be processed with further advances in this technology. Moreover, feed solutions consisting of mixed fractions such as hemi-cellulose and cellulose can be effectively handled without component separation. These results demonstrate the capability of the modifiable biphasic system to fine-tune the reaction conditions to process diverse biomass-derived feedstock molecules, which are inexpensive and abundantly available, to valuable furanic compounds by dehydration reactions.

4.6. Effect of mineral acids

We conducted experiments to study whether HCl could be replaced by less-corrosive mineral acids such as H₂SO₄ and H₃PO₄ and still achieve high HMF selectivity. These experiments were conducted using glucose as the feed molecule, at constant acidity (pH 1.5) with 5 : 5 (w/w) W : DMSO as the reacting mixture and MIBK : 2-butanol as the extracting solvent. Phosphoric acid achieved the highest selectivity of 48% (Table 2, run 20), HCl had an intermediate selectivity of 41% (Table 2, run 9), whereas sulfuric acid showed the lowest selectivity of 34% (Table 2, run 19). Unfortunately, the high selectivities achieved using H₃PO₄ are accompanied by the need to use twenty times more acid compared to HCl to achieve the same pH. It is clear, however, that the nature of the acid can influence the production of HMF.

4.7. Influence of dichloromethane as extracting solvent

We further studied the effects of changing the extracting solvent from a mixture of 7 : 3 (w/w) MIBK : 2-butanol to pure DCM. As seen in Fig. 5, the 3 : 7 (w/w) W : DMSO–DCM system converts all the carbohydrate feed molecules described above at a temperature of 413 K without an acid catalyst, with selectivities similar to those achieved using the HCl catalyst at 443 K. Fructose shows the highest HMF selectivity of 87%, while glucose dehydration achieves a selectivity of 48% (Table 2, runs 21 and 24). Sucrose is converted with an HMF selectivity of 62% at 82% conversion, comparing well with a predicted HMF selectivity of 59% at 100% conversion of fructose and 64% conversion of glucose monomer units (Table 2, run 25). In a separate experiment, 10 wt% fructose was dehydrated to produce HMF in a first cycle. After separating both the layers, the HMF remaining in the aqueous layer was extracted by contacting with two additional batches of fresh DCM solvent before charging a fresh feed of fructose

to recycle the aqueous layer. The recycle reaction system showed a selectivity of 83% at complete conversion, indicating excellent recycling ability of the solvent mixture. We also increased the initial fructose concentration from 10 to 30 wt%, and we achieved 78% HMF selectivity at complete conversion (Table 2, run 22). The decrease in HMF selectivity (from the value of 87%) resulting from the increase in feed concentration could be because of higher rates of condensation reactions.⁴ The ability of the W : DMSO–DCM system to process a variety of biomass feed molecules with good selectivity and recycling ability with no catalyst can prove beneficial to solve the corrosion problem caused by adding mineral acids. In addition, the extracting ratio of the organic phase is higher for DCM ($R = 1.35$) as compared to the mixture of MIBK : 2-butanol ($R = 0.8$). However, the DMSO carry over is higher in DCM (up to 20 wt%) than in the 7 : 3 (w/w) MIBK : 2-butanol solvent mixture, thereby increasing the subsequent recovery cost (see section 4.8). Thus, although the large-scale use of DCM would be restricted due to environmental concerns, DCM offers a valuable insight into the effects of different solvent properties on the selectivity.

DCM can undergo hydrolysis reactions in the presence of water at temperatures near 523 K to generate aqueous HCl.³⁹ In a blank run, we thus treated 3 : 7 (w/w) W : DMSO and DCM at 413 K for 3 h, and we observed a decrease of pH to 1.5, but no traces of HCl were observed by GC-MS analysis. These results suggest that water is not available for DCM hydrolysis to HCl, presumably because a high fraction of water is associated with DMSO.⁴⁰ However, traces of decomposition products from DMSO were observed that might impart acidity to the solvent mixture and cause the decrease in pH. Regardless of the origin for the decrease in pH upon reaction, this system shows promise because it can effectively deal with insoluble and soluble biomass feedstocks.

4.8. Effect of DMSO on energy requirements for separation

Previous work has shown that high yields (~90%) of HMF can be obtained by dehydration of fructose in pure DMSO as a solvent.²⁶ However, the reactive nature of pure HMF at high temperature leads to substantial carbonization of the isolated product upon distilling HMF from DMSO.²⁴ Low-temperature separation processes, such as vacuum evaporation and vacuum distillation, are thus necessary to separate HMF from DMSO.^{24,41} During our process, a fraction of the DMSO from the aqueous layer is carried over to the organic layer (Table 1), thereby necessitating use of vacuum distillation to remove the small amounts of DMSO from the product. Since experimental data for separation of HMF from DMSO have not been reported in the literature, we performed process simulation calculations using Aspen Plus[®] Simulation Software (Aspen Technology Inc., Cambridge) to compare the energy requirements of our process using MIBK–2-butanol and DCM as solvents with a process using pure DMSO (see ESI†). For product purification in the biphasic system, the organic phases are fed first to an adiabatic flash unit to remove most of the volatile solvent (for a temperature at or above room temperature), followed by 2 vacuum distillation columns to remove the remaining organic solvent and DMSO, respectively. The initial

adiabatic flash does not prove to be useful for the pure DMSO system, because it leads to HMF loss (>20%). Simulation results show that a biphasic system using 7 : 3 MIBK–2-butanol and DCM solvents achieves 55% and 30% higher energy efficiencies, respectively, when compared to using pure DMSO. The separation schemes we have employed may not be the optimal strategies for each case, but they allow a preliminary comparative estimate of the energy requirements for the three processes on the same basis for similar equipment and operating conditions. To improve the energy efficiency further, the DMSO content can be optimized for each sugar by comparing the gain of HMF yield against the penalty paid by the increase in energy requirements caused by increasing the level of DMSO.

While volatile organic solvents such as DCM and aprotic polar solvents such as DMSO have benefits in terms of improved extracting capability and higher selectivity for HMF, their use poses environmental concerns, and future work must address this issue. As shown in our earlier work, the addition of the aprotic solvent *N*-methylpyrrolidone (NMP) to the aqueous-phase in the biphasic system increases the selectivity to HMF, similar to the effect of DMSO. Importantly, replacing NMP with PVP,³⁴ a hydrophilic polymer that has NMP moieties along the polyethylene chain, retains the advantage of increased selectivity, but significantly reduces carry over into the organic phase. In a similar manner, grafting DMSO onto a hydrophilic polymeric backbone⁴² or a catalyst surface⁴³ could be used as a strategy to provide a suitable reacting environment for HMF production and avoid organic phase contamination. In addition, this strategy would eliminate the risk associated with DMSO handling in the aqueous phase. Similarly, environmentally benign solvents (such as lower alcohols like 2-butanol, esters, PEG) that exhibit desirable properties for HMF extraction from the reactive aqueous phase should be explored. As shown in our previous work, solid acid catalysts such as ion-exchange resins (at low temperature) and niobium phosphate (at high temperature) can be employed to replace the use of mineral acids.³⁴

5. Conclusions

We demonstrate in this work that a biphasic system can be tuned to process diverse feedstock molecules to produce HMF and furfural. By using preferred reaction conditions for representative monosaccharide units, it is possible to process the corresponding polysaccharides, such as sucrose (from sugarcane), inulin (from chicory), starch (from corn, rice), cellobiose (from cellulose), and xylan (from hemi-cellulose), in the same reactor system with equally good selectivities (from 50 to 90%) at high conversions, thereby eliminating the separate hydrolysis step before the dehydration reaction. The process variables that influence the yields of HMF and furfural for different carbohydrate feed molecules are the pH of the solution, the DMSO content in aqueous phase, the initial sugar concentration, the nature of the acid, and the extracting solvent. This biphasic reaction system is a step toward the more economical production of HMF and furfural through the processing of inexpensive and abundantly available renewable feedstocks.

Acknowledgements

This work was supported by the U.S. Department of Agriculture (USDA) and the National Science Foundation (NSF) Chemical and Transport Systems Division of the Directorate for Engineering. We would like to thank Prof. Swaney and Prof. Maravelias for providing technical consultation. We thank R. West, C. Loeb, D. Spence, D. Komula, and J. Philipsek for technical assistance. We would also like to acknowledge R. McClain for allowing us to use the GC-MS facility at the Chemistry Instructional Instrumental Laboratory.

References

- 1 A. J. Ragauskas, C. K. Williams, B. H. Davison, G. Britovsek, J. Cairney, C. A. Eckert, W. J. F. Jr., J. P. Hallett, D. J. Leak, C. L. Liotta, J. R. Mielenz, R. Murphy, R. Templer and T. Tschaplinski, *Science*, 2006, **311**, 484.
- 2 M. Bicker, J. Hirth and H. Vogel, *Green Chem.*, 2003, **5**, 280.
- 3 K. W. Pentz, *Br. Pat.* 2 131 014, 1984; T. Werpy and G. Petersen, *Top Value Added Chemicals From Biomass*, 2004, available electronically at <http://www.osti.gov/bridge>.
- 4 B. M. F. Kuster, *Starch*, 1990, **42**, 314.
- 5 J. Lewkowsky, *ARKIVOC*, 2000, **2**, 17. Available electronically at http://www.arkat-usa.org/ARKIVOC/JOURNAL_CONTENT/manuscripts/2001/01-403CR%20as%20published%20mainmanuscript.pdf.
- 6 C. Moreau, M. N. Belgacem and A. Gandini, *Top. Catal.*, 2004, **27**, 11.
- 7 A. Gandini and M. N. Belgacem, *Prog. Polym. Sci.*, 1997, **22**, 1203.
- 8 A. Chaabouni, S. Gharbi, M. Abid, S. Boufi, R. E. Gharbi and A. Gandini, *J. Soc. Chim. Tunis.*, 1999, **4**, 547.
- 9 R. Storbeck and M. Ballauff, *Polymer*, 1993, **34**, 5003; J. A. Moore and J. E. Kelly, *J. Polym. Sci.*, 1978, **16**, 2407; J. A. Moore and J. E. Kelly, *Polymer*, 1979, **20**, 627; J. A. Moore and J. E. Kelly, *J. Polym. Sci.*, 1984, **22**, 863.
- 10 W. J. McKillip, *Kirk-Othmer Encycl. Chem. Technol.*, 1981, **11**, 501.
- 11 S. F. Paul, *US Pat.* 6 309 430, 2001.
- 12 G. W. Huber, J. N. Chheda, C. J. Barret and J. A. Dumesic, *Science*, 2005, **308**, 1446; C. J. Barrett, J. N. Chheda, G. W. Huber and J. A. Dumesic, *Appl. Catal., B*, 2006, **66**, 111.
- 13 H. Schiweck, M. Munir, K. Rapp and M. Vogel, *Carbohydr. Org. Raw Mat.*, 1990, **115**, 555.
- 14 K. M. Rapp, *US Pat.* 4 740 605, 1987.
- 15 R. M. Musau and R. M. Munavu, *Biomass*, 1987, **13**, 67.
- 16 D. Mercadier, L. Rigal, A. Gaset and J. P. Gorrichon, *J. Chem. Technol. Biotechnol.*, 1981, **31**, 489.
- 17 C. Moreau, R. Durand, S. Razigade, J. Duhamet, P. Faugeras, P. Rivalier, P. Ros and G. Avignon, *Appl. Catal., A*, 1996, **145**, 211.
- 18 F. S. Ashgari and H. Yoshida, *Ind. Eng. Chem. Res.*, 2006, **45**, 2163.
- 19 S. Tyrlik, D. Szerszen, M. Olejnik and W. Danikiewicz, *J. Mol. Catal. A: Chem.*, 1996, **106**, 223.
- 20 K. Seri, Y. Inoue and H. Ishida, *Chem. Lett.*, 2000, **29**, 22.
- 21 C. Carlini, P. Patrono, A. M. R. Galletti and G. Sbrana, *Appl. Catal., A*, 2004, **275**, 111.
- 22 C. Carlini, M. Giuttari, G. Raspolli, A. Maria, G. Sbrana, T. Armaroli and G. Busca, *Appl. Catal., A*, 1999, **183**, 295.
- 23 Q. P. Peniston, *U.S. Pat.*, 2 750 394, 1956; P. Rivalier, J. Duhamet, C. Moreau and R. Durand, *Catal. Today*, 1995, **24**, 165.
- 24 D. W. Brown, A. J. Floyd, R. G. Kinsman and Y. Roshan-Ali, *J. Chem. Technol. Biotechnol.*, 1982, **32**, 920.
- 25 Y. Nakamura and S. Morikawa, *Bull. Chem. Soc. Jpn.*, 1980, **53**, 3705.
- 26 H. H. Szmant and D. D. Chundury, *J. Chem. Technol. Biotechnol.*, 1981, **31**, 135.
- 27 H. E. van Dam, A. P. G. Kieboom and H. van Bekkum, *Starch*, 1986, **38**, 95.

- 28 K. Seri, Y. Inoue and H. Ishida, *Bull. Chem. Soc. Jpn.*, 2001, **74**, 1145.
- 29 K. J. Zeitsch, *The chemistry and technology of furfural and its many by-products*, Elsevier, Amsterdam, Sugar Series, vol. 13, 1st edn, pp 34–69, 2000.
- 30 H. D. Mansilla, J. Baeza, S. Urzua, G. Maturana, J. Villasenor and N. Duran, *Bioresour. Technol.*, 1998, **66**, 189.
- 31 C. Moreau, R. Durand, D. Peyron, J. Duhamet and P. Rivalier, *Ind. Crop Prod.*, 1998, **7**, 95.
- 32 A. S. Dias, M. Pillinger and A. A. Valente, *J. Catal.*, 2005, **229**, 414.
- 33 A. S. Dias, M. Pillinger and A. A. Valente, *Appl. Catal., A*, 2005, **285**, 126.
- 34 Y. Roman-Leshkov, J. N. Chheda and J. A. Dumesic, *Science*, 2006, **312**, 1933.
- 35 M. J. Antal, Jr., T. Leesomboon, W. S. Mok and G. N. Richards, *Carbohydr. Res.*, 1991, **217**, 71; X. Qian, M. R. Nimlos, M. Davis, D. K. Johnson and M. E. Himmel, *Carbohydr. Res.*, 2005, **340**, 2319.
- 36 M. J. Antal, T. Leesomboon and W. S. Mok, *Carbohydr. Res.*, 1991, **217**, 71.
- 37 B. F. M. Kuster and H. S. van der Baan, *Carbohydr. Res.*, 1977, **54**, 165; B. M. F. Kuster and H. J. C. van der Steen, *Carbohydr. Res.*, 1977, **54**, 177.
- 38 P. Dais, *Carbohydr. Res.*, 1987, **169**, 159; F. Franks, *Pure Appl. Chem.*, 1987, **59**, 1189; M. Bicker, D. Kaiser, L. Ott and H. Vogel, *J. Supercrit. Fluids*, 2005, **36**, 118.
- 39 C. Wakai, S. Morooka, N. Matubayasi and M. Nakahara, *Chem. Lett.*, 2004, **33**, 302.
- 40 J. M. G. Cowie and P. M. Toporowski, *Can. J. Chem.*, 1961, **39**, 2240.
- 41 R. E. Jones and H. B. Lange, *U.S. Pat.* 2 994 645, 1958; R. H. Hunter, *US Pat.* 3 201 331, 1965; J. Harris, J. Saeman and L. Zoch, *For. Prod. J.*, 1960, **10**, 125.
- 42 S. Kondo, K. Ohta, Y. Inagaki, M. Minafuji, H. Yasui, N. Nakashima, M. Iwasaki, K. Furukawa and K. Tsuda, *Pure Appl. Chem.*, 1988, **60**, 387.
- 43 E. M. Soliman, M. B. Saleh and S. A. Ahmed, *Talanta*, 2006, **69**, 55.

Textbooks from the RSC

The RSC publishes a wide selection of textbooks for chemical science students. From the bestselling *Crime Scene to Court*, 2nd edition to groundbreaking books such as *Nanochemistry: A Chemical Approach to Nanomaterials*, to primers on individual topics from our successful *Tutorial Chemistry Texts series*, we can cater for all of your study needs.

Find out more at www.rsc.org/books

Lecturers can request inspection copies – please contact sales@rsc.org for further information.



Registered Charity No. 207890

RSC Publishing

www.rsc.org/books

On-line *in-situ* characterization of CO₂ RESS processes for benzoic acid, cholesterol and aspirin

Jeremy J. Harrison, Changyoul Lee, Thomas Lenzer* and Kawon Oum*

Received 21st August 2006, Accepted 22nd December 2006

First published as an Advance Article on the web 18th January 2007

DOI: 10.1039/b612055e

Rapid expansions of supercritical solutions (RESS) of benzoic acid, cholesterol and aspirin in supercritical CO₂ have been used to investigate the influence of a systematic variation of the pre-expansion temperature and pressure, the distance from the RESS nozzle and the amount of added co-solvent on properties like the average particle diameter D_{av} and the width of the particle size distribution σ . The properties of the CO₂ expansion have been characterized by a 1-dimensional flow-field model using the Span–Wagner equation of state. Particle detection was performed on-line and *in-situ* using laser-based three wavelength extinction measurements (3-WEM). For benzoic acid we found a decrease in D_{av} with increasing pre-expansion pressure, and an increase in D_{av} with increasing pre-expansion temperature. This is probably due to a lower mass flow rate, which is associated with a lower pre-expansion pressure or higher pre-expansion temperature. This in turn results in a longer residence time in the expansion region and thus a longer particle growth time. Furthermore, a decrease in pre-expansion pressure or an increase in pre-expansion temperature is associated with a decrease in saturation, corresponding to an increase in the critical particle radius and a decrease in the nucleation rate. The size of the benzoic acid particles ranged from about 100 to 500 nm. In addition, we found no obvious correlation between D_{av} and the distance from the RESS nozzle for benzoic acid and aspirin particles. The particle size was roughly 350 nm and 160 nm for these two solutes, respectively. Obviously, the particle growth processes have already ceased not too far away from the Mach disc. In addition, for cholesterol expansions in CO₂ there was no correlation between the amount and type of co-solvent added. Particle sizes of ~100 nm were obtained for methanol, ethanol and isopropanol co-solvents. This is most likely due the low solubility of cholesterol in supercritical CO₂, compared with molecules such as benzoic acid, which results in a change of D_{av} which is too small to be detected using 3-WEM.

1. Introduction

RESS (rapid expansion of supercritical solutions) has been shown to be an environmentally benign technique for the production of nanometre- to micrometre-sized particles with narrow size distributions. The process involves expansion of a supercritical solution containing a solute of interest through a micrometre-sized orifice to atmospheric pressure. The rapid density drop and associated increase in supersaturation result in the solute being expelled from the solution as a collection of fine particles. The process has important applications in chemical engineering, the pharmaceutical industry, materials science and biotechnology.^{1–3}

Our laboratory employs a wide range of supercritical fluids, and uses *in-situ* and on-line laser-based methods to determine the size of the particles. On-line particle detection methods are useful, because they allow the checking of properties of particles during their production in a non-invasive way, without possible problems occurring when using off-line techniques like, for example, scanning electron microscopy (SEM),

where the particle properties might be changed during the collection and analysis process. For the first time, we have used a laser-based shadowgraphy method (LABS)⁴ to investigate the particle size and shape within the RESS expansion. This method gives detailed information, because it records the size and shape of each individual particle passing through a well-defined volume interrogated by a combination of a far-field microscope and a high resolution CCD camera. However, it is limited to particle sizes down to about 1 μm . To cover smaller particle sizes, light scattering techniques are used. In our laboratory we apply the three-wavelength extinction method (3-WEM) as the method of choice.⁵ It yields reliable values for the average particle diameter (in the range between about 100 nm and 10 μm), the width of the particle size distribution (PSD) and the volume concentration of the particles. However, in contrast to LABS, no information on the morphology of individual particles can be extracted.

Most of the previous RESS work has concentrated on small organic molecules and larger biomolecules such as cholesterol, which is used as a model for pharmaceuticals.^{6,7} The present work has the aim of characterizing the dependence of the particle size on pre-expansion temperature and pressure, the variation of particle size with distance from the RESS nozzle and the influence of adding co-solvents, which is a viable way of increasing the solubility of the organic solute in CO₂ RESS

Institut für Physikalische Chemie, Universität Göttingen,
Tammannstrasse 6, 37077 Göttingen, Germany.
E-mail: tlenzer@gwdg.de; koum@gwdg.de; Fax: +49 551 393150;
Tel: +49 551 3912598

expansions.^{8–19} The current study is intended as one step in the direction of ultimately being able to understand and control particle sizes in RESS processes for industrial applications.

2. Experimental

Our RESS apparatus has been described in detail elsewhere.⁴ Briefly, liquefied CO₂ (Praxair) at room temperature was pressurized using an Isco syringe pump (Model 100 DX) in continuous flow mode, before passing through a preheater (*ca.* 323 K), which brought the CO₂ into the supercritical state. The CO₂ was then flowed through the heated and stirred extraction cell, where it was saturated with the solute of interest (cholesterol from Acros Organics, aspirin and benzoic acid from Sigma–Aldrich). Two high pressure filters with a pore size of 50 μm were used to save the nozzle from any possible clogging with undissolved particles. A buffer volume (*ca.* 10 mL) was used to ensure that the solution reached the correct pre-expansion temperature. For the aspirin measurements a slightly smaller buffer volume was used. The supercritical solution was then expanded through a home-built heated nozzle into an expansion chamber equipped with quartz windows. The nozzle consisted of a holder with Teflon seals and a laser-drilled sapphire orifice (Bird Precision, length 254 μm, diameter 51 μm, with tapered inlet, “V-hole type”).

For the benzoic acid measurements with varying pre-expansion conditions and the cholesterol/co-solvent measurements, an acrylic-glass expansion chamber was utilized, as in our earlier experiments.⁴ For the distance-dependence measurements a new expansion chamber was constructed. It consisted of two rubber bellows either side of a quartz-window assembly which could be moved precisely using an electric motor. Such a chamber allows measurements to be performed at a range of distances from the nozzle along the expansion. A fan with variable speed was attached to the bottom of the chamber to allow for exchange of the expanded mixture.

Experiments were carried out in a systematic variation of the extraction temperature (T_{extr}) and extraction pressure (P_{extr}) within the extraction cell, the pre-expansion temperature (T_0) and pre-expansion pressure (P_0) prior to the expansion, and the nozzle temperature (T_{nozzle}). In this work, the extraction and pre-expansion pressures were equivalent, as were the pre-expansion and nozzle temperatures.

The 3-WEM technique⁵ was used for the characterization of the average particle diameter D_{av} and the width of the PSD. It has already been explained in detail in our previous paper.⁴ Essentially, it is based on the extinction of monochromatic light by particles due to Mie scattering.²⁰ Extinction measurements were performed for three wavelengths at a fixed angle of 180°, from which two extinction quotients were obtained. A comparison of these with a data field calculated using Mie scattering theory allowed a determination of the average particle diameter, the width of the PSD, and the volume concentration of the particles. Important approximations are that the particles are assumed to be spherical and the size distribution log(arithmetic)-normal,

$$p(D) = \frac{1}{\sqrt{2\pi}\sigma D} \exp\left(-\frac{[\ln(D) - \ln(D_{\text{av}})]^2}{2\sigma^2}\right) \quad (1)$$

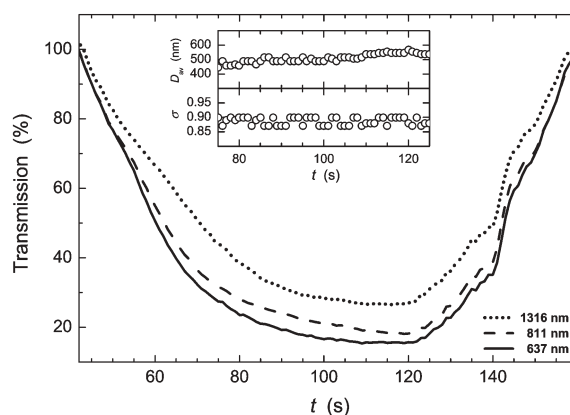


Fig. 1 Typical 3-WEM signals for benzoic acid RESS nanoparticles. The optical transmission is shown as a function of the measurement time for the three wavelengths 1316 nm (dotted line), 811 nm (broken line) and 637 nm (continuous line). $P_{\text{extr}} = P_0 = 150$ bar, $T_0 = T_{\text{nozzle}} = 378$ K and $T_{\text{extr}} = 326$ K. Upper inset: 3-WEM on-line *in-situ* determination of the average particle size D_{av} extracted from the transmission data. Lower inset: Corresponding standard deviation σ of the logarithmic-normal distribution. Values see Table 1.

where D is the particle diameter, D_{av} the average diameter of the particles, and σ the associated standard deviation of the log-normal distribution. A typical example of a 3-WEM measurement for a RESS expansion of benzoic acid in CO₂ is shown in Fig. 1. The transmission of the particle cloud at a scattering angle of 180° was clearly wavelength dependent, as is shown by the three different curves at the wavelengths 1316, 811 and 637 nm. The two insets show the D_{av} and σ values determined from the on-line measurement. In this case the averaged values $D_{\text{av}} = 506$ nm and $\sigma = 0.87$ were obtained. As was shown in our previous study, particles obtained from RESS expansions under similar conditions using a variety of solid and liquid substances have only a slightly elliptical shape, so that the application of standard Mie theory for spherical particles is sufficient. We also note that the PSD width as determined by 3-WEM is reliable, as demonstrated in our earlier paper, where good agreement with shadowgraphy measurements was obtained, which accurately characterizes the PSD tail at larger diameters.⁴ To increase sensitivity at low particle concentrations, in some of the experiments a multi-pass arrangement employing broadband mirrors was used to extend the effective scattering path length. The accuracy of the 3-WEM set-up was routinely checked against different monodisperse polystyrene latex suspensions in water. In addition to the 3-WEM technique, for some measurements of the size of cholesterol particles we also used a laser diffraction based particle analyzer (Spraytech, Malvern Instruments), which measured the angular intensity of diode laser light (670 nm) scattered from the RESS particles.

3. Results and discussion

3.1. Expansion conditions in the current experimental RESS setup

To characterize the supercritical CO₂ expansion, we performed a modelling of a 1-D steady-state flow field to calculate central

quantities, like pressure, temperature, density and velocity, along the nozzle for our specific setup. For a schematic cross-sectional view of the “V-hole” type laser-drilled sapphire orifice see the inset in Fig. 2(a). It had the following dimensions: “V” entrance width 1700 μm , length 940 μm , capillary length $L = 254 \mu\text{m}$, and diameter $D = 50.8 \mu\text{m}$, *i.e.*, an L/D ratio of 5:1. A conical shape of the emerging supersonic free jet was assumed. For the calculation of the flow field the equations for the mass, momentum and energy balances were solved.^{7,21}

$$v \frac{d\rho}{dx} + \rho \frac{dv}{dx} + \frac{\rho v dA}{A dx} = 0 \quad (2)$$

$$\rho v \frac{dv}{dx} + \frac{dP}{dx} = -\frac{2fv^2\rho}{D} \quad (3)$$

$$\frac{dh}{dx} + v \frac{dv}{dx} = \frac{dq}{dx} \quad (4)$$

with the following variables and parameters: v = velocity, ρ = density, x = position along nozzle, A = cross-sectional area of the nozzle, P = pressure, f = Fanning friction factor, D = internal diameter of nozzle, h = enthalpy per unit mass and q = heat transferred to the nozzle. Calculations were performed for the pure solvent (high dilution) assuming an isentropic capillary inlet flow. In the capillary nozzle, heat exchange and friction were included. We also incorporated heat exchange for the supersonic free jet. Initial conditions for the expansion were $P_0 = 130$ bar and $T_0 = 388$ K. h_0 and ρ_0 were calculated from P_0 and T_0 using the Span–Wagner equation of state (SW-eos) for CO_2 , which is known to give an excellent representation for CO_2 under the conditions used in this study.^{22,23} Because v_0 is unknown, we used v_s (the sonic velocity) at the nozzle exit, which was calculated using the SW-eos. The heat transmitted to the nozzle was calculated from a model for turbulent flow in a pipe with constant wall temperature. In the supersonic free jet, a constant heat transfer coefficient of $1.0 \times 10^7 \text{ W m}^{-2} \text{ K}^{-1}$ was assumed. Transport properties needed for the calculations were obtained *via* the SW-eos. The Fanning friction factor was calculated from the Blasius equation.⁷

Fig. 2 shows the modelling results for our particular nozzle. Fig. 2(a) demonstrates the drop in CO_2 pressure and temperature during the expansion, with a noticeable decrease in the 254 μm long capillary part of the nozzle and a much stronger decrease at the nozzle exit, *i.e.*, the transition from the capillary to the region of the supersonic free jet. The final increase of the temperature is due to the fact that heat exchange with the surrounding gas is considered in the model. The large drop in pressure and temperature is responsible for the rapid drop in density, as shown in Fig. 2(b), which results in particle formation due to the loss of solvent power. The velocity profile allows an estimate of the residence time in the capillary part, which is in the range of 1 μs .

We will extend the present modelling in a forthcoming publication to determine particle sizes, including nucleation, condensation and coagulation processes.²⁴ Recent simulations show that this should be feasible, although they still overestimate the experimental particle diameters.²⁵

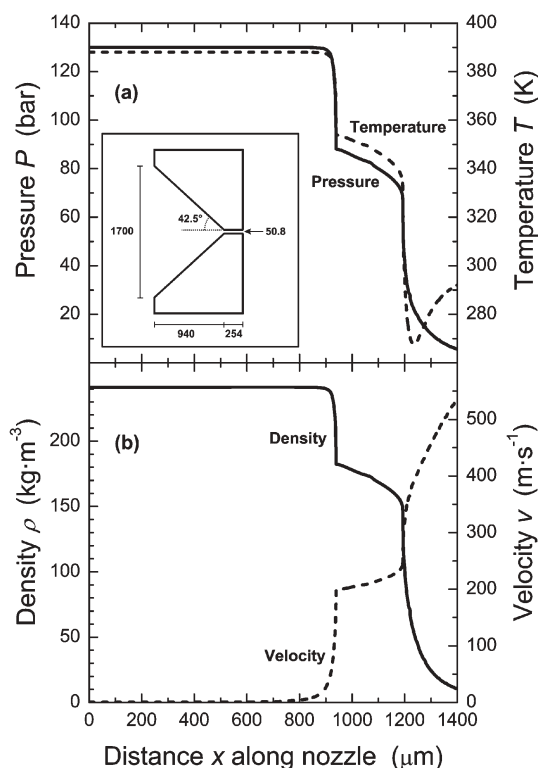


Fig. 2 Numerical simulation of a pure CO_2 RESS expansion. (a) CO_2 pressure profile (continuous line) and temperature profile (broken line). (b) CO_2 density profile (continuous line) and velocity profile (broken line). The inset in (a) shows a cross-sectional view of the laser-drilled sapphire orifice used in our experiments, where numbers indicate the dimensions in μm .

3.2. Dependence of benzoic acid particle size on pre-expansion temperature and pressure

Several studies using off-line detection techniques show a rather heterogeneous picture of the influence of quantities like pre-expansion temperature and pressure on particle size, and no clear systematic trends or correlations have been observed.^{26–28} Systematic studies using on-line techniques can be helpful in this respect, as the particle size is detected in a non-invasive manner.

We have obtained experimental results for the variation of the pre-expansion pressure and temperature of a benzoic acid– CO_2 RESS expansion. For benzoic acid, we find a decrease in particle size with increasing pre-expansion pressure (Fig. 3), and an increase in particle size with increasing pre-expansion temperature (Fig. 4). The particle sizes range from about 100 to 500 nm for the conditions utilized in this work (see Tables 1 and 2). The most likely explanation for this dependence is that a lower mass flow rate, which is associated with a lower pre-expansion pressure or higher pre-expansion temperature, results in a longer residence time in the expansion region and thus a longer particle growth time. Furthermore, a decrease in pre-expansion pressure or an increase in pre-expansion temperature is associated with a decrease in saturation, corresponding to an increase in the critical particle radius and a decrease in the nucleation rate.^{6,7} Our results compare favourably with earlier data of Helfgen *et al.* which found

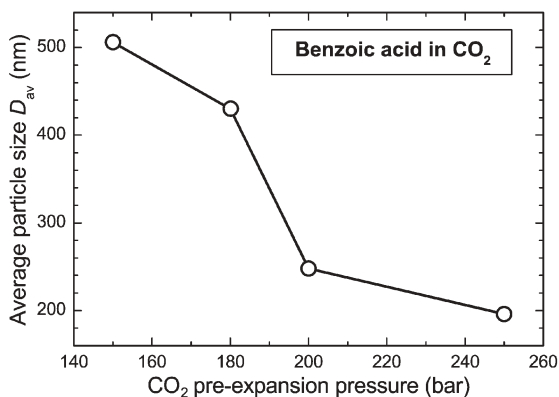


Fig. 3 Average particle size D_{av} as a function of pre-expansion pressure P_0 for the system benzoic acid–CO₂, with $T_0 = T_{nozzle} = 378$ K and $T_{extr} = 326$ K.

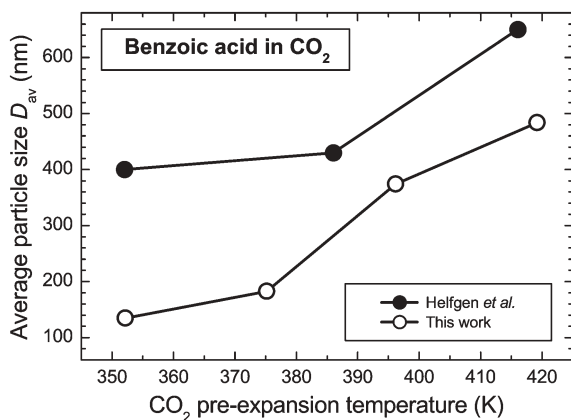


Fig. 4 Average particle size D_{av} as a function of pre-expansion temperature T_0 for the system benzoic acid–CO₂, with $P_{extr} = P_0 = 200$ bar and $T_{extr} = 332$ K. ●, Data from Helfgen *et al.*^{6,7}; ○, this work.

similar trends. However, the magnitudes of the particle sizes in comparison with those of Helfgen *et al.* differ somewhat. A visual comparison of data in this work with a sample from ref. 7 is provided in Fig. 4 for the dependence on pre-expansion temperature. It can clearly be seen that the particle sizes of Helfgen *et al.* are larger. Reasons for this may include differences in the extraction conditions, nozzle temperature and design, and even the RESS set-ups themselves. Unfortunately, it is difficult to ascertain the exact T_{extr} and T_{nozzle} used by Helfgen *et al.* in order to compare with the results of this work. However, the most important factors are likely to be the conditions within the expansion chamber,

Table 1 Average particle diameter D_{av} and associated standard deviation σ as a function of pre-expansion pressure P_0 determined from the 3-WEM data of benzoic acid–CO₂ expansions, with $T_0 = T_{nozzle} = 378$ K and $T_{extr} = 326$ K

P_0 /bar	D_{av} /nm	σ
150	506	0.87
180	430	0.60
200	248	0.85
250	196	0.85

Table 2 Average particle diameter D_{av} and associated standard deviation σ as a function of pre-expansion temperature T_0 determined from the 3-WEM data of benzoic acid–CO₂ expansions, with $P_{extr} = P_0 = 200$ bar and $T_{extr} = 332$ K

T_0 /K	D_{av} /nm	σ
352	135	0.87
375	182	0.79
396	374	0.58
419	484	0.58

including the air flow rate, because these conditions are thought to ultimately influence the final particle size.^{6,7,25}

3.3. Dependence of benzoic acid and aspirin particle size on distance from the nozzle

To the best of our knowledge no systematic *in-situ* on-line particle-size measurements have been previously performed as a function of distance from the nozzle. When using off-line techniques varying results have been obtained. For instance, Kayrak *et al.* found an increase of ibuprofen particle diameter by a factor of two when increasing the spraying distance from 2 to 6 cm.²⁶ For the same substance, Foster and co-workers observed a slight decrease in particle size between 7 and 11 cm spraying distance.²⁷ The analysis of such data is complicated by the fact that particles may aggregate due to the collection process and have to be dispersed by a solvent, with unknown impact on the determined PSD.

It is recognized that RESS-produced particles continue to grow behind the Mach disc within the expansion chamber as a result of coagulation,^{6,7,25} hence measurements such as those in the current study will hopefully provide important information on this process and input for future theoretical studies of RESS expansions.

We have determined the size of benzoic acid and aspirin particles as a function of the distance from the RESS nozzle. The experimental conditions and results are given in Fig. 5 and Table 3. There is no obvious correlation between size and distance. The particle sizes are roughly 350 nm and 160 nm for benzoic acid and aspirin, respectively. Obviously, the particle

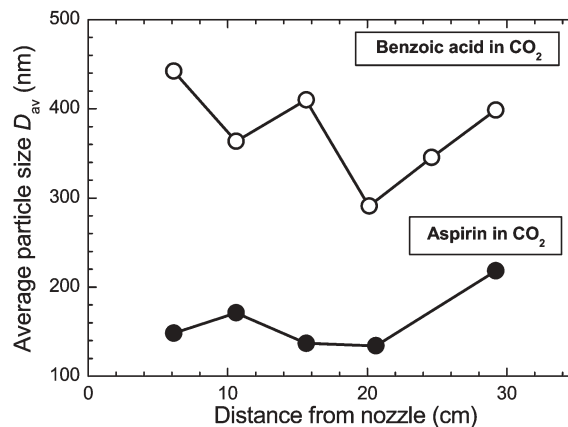


Fig. 5 Average particle size D_{av} as a function of distance from the RESS nozzle for the systems benzoic acid–CO₂ ($P_{extr} = P_0 = 200$ bar; $T_{extr} = 336$ K; $T_0 = T_{nozzle} = 376$ K) and aspirin–CO₂ ($P_{extr} = P_0 = 250$ bar; $T_{extr} = 333$ K; $T_0 = T_{nozzle} = 372$ K).

Table 3 Average particle diameter D_{av} and associated standard deviation σ as a function of distance from the RESS nozzle determined from the 3-WEM data of benzoic acid–CO₂ expansions ($P_{extr} = P_0 = 200$ bar, $T_{extr} = 336$ K, and $T_0 = T_{nozzle} = 376$ K) and aspirin–CO₂ expansions ($P_{extr} = P_0 = 250$ bar, $T_{extr} = 333$ K, and $T_0 = T_{nozzle} = 372$ K)

Distance/cm	D_{av}/nm	σ
Benzoic acid–CO ₂		
6.1	442	0.59
10.6	363	0.68
15.6	410	0.61
20.1	291	0.78
24.6	345	0.65
29.2	399	0.62
Aspirin–CO ₂		
6.1	148	0.79
10.6	171	0.73
15.6	137	0.86
20.6	134	0.87
29.2	218	0.88

growth processes have already ceased not too far away from the Mach disc, which is extremely close to the throat of the sapphire nozzle used in the current experiments. The processes of particle growth behind the Mach disc are still not very well understood, although the dominant process is most likely coagulation. The calculations of Helfgen *et al.* indicate that the average particle size is only a few nanometres at the Mach disk, and that substantial particle growth still occurs at a considerable distance behind the Mach disc. Our results show, however, that this growth has definitely stopped at a distance of centimetres. On the other hand, there is some experimental evidence that additional particle growth in the expansion chamber can be achieved if the residence time of the particles is deliberately increased. Helfgen *et al.* carried out experiments in which additional air was supplied to the expansion chamber in order to vary the residence time and therefore the growth time of the particles inside the expansion chamber.²⁵ Their results indicated a decrease in particle size with increasing volume flow of air. Although it is an appealing interpretation that additional air flow shortens the residence time and leads to smaller particles, these results have to be taken with caution. It is also possible that the additional flow of air skews the particle size distribution by removing particles from the expansion chamber at different rates depending on their size.

3.4. Dependence of cholesterol particle size on the amount and type of co-solvent added

The addition of small amounts of liquid co-solvents to supercritical CO₂ is known to significantly enhance the solubility of cholesterol, aspirin and other substances in CO₂, and has recently received considerable attention.^{8–19} For instance, the solubility of cholesterol in CO₂ increases by roughly a factor of 2 when different organic solvents are used as co-solvent.^{8,9} An even larger effect is observed for aspirin, where its solubility increases 14 times when adding 3 mol% ethanol or methanol,¹⁰ and 5 times by adding 3 mol% acetone.¹¹

So far there has been no systematic RESS study in the literature as to whether the addition of co-solvent has any effect on particle size. Therefore, we carried out 3-WEM measurements for cholesterol–CO₂ expansions for different

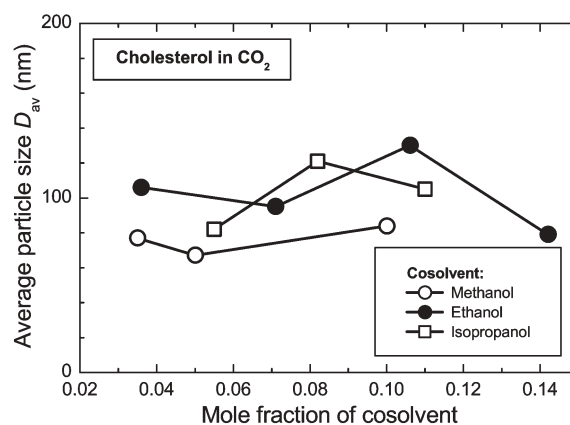


Fig. 6 Average particle size D_{av} as a function of mole fraction of co-solvent methanol, ethanol and isopropanol for RESS expansions of cholesterol–CO₂–alcohol co-solvent mixtures. See Table 4 for pre-expansion conditions.

types and amounts of added alcohols. The results are plotted in Fig. 6 and tabulated in Table 4. Interestingly, there is no correlation between the amount and type of co-solvent added, and the particle size (~ 100 nm in all cases). This might be explained by the low solubility of cholesterol in CO₂, compared with molecules such as benzoic acid, resulting in the changes in particle size being too small to detect using 3-WEM. Our results imply that addition of a liquid co-solvent might be a viable way to increase the particle yield for substances having low solubilities in CO₂, without affecting the desired average particle diameter.

It should be noted that our data for cholesterol are already approaching the lower limit of particle-size detection using 3-WEM. As can be observed, the cholesterol particle sizes with methanol as co-solvent are generally smaller: however, it is difficult to assess whether this is meaningful because of the errors one would expect at the lower limit of the 3-WEM set-up. In any case, the average diameters from the 3-WEM measurements were also consistent with our preliminary results for pure cholesterol–CO₂ expansions using a laser

Table 4 Average particle diameter D_{av} and associated standard deviation σ as a function of distance from the RESS nozzle determined from the 3-WEM data for RESS expansions of cholesterol–CO₂ with added alcohol co-solvent. Methanol: $P_{extr} = P_0 = 250$ bar, $T_{extr} = 333$ K, and $T_0 = T_{nozzle} = 371$ K; ethanol: $P_{extr} = P_0 = 250$ bar, $T_{extr} = 336$ K, and $T_0 = T_{nozzle} = 374$ K; isopropanol: $P_{extr} = P_0 = 250$ bar, $T_{extr} = 338$ K, and $T_0 = T_{nozzle} = 373$ K

Mole fraction	D_{av}/nm	σ
Cholesterol–CO ₂ –methanol		
0.035	77	0.96
0.050	67	0.84
0.100	84	0.95
Cholesterol–CO ₂ –ethanol		
0.036	106	0.95
0.071	95	0.94
0.106	130	0.98
0.142	79	0.96
Cholesterol–CO ₂ –isopropanol		
0.055	82	0.97
0.082	121	0.98
0.110	105	0.96

diffraction set-up (Malvern Spraytech). The latter had a lower detection limit of about 200 nm, and a satisfactory agreement with the upper level of the PSDs determined by the 3-WEM and Spraytech systems was found. The particle sizes we obtained were also in agreement with the experimental data of Helfgen *et al.* for cholesterol–CO₂ expansions without co-solvent.^{6,7}

4. Conclusions

We have performed RESS studies on benzoic acid, cholesterol and aspirin, in which the influence of several expansion parameters on the particle size has been studied using 3-WEM detection. For benzoic acid, the average particle diameter D_{av} decreased with increasing pre-expansion pressure, and increased with increasing pre-expansion temperature. This is probably due to a lower mass flow rate, which is associated with a lower pre-expansion pressure or higher pre-expansion temperature, as outlined above. Careful regulation of the mass flow rate therefore allows us to control the particle size within certain (relatively narrow) limits, in the specific case of benzoic acid between *ca.* 100 and 500 nm. No obvious correlation between D_{av} and the distance from the RESS nozzle has been found for benzoic acid and aspirin particles, indicating that particle growth processes have already stopped not too far away from the Mach disc. In addition, no correlation between the amount and type of co-solvent could be found for cholesterol expansions in CO₂, where particle sizes of ~100 nm were obtained for a range of alcohols. The addition of non-toxic co-solvents to RESS expansions might therefore be a viable way to produce a larger particle density in cases where solutes with extremely low solubility are to be micronized. Clearly, a detailed flow-field modelling, preferably using 3-D simulations, will be required to understand all the systematic trends observed in the current study, and ultimately predict particle sizes in RESS expansions for arbitrary systems.

Acknowledgements

We are grateful to the Alexander von Humboldt Foundation (“Sofja Kovalevskaja Program”) for the generous financial support and Professor Wolfgang Wagner for providing the numerical code for the implementation of the Span–Wagner equation of state. We also thank Malvern Instruments for their generous loan of a Spraytech system, and especially

Michael Saar for his support and assistance in some of the measurements.

References

- 1 R. C. Petersen, D. W. Matson and R. D. Smith, *J. Am. Chem. Soc.*, 1986, **108**, 2102.
- 2 M. Weber and M. C. Thies, in *Supercritical Fluid Technology in Materials Science and Engineering*, ed. Y.-P. Sun, Marcel Dekker, New York, 2002, p. 387.
- 3 Z. Knez and E. Weidner, *Curr. Opin. Solid State Mater. Sci.*, 2003, **7**, 353.
- 4 K. Oum, J. J. Harrison, C. Lee, D. A. Wild, K. Luther and T. Lenzer, *Phys. Chem. Chem. Phys.*, 2003, **5**, 5467.
- 5 K. Schaber, A. Schenkel and R. A. Zahoransky, *Tech. Mess.*, 1994, **61**, 295.
- 6 B. Helfgen, M. Türk and K. Schaber, *Powder Technol.*, 2000, **110**, 22.
- 7 B. Helfgen, P. Hils, C. Holzknicht, M. Türk and K. Schaber, *J. Aerosol Sci.*, 2001, **32**, 295.
- 8 N. R. Foster, H. Singh, S. L. J. Yun, D. L. Tomasko and S. J. Macnaughton, *Ind. Eng. Chem. Res.*, 1993, **32**, 2849.
- 9 Z. Huang, S. Kawi and Y. C. Chiew, *J. Supercrit. Fluids*, 2004, **30**, 25.
- 10 Z. Huang, Y. C. Chiew, W.-D. Lu and S. Kawi, *Fluid Phase Equilib.*, 2005, **237**, 9.
- 11 Z. Huang, W. D. Lu, S. Kawi and Y. C. Chiew, *J. Chem. Eng. Data*, 2004, **49**, 1323.
- 12 Ö. Güclü-Üstündag and F. Temelli, *J. Supercrit. Fluids*, 2005, **36**, 1.
- 13 B. Wang, Q. Li, Z. Zhang, J. Yang and Y. Liu, *Korean J. Chem. Eng.*, 2006, **23**, 131.
- 14 Q. Li, C. Zhong, Z. Zhang and Q. Zhou, *Korean J. Chem. Eng.*, 2004, **21**, 1173.
- 15 F. E. Wubbolts, O. S. L. Bruinsma and G. M. van Rosmalen, *J. Supercrit. Fluids*, 2004, **32**, 79.
- 16 M. J. Noh, T. G. Kim, I. K. Hong and K.-P. Yoo, *Korean J. Chem. Eng.*, 1995, **12**, 48.
- 17 E. Ruckenstein and I. Shulgin, *Ind. Eng. Chem. Res.*, 2003, **42**, 1106.
- 18 P. Muthukumar, R. B. Gupta, H.-D. Sung, J.-J. Shim and H.-K. Bae, *Korean J. Chem. Eng.*, 1999, **16**, 111.
- 19 N. Vedaraman, G. Brunner, C. Srinivasakannan, C. Muralidharan, P. G. Rao and K. V. Raghavan, *J. Supercrit. Fluids*, 2004, **32**, 231.
- 20 G. Mie, *Ann. Phys.*, 1908, **25**, 377.
- 21 R. Ehrig and U. Nowak, LIMEX 4.2A, Konrad-Zuse-Zentrum für Informationstechnik (ZIB), Berlin, 2000.
- 22 R. Span and W. Wagner, *J. Phys. Chem. Ref. Data*, 1996, **25**, 1509.
- 23 M. Türk, *J. Supercrit. Fluids*, 1999, **15**, 79.
- 24 J. J. Harrison, T. Lenzer and K. Oum, to be published.
- 25 B. Helfgen, M. Türk and K. Schaber, *J. Supercrit. Fluids*, 2003, **26**, 225.
- 26 D. Kayrak, U. Akman and Ö. Hortacsu, *J. Supercrit. Fluids*, 2003, **26**, 17.
- 27 M. Charoenchaitrakool, F. Dehghani, N. R. Foster and H. K. Chan, *Ind. Eng. Chem. Res.*, 2000, **39**, 4794.
- 28 Z. Huang, G.-B. Sun, Y. C. Chiew and S. Kawi, *Powder Technol.*, 2005, **160**, 127.

Synthesis of bi- and tricyclic β -lactam libraries in aqueous medium†

Iván Kanizsai,^a Szilvia Gyónfalvi,^a Zsolt Szakonyi,^a Reijo Sillanpää^b and Ferenc Fülöp^{*a}

Received 12th September 2006, Accepted 21st December 2006

First published as an Advance Article on the web 18th January 2007

DOI: 10.1039/b613117d

Water as a solvent is not only inexpensive and environmentally benign, but may allow good reactivity. The present work focuses on the application of a modified Ugi reaction, *i.e.* the Ugi four-centre three-component reaction (U-4C-3CR), in aqueous medium to construct β -lactam libraries. All the attempted reactions could be successfully performed in water. The reaction conditions under which the precipitation process was effective were investigated; no further work-up or purification was necessary. In several cases when less water-soluble β -amino acids were used, the precipitated products were isolated easily by simple filtration. In other cases, evaporation of the solvent was appropriate for isolation; when the product was crystalline, recrystallization was necessary to obtain the pure final compounds. In water, the yields were higher as compared with the reactions in organic solvents. When bicyclic β -amino acids and the bulky *tert*-butyl isocyanide were used as starting materials, noteworthy increases in diastereoselectivity were observed.

Introduction

In most cases, water comprises a contaminant for organic chemists, unless it is used as a reactant. However, attention has recently turned to the possibility of using water as a solvent for organic reactions.^{1,2} Pirrung *et al.* reported higher reaction rates in aqueous medium as compared with organic solvents for multicomponent reactions such as the Ugi reaction.^{3–5} This difference was attributed to the hydrophobic effect, enhanced hydrogen bonding in the transition state, and the high cohesive energy density of water. In contrast, Mironov *et al.* observed a considerably lower rate when an aqueous medium was applied for the Ugi reaction.⁶ The use of water as a solvent for organic transformations offers several advantages, such as less environmental pollution and the cheapness relative to organic solvents. A further benefit is that the products are often insoluble in water and this can facilitate their isolation.

Multicomponent reactions such as the isocyanide-based Ugi condensations may afford a possibility to prepare numerous and very diverse products in fewer steps than was possible before.^{7–11} The traditional Ugi 4-component condensation incorporates a carboxylic acid, an amine, a carbonyl compound and an isocyanide in a one-pot condensation. For example, α -acetocarboxamides are synthesized in good yields and with good diastereoselectivity by this method. In modified Ugi 4- or 5-centre, 3- or 4-component reactions (U-4C-3CR or U-5C-4CR), α - or β -amino acids containing two functional groups (a carbonyl and an amine) in the same compound are obtained. This amended protocol provides a chance to prepare α - or β -amino acid derivatives and heterocyclic libraries,

e.g. β -lactams, benzodiazepines, piperazines, morpholines and other derivatives.^{12–19} In the past few years, much attention has been paid to the synthesis of β -lactam derivatives as selective protease inhibitors against serine protease, elastase, cysteine protease and papain.^{20–22}

Racemic and enantiopure β -amino acids are of increasing significance as building blocks in the synthesis of β -lactam pharmacophores, and as segments in peptides. These molecules possess a great variety of biological activities.^{23,24} In recent years, the diversity of β -amino acids has rapidly increased and has opened the door to the design and synthesis of biologically active peptidomimetics, β -lactam antibiotics, heterocycles and related compounds, *e.g.* taxol derivatives.^{25–28} These structurally diverse β -amino acids are also popular as starting materials for combinatorial synthesis. Combinatorial libraries of β -lactams have been successfully prepared in MeOH using the U-4C-3-CR, *cis* alicyclic and *diexo* bicyclic β -amino acids being used as bifunctional starting materials for intramolecular cyclization.^{29–31}

The aim of the present work was to create a β -lactam library in aqueous medium similarly to that obtained in MeOH, with optimization of the reaction condition, the yields, the stereoselectivity and the isolation technique.

Results and discussion

Fig. 1 shows the compounds selected for the construction of the β -lactam library: 4 aliphatic or aromatic aldehydes (**A–D**), 8 cyclic β -amino acids (*cis*-2-aminocyclopentane- (**I**), *cis*-2-aminocyclohexane- (**II**), 6-aminocyclohex-3-ene- (**III**), 2-aminocyclohex-3-ene- (**IV**), *diendo*-3-aminobicyclo[2.2.1]heptane-2- (**V**), *diexo*-3-aminobicyclo[2.2.1]heptane-2- (**VI**), *diendo*-3-aminobicyclo[2.2.1]hept-5-ene-2- (**VII**) or *diexo*-3-aminobicyclo[2.2.1]hept-5-ene-2-carboxylic acid (**VIII**)), and cyclohexyl (**a**) or *tert*-butyl isocyanide (**b**). Fig. 2 shows the *N*-substituted β -lactams synthesized (**2a–q**).

^aInstitute of Pharmaceutical Chemistry, University of Szeged, POB 427, H-6701, Szeged, Hungary. E-mail: fulop@pharm.u-szeged.hu; Fax: +36-62-545705; Tel: +36-62-545564

^bDepartment of Chemistry, University of Jyväskylä, POB 35, 40351, Jyväskylä, Finland

† Electronic supplementary information (ESI) available: Compound characterization details. See DOI: 10.1039/b613117d

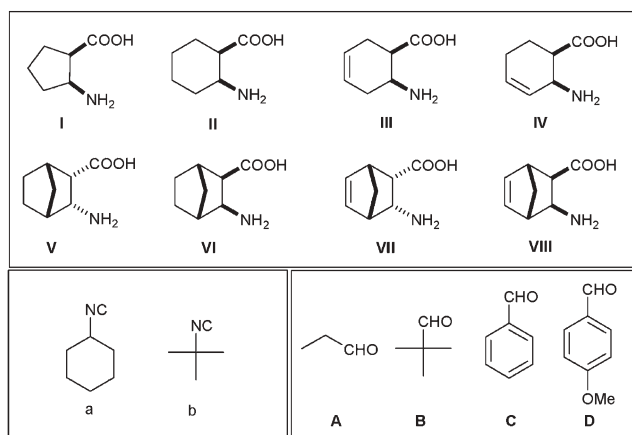


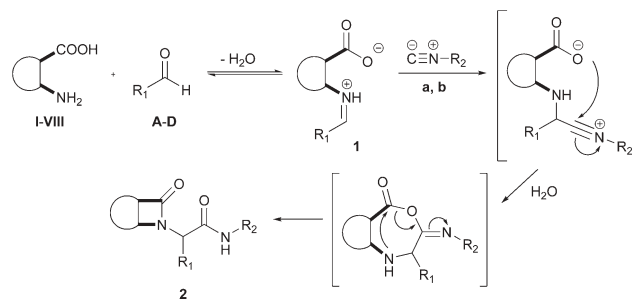
Fig. 1 Building blocks of Ugi libraries generated from β -amino acids (I–VIII), isocyanides (a, b) and aldehydes (A–D).

In the first step of the general method, the β -amino acid (I–VIII) was reacted with the appropriate aldehyde (A–D), resulting in protonated Schiff base **1**, followed by addition of the isocyanide (a, b) to afford β -lactam **2** via intramolecular cyclization and rearrangement (Scheme 1).

Racemic β -amino acids were used in 10% excess, with equimolar amounts of the aldehyde and isocyanide. The diversity of the final Ugi products was increased by the aldehyde constituent, since aldehydes are available commercially in a great structural variety. It should be mentioned that the relatively poor solubility of the different aldehydes in aqueous medium reduced their applicability. Because of the high number of possible combinations, only representative members of the library were prepared.

In all cases, the condensation of the three participants led to the formation of a new stereogenic centre at position C2 of the acetamido group in the β -lactam product and afforded diastereoselective reactions (Table 1).

For this protocol, different quantities of water were used to achieve a critical concentration of the corresponding intermediate Schiff bases. We experienced that the concentration



Scheme 1

was a determining factor. Precipitation occurred when less water-soluble β -amino acids and an appropriate amount of water were used. In this way, the reactions were complete in 1 day at room temperature, as compared with a 3 day reaction in methanol. Products **2j**, **2l** and **2p** were precipitated in moderate yields, in purities of 65–91%. When precipitation was not observed, products were isolated in moderate to good yields by evaporation of the water. In most cases, the crude products (**2**) were sufficiently pure to allow analytical identification and further purification was not required. With anisaldehyde (D), solid β -lactams (**2b**, **2f**, **2k**, **2m** and **2q**) were isolated in yields of 44–57%; in consequence of decomposition of the aldehyde, crystallization was necessary to remove the remaining contamination. With aliphatic aldehydes such as propion- and pivalaldehyde, good yields were obtained.

The diastereomeric ratio ranged from 60 : 40 to 100 : 0. Quantitatively diastereoselective reactions were mainly observed when the β -amino acid component contained a norbornane or norbornene skeleton. Comparison of the diastereomeric ratios obtained in the aqueous phase or in an organic solvent did not reveal appreciable differences. However, the yields were slightly better in water than in organic media.¹³ The structures of the major isomers **2a–q** were determined, with **2q** as a representative example, by X-ray crystallography (Fig. 3).

In conclusion, we found that the U-4C-3CR functions efficiently in aqueous medium. Relative to organic media,

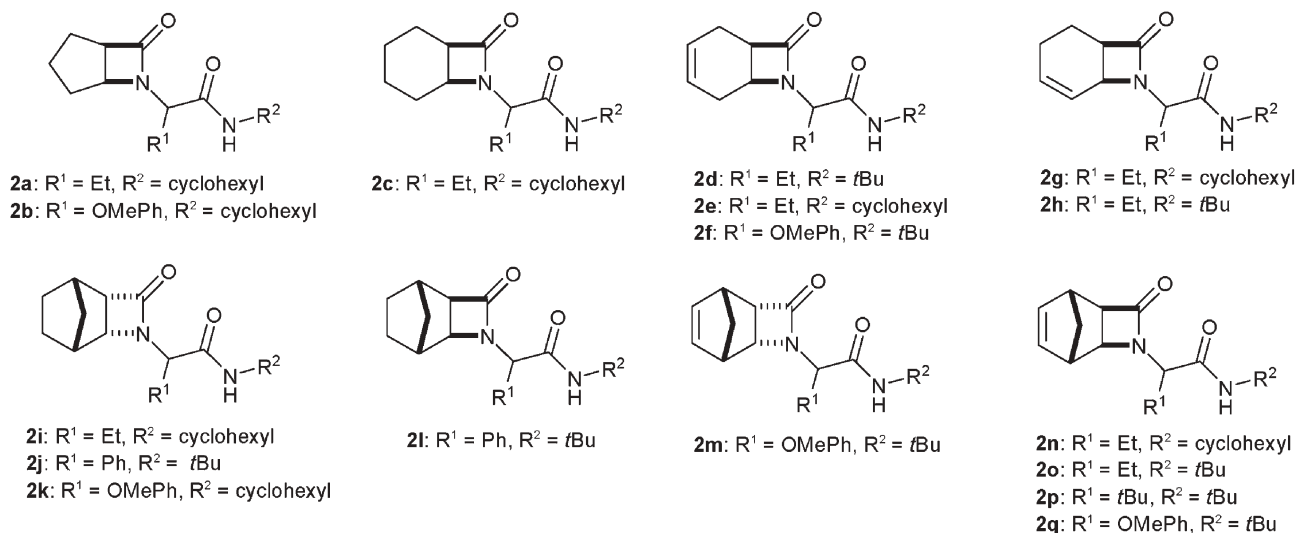


Fig. 2 Structures of the β -lactam derivatives prepared **2a–q**.

Table 1 Yields, melting points and diastereomeric ratios of compounds **2a–q**

Product	β -Amino acid	Aldehyde (R^1)	Isocyanide (R^2)	Yield (%)	Mp/ $^{\circ}$ C	d.r. ^a
2a	I	A (Et)	a (cyclohexyl)	87 ^b	oil	68 : 32
2b	I	D (OMePh)	a (cyclohexyl)	44 ^c	208–210	100 : 0
2c	II	A (Et)	a (cyclohexyl)	72 ^b	oil	75 : 25 ^e
2d	III	A (Et)	b (<i>t</i> Bu)	74 ^b	oil	66 : 34 ^e
2e	III	A (Et)	a (cyclohexyl)	70 ^b	oil	66 : 34
2f	III	D (OMePh)	b (<i>t</i> Bu)	50 ^c	204–207	63 : 36
2g	IV	A (Et)	a (cyclohexyl)	86 ^b	oil	68 : 32
2h	IV	A (Et)	b (<i>t</i> Bu)	91 ^b	oil	67 : 33
2i	V	A (Et)	a (cyclohexyl)	79 ^b	oil	86 : 14
2j	V	C (Ph)	b (<i>t</i> Bu)	45 ^d	117–120	100 : 0
2k	V	D (OMePh)	a (cyclohexyl)	51 ^c	251–254	100 : 0
2l	VI	C (Ph)	b (<i>t</i> Bu)	35 ^d	140–146	92 : 8
2m	VII	D (OMePh)	b (<i>t</i> Bu)	48 ^c	193–196	100 : 0
2n	VIII	A (Et)	a (cyclohexyl)	90 ^b	oil	62 : 38
2o	VIII	A (Et)	b (<i>t</i> Bu)	95 ^b	oil	60 : 40
2p	VIII	B (<i>t</i> Bu)	b (<i>t</i> Bu)	51 ^d	200–202	100 : 0
2q	VIII	D (OMePh)	b (<i>t</i> Bu)	57 ^c	218–222	83 : 17

^a The diastereomeric ratios were established by ¹H-NMR on the crude products. ^b The compounds were isolated by evaporation of the solvent; the yields and purities were estimated by ¹H-NMR. ^c The final compounds were isolated as crystalline forms after evaporation; the yields are given for the recrystallized products. ^d The products precipitated from the aqueous solution. ^e The diastereomeric ratios matched those reported previously (**2c** 3 : 1 and **2d** 2 : 1).²⁹

water as a solvent has several advantages, such as the environmentally benign and mild conditions and a shorter reaction time. Additionally, the experimental procedures may be simplified since the final products may be isolated by simple filtration. This benefit can be exploited when less water-soluble, *e.g.* norbornene-based β -amino acids are utilized. As exemplified in this publication, the unique solvating properties of water have beneficial effects on the Ugi reaction with respect to the diastereoselectivity and the shorter reaction time.

Experimental

General procedure for the preparation of β -lactams (**2a–q**)

To the β -amino acid (**I–VIII**) (1.1 mmol) dissolved in a few drops of water, the corresponding aldehyde (**A–D**) (1.0 mmol) was added dropwise. Further water was then cautiously added

dropwise until the generated Schiff base just dissolved. The reaction was stirred for 1 h at room temperature, followed by addition of the isocyanide (**a**, **b**) (1.0 mmol). The resulting mixture was stirred for 1 day at room temperature. The precipitate (**2j**, **2l** and **2p**) was then filtered off. When the product did not precipitate, the aqueous solution was evaporated *in vacuo*, which resulted in **2a**, **2c–e**, **2g–i**, **2n** and **2o** in more than 85% purity. For **2b**, **2f**, **2k**, **2m**, and **2q**, the β -lactams were obtained as solids and were crystallized with EtOH/EtOAc to remove the remaining aldehyde **D** and other decomposed material.

The preparations of **2i** and **2q** are presented with physical and spectroscopic data below. Details on the other fully characterized compounds are available in the ESI.†

diendo-N-Cyclohexyl-2-(4-oxo-3-azatricyclo[4.2.1.0^{2,5}]non-3-yl)butyramide (2i)

This compound was obtained as a yellow oil, diastereoisomeric ratio 86 : 14, (0.18 g, 79%); (found: C, 71.14; H, 9.31; N, 9.19. C₁₈H₂₈N₂O₂ requires C, 71.02; H, 9.27; N, 9.20%); ν_{\max} (film)/cm⁻¹ 3284, 3078, 2936, 2848, 2664, 2364, 1740, 1647, 1550, 1444, 1260; δ_{H} (400 MHz, CDCl₃, Me₄Si): major diastereomer: 0.93 (3H, t, *J* 7.55, CH₂CH₃), 1.12–1.99 (18H, m, 8 \times CH₂ and 2 \times CH), 2.33–2.45 (2H, m, CHCH₂CH), 3.37 (1H, dd, *J* 2.01 and 6.04, CHCHCO), 3.67–3.80 (1H, m, NHCH), 3.94 (1H, t, *J* 8.05, CHCHN), 3.99 (1H, t, *J* 5.04, NCHCO) and 6.58 (1H, d, *J* 7.06, NH); minor diastereomer: 0.96 (3H, t, *J* 7.55, CH₂CH₃), 1.12–1.99 (18H, m, 8 \times CH₂ and 2 \times CH), 2.33–2.45 (2H, m, CHCH₂CH), 3.55 (1H, t, *J* 7.71, CHCHCO), 3.67–3.80 (1H, m, NHCH), 3.87 (1H, t, *J* 8.06, CHCHN), 3.93 (1H, t, *J* 5.04, NCHCO) and 7.35 (1H, d, *J* 7.06, NH); δ_{C} (100 MHz, CDCl₃, Me₄Si): major diastereomer: 11.2, 23.8, 24.7, 25.3, 26.1, 26.6, 33.2, 36.8, 38.9, 43.3, 48.7, 58.6, 59.1, 59.4, 61.5, 63.4, 168.8 and 171.7; minor diastereomer: 11.3, 23.8, 24.9, 25.2, 26.0, 26.4, 36.8, 38.5, 43.4, 48.7, 58.6, 58.9, 59.1, 59.4, 61.5, 63.4, 170.3 and 171.7; *m/z* (EI) 306 (M⁺ + 2H, 1), 305 (M⁺ + H, 3), 304 (M⁺, 2), 211(6), 180 (3), 179 (35), 178

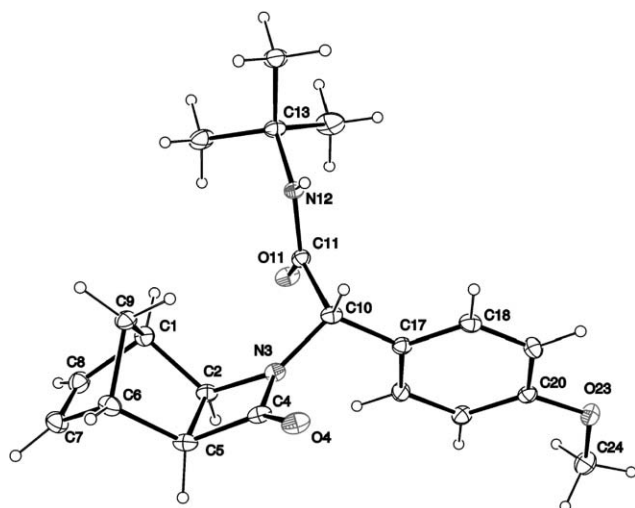


Fig. 3 Perspective view of **2q**. Thermal ellipsoids have been drawn with a probability level of 20% (ORTEP plot).

(100), 150 (4), 123 (18), 122 (4), 121 (8), 93 (8), 83 (4), 67 (12), 66 (10), 57 (7), 41 (7).

diexo-2-(4-Methoxyphenyl)-N-tert-butyl-2-(4-oxo-3-azatricyclo[4.2.0.1^{2,5}]non-7-en-3-yl) acetamide (2q)

This compound was obtained as yellowish crystals, diastereoisomeric ratio 83 : 17, (0.14 g, 57%); mp 218–222 °C; (found: C, 71.23; H, 7.40; N, 7.91. C₂₁H₂₆N₂O₃ requires C, 71.16; H, 7.39; N, 7.90%); ν_{\max} (film)/cm⁻¹ 3332, 3058, 2973, 1731, 1672, 1513, 1454, 1299; δ_{H} (400 MHz, CDCl₃, Me₄Si): major diastereomer: 1.26 (9H, s, *t*Bu), 1.54 (1H, d, *J* 9.56, CHCHCO), 1.66 (1H, d, *J* 10.07, CHCHN), 2.81–2.85 (2H, m, CHCH₂CH), 2.98–3.03 (1H, m, CHCHCO), 3.32 (1H, d, *J* 3.53, CHCHN), 3.73 (3H, s, OCH₃), 5.08 (1H, s, NCHCO), 5.96 (1H, 2 × d, *J* 3.02 and 5.54, CHCH), 6.12 (1H, *J* 3.02 and 5.54, CHCH), 6.36 (1H, br s, NH), 6.80 (2H, d, *J* 8.06, C₆H₄OMe-*p*) and 7.26 (2H, d, *J* 8.06, C₆H₄OMe-*p*); minor diastereomer: 1.32 (9H, s, 3 × Me), 1.35–1.41 (2H, m, CHCH₂CH), 2.16–2.21 (1H, m, CHCHCO), 2.84–2.89 (1H, m, CHCHN), 3.02 (1H, d, *J* 3.53, CHCHCO), 3.81 (3H, s, OMe), 3.83 (1H, d, *J* 4.03, CHCHN), 5.21 (1H, s, NCHCO), 5.92 (1H, 2 × d, *J* 3.02 and 5.54, CHCH), 6.10 (1H, br s, NH), 6.16 (1H, 2 × d, *J* 3.02 and 5.54, CHCH), 6.86–6.92 (2H, m, C₆H₄OMe-*p*) and 7.31–7.36 (2H, m, C₆H₄OMe-*p*); δ_{C} (100 MHz, CDCl₃, Me₄Si): major diastereomer: 29.1, 39.7, 41.9, 43.8, 52.1, 55.8, 56.4, 58.1, 61.1, 114.8, 128.2, 130.2, 136.2, 139.2, 160.1, 168.4 and 170.0; minor diastereomer: 29.3, 39.9, 41.9, 43.8, 56.5, 58.1, 61.6, 114.9, 130.4, 136.2, 139.3, 160.1, 168.5 and 170.1; *m/z* (EI) 355 (M + H⁺, 1), 271 (1), 255 (52), 254 (100), 189 (8), 188 (24), 162 (82), 136 (4), 121 (16), 120 (4), 88 (60), 70 (10), 66 (24), 58 (1).

X-ray crystallographic study. Crystallographic data were collected at 173 K with a Nonius-Kappa CCD area detector diffractometer using graphite-monochromatized Mo-K α radiation ($\lambda = 0.71073$ Å). The data were collected by φ and ω rotation scans and processed with the DENZO-SMN v0.93.0 software package.³²

Crystal data for **2q**: C₂₁H₂₆N₂O₃, *M*_r = 354.44, triclinic, space group *P*-1 (no. 2), *a* = 9.4031(5), *b* = 9.3855(5), *c* = 11.0060(6) Å, $\alpha = 78.010(3)$, $\beta = 84.307(3)$, $\gamma = 82.744(3)^\circ$, *V* = 939.84(9) Å³, *T* = 173 K, *Z* = 2, $\mu(\text{Mo-K}\alpha) = 0.084$ mm⁻¹, 3897 unique reflections (*R*_{int} = 0.0348) which were used in calculations. The final *wR*(*F*²) was 0.1110 (all data).

The structure was solved by direct methods by use of the SIR97 program³³ and full-matrix, least-squares refinements on *F*² were performed by use of the SHELXL-97 program.³⁴ The CH hydrogen atoms were included at the fixed distances with the fixed displacement parameters from their host atoms. The NH hydrogen atom was refined isotropically. The figure was drawn with ORTEP-3 for Windows.³⁵

Acknowledgements

We are grateful to the Hungarian Research Foundation (OTKA No. T047186) and the National Research and Development Office, Hungary (GVOP-311-2004-05-0255/3.0

and GVOP-3.2.1-2004-04-0345/3.0) for financial support. We thank Dr Anasztázia Hetényi for the NMR interpretations.

References

- C.-J. Li, *Chem. Rev.*, 1993, **93**, 2023–2035.
- U. M. Lindström, *Chem. Rev.*, 2002, **102**, 2751–2771.
- M. C. Pirrung and K. Das Sarma, *J. Am. Chem. Soc.*, 2004, **126**, 444–445.
- M. C. Pirrung and K. Das Sarma, *Synlett*, 2004, **8**, 1425–1427.
- M. C. Pirrung and K. Das Sarma, *Tetrahedron*, 2005, **61**, 11456–11472.
- M. A. Mironov, M. N. Ivantsova, M. I. Tokareva and V. S. Mokrushin, *Tetrahedron Lett.*, 2005, **46**, 3957–3960.
- A. Dömling and I. Ugi, *Angew. Chem., Int. Ed.*, 2000, **39**, 3169–3210.
- A. Dömling, *Curr. Opin. Chem. Biol.*, 2002, **6**, 306–313.
- L. Weber, *Curr. Med. Chem.*, 2002, **9**, 2085–2093.
- M. Yus and D. J. Ramón, *Angew. Chem., Int. Ed.*, 2005, **44**, 1602–1634.
- A. Dömling, *Chem. Rev.*, 2006, **106**, 17–89.
- J. Kolb, B. Beck and A. Dömling, *Tetrahedron Lett.*, 2002, **43**, 6897–6901.
- C. Hulme, L. Ma, V. Kumar, P. H. Krolkowski, A. C. Allen and R. Labaudiniere, *Tetrahedron Lett.*, 2000, **41**, 1509–1514.
- C. Hulme and M. P. Cherrier, *Tetrahedron Lett.*, 1999, **40**, 5295–5299.
- T. Nixey, M. Kelly and K. Hulme, *Tetrahedron Lett.*, 2000, **41**, 8729–8733.
- A. Golebiowski, J. Jozwik, S. R. Klopfenstein, A.-O. Colson, A. L. Grieb, A. F. Russell, V. L. Rastogi, C. F. Diven, D. E. Portlock and J. J. Chen, *J. Comb. Chem.*, 2002, **4**, 584–590.
- Y. B. Kim, E. H. Choi, G. Keum, S. B. Kang, D. H. Lee, H. Y. Koh and Y. Kim, *Org. Lett.*, 2001, **3**, 4149–4152.
- S. Marcaccini, R. Pepino, T. Torroba, D. Miguel and M. Garcia-Valvedere, *Tetrahedron Lett.*, 2002, **43**, 8591–8593.
- G. Dyker, K. Breitenstein and G. Henkel, *Tetrahedron: Asymmetry*, 2002, **13**, 1929–1936.
- M. Schneider and H.-H. Otto, *Arch. Pharm. (Weinheim, Ger.)*, 2001, **334**, 167–172.
- B. Macchia, D. Gentili, M. Macchia, F. Mamone, A. Martinelli, E. Orlandini, A. Rossello, G. Cercignani, R. Pierotti, M. Allegretti, C. Asti and G. Caselli, *Eur. J. Med. Chem.*, 2000, **35**, 53–67.
- A. Clemente, A. Domingos, A. Grancho, A. P. Iley, R. Moreira, J. Neres, N. Palma, A. B. Santana and E. Valente, *Bioorg. Med. Chem. Lett.*, 2001, **11**, 1065–1068.
- F. Fülöp, *Chem. Rev.*, 2001, **101**, 2181–2204.
- F. Fülöp, T. A. Martinek and G. K. Tóth, *Chem. Soc. Rev.*, 2006, 323–334.
- I. Ugi, *Pure Appl. Chem.*, 2001, **73**, 187–191.
- J. Pitlik and C. Townsend, *Bioorg. Med. Chem. Lett.*, 1997, **7**, 3129–3134.
- C. Hanusch-Kompa and I. Ugi, *Tetrahedron Lett.*, 1998, **39**, 2725–2728.
- M. Liu and M. P. Sibi, *Tetrahedron*, 2002, **58**, 7991–8035.
- S. Gedey, P. Vainiotalo, I. Zupkó, A. M. Peter de Witte and F. Fülöp, *J. Heterocycl. Chem.*, 2003, **40**, 951–956.
- S. Gedey, J. Van der Eycken and F. Fülöp, *Org. Lett.*, 2002, **4**, 1967–1969.
- S. Gedey, J. Van der Eycken and F. Fülöp, *Lett. Org. Chem.*, 2004, **1**, 215–220.
- Z. Otwinowski and W. Minor, *Methods Enzymol.*, 1997, **276**, 307–326.
- A. Altomare, M. Cascarano, C. Giacovazzo, A. Guagliardi, M. C. Burla, G. Pilodori and M. Camalli, *J. Appl. Crystallogr.*, 1994, **27**, 435–436.
- G. M. Sheldrick, *SHELXL-97, Program for refinement of crystal structures*, University of Göttingen, Germany, 1997.
- L. J. Farrugia, *J. Appl. Crystallogr.*, 1997, **30**, 565–567.

‡ CCDC reference numbers 625418. For crystallographic data in CIF or other electronic format see DOI: 10.1039/b613117d

Influence of high pressure on solubility of ionic liquids: experimental data and correlation†‡

Urszula Domańska* and Piotr Morawski

Received 6th June 2006, Accepted 22nd December 2006

First published as an Advance Article on the web 22nd January 2007

DOI: 10.1039/b608059f

The solid–liquid phase equilibrium (SLE) in binary mixtures that contain a room-temperature ionic liquid, IL, and an organic solvent: {1-ethyl-3-methylimidazolium tosylate, [EMIM][TOS] (1) + cyclohexane, or benzene (2)} and {1,3-dimethylimidazolium methylsulfate, [MMIM][CH₃SO₄] (1) + hexan-1-ol (2)} have been measured under very high pressures up to about 900 MPa at the temperature range from $T = 328$ to 363 K. The thermostatted apparatus for the measurements of transition pressures from the liquid to the solid state was used. The pressure–temperature–composition relation of the high pressure solid–liquid phase equilibria polynomial based on the Yang model was satisfactorily used. The freezing and melting temperatures at a constant composition increase monotonously with pressure. The high pressure experimental results obtained at isothermal conditions (p – x) were interpolated to well known T – x diagrams. Additionally, the SLE of binary systems {[EMIM][TOS] (1) + cyclohexane, or benzene (2)} at normal pressure have been measured by a dynamic method from 270 K to the melting point of the IL. Experimental solubility results are compared with values calculated by means of the non-random, two-liquid equation (NRTL) utilizing parameters derived from SLE and liquid–liquid equilibria (LLE) results. The experimental results at high pressures were compared for every system to these at normal pressure. The paper includes thermophysical basic characterization of pure ionic liquids obtained *via* differential scanning calorimetry (DSC), temperatures and enthalpies of melting. The influence of the interaction between the IL and solvent on the solubility at 0.1 MPa and high pressure up to 900 MPa was discussed.

Introduction

Room Temperature Ionic Liquids (ILs), are being explored as potential environmentally benign solvents^{1–4} because of their negligible vapour pressure^{5–7} in comparison with the traditional volatile organic solvents used in industry. ILs have been studied in many chemical processes, for example, in bio processing operations, as electrolytes in electrochemistry, in gas separations such as the capturing of CO₂, in liquid–liquid extractions, and as heat-transfer fluids.^{6–12} It was found that non-volatile organic compounds can be extracted from ionic liquids using supercritical carbon dioxide, which is widely used to extract large organic compounds with minimal pollution.^{13–16} Carbon dioxide dissolves in the liquid to facilitate extraction, but the ionic liquid does not dissolve in carbon dioxide, so a pure product can be recovered. To design any process involving ionic liquids on an industrial scale it is necessary not only to know a range of physical properties including viscosity and density, but also heat capacity and

other thermodynamic properties including phase equilibria such as vapour–liquid equilibria (VLE), liquid–liquid equilibria (LLE) and solid–liquid equilibria (SLE).^{17–27}

The influence of pressure as well as that of the cation's alkyl chain length on several properties (speed of sound, density, heat capacity) of the ILs have been measured.²⁸ It was concluded that as the anion increases in size the density increases, while the sound speed shows the opposite trend: when pressure rises, density increases, compressibility decreases and the sound speed increases.²⁸ The effect of pressure on heat capacity depends on nature of the IL.²⁸ The influence of pressure (60–120 MPa) is greater when the higher temperature dependence of the isobaric expansivity of the IL is observed.²⁸

Our previous study of phase equilibria with ILs, *e.g.* of 1,3-dimethylimidazolium methylsulfate, [MMIM][CH₃SO₄], were performed with typical solvents: with *n*-alkanes (pentane, or hexane, or heptane, or octane, or decane), or cycloalkanes (cyclohexane or cycloheptane) and with aromatic hydrocarbons (benzene, or toluene, or ethylbenzene, or propylbenzene, or *o*-xylene, or *m*-xylene, or *p*-xylene).^{23–26} In these systems, the liquid–liquid phase equilibrium was mainly observed.

The present work is the continuation of our studies concerning the solid–liquid phase equilibria of binary mixtures involving *n*-alkanes and highly polar compounds, as ether, or diacetate under high pressures up to 900 MPa.^{29–31} Besides its

Physical Chemistry Division, Faculty of Chemistry, Warsaw University of Technology, Noakowskiego 3, 00-664 Warsaw, Poland.

E-mail: ula@ch.pw.edu.pl; Fax: +48-22-6282741; Tel: +48-22-6213115

† Electronic supplementary information (ESI) available: Tabulated data (Tables 1S–3S) of the experimental phase diagrams. See DOI: 10.1039/b608059f

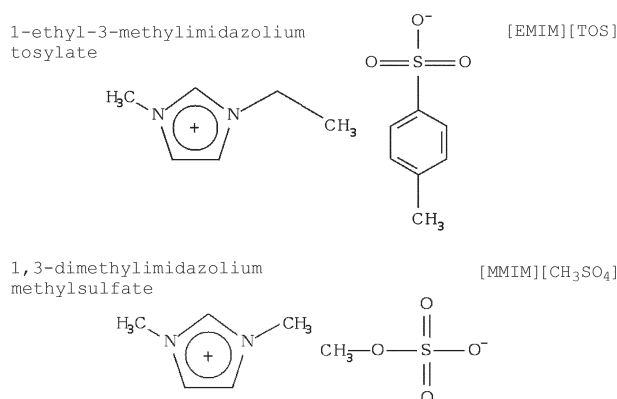
‡ Presented at the XLIX National Meeting of PTChem and SITPChem, Gdańsk, Poland, September 18–22, 2006.

importance for technological processes such as crystallization and purification at high pressure, the SLE provides a good tool for examining the thermodynamic nature of many systems.

From a historical perspective, the very first (solid + liquid) phase equilibria measurements of organic liquids at high pressure conditions were presented by Baranowski and Dudek.^{32,33} Simultaneously, results for different organic mixtures were presented by Nagaoka and Makita,^{34,35} Nagaoka *et al.*³⁶ and Tanaka and Kawakami.³⁷ Recently, Yang *et al.* presented results involving *n*-alkane mixtures with alcohols.^{38,39} The pressure effect on phase behaviour of binary mixtures of fatty acids up to 200 MPa was measured and well described by Inoue *et al.*⁴⁰ The eutectic mixtures become usually richer in the component with the highest slope dp/dT of the melting curve and the eutectic temperature rises with increasing pressure; also, different compositions of the eutectic point are observed.^{29,30,36,37}

The current study focuses on solutions of binary mixtures that contain a room-temperature ionic liquid, IL, and an organic solvent: {1-ethyl-3-methylimidazolium tosylate, [EMIM][TOS] (1) + cyclohexane, or benzene (2)} and of {1,3-dimethylimidazolium methylsulfate, [MMIM][CH₃SO₄] (1) + hexan-1-ol (2)}. The solid–liquid and liquid–liquid equilibria at normal pressure and solid–liquid under very high pressures up to about 900 MPa have been measured at the temperature range from $T = 328$ to 363 K. These (IL + solvent) binary systems were chosen from many measured by us. Pressometry is usually used for detecting the influence of pressure on the melting point, the eutectic point and the changes on liquidus curves. Thus the choice of the IL system is for low melting point and for a binary system exhibiting a simple eutectic point at ambient pressure. The influence of high pressure on the LLE cannot be observed. In the chosen systems only {[EMIM][TOS] (1) + cyclohexane (2)} presents the binary system with immiscibility in the liquid phase. The data presented here will be useful from the technological perspective, because they show the influence of high pressure on the melting temperature and liquidus curves.

The formulas of ionic liquids under study are as follows:



Phase equilibria under 0.1 MPa were correlated by the non-random, two-liquid equation (NRTL).⁴¹ The Yang equation was a thermodynamic model that was used for the correlation of the SLE in (IL + solvent) binary mixtures.^{38,39} Acceptable agreement with the experimental points was obtained.

Results and discussion

The thermophysical constants of pure ionic liquids and solvents are shown in Table 1. The salts investigated here show low melting temperatures, at normal pressure, of 322.93 and 308.90 K for [EMIM][TOS] and [MMIM][CH₃SO₄], respectively.

For this discussion, the SLE and LLE for new binary ionic liquid–organic solvent systems were determined. The experimental data of phase equilibria in binary systems of [EMIM][TOS] with cyclohexane and benzene are given in Table 1S in the ESI.† The table includes the direct experimental results of the SLE: temperatures, T/K or T_{LLE}/K versus x_1 , the mole fraction of the IL at the equilibrium temperatures for the investigated systems. The upper critical solution temperature, UCST, was observed in the system [EMIM][TOS] with cyclohexane. Maximum of the curve (above 370 K) was not observed because the boiling temperature of the solvent was lower. For the investigated mixture, it was impossible to detect by the visual method, the mutual solubility of the ILs in the solvent-rich phase. These data can be approached by the COSMO-RS calculations²⁶ and we expected the IL mole fraction of about 1×10^{-4} , as was observed in many systems. The experimental data of phase equilibria in binary systems of [MMIM][CH₃SO₄] with hexan-1-ol at normal pressure were given in our previous discussion.⁴⁸ For the {[MMIM][CH₃SO₄] + hexan-1-ol, or heptan-1-ol} simple eutectic mixtures were observed with complete miscibility in the liquid phase. Immiscibility was observed with UCSTs for the longer chain alcohols.

The ability of an IL to form hydrogen bonds or other possible interactions with potential solvents is an important feature of its behaviour. With aromatic hydrocarbons–benzene, the stronger interaction was observed of possible $n-\pi$ or $\pi-\pi$ interactions between the IL and benzene (interaction may be expected between the imidazolium ring and benzene ring). The liquidus curve was very flat, but the immiscibility in the liquid phase was not observed.

Experimental phase diagrams of SLE investigated at ambient pressure are characterized mainly by the following: (1) the shape of the equilibrium curve is similar for both [EMIM][TOS] and [MMIM][CH₃SO₄] with every solvent; (2) better solubility of [EMIM][TOS] was observed in benzene

Table 1 Thermophysical constants of pure substances: melting temperature, $T_{fus,1}$; enthalpy of fusion, $\Delta_{fus}H_1$ [as determined from differential scanning calorimetry (DSC) data]; change of heat capacity at melting temperature, $\Delta_{fus}C_{p,1}$; molar volume at 298.15 K, $V_m^{298.15}$

Compound	$T_{fus,1}/K$	$\Delta_{fus}H_1/kJ\ mol^{-1}$	$\Delta_{fus}C_{p,1}/J\ K^{-1}\ mol^{-1}$	$V_m^{298.15}/cm^3\ mol^{-1}$
[EMIM][TOS]	322.93	27.83	—	221.50 ^d
[MMIM][CH ₃ SO ₄]	308.90	16.58	—	156.68 ^b
Cyclohexane	279.82 ^c	2.677 ^c	14.63 ^c	108.75 ^d
	279.65			108.91 ^e
Benzene	278.61 ^c	9.834 ^c	4.01 ^c	89.40 ^f
	278.65			89.52 ^d
Hexan-1-ol	221.15	15.38 ^g	—	125.30 ^h

^a Calculated from group contribution method.⁴² ^b Ref. 43. ^c Ref. 44.

^d Ref. 45. ^e Calculated from *PhysProps*, © 1999–2003, Greg Rupert, G&P Engineering Software. ^f Ref. 46. ^g Ref. 44. ^h Ref. 47.

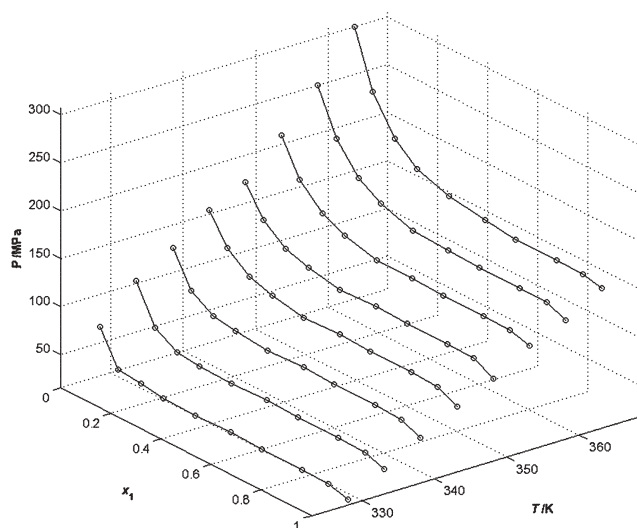


Fig. 1 Experimental data of solid–liquid equilibrium under high pressure of the system {[EMIM][TOS] (1) + cyclohexane (2)}; plot of pressure against mole fraction, x , of the IL.

than in cyclohexane; (3) the assumption was made that the phase diagram, measured for the binary systems exhibit simple eutectic behaviour mixtures.

Tables 2S and 3S in the ESI† show solid–liquid phase equilibrium data collected at high pressures. The system

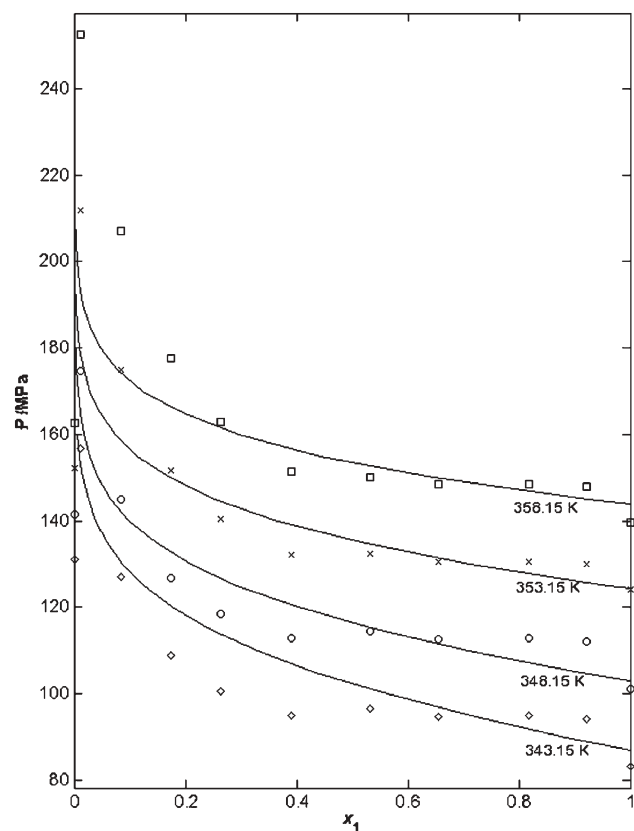


Fig. 2 Solid–liquid equilibrium of the {[EMIM][TOS] (1) + cyclohexane (2)} system at constant temperatures. Solid lines represent the Yang equation; plot of pressure against mole fraction, x , of the IL.

{[EMIM][TOS] (1) + cyclohexane (2)} exhibits immiscibility in the liquid phase which cannot be measured by the apparatus used by us, but it can be seen as a characteristic flat liquidus curve in a broad range of the IL's mole fraction (see Fig. 1). The effect of pressure on the solid–liquid phase equilibria of the binary mixtures has been measured at various constant compositions and temperatures. The liquid–solid transitions were determined for the whole IL concentration range from $x_1 = 0$ to 1. The solubility of [EMIM][TOS] in the two solvents tested is lower than that of [MMIM][CH₃SO₄], not only because of the higher melting temperature, but also because of the polar solvent (hexan-1-ol). At 0.1 MPa and at high pressure the solubility of [EMIM][TOS] in benzene is higher than in cyclohexane. These results are presented in Fig. 2 and Fig. 3 at constant temperatures and as an example in Fig. 4 at constant composition. Fig. 5 presents the [MMIM][CH₃SO₄] in hexan-1-ol system at constant temperatures. The difference between the melting point of cyclohexane (279.82 K) and the first experimental point (318.95 K) is a result of the position of the eutectic point, which is between these two points. For many ionic liquids the eutectic point is at a very low mole fraction of the solvent.

Unfortunately, the eutectic points in the solvents tested were not found because they are shifted to the very low mole fraction of the IL. The influence of high pressure on the liquidus curve in the tested systems is typical: with increasing pressure the freezing curves shift monotonously to higher temperatures (see Fig. 2, 3 and 5). The high pressure experimental results obtained at isothermal conditions (p – x) were interpolated to well known T – x diagrams as is shown in

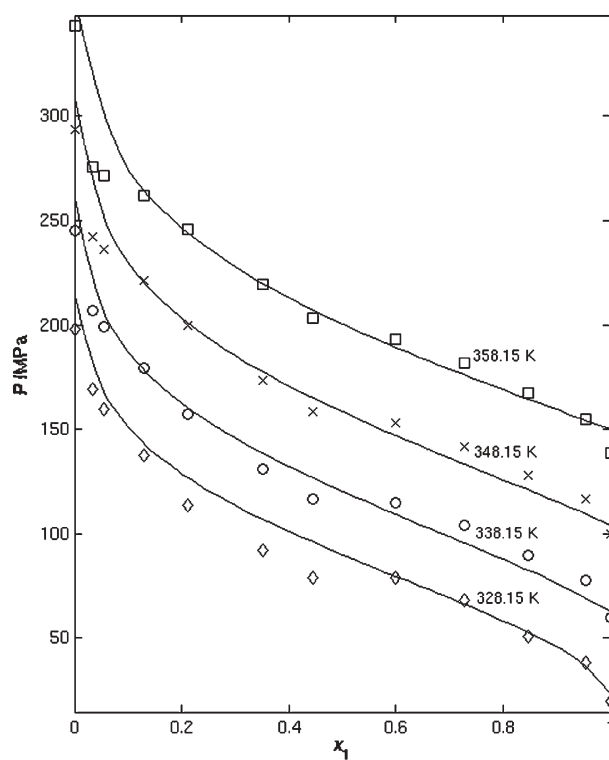


Fig. 3 Solid–liquid equilibrium of the {[EMIM][TOS] (1) + benzene (2)} system at constant temperatures. Solid lines represent the Yang equation; plot of pressure against mole fraction, x , of the IL.

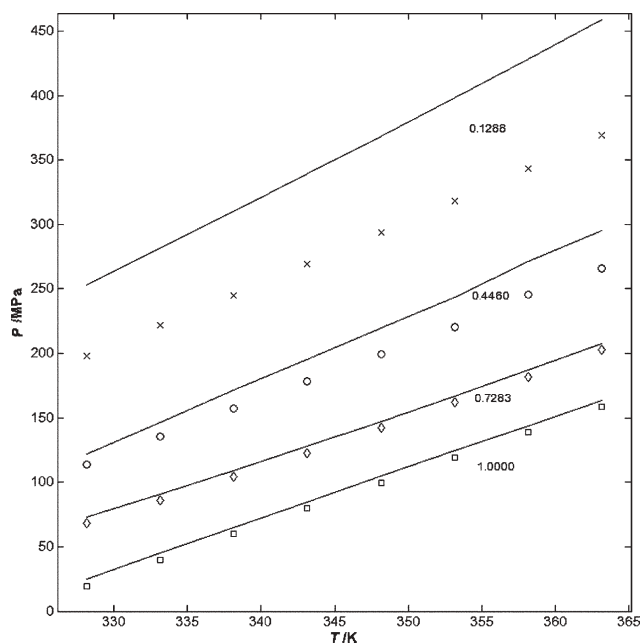


Fig. 4 Solid-liquid equilibrium of the {[EMIM][TOS] (1) + benzene (2)} system at constant composition. Solid lines represent the Yang equation; plot of pressure against temperature.

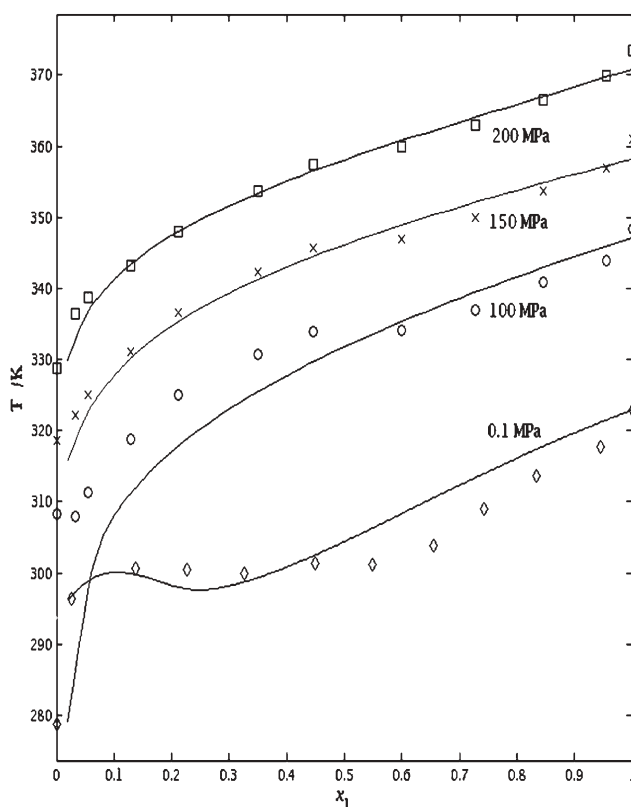


Fig. 6 Solid-liquid equilibrium of the {[EMIM][TOS] (1) + benzene (2)} system at constant pressures (interpolated values). Solid lines represent the Yang equation (high pressure), or the NRTL equation (0.1 MPa).

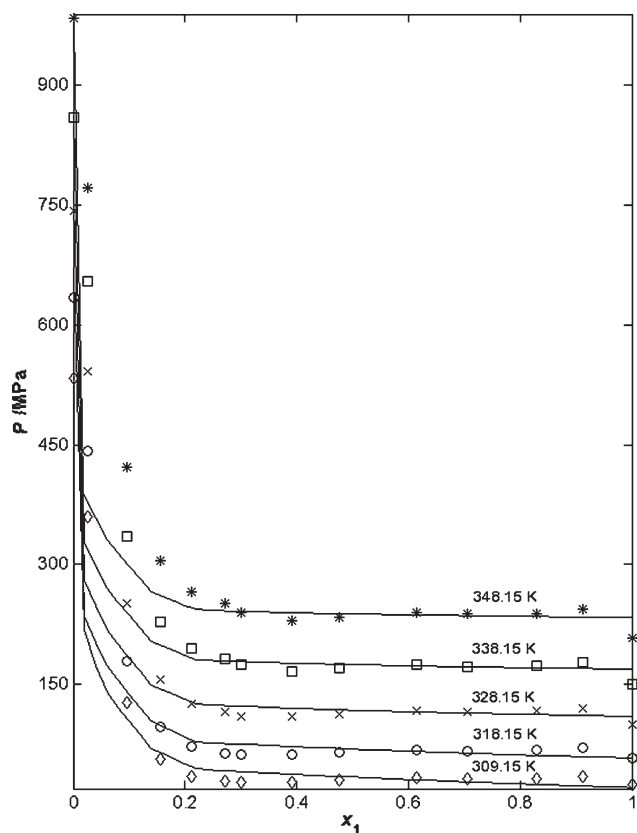


Fig. 5 Solid-liquid equilibrium of the {[MMIM][CH₃SO₄] (1) + hexan-1-ol (2)} system at constant temperatures. Solid lines represent the Yang equation; plot of pressure against mole fraction, x_1 , of the IL.

Fig. 6 and Fig. 7 for {[EMIM][TOS] (1) + benzene (2)} and for {[MMIM][CH₃SO₄] (1) + hexan-1-ol (2)}, respectively.

The difference of the pressure from 0.1 MPa to 160 MPa increases the melting temperature of the [EMIM][TOS] giving $\Delta T = 40.1$ K. The melting temperature, $T_{\text{fus},1}$, of [EMIM][TOS] has changed from $T_{\text{fus},1} = 322.9$ K (0.1 MPa) to $T_{\text{fus},1} = 363.1$ K at 160 MPa and that of [MMIM][CH₃SO₄] has changed from $T_{\text{fus},1} = 308.9$ K (0.1 MPa) to $T_{\text{fus},1} = 343$ K at 160 MPa. These results show that high pressure has a much stronger influence on the thermophysical properties of [EMIM][TOS] than on [MMIM][CH₃SO₄]. The influence of high pressure on the melting temperatures of the ILs and of the solvents is presented in Fig. 8. The slope of dp/dT is totally different for the ILs and the solvents. ILs, as hydrogen-bonded substances and much bigger molecules, show lower influence especially comparing with cyclohexane. There is disagreement between the point at 0.1 MPa and the first point at higher pressure for [MMIM][CH₃SO₄], which can be seen in Fig. 8. It can be the experimental error, which is normally lower for the higher pressure.

For the system {[EMIM][TOS] (1) + benzene (2)}, it can be seen in Fig. 6 the characteristic inflection on the liquidus curves at normal and high pressures. We think it may be the result of possible solid-solid phase transition observed also on DSC of the pure substance at 293 K. Unfortunately, it was impossible to separate two of the peaks in the DSC, one from

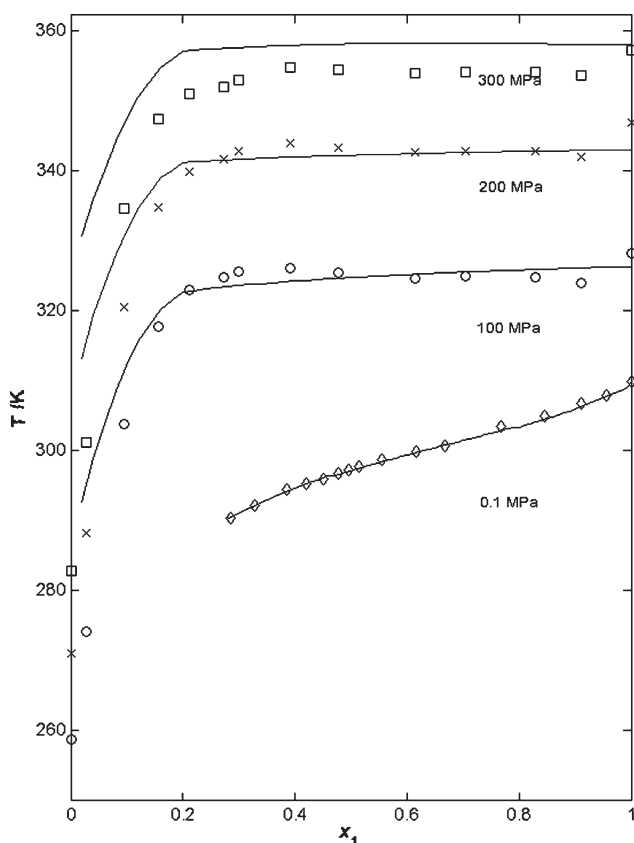


Fig. 7 Solid-liquid equilibrium of the {[MMIM][CH₃SO₄] (1) + hexan-1-ol (2)} system at constant pressures (interpolated values). Solid lines represent the Yang equation (high pressure), or the NRTL equation (0.1 MPa). Data at 0.1 MPa from ref. 47; plot of pressure against temperature.

melting and the second from a solid-solid phase transition. It is also worth mentioning that during the second and third turn of heating and cooling the DSC curve showed only the glass transition temperature at 214.1 K with ΔC_p equal to 61 J K mol⁻¹. It means that this IL demonstrates strong precooling.

Correlation at ambient pressure

The solubility of a solid (1) in a liquid may be expressed in a very general manner by eqn (1)

$$-\ln x_1 \gamma_1 = \frac{\Delta_{\text{fus}} H_1}{R} \left(\frac{1}{T} - \frac{1}{T_{\text{fus},1}} \right) - \frac{\Delta_{\text{fus}} C_{p,1}}{R} \left(\ln \frac{T}{T_{\text{fus},1}} + \frac{T_{\text{fus},1}}{T} - 1 \right) \quad (1)$$

where x_1 , γ_1 , $\Delta_{\text{fus}} H_1$, $\Delta_{\text{fus}} C_{p,1}$, $T_{\text{fus},1}$ and T stand for mole fraction, activity coefficient of the IL in the saturated solution, enthalpy of fusion, difference in solute heat capacity between the liquid and solid phase at the melting temperature, melting temperature of the solute (1) and equilibrium temperature, respectively. Eqn (1) is valid for simple eutectic mixtures with complete immiscibility in the solid phase. Only the first term of the eqn (1) was used in the tested systems, because the $\Delta_{\text{fus}} C_{p,1}$ values of the ILs were not known.

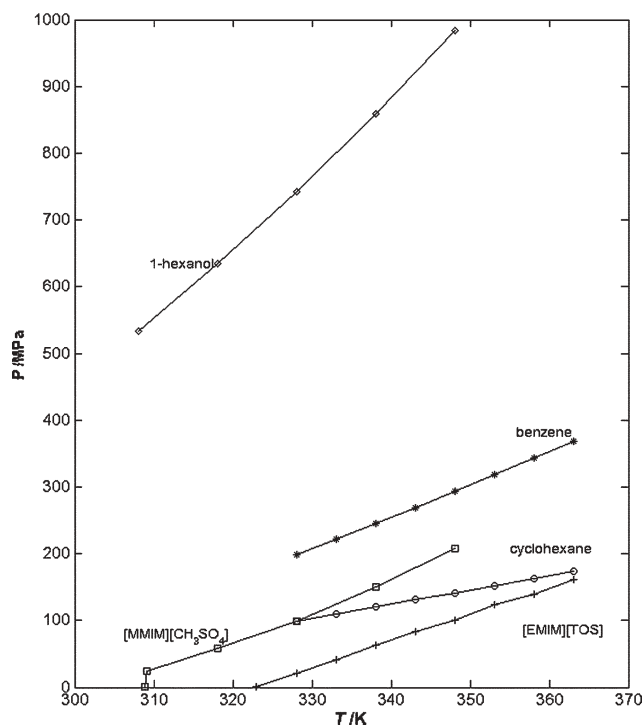


Fig. 8 Influence of pressure on the melting temperatures of ILs and solvents; plot of pressure against temperature.

For the solid-liquid equilibria the parameters of the excess Gibbs energy equation were fitted by an optimization technique. The objective function, OF , was as follows,

$$OF(A_1 A_2) = \sum_{i=1}^n w_i^{-2} [\ln x_{1i} \gamma_{1i}(T_i, x_{1i}, A_1 A_2) - \ln a_{1i}]^2 \quad (2)$$

where $\ln a_{1i}$ denotes an 'experimental' value of the logarithm of the solute activity, taken as the right-hand side of eqn (1), w_i is the weight of an experimental point, A_1 and A_2 are the two adjustable parameters of the correlation equations, i denotes the i th experimental point and n is the number of experimental data points.

The weights of the experimental points were calculated by means of the error propagation formula,

$$w_i^2 = \left(\frac{\partial \ln x_1 \gamma_1}{\partial T} \right)_{T=T_i}^2 (\Delta T_i)^2 + \left(\frac{\partial \ln x_1 \gamma_1}{\partial x_1} \right)_{x_1=x_{1i}}^2 (\Delta x_{1i})^2 \quad (3)$$

where ΔT and Δx_1 are the estimated errors in T and x_{ji} , respectively. According to the eqn (3) above, the objective function was obtained by solving the non-linear equation [eqn (1)]. The root-mean-square deviation of temperature, σ_T , defined by eqn (4) was used as a measure of the goodness of the solid-liquid equilibria correlation,

$$\sigma_T = \left(\sum_{i=1}^n \frac{(T_i^{\text{exp}} - T_i^{\text{cal}})^2}{n-2} \right)^{1/2} \quad (4)$$

where n is the number of experimental points (including the melting point) and 2 is the number of adjustable parameters.

Table 2 Correlation of the SLE/LLE data of the {[EMIM][TOS] (1) + cyclohexane, or benzene (2)} systems and of {[MMIM][CH₃SO₄] (1) + hexan-1-ol (2)}⁴⁷ by means of the NRTL equation; values of parameters and root-mean-square deviations σ_T , or σ_x

NRTL	IL + cyclohexane	IL + benzene	IL + hexan-1-ol
α	0.37	0.30	0.60
$\Delta g_{12}/\text{J mol}^{-1}$	7578.47	-1562.12	4215.61
$\Delta g_{21}/\text{J mol}^{-1}$	17 822.21	10 120.57	4594.65
$\sigma_T^{\text{SLE}}/\text{K}^a$	—	3.70	0.47
$\sigma_x^{\text{LLE}b}$	0.0120	—	—

^a According to eqn (4). ^b According to eqn (11).

The SLE of three binary systems was correlated by the NRTL equation.⁴¹ Table 2 lists the results of fitting the solubility curves. For the systems presented in this table the description of the solid–liquid phase equilibrium for both ILs, given by the two-parameter equation, was in the same range of accuracy with the average standard deviation $\sigma_T = 2.08$ K.

A simultaneous correlation of the solid–liquid and liquid–liquid phase equilibrium data for the mixtures of {[EMIM][TOS] (1) + cyclohexane (2)} was done also with the simple NRTL equation,⁴¹ where G^E is the excess Gibbs energy for the equilibria

$$\frac{G^E}{RT} = x_1 x_2 \left[\frac{\tau_{21} G_{21}}{x_1 + x_2 G_{21}} + \frac{\tau_{12} G_{12}}{G_{12} x_1 + x_2} \right] \quad (5)$$

where

$$\tau_{12} = (g_{12} - g_{22})/RT \quad (6)$$

$$\tau_{21} = (g_{21} - g_{11})/RT \quad (7)$$

$$G_{12} = \exp(-\alpha_{12}\tau_{12}) \quad (8)$$

$$G_{21} = \exp(-\alpha_{12}\tau_{21}) \quad (9)$$

The activity coefficients and the model adjustable parameters ($g_{12} - g_{22}$) and ($g_{21} - g_{11}$) were usually found by the optimization technique, widely discussed previously.⁴⁹ For this work the minimization of the objective function OF , presented by eqn (10), was proposed,

$$OF(A_1, A_2) =$$

$$\sum_{i=1}^n \left[(x_i^{\text{exp}} - x_i^{\text{cal}}(A_1, A_2))^2 + (x_i^{*\text{exp}} - x_i^{*\text{cal}}(A_1, A_2))^2 \right]_{\text{LLE}} \quad (10)$$

$$+ 0.001 \sum_{i=1}^n \left[\ln a_i^{\text{exp}}(x_i, T_i) - \ln a_i^{\text{cal}}(x_i, T_i, A_1, A_2) \right]^2_{\text{SLE}}$$

where n is the number of experimental points and x_i^* is the mole fraction of i in the second liquid phase. The first term is dedicated to the liquid–liquid equilibrium and deviations of the n -alkane mole fraction; the second term is connected to the solid–liquid equilibrium and is multiplied by the factor 0.001 to get lower influence of the order of magnitude of deviations of temperature on the correlation. A_1 and A_2 are two adjustable parameters.

The root-mean-square deviation of mole fraction, σ_x , for the LLE was defined as follows:

$$\sigma_x = \left\{ \sum_{i=1}^n \frac{(x_i^{\text{exp}} - x_i^{\text{cal}})_i^2}{n-2} + \sum_{i=1}^n \frac{(x_i^{*\text{exp}} - x_i^{*\text{cal}})_i^2}{n-2} \right\}^{1/2} \quad (11)$$

The calculated values of the equation parameters and corresponding root-mean-square deviations are presented in Table 2.

High pressure correlation

The experimental high pressure data (P , x_1) at constant temperature were correlated by the equation proposed by Yang *et al.*^{38,39} It was shown that the activity coefficient γ_1 at high pressure can be expressed as,

$$\ln \gamma_1 = \sum_{i=0}^3 a_i \left(\frac{1}{T} - \frac{1}{T_{\text{fus},1}} \right)^i + a' \left(\ln \frac{T}{T_{\text{fus},1}} + \frac{T_{\text{fus},1}}{T} - 1 \right) \quad (12)$$

where a_i and a' are two adjustable parameters. After substituting eqn (12) into eqn (1) some simplifications were obtained,

$$\ln x_1 = \sum_{i=0}^3 b_i \left(\frac{1}{T} - \frac{1}{T_{\text{fus},1}} \right)^i + b' \left(\ln \frac{T}{T_{\text{fus},1}} + \frac{T_{\text{fus},1}}{T} - 1 \right) \quad (13)$$

where $b_0 = -a_0$, $b_1 = -a_1 - \Delta_{\text{fus}}H_1/R$, $b_2 = -a_2$, $b_3 = -a_3$, $b' = -a' + \Delta_{\text{fus}}C_{p,1}/R$.

The value of the second term on the right-hand side of eqn (13) is small and this term can be neglected. Thus, the eqn (13) may be rewritten in a simple form:

$$\ln x_1 = \sum_{i=0}^3 b_i \left(\frac{1}{T} - \frac{1}{T_{\text{fus},1}} \right)^i \quad (14)$$

Solid–liquid phase equilibrium curves are dependent on pressure. With increasing pressure, the SLE curves shift to a higher temperature. In eqn (14) the b_i terms were found to be pressure-dependent and this dependence can be expressed as follows:

$$b_i = \sum_{j=0}^2 D_{ji} P^j \quad (15)$$

The objective function OF used in the fit of the parameters of eqn (14) and eqn (15) was as follows,

$$OF = \sum_{i=1}^n w_i^{-2} (\ln x_{1i}^{\text{cal}}(T_i, P_i, D_{ji}) - \ln x_{1i}) \quad (16)$$

where $\ln x_{1i}^{\text{cal}}$ denotes values of the logarithm of the solute mole fraction calculated from the eqn (14), $\ln x_{1i}$ denotes the logarithm of the experimental solute mole fraction and the symbols, T_i , P_i , D_{ji} express temperature, pressure and coefficients from eqn (15), respectively; w_i is the weight of the calculated values, described by means of the error propagation formula.

Table 3 contains the coefficients D_{ji} of eqn (15) for the studied systems. The pressure during the experiments was

Table 3 Parameters D_{ji} of the Yang equation for measured {[EMIM][TOS] (1) + cyclohexane, or benzene (2)} or {[MMIM][CH₃SO₄] (1) + hexan-1-ol (2)} systems

	IL + cyclohexane	IL + benzene	IL + hexan-1-ol
D_{00}	-1.0224	-2.9960×10^{-1}	-9.9607×10^{-1}
D_{10}	-1.3411×10^{-1}	-7.6541×10^{-3}	-5.1806×10^{-1}
D_{20}	-2.6342×10^{-4}	-4.6026×10^{-4}	-1.3200×10^{-3}
D_{01}	-1.5983×10^3	-5.2901×10^2	-1.1601×10^3
D_{11}	-2.5324×10^2	-2.1246×10^1	-3.9897×10^2
D_{21}	2.3419×10^{-1}	-8.8144×10^{-1}	-3.3996×10^{-1}
D_{02}	2.1283×10^3	-7.7870×10^1	2.0277×10^3
D_{12}	1.7817×10^2	-6.7513×10^2	6.1105×10^2
D_{22}	-2.0412×10^1	-4.8161×10^2	4.9706×10^1
D_{03}	-1.8081×10^3	1.2908×10^3	-2.5728×10^3
D_{13}	4.7572×10^1	1.8434×10^3	-6.9634×10^2
D_{23}	5.7063	1.2789×10^3	-1.6003×10^2
σ^a	0.169	0.054	0.120

$$^a \text{ The standard deviation } \sigma = \left[\frac{\sum_{i=1}^n (x_i^{\text{cal}}(P_i, T_i, A_1, A_2, \dots, A_{12}) - x_i^{\text{exp}})^2}{n-k} \right]^{1/2}$$

measured at constant composition–temperature conditions. The relation between temperature T and pressure p of the SLE at constant x_1 can be satisfactorily described with a simple quadratic equation, so the p - x diagram can be transformed into the T - x diagram. Direct experimental points and the results of the correlation are shown in the 3D diagram in Fig. 1. The solid lines represent the results of the fit with eqn (14).

The description of the experimental data is quite good. The standard deviation in mole fraction is 0.169 for {[EMIM][TOS] + cyclohexane}, 0.054 for {[EMIM][TOS] + benzene} and 0.120 for {[MMIM][CH₃SO₄] + hexan-1-ol}.

Experimental

Materials

The origins of the chemicals (in parentheses Chemical Abstract registry numbers, the manufacturer, and mass percent purities) were as follows: [EMIM][TOS] (CAS No. 328090-25-1, Solvent Innovation GmbH, >98%); [MMIM][CH₃SO₄] (CAS No. 97345-90-9, Solvent Innovation GmbH, >98; cyclohexane (CAS No. 110-82-7, Intern. Enz. Lim., for spectroscopy); benzene (CAS No. 71-43-2, Sigma-Aldrich, 99.97%); hexan-1-ol (CAS No. 111-27-3, Reachim, 0.99). ILs were dried for 24 h at 330 K in a vacuum before use. All solvents were fractionally distilled over different drying reagents to mass fraction purity better than 99.8% and were stored over freshly activated molecular sieves of type 4Å (Union Carbide). All compounds were checked by GLC analysis and no significant impurities were found. Analysis, using the Karl-Fischer technique, showed that the water content in solvents was less than 0.02 mass%. Samples of ionic liquids used in the experiment have been checked regularly concerning water content using Karl-Fischer titration. In all cases, the content of water was less than 160 ppm.

Differential scanning microcalorimetry (DSC)

The melting temperature and the enthalpy of fusion were measured by a Perkin-Elmer Pyris 1 differential scanning calorimetry (DSC) instrument. Measurements were carried out

at a scan rate of 10 K min⁻¹, with a power sensitivity of 16 mJ s⁻¹ and with the recorder sensitivity of 5 mV. Each time the instrument was used, it was calibrated with the 99.9999 mol% purity indium sample. The calorimetric accuracy was $\pm 1\%$, and the calorimetric precision was $\pm 0.5\%$. The thermophysical properties are shown in Table 1.

Phase equilibria apparatus at ambient pressure and measurements

SLE and LLE temperatures have been determined using a dynamic method that has previously been described in detail.^{25,26} Appropriate mixtures of IL and solvent placed under a nitrogen atmosphere in a drybox into a Pyrex glass cell were heated very slowly (less than 2 K h⁻¹ near the equilibrium temperature) with continuous stirring inside the cell. The sample was placed in a glass thermostat filled with silicone oil, or water. The temperature of the liquid bath was varied slowly until the one phase was obtained. The two phase disappearance temperatures in the liquid phase were detected visually during an increasing temperature regime. The temperature was measured with an electronic thermometer P 550 (DOSTMANN electronic GmbH) with the probe totally immersed in the thermostating liquid. The thermometer was calibrated on the basis of ITS-90. The accuracy of the temperature measurements was judged to be ± 0.01 K. Mixtures were prepared by mass, and the errors did not exceed $\delta x_1 = 0.0002$ and $\delta T_1 = 0.1$ K in the mole fraction and temperature, respectively.

Solid–liquid phase equilibria apparatus at high pressure and measurements

A simple piston-cylinder device, presented in detail in previous papers, was used.^{29–31} The mobile piston was moved by a hydraulic press. The device was thermostatted with the water thermostat linked to a thermocouple, and the temperature was measured by a Pt-resistance thermometer Delta HD 9215 (Poland) with an accuracy of ± 0.1 K. The pressure was measured up to 1.5 GPa with an error of $\pm 2\%$. (Liquid + solid) phase transitions were determined by discontinuities of volume–pressure curves. The accuracy of the discontinuity in the P–V curves following the measurement of pressure at the crystallization point is assumed to be $\pm 2\%$. The initiation of freezing was noticed at a higher pressure than the equilibrium value of this phase transition, observed as an ‘overpressure’ effect (the intersection between the lines of the one- and two-phase regions). The equilibrium point was the first from the solid phase line (see our previous work).^{29–31} The results published are the average of three or more measurements at the intersection point.

Conclusion

Knowledge of the impact of different factors on the phase behaviour of the IL with other liquids is useful for developing ILs as designer solvents. The observation of the liquid–liquid demixing at the solvent-rich phase was inhibited by the permanently foggy solution. The existence of the liquid–liquid equilibria in the mixture of [EMIM][TOS] with cyclohexane is

the evidence that the interaction between the IL and the solvent is not high, because two phases exist in the liquid phase. The saturated solution of [EMIM][TOS] with benzene is very close to the separation of phases, but it was not observed. This means that the $n-\pi$ interaction between the electron pair on the oxygen of the anion, or the $\pi-\pi$ interaction between the benzene ring and imidazolium ring, or between two benzene rings (one from solvent and the other from an anion) has an influence on the phase equilibria.

The noticeable differences in the solubilities of [EMIM][TOS] and [MMIM][CH₃SO₄] is a result of the melting temperature of the IL. The influence of high pressure on the melting temperature and the liquidus curve is different for different ionic liquids. In this work it is much bigger for [EMIM][TOS].

Owing to the differences in solubilities, ILs used in this work have attracted significant attention as potential solvents for industrial reactions, also at high pressures. Finally, it should be noted that the models used in this work for the correlation can be very useful for practical purposes.

Acknowledgements

This research has been supported by the Polish Committee for Scientific Research (Grant 3 T09B 004 27). Authors would like to thank Mrs A. Wiśniewska for cooperation.

References

- R. D. Rogers and K. R. Seddon, *Ionic Liquids. Industrial Applications to Green Chemistry*, ACS Symposium Series, American Chemical Society, Washington DC, 2002, p. 818.
- J. Dupont, R. F. De Souza and P. A. Z. Suarez, *Chem. Rev.*, 2002, **102**, 3667.
- Ch. J. Adams, M. J. Earle and K. R. Seddon, *Green Chem.*, 2000, **2**, 21.
- K. R. Seddon, A. Stark and M. J. Torres, *Pure Appl. Chem.*, 2000, **72**, 1391.
- J. L. Scott, D. R. MacFarlane, C. L. Raston and Ch. M. Teoh, *Green Chem.*, 2000, **2**, 123.
- P. A. Z. Suarez, J. E. L. Dullius, S. Einloft, R. F. De Souza and J. Dupont, *Polyhedron*, 1996, **15**, 1217.
- J. Dupont, P. A. Z. Suarez, R. F. De Souza, R. A. Burrow and J.-P. Kintzinger, *Chem.-Eur. J.*, 2000, **6**, 2377.
- P. Wasserscheid and W. Keim, *Angew. Chem., Int. Ed.*, 2000, **39**, 3773.
- R. S. Varma and V. V. Namboodiri, *Chem. Commun.*, 2001, 643.
- F. Zulficar and T. Kitazume, *Green Chem.*, 2000, **2**, 296.
- C. W. Lee, *Tetrahedron Lett.*, 1999, **40**, 2461.
- C. Cadena, J. L. Anthony, J. K. Shah, T. I. Morrow, J. F. Brennecke and E. J. Maginn, *J. Am. Chem. Soc.*, 2004, **126**, 5300.
- N. M. B. Flichy, S. G. Kazarin, C. J. Lawrence and B. J. Briscoe, *J. Phys. Chem. B*, 2002, **106**, 754.
- L. A. Blanchard, Z. Gu and J. F. Brennecke, *J. Phys. Chem. B*, 2001, **105**, 2437.
- A. M. Scurto, S. N. V. K. Akai and J. F. Brennecke, *J. Am. Chem. Soc.*, 2002, **124**, 10276.
- J. D. Holbrey and K. R. Seddon, *Clean Prod. Process.*, 1999, **1**, 223.
- S. P. Verevkin, J. Safarov, E. Bich, E. Hassel and A. Heintz, *Fluid Phase Equilib.*, 2005, **236**, 222.
- R. Kato and J. Gmehling, *Fluid Phase Equilib.*, 2005, **231**, 38.
- V. N. Najdanovic-Visac, J. M. S. S. Esperanca, L. P. N. Rebelo, M. Nunes da Ponte, H. J. R. Guedes, K. R. Seddon and J. Szydlowski, *J. Phys. Chem. B*, 2003, **107**, 12797.
- R. Kato, M. Krummen and J. Gmehling, *Fluid Phase Equilib.*, 2004, **224**, 47.
- J. M. Crosthwaite, S. N. V. K. Aki, E. J. Maginn and J. F. Brennecke, *Fluid Phase Equilib.*, 2005, **228–229**, 303.
- T. M. Letcher and N. Deenadayalu, *J. Chem. Thermodyn.*, 2003, **35**, 67.
- U. Domańska and A. Marciniak, *J. Chem. Eng. Data*, 2003, **48**, 451.
- U. Domańska, *Pure Appl. Chem.*, 2005, **77**, 543.
- U. Domańska and A. Marciniak, *J. Phys. Chem. B*, 2004, **108**, 2376.
- U. Domańska, A. Pobudkowska and F. Eckert, *Green Chem.*, 2006, **8**, 268.
- R. Kato and J. Gmehling, *J. Chem. Thermodyn.*, 2005, **37**, 603.
- R. Gomes de Azavedo, J. M. S. S. Esperanca, J. Szydlowski, Z. P. Visak, P. F. Pires, H. J. R. Guedes and L. P. N. Rebelo, *J. Chem. Thermodyn.*, 2005, **37**, 888.
- U. Domańska and P. Morawski, *Phys. Chem. Chem. Phys.*, 2002, **4**, 2264.
- U. Domańska, J. A. P. Coutinho and P. Morawski, *Fluid Phase Equilib.*, 2005, **230**, 72.
- U. Domańska, P. Morawski and R. Wierzbicki, *Fluid Phase Equilib.*, 2006, **242**, 154.
- B. Baranowski, *Pol. J. Chem.*, 1978, **52**, 1789.
- D. Dudek and B. Baranowski, *Pol. J. Chem.*, 1994, **68**, 1267.
- K. Nagaoka and T. Makita, *Int. J. Thermophys.*, 1998, **9**, 61.
- K. Nagaoka and T. Makita, *Int. J. Thermophys.*, 1988, **9**, 535.
- K. Nagaoka, T. Makita, N. Nishiguchi and M. Moritoki, *Int. J. Thermophys.*, 1989, **10**, 27.
- Y. Tanaka and M. Kawakami, *Fluid Phase Equilib.*, 1996, **125**, 103.
- M. Yang, E. Terakawa, Y. Tanaka, T. Sotani and S. Matsuo, *Fluid Phase Equilib.*, 2002, **194–197**, 1119.
- M. Yang, T. Narita, Y. Tanaka, T. Sotani and S. Matsuo, *Fluid Phase Equilib.*, 2003, **204**, 55.
- T. Inoue, I. Motoda, N. Hiramatsu, M. Suzuki and K. Sato, *Chem. Phys. Lipids*, 1996, **82**, 63.
- H. Renon and J. M. Prausnitz, *AIChE J.*, 1968, **14**, 135.
- A. F. M. Barton, *CRC Handbook of Solubility Parameters & Other Cohesion Parameters*, CRC Press Inc., Boca Raton, Florida, USA, 1995, p. 48.
- U. Domańska, A. Pobudkowska and A. Wiśniewska, *J. Solution Chem.*, 2006, **35**, 311.
- M. Palczewska-Tulińska, D. Wyrzykowska-Stankiewicz, A. M. Szafranski and J. Choliński, *Solid And Liquid Heat Capacity Data Collection, Part 2*, DECHEMA e.V., Frankfurt, 1997, vol. 4.
- C. A. Cerdeirina, C. A. Tovar and D. Gonzales-Solgado, *Phys. Chem. Chem. Phys.*, 2001, **3**, 5230.
- J. A. Riddick, W. B. Bunger and T. K. Sakano, *Organic Solvents, Physical Properties and Methods of Purification*, Wiley-Interscience, New York, 1986, vol. II.
- R. Malhotra and L. A. Woolf, *J. Chem. Thermodyn.*, 1996, **28**, 1411.
- U. Domańska, A. Pobudkowska and F. Eckert, *J. Chem. Thermodyn.*, 2006, **38**, 685.
- S. M. Walas, *Phase Equilibria in Chemical Engineering*, Butterworth, New York, 1985.

A method for the synthesis of 2-oxazolidinones and 2-imidazolidinones from five-membered cyclic carbonates and β -aminoalcohols or 1,2-diamines†

Lin-fei Xiao, Li-wen Xu and Chun-gu Xia*

Received 13th July 2006, Accepted 20th December 2006

First published as an Advance Article on the web 23rd January 2007

DOI: 10.1039/b609967j

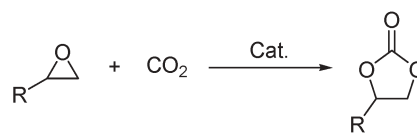
The first, highly efficient synthesis of 2-oxazolidinones from five-membered cyclic carbonates and β -aminoalcohols or 1,2-diamines, which gave excellent yields, are described. The effects of temperature, reaction time, solvent and the amount of catalyst were investigated.

Introduction

2-Oxazolidinones and cyclic ureas have been extensively used in organic synthesis, for example, pharmaceuticals, cosmetics, pesticides, and so on.¹ In particular, the chiral 2-oxazolidinones (Evans' chiral auxiliaries) have been used as chiral auxiliaries in a wide range of asymmetric syntheses.^{2,3} Conventionally, 2-oxazolidinones and cyclic urea are synthesized by using phosgenation of the corresponding 1,2-aminoalcohols or 1,2-diamines with toxic phosgene or its derivative,⁴ which may cause serious environmental pollution and equipment corrosion. Therefore, a number of non-toxic procedures have been suggested: (1) oxidative carbonylation using CO/O₂ and β -aminoalcohols or 1,2-diamines, (2) they are prepared by dialkyl carbonates and β -aminoalcohols or 1,2-diamines, (3) direct synthesis of 2-oxazolidinones and cyclic ureas from carbon dioxide and 1,2-aminoalcohols, aziridines or 1,2-diamines.

The intramolecular oxidative cyclocarbonylation of β -aminoalcohols or 1,2-diamines catalyzed by transition metals is a way to produce these heterocyclic compounds,^{5,6} but the oxidative carbonylation is expensive in using carbon monoxide and it has potential explosion hazards. As an alternative, dialkyl carbonates were used for the synthesis of 2-oxazolidinones and cyclic ureas.⁷ It should be noted that dimethyl carbonate is currently produced by phosgenation and oxidative carbonylation routes.⁸ There are several reports on the direct synthesis of 2-oxazolidinones or cyclic ureas by carbon dioxide and β -aminoalcohols, aziridines or diamines,⁹ however, toxic catalysts and high pressure and/or high temperature are required in most of those work. Development of a simple, highly efficient and environmentally benign method for synthesis of 2-oxazolidinone derivatives is still highly desired.

Herein, we report a novel method for synthesis of 2-oxazolidinones and cyclic ureas from five-membered cyclic carbonates under mild conditions. To the best of our



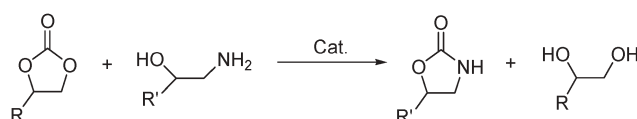
Scheme 1

knowledge, it is the first example of the preparation of 2-oxazolidinones and cyclic ureas from cyclic carbonates. This synthetic method has several advantages: (1) five-membered cyclic carbonates were synthesized from epoxides and carbon dioxide (Scheme 1),¹⁰ so it implies the use carbon dioxide as a starting material; (2) the 2-oxazolidinones or cyclic ureas and diol were obtained under mild conditions that are neither dangerous or noxious; (3) this reaction was potentially safe and wasteless, diol was the sole co-product, which can be sold as anti-freeze. So, this reaction process was environmentally benign and atom economic (Scheme 2).

Results and discussion

The reaction of 2-aminoethanol and propylene carbonate was investigated as a model. As shown in Table 1, 2-oxazolidinone was obtained in very low yield (8%) (Table 1, entry 14). When potassium carbonate was used as catalyst, the excellent yield (93%) of 2-oxazolidinone was obtained in *N,N*-dimethylformamide (DMF) (Table 1, entry 8), and the sole co-product was propane-1,2-diol.

The effects of the various of solvents on the reaction of the synthesis of 2-oxazolidinone using 2-aminoethanol and propylene carbonate were also investigated (Table 1). In tetrahydrofuran (THF), little 2-oxazolidinone was obtained (30%). In contrast to THF, high yield is obtained in polar organic solvents other than ethanol. The lower yield (79%) of 2-oxazolidinone was obtained in ethanol due to the side product of diethyl carbonate, obtained by transesterification between propylene carbonate and ethanol. Among the polar



Scheme 2

State Key Laboratory for Oxo Synthesis and Selective Oxidation, Lanzhou Institute of Chemical Physics, Chinese Academy of Sciences and Graduate School of Chinese Academy of Science, Lanzhou, 730000, P. R. China. E-mail: cgxia@lzb.ac.cn; Fax: +86-931-827-7147; Tel: +86-931-496-8089

† Electronic supplementary information (ESI) available: ¹H and ¹³C NMR spectra for 2-oxazolidinones and 2-imidazolidinones. See DOI: 10.1039/b609967j

Table 1 Effects of reaction conditions on the synthesis of 2-oxazolidinone from 2-aminoethanol and propylene carbonate^a

Entry	Catalyst	Solvent	Temperature/ °C	Yield ^b Time/h (%)
1	K ₂ CO ₃	THF	70	5 30
2	K ₂ CO ₃	1,2-Dimethoxyethane	70	5 45
3	K ₂ CO ₃	Acetonitrile	70	5 51
4	K ₂ CO ₃	1,4-Dioxane	70	5 87
5	K ₂ CO ₃	Ethanol	70	5 79
6	K ₂ CO ₃	DMF	70	5 90
7	K ₂ CO ₃	DMF	60	5 79
8	K ₂ CO ₃	DMF	80	5 93
9	K ₂ CO ₃	DMF	90	5 91
10	K ₂ CO ₃	DMF	80	4 83
11	K ₂ CO ₃	DMF	80	6 93
12	K ₂ CO ₃ ^c	DMF	80	5 65
13	K ₂ CO ₃ ^d	DMF	80	5 85
14	—	DMF	80	5 8
15	KHCO ₃	DMF	80	5 90
16	K ₃ PO ₄	DMF	80	5 77
17	Na ₂ CO ₃	DMF	80	5 85

^a Reaction conditions: propylene carbonate 10 mmol, ethanolamine 10 mmol, potassium carbonate 0.1 mmol. ^b GC yield. ^c 0.04 mmol. ^d 0.08 mmol.

organic solvents effective for the synthesis of 2-oxazolidinone, DMF was proved to be the best (Table 1, entries 1–6).

In order to establish the optimized reaction conditions, we examined the effect of temperature, reaction time, the amount of the catalyst and different catalysts. We found that increasing the reaction temperature had a pronounced positive effect on the yield of 2-oxazolidinone under 80 °C. However, the enhancement of the reaction temperature up to 90 °C gave the slight drop of the yield (Table 1, entries 6–9). This is probably due to the decomposability of propylene carbonate in the presence of potassium carbonate. The yield was affected by

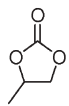
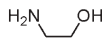
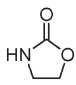
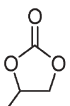
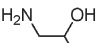
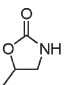
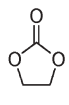
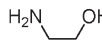
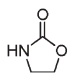
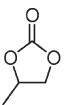
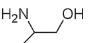
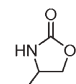
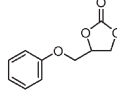
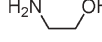
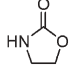
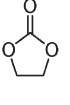
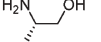
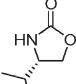
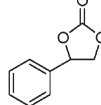
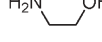
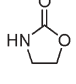
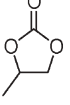
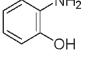
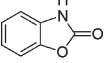
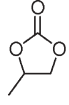

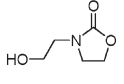
the reaction time, and increasing reaction time was propitious to improve the yield of 2-oxazolidinone (Table 1, entries 9–11). A higher yield is obtained by increasing the amount of the catalyst (Table 1, entries 8, 12, 13). In the reaction of the 2-aminoethanol and propylene carbonate, the yield of 2-oxazolidinone was greatly affected by basic metal salts (Table 1, entry 8, 15–17).

Under the optimized reaction conditions (the molar ratio of the substrate to catalyst was 100 : 1, at 80 °C in DMF for 5 h), it was found that this method was applicable to the synthesis of corresponding 2-oxazolidinones from different β -aminoalcohols and five-membered cyclic carbonates. The results are summarized in Table 2. As can be seen, this method showed excellent yields for almost all the employed β -aminoalcohols and five-membered cyclic carbonates, providing the corresponding 2-oxazolidinones. It is notable that optical activity of 2-oxazolidinone was obtained (57%) by this method (Table 2, entry 8). It is regrettable that 2-benzoxazolinone wasn't obtained when the substrate was 2-aminophenol (Table 2, entry 9).

The results of cyclic ureas obtained for the reaction between cyclic carbonates and 1,2-diamines are presented in Table 3. The results showed that satisfactory yields of 2-imidazolidinones were obtained from the aliphatic 1,2-diamines and five-membered cyclic carbonates. In this reaction, the yield of the cyclic urea was affected by the structure of the substrate used. When we used *o*-phenylenediamine as the substrate, the product of 2-hydroxybenzimidazole wasn't obtained (Table 3, entry 6).

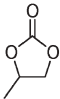
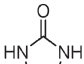
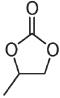
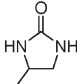
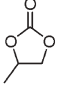
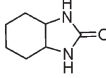
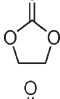
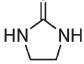
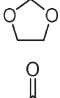
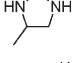
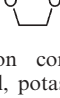
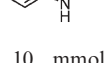
In a previous study,^{9e} Bhanage carried out the reaction of carbon dioxide with various 1,2-diamines and β -aminoalcohols, excellent yields of 2-oxazolidinones and 2-imidazolidinones were obtained. However, high pressure (6 MPa) and

Table 2 The synthesis of 2-oxazolidinones from the different substrates^a

Entry	Cyclic carbonate	β -Aminoalcohols	Products	Yield ^b (%)	Entry	Cyclic carbonate	β -Aminoalcohols	Products	Yield ^b (%)
1				89	6				89
2				90	7				74
3				78	8				57 ^c
4				80	9				—
5				92					

^a Reaction conditions: cyclic carbonate 10 mmol, β -aminoalcohol 10 mmol, potassium carbonate 0.1 mmol, DMF 5 mL, temperature 80 °C, time 5 h. ^b Isolated yield. ^c $[\alpha]_D^{20} = -15^\circ$ ($c = 0.4$, ethanol).

Table 3 The synthesis of cyclic ureas from the different 1,2-diamines and cyclic carbonates^a

Entry	Cyclic carbonate	Diamines	Products	Yield ^b (%)
1		$\text{H}_2\text{N}-\text{CH}_2-\text{NH}_2$		57
2		$\text{H}_2\text{N}-\text{CH}(\text{Me})-\text{NH}_2$		50
3		$\text{H}_2\text{N}-\text{C}_6\text{H}_{10}-\text{NH}_2$		43
4		$\text{H}_2\text{N}-\text{CH}_2-\text{NH}_2$		89
5		$\text{H}_2\text{N}-\text{CH}(\text{Me})-\text{NH}_2$		88
6		$\text{H}_2\text{N}-\text{C}_6\text{H}_3(\text{NH}_2)-\text{NH}_2$		—

^a Reaction conditions: cyclic carbonate 10 mmol, 1,2-diamine 10 mmol, potassium carbonate 0.1 mmol, DMF 5 mL, temperature 80 °C, time 5 h. ^b Isolated yield.

high temperature (150 °C) were required. In the literature,¹¹ 2-oxazolidinones and 2-imidazolidinones were synthesized from urea and aliphatic 1,2-diamines or β -aminoalcohols. However, 2-imidazolidinones were obtained with low yield, whereas high yields were obtained in this study (Table 3). Thus, five-membered cyclic carbonates are useful reagents for the syntheses of 2-oxazolidinones and 2-imidazolidinones.

Conclusion

In summary, we have found that the synthesis of 2-oxazolidinones cyclic ureas from five-membered cyclic carbonates and corresponding aliphatic β -aminoalcohols or 1,2-diamines could be performed with excellent yields by using potassium carbonate as catalyst under mild conditions. This atom-economical methodology represents a valuable and environmentally benign non-phosgene alternative to the use of toxic phosgene or expensive dimethyl carbonate. Since five-membered cyclic carbonates were prepared from epoxides and carbon dioxide, the title reactions will be chemical fixation of carbon dioxide to important chemicals indirectly.

Experimental

For each reaction, cyclic carbonate (10 mmol), β -aminoalcohols or 1,2-diamines (10 mmol) in DMF (5 ml) and potassium carbonate (0.1 mmol) were charged into a 25 ml round-bottomed flask equipped with a magnetic stirrer at 80 °C for 5 h. The resulting products were analyzed on a Hewlett-Packard 6890/5973 GC-MS and NMR. Quantitative analyses were carried out over a Agilent 6820 GC and column

chromatography on a silica gel (200–300 mesh, eluent: methanol–dichloromethane 1 : 10).

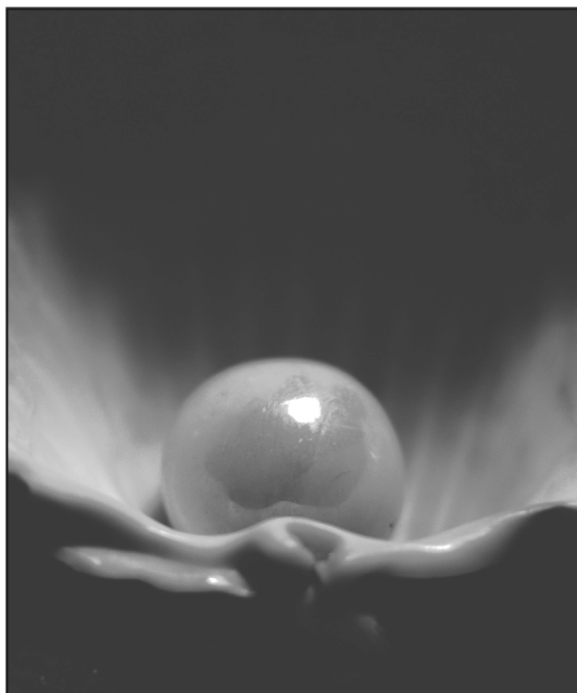
Acknowledgements

We are grateful to the Chinese National Sciences Foundation (20533080) and The National Science Fund for Distinguished Young Scholars (20625308) for financial support.

References

- M. E. Dyen and D. Swern, *Chem. Rev.*, 1967, **67**, 197; T. Wilson, *J. Org. Chem.*, 1986, **51**, 2977; N. Kudo, M. Taniguchi, S. Furuta, K. Sato, T. Endo and T. Honma, *J. Agric. Food Chem.*, 1998, **46**, 5305; L. M. Ednie, M. R. Jacobs and P. C. Appelbaum, *J. Antimicrob. Chemother.*, 2002, **50**, 101; M. B. Gravestock, D. G. Acton, M. J. Betts, M. Dennis, G. Hatter, A. McGregor, M. L. Swain, R. G. Wilson, L. Woods and A. Wookey, *Bioorg. Med. Chem. Lett.*, 2003, **13**, 4179.
- W. A. Gregory, D. R. Brittelli, C. L.-J. Wang, M. A. Wuonola, R. J. McRipey, D. C. Eustice, V. S. Everly, P. T. Bartholomew, A. M. Slee and M. Forbes, *J. Med. Chem.*, 1989, **32**, 1673; P. Seneci, M. Caspani, F. Ripamonti and R. Ciabatti, *J. Chem. Soc., Perkin Trans. 1*, 1994, 2345; K. C. Grega, M. R. Barbachyn, S. J. Brickner and S. A. Mzszak, *J. Org. Chem.*, 1995, **60**, 5255; S. J. Brikner, D. K. Hutchinson, M. R. Barbachyn, R. R. Manninen, D. A. Ulanowicz, S. A. Garmon, K. C. Grega, S. K. Hendges, D. S. Toops, C. W. Ford and G. E. Zurenko, *J. Med. Chem.*, 1996, **39**, 673; B. B. Lohray, S. Baskaran, B. S. Rao, B. Y. Reddy and I. N. Rao, *Tetrahedron Lett.*, 1999, **40**, 4855; D. J. Ager, I. Prakash and D. R. Schaad, *Aldrichim. Acta*, 1997, **30**, 3; J. Bach, S. D. Bull, S. G. Davies, R. L. Nicholson, H. J. Sanganeer and A. D. Smith, *Tetrahedron Lett.*, 1999, **40**, 6677; D. O'Hagan and M. Tavassli, *Tetrahedron: Asymmetry*, 1999, **10**, 1189.
- J. Seydenpenne, *Chiral Auxiliaries and Ligands in Asymmetric Synthesis*, Wiley, New York, 1995; D. J. Ager, I. Prakash and D. R. Schaad, *Chem. Rev.*, 1996, **96**, 835; P. Köll and A. Lützen, *Tetrahedron: Asymmetry*, 1996, **7**, 637; A. Lützen and P. Köll, *Tetrahedron: Asymmetry*, 1997, **8**, 29; A. Lützen and P. Köll, *Tetrahedron: Asymmetry*, 1997, **8**, 1193; S. Fonquerna, A. Moyano, M. A. Pericás and A. Riera, *Tetrahedron: Asymmetry*, 1997, **8**, 1685; P. Bravo, S. Fustero, M. Guidetti, A. Volonterio and M. Zanda, *J. Org. Chem.*, 1999, **64**, 8731; *Catalytic Asymmetric Synthesis*, ed. I. Ojima, Wiley, New York, 2000.
- N. A. Puschin and R. V. Mitic, *Justus Liebigs Ann. Chem.*, 1937, **532**, 300.
- T. Wilson, *J. Org. Chem.*, 1986, **51**, 2977; Y. Imada, Y. Mitsue, K. Ike, K. Washizuka and S. Murahashi, *Bull. Chem. Soc. Jpn.*, 1996, **69**, 2079; A. Bacchi, G. P. Chiusoli, M. Costa, B. Gabriele, C. Righi and G. Salerno, *Chem. Commun.*, 1997, 1209; J. E. Mccusker, C. A. Grasso, A. D. Main and L. M. Whit, *Org. Lett.*, 1999, **1**, 961; B. Gabriele, G. Salerno, D. Brindisi, M. Costa and G. P. Chiusoli, *Org. Lett.*, 2000, **2**, 625; B. Gabriele, R. Mancuso, G. Salerno and M. Costa, *J. Org. Chem.*, 2003, **68**, 601.
- F. W. Li and C. G. Xia, *J. Catal.*, 2004, **227**, 542.
- M. Tingoli, L. Testaferri, A. Temperini and M. J. Tiecco, *J. Org. Chem.*, 1996, **61**, 7085; Y. Fu, T. Baba and Y. Ono, *J. Catal.*, 2001, **197**, 91; P. S. N. Vani, A. S. Chida, R. Srinivasan, M. Chandrasekharam and A. K. Singh, *Synth. Commun.*, 2001, **31**, 2043.
- Y. Ono, *Catal. Today*, 1997, **35**, 15; M. A. Pachenco and C. L. Marshall, *Energy Fuels*, 1997, **11**, 2; D. Delledonne, F. Rivetti and U. Romano, *Appl. Catal. A*, 2001, **221**, 241; Y. Cao, J. Hu, P. Yang, W. Dai and K. Fan, *Chem. Commun.*, 2003, 908.
- J. F. Mulvaney and R. L. Evans, *Ind. Eng. Chem.*, 1948, **40**, 397; H. Matsuda, A. Baba, R. Nomura, M. Kori and S. Ogawa, *Ind. Eng. Chem. Prod. Res. Dev.*, 1985, **24**, 239; R. Nomura, M. Yamamoto and H. Matsuda, *Ind. Eng. Chem. Res.*, 1987, **26**, 1056; Y. Kubota, M. Kodaka, T. Tomohiro and H. Okuno, *J. Chem. Soc., Perkin Trans. 1*, 1993, 5; B. M. Bhanage, S. Fujita, Y. Ikushima and M. Arai, *Green Chem.*, 2003, **5**, 340; K. Tominaga and Y. Sasaki, *Synlett*, 2002, 307; C. J. Dinsmore and S. P. Mercer,

- Org. Lett.*, 2004, **6**, 2885; A. W. Miller and S. T. Nguyen, *Org. Lett.*, 2004, **6**, 2301; A. Sudo, Y. Morioka, E. Koizumi, F. Sanda and T. Endo, *Tetrahedron Lett.*, 2003, **44**, 7889; M. Feroci, A. Gennaro, A. Inesi, M. Orsini and L. Palombi, *Tetrahedron Lett.*, 2002, **43**, 5863.
- 10 D. J. Darensbourg and M. W. Holtcamp, *Coord. Chem. Rev.*, 1996, **153**, 155; F. Shi, Q. H. Zhang, Y. B. Ma, Y. D. He and Y. Q. Deng, *J. Am. Chem. Soc.*, 2005, **127**, 4182; F. W. Li, L. F. Xiao and C. G. Xia, *Tetrahedron Lett.*, 2004, **45**, 8307; F. W. Li, C. G. Xia, L. W. Xu, W. Sun and G. X. Chen, *Chem. Commun.*, 2003, 2042; L. F. Xiao, F. W. Li and C. G. Xia, *Appl. Catal., A*, 2005, **279**, 125.
- 11 C. E. Schweitzer, *J. Org. Chem.*, 1950, **15**, 471; A. R. Buter and I. Hussain, *J. Chem. Soc., Perkin Trans. 2*, 1981, 317; P. Li and J. C. Xu, *Tetrahedron*, 2000, **56**, 9949; W. J. Close, *J. Am. Chem. Soc.*, 1951, **73**, 95; B. M. Bannge, S. I. Fujita, Y. Ikushima and M. Ari, *Green Chem.*, 2004, **6**, 78.



Looking for that **special** research paper from applied and technological aspects of the chemical sciences?

TRY this free news service:

Chemical Technology

- highlights of newsworthy and significant advances in chemical technology from across RSC journals
- free online access
- updated daily
- free access to the original research paper from every online article
- also available as a free print supplement in selected RSC journals.*

*A separately issued print subscription is also available.

Registered Charity Number: 207890

RSC Publishing

www.rsc.org/chemicaltechnology

22030683

A synchrotron radiation study of the hydrothermal synthesis of layered double hydroxides from MgO and Al₂O₃ slurries

Sharon Mitchell,^a Timothy Biswick,^a William Jones,^{*a} Gareth Williams^b and Dermot O'Hare^b

Received 22nd September 2006, Accepted 18th December 2006

First published as an Advance Article on the web 23rd January 2007

DOI: 10.1039/b613795d

The hydrothermal reaction of slurries containing MgO and Cp3 alumina has been investigated *in situ* using energy dispersive X-ray diffraction (EDXRD). A range of temperatures (100, 150, 180 and 240 °C) were studied. Kinetic data for the formation of the hydrotalcite-like Mg–Al layered double hydroxide (LDH) have been determined. At 100 °C the LDH is the predominant phase that is formed but at higher temperatures the impurity phases brucite and boehmite become more significant. The rate of reaction increases with temperature in agreement with Arrhenius behaviour and the LDH growth curves exhibit sigmoidal kinetics. The rate of formation of the LDH phase was found to be approximately equal to the rate of consumption of MgO, indicating that the mechanism of LDH formation is unlikely to proceed *via* a long-lasting intermediate phase.

Introduction

Interest in layered double hydroxides (LDHs) remains high as new applications continue to be discovered.^{1,2} A knowledge of the basic chemistry of these materials is therefore fundamental for the efficient, targeted development of future uses and the exploitation of their full potential.

Also known as anionic clays or hydrotalcite-like materials, the structure of LDHs is similar to that of the mineral brucite, Mg(OH)₂.³ Substitution of the divalent layer cations by trivalent cations generates positively charged sheets which necessitates the incorporation of charge balancing anions in the interlayer region. Although some LDHs occur naturally the majority are produced synthetically. This enables experimentation with a range of synthetic variables, including incorporation of different metal species into the layers and anionic species into the interlayer. Furthermore, variations in the stoichiometry and synthesis conditions have created a wide range of LDHs with general formula [M(II)_{1-x}M(III)_x(OH)₂ (Aⁿ⁻)_{x/n}·yH₂O]. This compositional flexibility permits the design of LDHs with selected functionality, and the numerous range of current applications have been recently reviewed.^{4,5}

The most commonly used method for preparation of LDHs is that of coprecipitation.⁶ Many other synthesis routes have been developed in attempts to improve or extend the chemical and physical properties both of the LDH product itself, and of more complex LDH containing systems, for example LDH-polymer nanocomposites.⁷

Modifications of the coprecipitation method include hydrothermal synthesis,⁸ the use of microwave irradiation,⁹ and homogeneous precipitation, by for example, urea hydrolysis.¹⁰

Alternatively, a precursor, 'parent' LDH may be used for synthesis as in ion exchange reactions.¹¹ The dehydration–reconstruction method, which involves the decomposition of a pre-existing LDH by mild calcination (*e.g.* 500 °C), exploits the rehydration properties of the resulting mixed oxide, and also enables the incorporation of interlayer anions at low temperatures.^{12,13} Reducing the temperature of reactions and minimising waste, for example by the use of one-pot syntheses,¹⁴ are important targets in the development of more environmentally friendly, 'green' synthesis strategies.

The MgO–Al₂O₃–H₂O system has previously been reported in the synthesis of Mg–Al LDHs,^{15–19} and has been used as a method for preparing synthetic meixnerite in substantially carbonate free environments.^{18,19} Sealed reaction vessels are usually employed to allow accurate control of the anionic species.²⁰ The hydrothermal reaction of MgO and Al₂O₃ is of interest, as the elevated temperature and pressure produced is known to create the possibility of forming different chemical compositions of different structural arrangements, *i.e.* polytypes.¹⁸

The occurrence of polytypism is important, as polytypes may have different physical and chemical properties. Bookin and Drits studied the theoretically possible²¹ and naturally occurring²² polytypes of hydrotalcite-like minerals. The naturally occurring mineral hydrotalcite which has approximate composition Mg₆Al₂(OH)₁₆CO₃·4H₂O was found to have a three layer structure with rhombohedral (R) symmetry—designated by Bookin and Drits as the 3R₁ polytype. CO₃²⁻ is the most common anionic species found in LDHs due to the strong interaction of the carbonate within the interlayer.²³ The nature of this interaction limits the number of polytypes observed for LDHs containing CO₃²⁻ to two; a two-layer polytype with hexagonal symmetry (2H₁) and a three-layer polytype with rhombohedral (3R₁) symmetry.²⁴ The structures of synthetically prepared CO₃²⁻ bearing LDHs have all been identified as the 3R₁ polytype. Synthetically prepared OH⁻ containing LDHs, however, have been observed to form in two polytypes, both three-layer with rhombohedral symmetry,

^aDepartment of Chemistry, University of Cambridge, Lensfield Road, Cambridge, UK CB2 1EW. E-mail: wj10@cam.ac.uk; Fax: +44 1223 336362; Tel: +44 1223 336468

^bChemistry Research Laboratory, Department of Chemistry, University of Oxford, Mansfield Road, Oxford, UK OX1 3TA. E-mail: dermot.ohare@chem.ox.ac.uk; Fax: +44 1865 285131; Tel: +44 1865 285130

designated as the $3R_1$ and $3R_2$ polytypes respectively. Both polytypes have a fairly homogeneous distribution of cations, but in the $3R_2$ polytype the layers are shifted by lattice translations of $(1/3, 2/3)$ or $(2/3, 1/3)$ from the $3R_1$ structure. The $3R_2$ polytype is rarely observed in naturally occurring minerals, and, to date, has only been observed for sulfate containing forms.²² It is only possible to distinguish between these two polytypes by careful analysis of the reflection intensities—the appearance of the $3R_2$ polytype can be observed by comparison of the reflections appearing in the mid 2θ region ($30\text{--}50^\circ$). Specifically, the 012, 015 and 018 reflections will be relatively strong for the $3R_1$ polytype and the 101, 104 and 107 reflections will be relatively strong for the $3R_2$. Newman *et al.* reported the direct synthesis of this polytype by the hydrothermal treatment of Cp 1.5 (a flash calcined gibbsite) and MgO at 180°C , with hydroxyl groups as the dominant interlayer species.¹⁸

Despite the wealth of literature on the subject of LDHs, the mechanism of LDH formation remains unclear, perhaps due to the diversity of potential approaches to LDH synthesis or the numerous corresponding synthetic variables. Eliseev *et al.* reported that during formation of a Mg–Al LDH by coprecipitation, initially an amorphous phase is formed which then converts to a layered structure.²⁵ Using ^{27}Al solid state NMR, they observed a tetrahedral–octahedral change in Al geometry associated with this transition, which they suggested may be used as a measure of crystallisation. Sato *et al.* studied the thermal decomposition and reconstruction of LDHs by SEM, and proposed a topotactic mechanism based on their observations that the initial lamellar microstructure was retained.²⁶ More recently Xu and Lu presented evidence supporting a dissociation–deposition–diffusion mechanism based on their studies of the hydrothermal treatment of MgO and Al_2O_3 at 110°C .¹⁷ Before and during LDH formation, some reactions, such as hydrolysis of MgO and Al_2O_3 and the dissociation of $\text{Mg}(\text{OH})_2$ and $\text{Al}(\text{OH})_3$ formed *in situ*, may occur simultaneously. The type and rate of these reactions are dependent on temperature, which is controlled during hydrothermal synthesis, pH, which is not controlled, and pressure, which will initially increase but then remain fairly constant.

Synchrotron radiation enables *in situ* energy dispersive X-ray diffraction (EDXRD) analysis, which allows direct observation of the growth of crystalline phases during reaction.^{27–29} Millange and co-workers have already effectively used this technique for the time resolved study of the rehydration of an LDH providing insight into the kinetics of this process.²⁹

In this investigation we report on the use of EDXRD to study the hydrotalcite formation from a physical mixture of the MgO and Cp3 alumina. We have used the real time measurements obtained to establish the kinetics and improve our understanding of the mechanism of LDH formation under hydrothermal conditions.

Experimental

MgO (reagent grade, Aldrich) and Cp 3 Al_2O_3 (a transition alumina prepared by flash calcination of gibbsite) were combined with distilled water to give slurries of composition

R (Mg/Al) = 2, 10 wt% solids. A partially amorphous form of Al_2O_3 was selected since crystalline Al_2O_3 has a low reactivity.³⁰

Time-resolved *in situ* EDXRD was undertaken at the U.K. Synchrotron Radiation Source (SRS), Daresbury Laboratory, which operates using the radiation from the storage ring running at 2 GeV with an average stored current of 200 mA. Experiments were conducted on station 16.4, a wiggler magnet working at a peak frequency of 6 T supplies the station with X-ray frequency radiation. The station receives usable X-ray flux continuous in the range 5–120 KeV, with a maximum flux of 3×10^{10} photons s^{-1} at approximately 13 KeV. A three-element detector system was employed. Each detector was separated by a 2θ angle of 2.8° . In this investigation, the detectors were situated at 2θ angles of 1.6° (bottom), 4.4° (middle) and 7.2° (top). Using the relationship between energy, E/KeV , and d spacing, $d/\text{\AA}$, $E = 6.19926/d \sin\theta$. This corresponds to an observable d -spacing range of 1–14 \AA . Data collection times were 30 s throughout.

The slurries were treated in a stainless steel hydrothermal cell with a Teflon lining specifically designed to enable *in situ* measurements to be taken over a wide range of temperatures (up to 240°C).³¹ A Teflon coated magnetic stirrer bar ensured that a homogeneous portion of the reacting mixture remained in the beam. Reactions were undertaken at 100, 150, 180 and 240°C .

An automated Gaussian fitting routine was used to study the variation in integrated reflection area of the identifiable Bragg reflections with time. This permitted visualisation of the development and loss of crystalline phases during the hydrothermal reaction.³² The program was designed to enable manageable data analysis of the large numbers of powder diffraction patterns generated during time resolved experiments. Generally the results obtained showed little scatter. In order to compare several sets, the data was normalised and in some cases a 3-parameter sigmoidal trendline was fitted to improve visualisation.

For subsequent *ex situ* analysis, the products from the *in situ* study were dried at 70°C without filtering or washing. Angle dispersive powder X-ray diffraction (PXRD) patterns of the resulting materials were recorded with a Phillips X'Pert MPD diffractometer in reflection geometry using Cu $K\alpha$ radiation ($\lambda = 1.5418 \text{\AA}$). Data were collected from finely ground samples pressed on a flat plate, glass sample holder. The 2θ range explored was between $5\text{--}80^\circ$.

Phase identification was achieved by comparison with PXRD patterns simulated, using the X'Pert Plus software, from single crystal structural information data obtained from the International Crystal Structure Database, as well as with the diffraction patterns collected from known $3R_1$ and $3R_2$ polytypes synthesised in our laboratory.

Results

The dried products were all off-white powders for which the PXRD patterns collected *ex situ* are summarised in Fig. 1. It is evident that the Mg–Al LDH is the predominant phase formed in all cases. For the material prepared at 100°C , the reflections correspond well to the structure of the $3R_1$ polytype. At higher

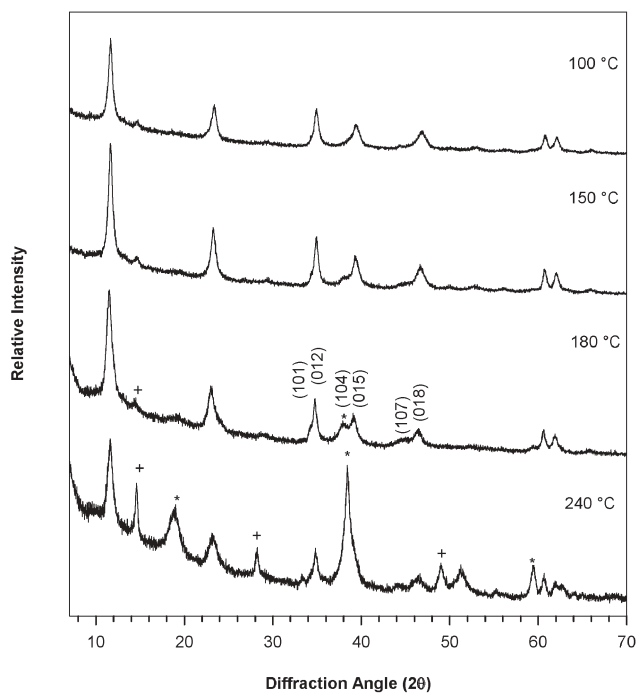


Fig. 1 *Ex situ* PXRD patterns of materials prepared during the *in situ* studies of the hydrothermal reaction of MgO and Cp3 alumina. + marks boehmite reflection and * marks brucite reflection.

reaction temperatures, reflections corresponding to both the 3R₁ and the 3R₂ polytypes are observed. It is noted, however, that the principal LDH structure in the dried products resulting from all reaction temperatures undertaken is that of the 3R₁ polytype. At 240 °C there is also significant formation of the impurity phases boehmite and brucite (marked).

A schematic diagram of the *in situ* spectra recorded from the top, middle and bottom detector is shown in Fig. 2. The data from two consecutive 30 s measurements were combined to improve the signal to noise ratio in the spectra. The presented spectra therefore show the data collected during Minute 1 (left) and Minute 30 (right). The high background intensity is due to diffraction from the water present in the reaction vessel. There are also some observable reflections which arise due to interaction between the X-ray beam and the reaction vessel—most notably, the strong reflection visible in spectra acquired from the bottom detector (marked Exp. Ref. in Fig. 2), which is due to diffraction from the Teflon lining of the reaction vessel. Additionally, there are sharp reflections (marked * in Fig. 2), which are thought to be due to diffraction from metals in the reaction vessel. These reflections are seen at all reaction temperatures and their intensity remains constant throughout. These reflections are not taken into account in the results presented below.

In order to assign the reflections observed in the EDXRD spectra, each potential phase which could be present during the reaction was analysed to calculate the expected energies at which the reflection would occur from the corresponding value of 2θ . In the initial spectra, collected during the first minute, only reflections arising from the MgO phase are visible. After 30 minutes of reaction, these reflections have disappeared and only reflections corresponding to the LDH are identifiable. These phases have been indexed LDH *hkl* and MgO *hkl* respectively. It was not possible to differentiate between reflections corresponding to the 3R₁ and 3R₂ LDH polytype in the EDXRD spectra.

Fig. 3 shows the variation in EDXRD spectra collected from the middle detector with time for the reaction at 100 °C. No reflections additional to MgO and LDH are seen to develop during the intermediate stages of the reaction. The variation

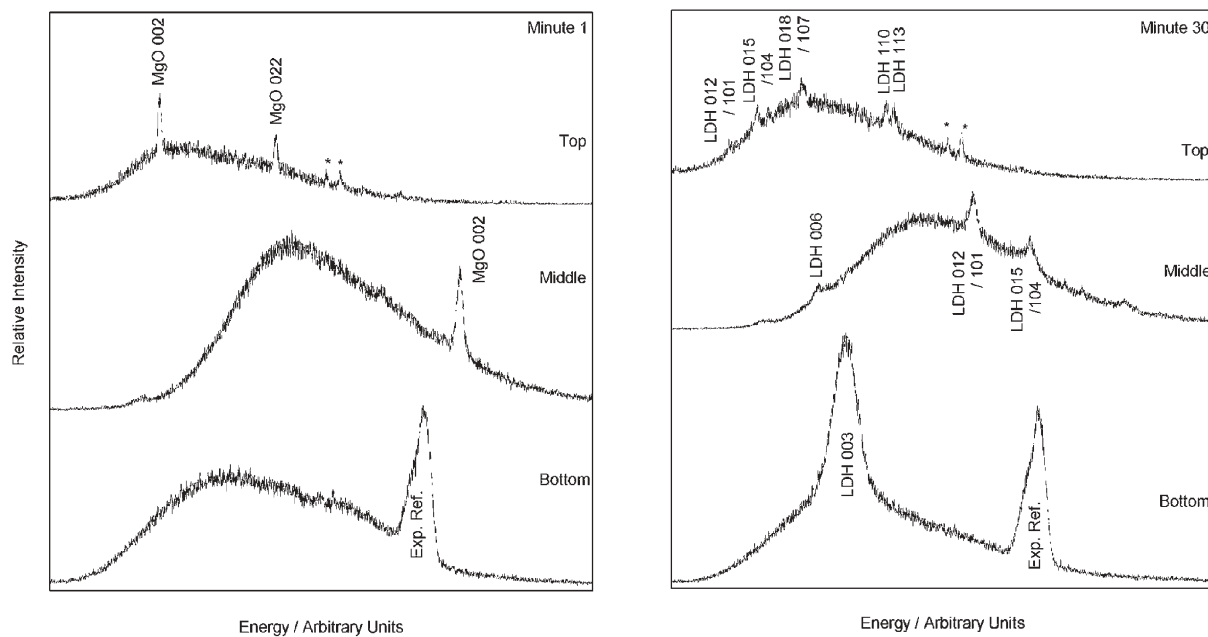


Fig. 2 Schematic diagram showing the initial (Minute 1) *in situ* spectra recorded by the top (28–100°/2θ), middle (18–50°/2θ) and bottom (6–18°/2θ) detectors compared with those recorded during Minute 30 of reaction at 180 °C. Identifiable reflections are indexed. The reflections marked Exp. Ref. and * are experimental artefacts arising from the apparatus used.

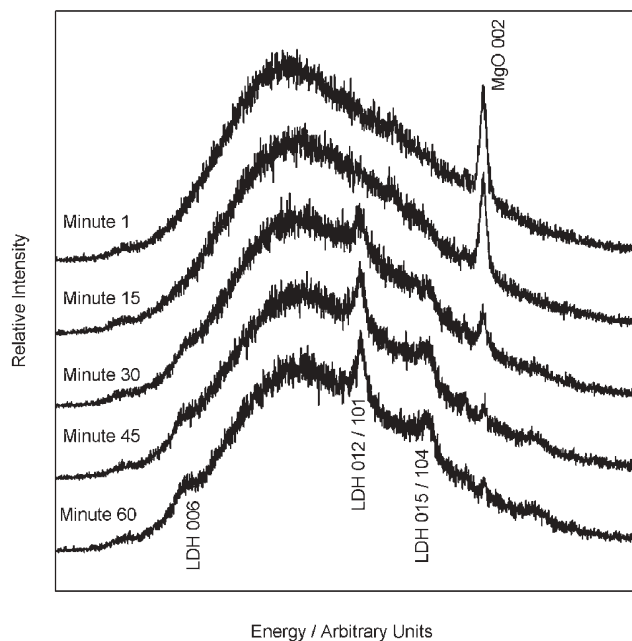


Fig. 3 Variation with time of the *in situ* spectra collected from the middle detector ($18\text{--}50^\circ/2\theta$) for the reaction at 100°C .

with time of the EDXRD spectra collected for reactions at 150 , 180 and 240°C is found to have similar trends. From the data collected at 240°C it was possible to identify additional reflections in the EDXRD spectra corresponding to the impurity phase boehmite.

Analysis of the EDXRD data obtained using the Gaussian fitting routine yielded information about the kinetics of the consumption and growth of crystalline phases during reaction. The strong 003 basal reflection of the LDH, the 002 reflection of MgO and (at 240°C) the 020 boehmite reflection, were selected to study the variation of these phases with time.

Fig. 4 summarises the data for LDH and MgO with reaction temperature. The LDH growth curves closely reflect, in terms of rate, the consumption of the MgO phase. In agreement with Arrhenius behaviour, the kinetics of reaction are seen to increase with temperature of hydrothermal reaction. Two effects are noticeable: the point at which the LDH reflection becomes distinguishable (LDH crystallisation) occurs earlier as the temperature is increased, and the rate at which the reaction occurs (measured by the slope of the nucleation controlled growth area of the curve) increases. In all cases, the normalised intensity vs. time curves of the MgO and LDH phases cross at approximately 0.5. As coherent diffraction from the starting material declines, it is matched by a gain in coherence from the product phase. This is consistent with a process in which MgO is transformed directly into the LDH: if an intermediate phase was forming, one might expect the reactant and product phase curves to cross at a lower normalised intensity, as seen by Geselbracht *et al.*, where two intermediate phases were detected in a reaction and the reactant and product curves crossed at approximately 0.2.³³ The decay of overall intensity which can be seen in the results from 240°C is possibly the result of the stirrer bar being impeded by the developing product phases. In this situation the portion of the reacting

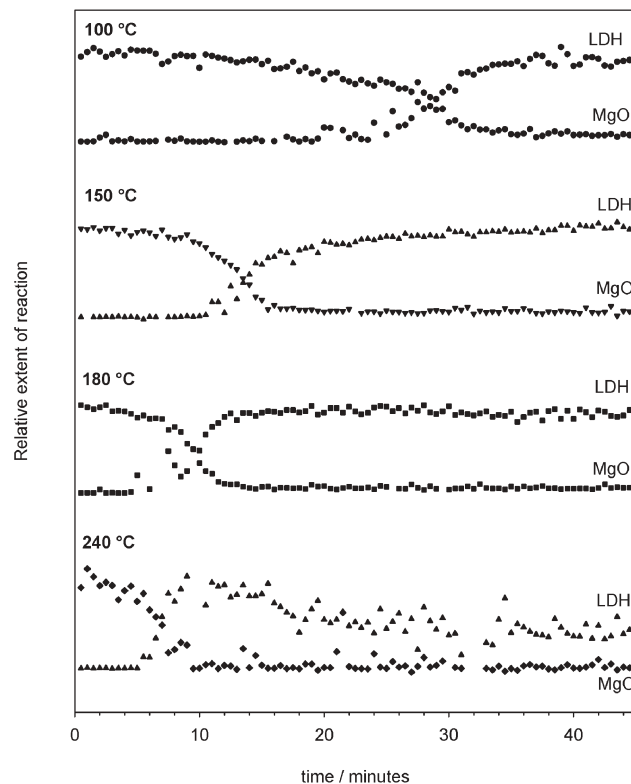


Fig. 4 Plot showing relationship between growth of LDH 003 reflection and consumption of MgO 002 reflection from the *in situ* data with time at the temperatures studied.

mixture remaining in the line of the beam would decrease and therefore lead to a loss of intensity.

Fig. 5 compares the extent of reaction with time for each reaction temperature. Sigmoidal trendlines are fitted to enable clear visualisation, as this shape was found to have the closest

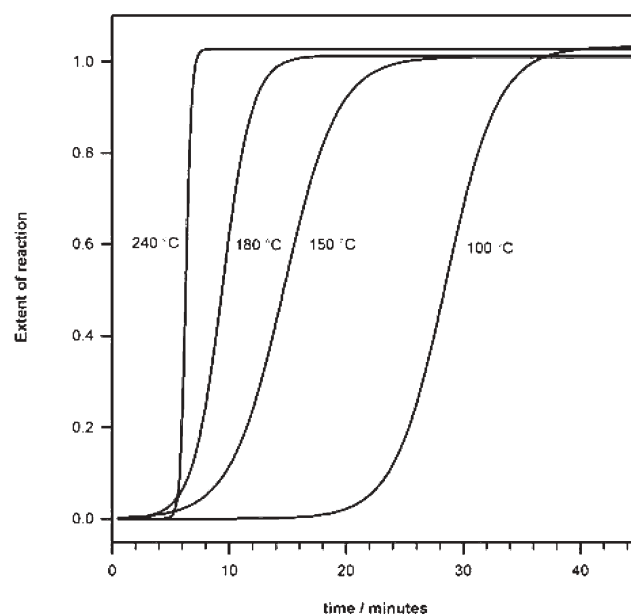


Fig. 5 Comparison of the rate of development of the LDH 003 basal reflection with the temperature of hydrothermal reaction.

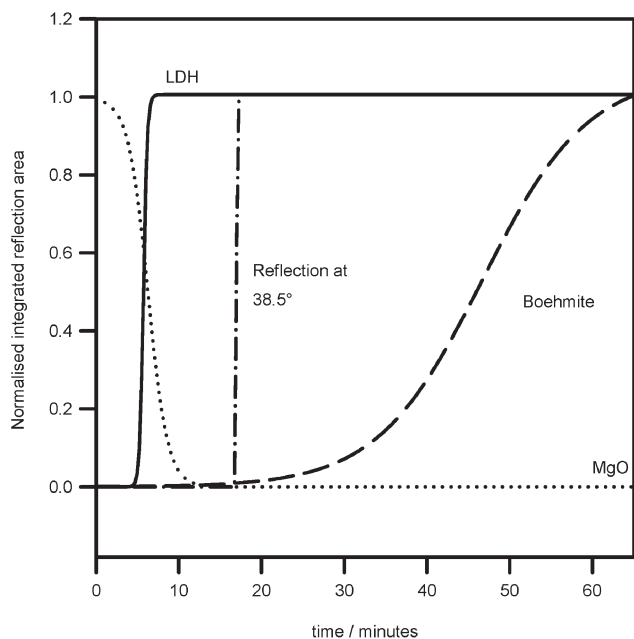


Fig. 6 Comparison of the normalised variation of integrated reflection area with time for the LDH 003, MgO 002 and Boehmite 020 reflections and the multi component reflection at 38.5° , for the reaction at 240°C .

fit with the data. Unfortunately, it was not possible to fit a full kinetic model to the data collected due to the low resolution during the initial stages of reaction.

For the reaction at 240°C it was also possible to study the development of boehmite and of the intense reflection at approximately 38.5° two-theta (which may have contributions from brucite 011 and LDH 015/104 reflections). The growth of these reflections with respect to the 003 LDH basal reflection and loss of 002 MgO reflection is shown in Fig. 6. It is interesting to note that the development of both the boehmite reflection and the reflection seen at 38.5° in the *ex situ* pattern, have different kinetics from that of the LDH phase. Both reflections appear after longer time intervals than the LDH 003 reflection and the rate of development of the boehmite reflection is slower. The fact that the development of the reflection at 38.5° has different kinetics from the LDH 003 reflection indicates that this reflection arises from one or more phase in addition to the LDH. If this is the case, then both the brucite and boehmite phases crystallise after the MgO phase has been fully consumed. These phases must, therefore, either be formed from amorphous phases present in the slurry or must be formed from the decomposition or structural alteration of the LDH present. It was not possible to study the development of impurity phases at other reaction temperatures as insufficient quantities were formed. The reflection intensities were, therefore, too weak for assignment to be made and to allow accurate determination of the reflection area compared with the background noise.

Discussions

Contrary to what was expected based on previous knowledge, in this investigation the *ex situ* data show that the predominant

LDH structure formed at all reaction temperatures was that of the $3R_1$ polytype.

A possible explanation for this observation would be if the LDH formed contained carbonate (due to the predisposition of carbonate containing LDHs towards the $3R_1$ polytype). Elemental analysis of the products obtained indicated the wt% of carbon to be approximately 1.3%. Assuming that the layer stoichiometry reflects the stoichiometry of the initial slurry, the corresponding LDH containing carbonate as the charge balancing anion would have approximate composition $\text{Mg}_4\text{Al}_2(\text{OH})_{12}(\text{CO}_3)\cdot 2\text{H}_2\text{O}$, corresponding to a wt% C of 2.66%. This indicates that the products formed contain both carbonate and hydroxyl anions. Possible sources of carbonate anions include CO_2 from the atmosphere or adsorbed on the reactants (as $\text{CO}_3^{2-}/\text{HCO}_3^-$). Alternatively, the absorption of CO_2 from air during the post-synthesis collection process may account for the presence of carbon, but this would not be expected to effect the structure of the LDH formed, as the interconversion between $3R_1$ and $3R_2$ structure is not thought to be possible.¹⁸

Another explanation for the formation of the $3R_1$ polytype may also be considered. It is possible that the $3R_2$ polytype is not formed directly on reaction of slurries containing MgO and Cp3 alumina but forms *via* a $3R_1$ intermediate. In this investigation, the maximum data collection time was 90 minutes. More data would be needed, to eliminate this possibility.

There is some debate over the assignment of reflections in the products resulting from hydrothermal reactions at temperatures sufficiently high to yield LDHs with the $3R_2$ structure. Reflections in positions approximately equivalent to those of brucite (marked * in Fig. 1) were left unassigned ('non-indexed') by Newman *et al.* when reporting the synthesis of the $3R_2$ polytype, observing that the reflections occurred at lower *d*-spacings than reported data for brucite. They noted that the reflection close to 19° has previously been assigned to the existence of a superlattice structure in LDHs, possibly due to cation ordering within the layers and/or to the ordered arrangement of anions within the gallery.¹⁸ Our results show the formation of brucite during the reaction at 240°C , indicating that the non-indexed reflections are likely to have at least some component (if not all) from brucite.

The presence of brucite and boehmite is observed in both the *in situ* and *ex situ* data collected from the material prepared by hydrothermal reaction at 240°C . This is consistent with the phase diagrams presented by Mascolo in his review on the hydrothermal synthesis of anionic clays from the amorphous precursors of M_2O_3 ($\text{M} = \text{Al}, \text{Cr}, \text{Fe}$) with an appropriate agent of crystallisation MO ($\text{M} = \text{Mg}, \text{Zn}, \text{Ni}$).¹⁶ Mascolo considers LDHs as low density phases whose formation is favoured by low temperature hydrothermal treatment (and hence a lower self generated pressure). Mascolo suggests that elevated pressures favour the formation of Al rich LDHs, and that as the temperature is increased ($>200^\circ\text{C}$) the LDH phase becomes less stable and brucite and boehmite become the more thermodynamically stable phases. The exact stability of the LDH is dependent on the layer composition and the nature of the interlayer anion.

Conclusions

Hydrothermal reaction of MgO and Cp Al₂O₃ occurs rapidly, yielding mainly the Mg–Al LDH product at all temperatures. Reaction at 100 °C yielded an LDH phase with a structure corresponding to the 3R₁ polytype. As the temperature of hydrothermal treatment is increased, a small amount of the 3R₂ structure and the presence of brucite and boehmite impurities is also detected.

In situ EDXRD has proved successful in furthering understanding of the mechanism of reaction and has enabled conclusions to be made regarding the kinetics. At all temperatures there is some delay before the LDH peak becomes visible (LDH crystallisation). This is followed by a rapid increase in intensity of the 003 reflection corresponding to mass crystallisation of LDH particles. After the reaction is complete (when there is no further rise in intensity) the LDH crystallites are thought to enter into a growth stage, although it was not possible to observe the corresponding decrease in the FWHM of the reflection from our data, which could indicate that the growth of LDH crystallites occurs on a slower timescale. Brucite and Boehmite are observed to crystallise less quickly than the LDH phase.

In agreement with the findings of Millange *et al.*²⁹ for the rehydration of an Mg–Al LDH, it is evident that increasing the temperature has a significant effect on the rate of hydrotalcite formation. However, unlike the results of that study, where the LDH 003 reflection appears almost instantaneously upon rehydration of the Mg–Al mixed metal oxide, for the formation of LDH by hydrothermal reaction of MgO and Al₂O₃ slurries, there is a delay of at least 5 minutes before the LDH reflection is detectable. This would be consistent with the postulation that the rehydration of a calcined Mg–Al LDH occurs topotactically, as it would be expected to have a lower activation energy than the hydrothermal reaction of MgO and Cp3 alumina to form Mg–Al LDH. In the situation reported here, the Mg and Al cations will be separated, thus requiring an additional diffusion step in order to form the LDH.

The MgO consumption curves appear to mirror the rate of the LDH growth curves. The curves cross where the normalised intensity of each is approximately 0.5, and no other crystalline phases are detected by EDXRD. Therefore, the mechanism for LDH formation by this method does not involve the formation of a long-lasting, either amorphous or crystalline, intermediate phase.

Acknowledgements

The authors would like to thank EPSRC for funding and the CCLRC for access to Station 16.4 of the UK SRS. Dr Dave

Taylor and Mr Alfie Neild are thanked for technical support at the SRS.

References

- 1 T.-Y. Tsai, S.-W. Lu, Y.-P. Huang and F.-S. Li, *J. Phys. Chem. Solids*, 2006, **67**, 938.
- 2 F. Leroux, *J. Nanosci. Nanotechnol.*, 2006, **6**, 303.
- 3 A. de Roy, C. Forano and J. P. Besse, in *Layered Double Hydroxides: Present and Future*, ed. V. Rives, Nova Sci. Pub., Inc., New York, ch. 1, 2001.
- 4 D. Evans and X. Duan, *Chem. Commun.*, 2006, **5**, 485.
- 5 S. Carlino, *Chem. Br.*, 1999, **33**, 59.
- 6 P. S. Braterman, Z. P. Xu and F. Yarberry, in *Handbook of Layered Materials*, ed. S. M. Auerbach, K. A. Carrado and P. K. Dutta, Marcel Dekker, Inc., New York, 2004.
- 7 N. S. Kottegoda and W. Jones, *Macromol. Symp.*, 2005, **222**, 65.
- 8 F. M. Labajos, V. Rives and M. A. Ulibarri, *J. Mater. Sci.*, 1992, **27**, 1546.
- 9 G. Fetter and F. Hernandez, *J. Porous Mater.*, 1997, **4**, 27.
- 10 M. Adachi-Pagano, C. Forano and J.-P. Besse, *J. Mater. Chem.*, 2003, **13**, 1988.
- 11 M. Meyn, K. Beneke and G. Lagaly, *Inorg. Chem.*, 1990, **29**, 5201.
- 12 K. Chibwe and W. Jones, *J. Chem. Soc., Chem. Commun.*, 1989, **14**, 926.
- 13 S. Aisawa, H. Kudo, T. Hoshi, S. Takahashi, H. Hirahara, Y. Umetsu and E. Narita, *J. Solid State Chem.*, 2004, **177**, 3987.
- 14 C. H. Greenwell, W. Jones, D. N. Stammers, P. O'Connor and M. F. Brady, *Green Chem.*, 2006, DOI: 10.1039/b605851e.
- 15 I. Pausch, H. H. Lohse, K. Schuermann and R. Allmann, *Clays Clay Miner.*, 1986, **34**, 507.
- 16 G. Mascolo, *Appl. Clay Sci.*, 1995, **10**, 21.
- 17 Z. P. Xu and G. Q. Lu, *Chem. Mater.*, 2005, **17**, 1055.
- 18 S. P. Newman, W. Jones, P. O'Connor and D. N. Stammers, *J. Mater. Chem.*, 2002, **12**, 153.
- 19 E. S. Martin and A. Pearson, *US Pat.* 5 514 361, 1996.
- 20 M. Ogawa and S. Asai, *Chem. Mater.*, 2000, **12**, 3253.
- 21 A. S. Bookin and V. A. Drits, *Clays Clay Miner.*, 1993, **41**, 551.
- 22 A. S. Bookin, V. I. Cherkashin and V. A. Drits, *Clays Clay Miner.*, 1993, **41**, 558.
- 23 G. S. Thomas, A. V. Radha, P. V. Kamath and S. Kannan, *J. Phys. Chem. B*, 2006, **110**, 12365.
- 24 V. A. Drits and A. S. Bookin, in *Layered Double Hydroxides: Present and Future*, ed. V. Rives, Nova Sci. Pub., Inc., New York, ch. 2, 2001.
- 25 A. A. Eliseev, A. V. Lukashin, A. A. Vertegel, V. P. Tarasov and Y. D. Tret'yakov, *Dokl. Chem.*, 2002, **387**, 339.
- 26 T. Sato, H. Fujita, T. Endo and M. Shimada, *React. Solids*, 1988, **5**, 219.
- 27 R. I. Walton, A. Norquist, R. I. Smith and D. O'Hare, *Faraday Discuss.*, 2003, **122**, 331.
- 28 A. Ragavan, A. I. Khan and D. O'Hare, *J. Mater. Chem.*, 2006, **16**, 602.
- 29 F. Millange, R. I. Walton and D. O'Hare, *J. Mater. Chem.*, 2000, **10**, 1713.
- 30 D. M. Roy, R. Roy and E. F. Osborn, *Am. J. Sci.*, 1953, **251**, 337.
- 31 J. S. O. Evans, R. J. Francis, D. O'Hare, S. J. Price, S. M. Clark, J. Flaherty, J. Gordon, A. Nield and C. C. Tang, *Rev. Sci. Instrum.*, 1995, **66**, 2442.
- 32 S. M. Clark, *J. Appl. Crystallogr.*, 1995, **28**, 646.
- 33 M. J. Geselbracht, R. I. Walton, E. S. Cowell, F. Millange and D. O'Hare, *Chem. Mater.*, 2002, **14**, 4343.

Superparamagnetic nanoparticle-supported palladium: a highly stable magnetically recoverable and reusable catalyst for hydrogenation reactions

Liane M. Rossi,^{*a} Fernanda P. Silva,^a Lucas L. R. Vono,^a Pedro K. Kiyohara,^b Evandro L. Duarte,^b Rosangela Itri,^b Richard Landers^c and Giovanna Machado^d

Received 7th September 2006, Accepted 2nd January 2007

First published as an Advance Article on the web 24th January 2007

DOI: 10.1039/b612980c

Here we present a magnetically recoverable palladium catalyst prepared by immobilization of palladium over silica-coated magnetite nanoparticles. The catalyst reduced by molecular hydrogen contains palladium nanoparticles well distributed and stabilized in the magnetizable support surfaces and converts cyclohexene to cyclohexane under mild reaction conditions (75 °C and 6 atm) with TOF of 11 500 h⁻¹. The catalyst was easily recovered with a permanent magnet in the reactor wall and reused for up to 20 recycles of 2500 TON each without any significant loss in catalytic activity, demonstrating an efficient recycling process for hydrogenation reactions.

Introduction

Superparamagnetic nanoparticles are now emerging as new supporting materials for catalysts immobilization with increased catalyst to products separation capabilities.¹ Nanometric iron oxides respond to an external magnetic field but do not remain magnetized when the magnetic field is removed. These properties permit superparamagnetic materials to be concentrated from the solution with a magnet and dispersed immediately after removing the magnetic field. The absence of remanence prevents particle-particle attraction and particle aggregation, which would dramatically decrease the surface area of a solid support. Magnetic separation is very promising to greatly improve separability and recycling of homogeneous and nanocluster catalysts. In this recycling process, the catalyst can be magnetically recovered inside the reactor vessel while draining the liquid products. It can be considered a greener technology that avoids the consequences of filtration steps such as catalyst mass loss, catalyst oxidation, use of additional solvents and the subsequent generation of organic residues.

Magnetic separation has been extensively used in biomedical applications such as drug targeting, cell sorting and isolation and separation of biochemical products.² The biomedical applicability of magnetic particles is greatly improved by coating their surfaces to protect the magnetic core and increase surface reactivity. It is worth mentioning the results of Philipse *et al.*³ and Xia *et al.*⁴ on the preparation of silica coated magnetic nanoparticles. Silica contains reactive silanol groups that can be easily functionalized by organosilanes yielding modified surfaces with a variety of functional groups, such as amino and thiol.⁵ Those functional groups can also work perfectly as coordinating sites for metals as well as starting

materials for the engineering of chelant ligands on silica surfaces. Thiol-modified mesoporous silica, for instance, has been shown as a remarkable scavenger for palladium.^{6,7} The palladium loaded solid obtained by Crudden *et al.*⁷ was also used as a heterogeneous and reusable catalyst for coupling reactions with no leaching of palladium (<3 ppb Pd in the filtrates). Immobilization of palladium on solid supports is a strategy to decrease the accumulation of palladium in the final products, especially important in the synthesis of pharmaceuticals, but leaching of palladium can occur. In some cases, it has been demonstrated that heterogeneous catalysts are merely reservoirs for highly active soluble forms of palladium.⁸ In an attempt to prepare a palladium-based magnetically separable catalyst we first coated the surfaces of superparamagnetic nanoparticles with silica and then modified their surfaces with thiol for the immobilization of palladium. The catalyst, reduced by molecular hydrogen, contains palladium nanoparticles well distributed and stabilized in the magnetizable support surfaces. The catalytic performance and recycling of the magnetizable palladium catalyst in hydrogenation reactions in solventless conditions were investigated.

Results and discussion

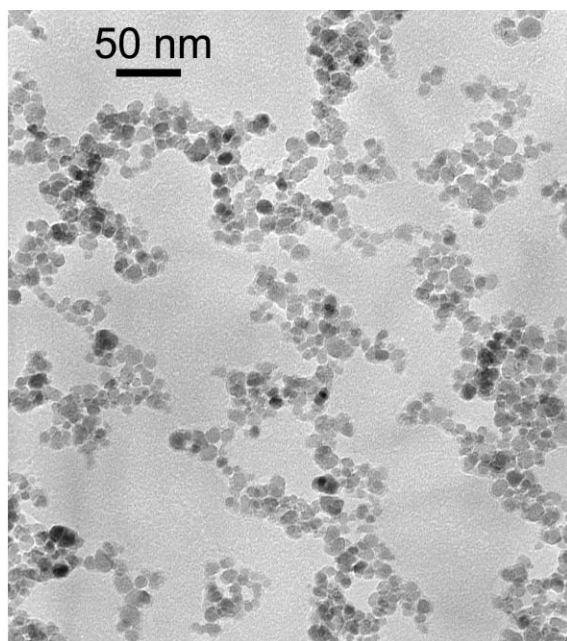
Silica-coated magnetic particles were prepared following the procedure described by Philipse *et al.*³ that consists of pre-coating magnetic particles surfaces with soluble silicate, and subsequent growth of a silica layer by condensation of tetraethylorthosilicate. The pre-coating step was necessary to improve the solubility of the magnetic particles in the alcohol mixture that is used for the silica layer growth. Without this step, precipitation and agglomeration of the magnetic nanoparticles take place immediately after addition of ethanol or isopropanol. The magnetic cores were prepared by coprecipitation of Fe²⁺/Fe³⁺ ions under alkaline conditions followed by stabilization with tetraethylammonium hydroxide.³ TEM images of the pre-coated magnetic particles and the silica-coated magnetic spheres are shown in Fig. 1 and 2. Analysis of the micrograph in Fig. 1a indicates that these

^aInstitute of Chemistry, University of São Paulo, USP, São Paulo, 05508-000, SP, Brazil and CEPEMA-USP, Cubatão, SP, Brazil. E-mail: lrossi@iq.usp.br; Fax: +55 11 38155579; Tel: +55 11 30912181

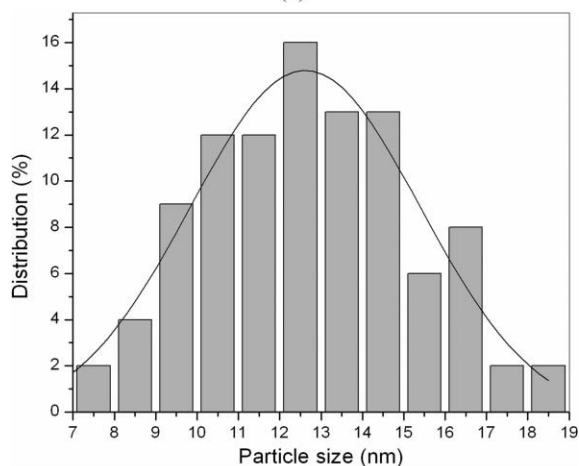
^bInstitute of Physics, USP, São Paulo, SP, 05508-090, Brazil

^cInstitute of Physics, UNICAMP, Campinas, SP, 13083-970, Brazil

^dInstitute of Chemistry, UFRGS, Porto Alegre, RS, 91501-970, Brazil



(a)



(b)

Fig. 1 (a) Transmission electron microscopy (TEM) of the pre-coated magnetite nanoparticles and (b) histogram showing particle size distribution.

nanoparticles display an irregular shape, but evaluating their characteristic diameter results in a mono modal distribution. The histogram of Fig. 1b shows that particle size distributions can be reasonably well fitted by a Gaussian curve. The average diameter of the nanoparticles after pre-coating with silicate, determined by measuring the diameter of 600 randomly selected particles in enlarged TEM images, was 12 ± 3 nm.

After a 10 nm silica layer growth, the particles size increased to approximately 30 to 40 nm diameter size (Fig. 2). Although most of the particles appear spherical in shape, some aggregation can be seen and we were not able to precisely determine particles size.

Magnetization curves revealed the superparamagnetic behavior of the silica coated-magnetic nanoparticles with a saturation magnetization of 12.6 emu g^{-1} (Fig. 3). This value is smaller than that of bulk magnetite (92 emu.g^{-1}), which is

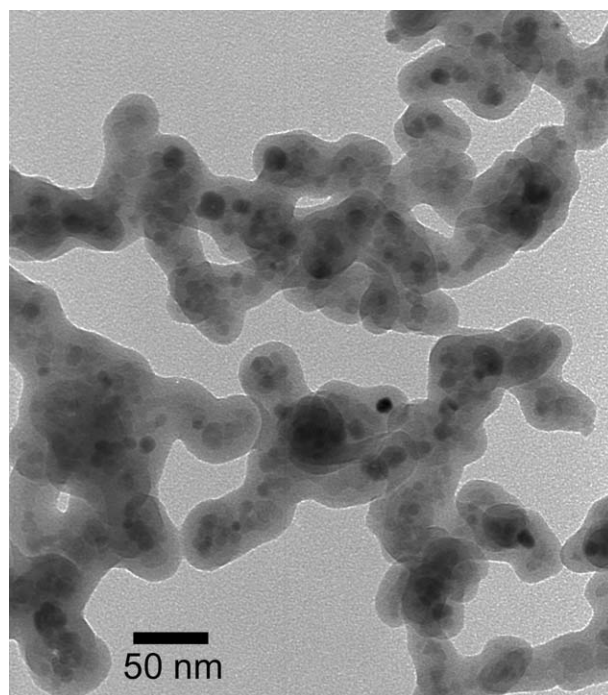


Fig. 2 TEM of silica-coated magnetic spheres.

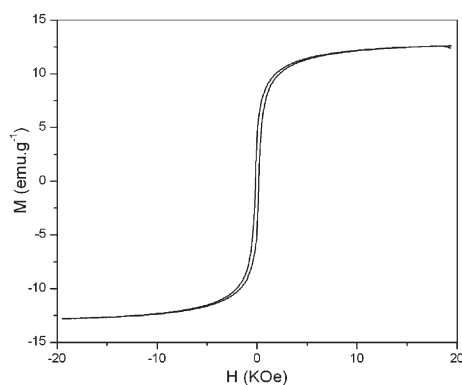


Fig. 3 Magnetization curve of silica-coated magnetic particles at 300 K.

consistent with the presence of a diamagnetic component. The decrease of the saturation magnetization suggests the presence of 30% of silica in the material.⁹ Even with this reduction in the saturation magnetization the solid can still be efficiently separated from solution with a small neodymium permanent magnet (~ 4400 G).

The silica-coated magnetic particles had their surfaces modified with thiol groups through hydrolysis and condensation with 3-mercaptopropyltrimethoxysilane (MPTMS), performed in dry toluene under nitrogen to minimize side-reaction. A thermal curing of the silanized solids was included to guarantee a stable, cross-linked and condensed silane layer.⁵ The mercaptopropyl-modified silica coated magnetic particles were submitted to an aqueous solution of $[\text{PdCl}_4]^{2-}$ (1.0 mg mL^{-1}). The isolated solid contains 1.21 wt% of palladium as determined by ICP-AES. The catalytic activity of the magnetizable palladium catalyst was investigated in

Table 1 Hydrogenation of cyclohexene to cyclohexane by Pd magnetically recoverable catalyst

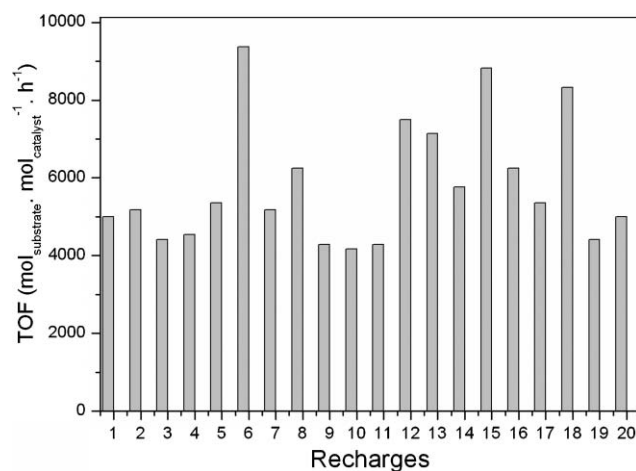
Entry	P/atm	$T/^\circ\text{C}$	Time/min	Conv. (%) ^a	TON ^b	TOF ^c /h ⁻¹
1	6	75	13	>99	2500	11 538
2	4	75	18	>99	2500	8333
3	2	75	51	>99	2500	2941
4	1	75	152	>99	2500	987
5	6	25	22	96	2400	6545
6	1	25	120	56	1400	700
7	6	75	510	>99	50 000	5882
8 ^d	6	75	600	>99	50 000	5000
9 ^e	10	75	240	3	27	7

^a Measured by GC. ^b Catalytic turnover number: mol of substrate transformed per mol of catalyst. ^c Catalytic turnover frequency: mol of substrate transformed per mol of catalyst per hour. ^d Catalyst reused after experiment described in entry 7. ^e Reaction performed without Pd: magnetic particles/substrate ratio = 1/1000.

hydrogenation reactions of olefins to the corresponding alkanes in solventless conditions. The reactor loaded with the catalyst and the olefin was submitted to the desired hydrogen pressure and temperature. The reaction is monitored by the consumption of hydrogen in a reservoir connected to the main reactor maintained at constant pressure. Curves of hydrogen pressure *versus* time were obtained for each experiment. At the desired time, the reactor was cooled down, the remaining hydrogen relieved and the catalyst recovered magnetically by placing a magnet in the reactor wall. The organic phase was easily separated and analyzed by gas chromatography. Table 1 summarizes the results.

The hydrogenation of cyclohexene at $P_{\text{H}_2} = 6 \text{ atm}$ and $T = 75 \text{ }^\circ\text{C}$ showed a very high turnover frequency of $11\,500 \text{ h}^{-1}$ (Table 1, entry 1). At a hydrogen pressure of 1 atm, the reaction became ten times slower at $75 \text{ }^\circ\text{C}$ (Table 1, entry 4) and did not go to completion after two hours at $25 \text{ }^\circ\text{C}$ (Table 1, entry 6). Similar experiments performed with non-supported PdCl_2 showed deposition of a metallic film and catalyst deactivation. The performance of commercially available Pd/C catalyst under the conditions used in this study is comparable to our results ($\text{TOF} = 18\,750 \text{ h}^{-1}$), but with the difficulty of separating the product. The catalytic parameters shown in Table 1 were calculated based on the total amount of palladium in the catalyst without taking into account the true number of active metal sites on nanoparticles surfaces, consequently those values may be underestimated.¹⁰ The values shown in Table 1 are higher than those reported for hydrogenation of cyclohexene by palladium¹¹ and other metal nanoparticles¹² stabilized in solid or liquid supports.

Further experiments were performed to verify the catalyst stability and recyclability. After a first run with complete conversion of 28 mmol of olefin ($11.2 \text{ } \mu\text{mol}$ palladium, $75 \text{ }^\circ\text{C}$ and 6 atm H_2), the magnetically recovered catalyst was reused in twenty successive runs of 2500 TON each (total turnover of 50 000 in 9 h), by addition of new portions of cyclohexene. The catalyst showed no significant loss of activity at the end of the 20th run (Fig. 4). Variations on the reaction rates in the series of experiments were observed, but the rate of the first and the 20th batch were the same (5000 h^{-1}), which means that the active metal sites were maintained. Moreover, the minimum activity (lower TOF values) did not change significantly, but peaks of increased activity were observed at recharges 6, 12,

**Fig. 4** Catalyst recycling in the hydrogenation of cyclohexene at 2500 mol substrate per mol catalyst each run, $75 \text{ }^\circ\text{C}$ and 6 atm H_2 .

13, 15 and 18. The organic products were collected and the Pd content was $<0.01 \text{ ppm}$ (ICP-AES analysis). In order to better estimate the catalyst lifetime, a new experiment was performed with an olefin/Pd ratio of 50 000 (Table 1 entry 7) and the catalyst was still active for a second run (Table 1, entry 8) corresponding to a total turnover (TTO) of 100 000.

In order to obtain evidence that reduction of the Pd(II) bonded to mercaptopropyl modified magnetic solid occurred when submitted to hydrogenation conditions, we carried out TEM (Fig. 5), X-ray diffraction (XRD) (Fig. 6) and X-ray photoelectron spectroscopy (XPS) (Fig. 7) analysis of the spent catalyst. The results shown in Fig. 5 and Fig. 6 are consistent with the formation of $[\text{Pd}(0)]_n$ nanoparticles on silica surfaces of the catalyst submitted to hydrogenation reactions.

The stabilization of metal nanoparticles on the magnetic support surface can explain the high reusability of our catalyst without losing activity. It is well established that high energy surface metal nanoparticles aggregate into larger particles or bulk materials in the absence of stabilizing agents or supports, resulting in decreased surface areas, loss of reactive sites and consequently deactivation of the catalyst by agglomeration.¹³

The TEM image of the spent catalyst (Fig. 5a) clearly shows the silica shell decorated with very small particles, attributed to palladium species since they were absent in the TEM image of the silica-coated magnetic particles shown in Fig. 2. Analysis of TEM enlarged micrographs, by measuring the diameter of 300 randomly selected particles, resulted in the particle size distribution histogram shown in Fig. 5b. The size distribution was found to be well described by a Gaussian distribution function from which we obtained an average particle diameter of $3.0 \pm 0.5 \text{ nm}$. The high resolution TEM (HRTEM) image (Fig. 5c) allowed us, by means of Gatan software, to obtain the Fourier transform from which lattice spacings of 2.16 and 2.02 \AA were (experimental error $<5\%$). These lattice spacings, corresponding to the interplanar distance (1 1 1) and (2 0 0) of the Pd(0), are depicted by the arrows in Fig. 5c.

The XRD pattern of the spent catalyst confirms the presence of crystalline Pd(0) by the appearance of the most representative Bragg reflections of Pd(0) metal as indicated in the Fig. 6(b). The mean diameter could be estimated from the

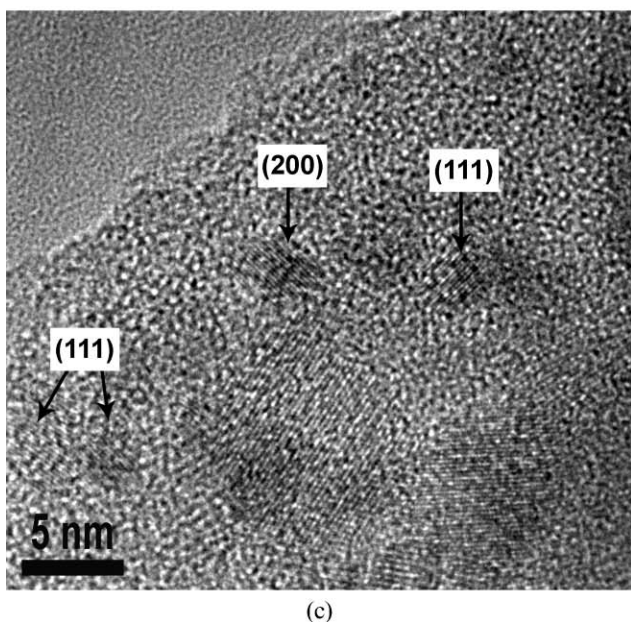
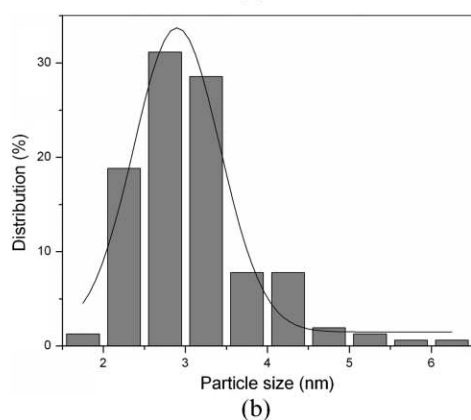
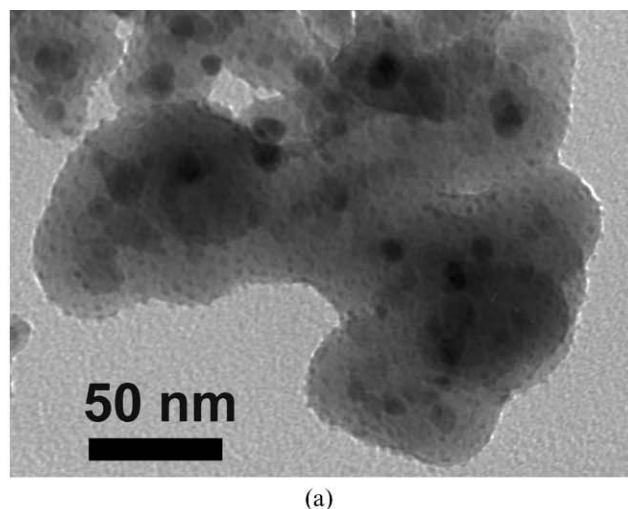


Fig. 5 (a) TEM micrographs, (b) histograms showing the particle size distribution of Pd(0), and (c) HRTEM image of the spent catalyst with the interplanar distance indicated by arrows.

XRD diffraction pattern by means of the Debye–Scherrer equation calculated from full width at half-maximum (fwhm) of the (111), (200), (220), (311), and (222) planes obtained from Rietveld's refinements. The most representative reflections of

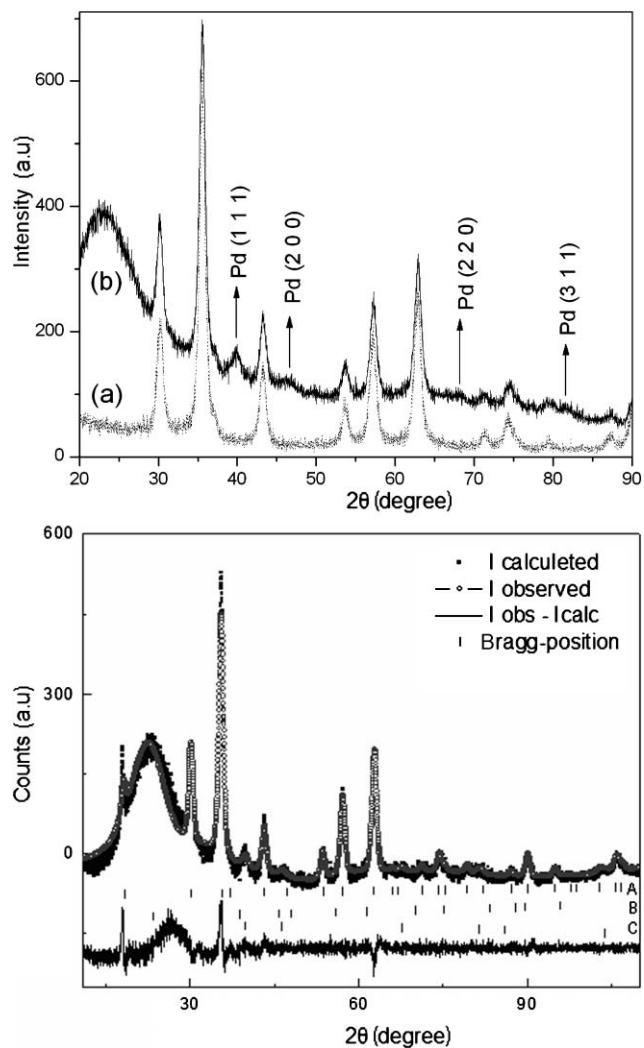


Fig. 6 X-ray diffraction pattern of (a) the magnetic core— Fe_3O_4 nanoparticles and (b) the spent catalyst (top) and Rietveld's refinement (bottom). (A = Bragg peak position Fe_3O_4 ; B = Bragg peak position SiO_2 ; C = Bragg peak position Pd (0)).

Pd(0) and Fe_3O_4 were indexed as face-centered cubic (fcc) with unit cell parameter $a = 3.9142 \text{ \AA}$ and $a = 8.3668 \text{ \AA}$, respectively. The simulations of Bragg reflections and Rietveld's refinement were performed with a pseudo-Voigt function using

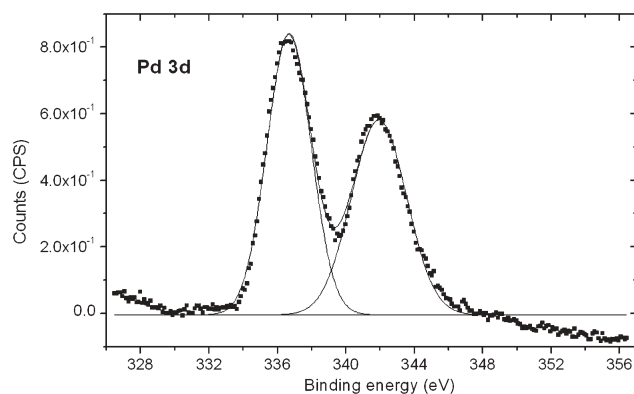


Fig. 7 XPS spectrum of the spent catalyst.

the FULLPROF code.¹⁴ It is important to point out that the use of fwhm of a peak to estimate the size of crystalline grain by means of the Scherrer equation has serious limitations, since it does not take into account the existence of a distribution of sizes and the presence of defects in the crystalline lattice. Therefore, the calculation of the average diameter of the grains from fwhm of the peak can overestimate the real value, since the larger grains give a strong contribution to the intensity, while the smaller grains just enlarge the base of the peak. Moreover, the presence of defects in a significant amount causes an additional enlargement of the diffraction line. Considering this enlargement, the obtained size can be smaller than the real size of the grains. These problems can be minimized by the use of Rietveld's refinement method. Indeed, these discrepancies are confirmed by the values found for the average diameter of the nanoparticles without the structural refinement (8.5 ± 3 nm and 6.5 nm), which significantly differ from those found by means of Rietveld's refinement (11.5 ± 3 nm and 4.5 nm) for the nanoparticles Fe₃O₄ and Pd(0), respectively. These latter values are much closer to those determined by TEM. Fig. 6 shows the X-ray diffraction pattern of the magnetic core—Fe₃O₄ nanoparticles, the spent catalyst (top) and Rietveld's refinement of this material (bottom).

Further analysis of the spent catalyst using XPS showed the palladium 3d doublet at 336.7 eV for 3d_{5/2} and 341.9 eV for 3d_{3/2} (Fig. 7). According to the literature,¹⁵ the Pd 3d_{5/2} peak binding energy for Pd(0) is 335.1 eV. However, we found the Pd 3d_{5/2} peak shifted to higher values, suggesting that the catalyst has electron-deficient palladium species on the surface. These oxidized forms of Pd might be palladium chloride or palladium oxide, which show Pd 3d_{5/2} peak binding energies at 337.5 or 336.9 eV, respectively.¹⁵ Considering the peak position, TEM and XRD results, the Pd(II) component found in our system can be attributed to PdO, probably resulting from surface reoxidation of high surface area palladium nanoparticles during workup procedures. Analysis of peak binding energies also confirms the absence of the metal precursor, palladium chloride, in the spent catalyst. Using the same sample portion, a new XRD analysis was performed and, again, the most representative Bragg reflections of Pd(0) metal were observed in the XRD pattern, whereas the expected Bragg reflections of crystalline PdO were not detected. These results are consistent with the presence of an amorphous layer of PdO over the palladium nanoparticles only detected by XPS and not detected by XRD.

Conclusions

In summary, we have prepared a highly stable magnetically recoverable catalyst formed by very small palladium nanoparticles well distributed and stabilized in the magnetizable support surfaces. A good agreement was found between TEM and XRD methods for determining the mean relative diameters of the nanoparticles. The values obtained were 3.0 and 4.5 nm from TEM and XRD, respectively. The catalyst showed excellent catalytic activity for hydrogenation of cyclohexene without catalyst leaching or deactivation after 20 cycles or 100 000 turnovers. After each reaction, the

catalyst could be easily separated magnetically from the reaction products minimizing the generation of organic residues and avoiding the use of additional solvents and environmentally non-friendly procedures.

Experimental

Materials and instrumentation

Iron(II) chloride hydrate, iron(III) chloride hydrate, ammonium hydroxide, 3-mercaptopropyltriethoxysilane, tetraethylammonium hydroxide, tetraethoxysilane and cyclohexene were purchased from Aldrich and Fluka and used without further purification.

GC analysis. Gas chromatography analyses were performed on a Shimadzu GC 17A, equipped with a 30 metre capillary column with a dimethylpolysiloxane stationary phase, using the following parameters: initial temperature: 40 °C, initial time: 5 min, ramp: 10 °C min⁻¹, final temperature: 250 °C, final time: 5 min, injector and detector temperature: 250 °C, injection volume: 2 μ L.

TEM analysis. The morphology of the obtained nanoparticles was obtained on a Philips CM 200 operating at an accelerating voltage of 200 kV. The samples for TEM were prepared by dispersion of the nanoparticles in aqueous solution at room temperature and then collected on a carbon-coated copper grid. The histograms of the nanoparticles size distribution, assuming spherical shape, were obtained from the measurement of about 600 particles and were reproduced in different regions of the Cu grid, found in an arbitrarily chosen area of enlarged micrographs. The high resolution electron microscopy work was performed with a JEM-3010 ARP microscope.

XRD analysis. The phase structures of nanoparticles were characterized by XRD. For the XRD analysis, the nanoparticles were isolated as a fine powder and placed in the sample holder. The XRD experiments were carried out on a Rigaku-Denki powder diffractometer equipped with a curved graphite crystal using Cu K α radiation $\lambda = 1.5418$ Å. The diffraction data were collected at room temperature in a Bragg–Brentano θ – 2θ geometry with scan range between 10° to 100°. The diffractograms were obtained with a constant step, $\Delta 2\theta = 0.02^\circ$. The indexation of Bragg reflections was obtained by a pseudo-Voigt profile fitting using the FULLPROF code.¹⁴

Magnetic measurements. A VSM was used to obtain the magnetization *versus* magnetic field loop at room temperature up to $H = 20$ kOe. The apparatus was calibrated with a Ni pattern. The magnetization measurements were carried out on a known quantity of powder samples, slightly pressed and conditioned in cylindrical holders of Lucite.

XPS analysis. The X-ray photoelectron spectra were obtained with a VSW HA-100 spherical analyzer using an aluminum anode (AlK α line, $h\nu = 1486.6$ eV) X-ray source. The high-resolution spectra were measured with constant

analyzer pass energies of 44 eV, which produce a full width at half-maximum (fwhm) line width of 1.7 eV for the Au(4f_{7/2}) line. The powdered samples were pressed into pellets and fixed to a stainless steel sample holder with double-faced tape and analyzed without further preparation. To correct for charging effects the spectra were shifted so that the Cls binding energy was 284.6 eV. Curve fitting was performed using Gaussian line shapes, and Shirley type background was subtracted from the data.

Synthesis of magnetic particles. Fe₃O₄ nanoparticles were prepared by the co-precipitation method: 10 mL of an aqueous solution of FeCl₃ (1 mol L⁻¹) were mixed with 2.5 mL of FeCl₂ (2 mol L⁻¹) dissolved in HCl 2 mol L⁻¹. Both solutions were freshly prepared with deoxygenated water before use. Immediately after being mixed under nitrogen, the solution containing the iron chlorides was added to 125 mL of ammonium hydroxide solution (0.7 mol L⁻¹, deoxygenated water) under vigorous mechanical stirring (10 000 rpm, Ultra-Turrax T18 Homogenizer, IKA Works), under nitrogen atmosphere. After 30 minutes, the black precipitate formed was separated magnetically and redispersed in a new portion of water (3 × 250 mL). The obtained precipitate was dispersed in 125 mL of water and stabilized after addition of 15 mL of tetraethylammonium hydroxide.

Synthesis of magnetic silica spheres. Silica-coated magnetic particles were prepared following the procedure described by Philipse *et al.*³ A 16 mL of a 0.58 wt% silicate solution (the silicate solution was previously passed through an acid exchange resin column and the pH adjusted to 9.5 using a small portion of the original silicate solution) was mixed with 85 mL of ferrofluid stabilized with tetraethylammonium hydroxide (1.4 g L⁻¹). After the mixture, the solution attained pH 12 and was adjusted to pH 10 with 0.5 mol L⁻¹ HCl. The solution was stirred for 2 h and submitted to dialysis against an aqueous solution of tetraethylammonium hydroxide with pH adjusted to 10 for 2 days. Further silica growth on the obtained particles was performed according to the Stöber method. To a solution containing 944 mL of ethanol, 34 mL of NH₄OH and 9.1 mL of the obtained particles was added 0.8 mL of TEOS. The solution was allowed to stand for 24 h under stirring. The product was isolated by centrifugation (6000 rpm, 20 min) and washed with ethanol (3 × 50 mL) and water (2 × 50 mL) and dried in oven at 100 °C overnight.

Synthesis of mercaptopropyl-modified magnetic silica spheres. The reaction was performed under nitrogen using Schlenk techniques and dry solvent. To a dispersion containing 200 mg of magnetic silica spheres in toluene (15 mL) was added 0.15 mL of 3-mercaptopropyltriethoxysilane (MPTS). The solution was stirred for 2 hours. The resulting precipitate was centrifuged (6000 rpm, 10 min) and washed with toluene and acetone and dried in oven at 100 °C for 20 h. Elemental analysis: 2.04% C, 0.85% H.

Preparation of palladium catalyst. To 50 mg of thiol-modified magnetic silica spheres was added 5 mL of a palladium chloride solution (1 mg mL⁻¹) (PdCl₂ was dissolved in

water by addition of NaCl and heating). The resulting solid was separated magnetically, washed with water and acetone and isolated as a powder. Palladium contents (analyzed by ICP-AES): 1.21 wt%

Hydrogenation experiments. The catalytic reactions were carried out in a Fischer–Porter reactor connected to an H₂ reservoir. In a typical experiment, catalyst (50 mg, 5.6 μmol Pd) and 1.16 g of cyclohexene (14 mmol) are added to the reactor under inert atmosphere. The reactor is connected to a hydrogen gas reservoir and the reaction is initiated by the gas admission at constant pressure. The reaction is monitored by the fall in hydrogen pressure in the H₂ reservoir as a function of time. H₂ uptake was measured in 10 sec intervals with a pressure transmitter interfaced *via* a Novus Field Logger converter to a computer. The pressure *versus* time data are collected by the FieldChart Novus Software, stored as a data file and exported to MicroCal Origin 7.0 for hydrogenation rates calculations. The catalyst is recovered magnetically by placing a magnet in the reactor wall and the products are collected and analyzed by GC and GC-MS. The isolated catalyst can be reused by addition of new portions of substrate.

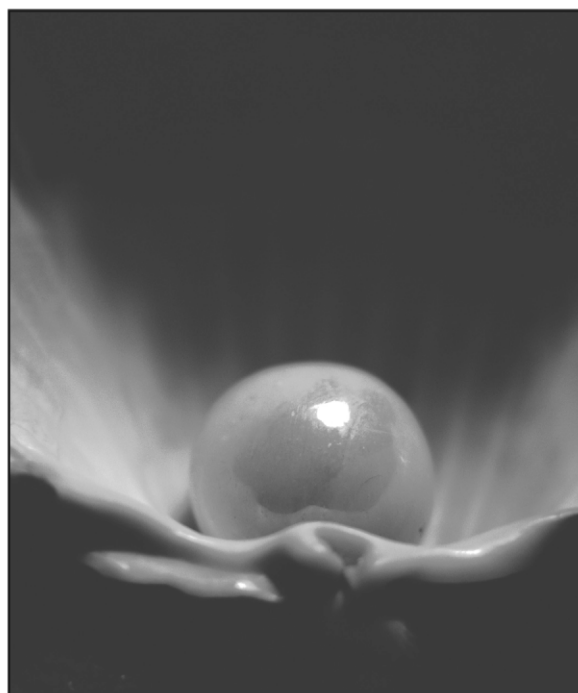
Acknowledgements

We are grateful to FAPESP, CNPq and TWAS for financial support. We also thank the Laboratory of Magnetism of IF-USP for VSM measurements, and the Laboratory of Electron Microscopy of LNLS, Campinas, SP for HRTEM images.

References

- 1 T.-J. Yoon, W. Lee, Y.-S. Oh and J. K. Lee, *New J. Chem.*, 2003, **27**, 227; P. D. Stevens, G. Li, J. Fan, M. Yen and Y. Gao, *Chem. Commun.*, 2005, 4435; P. D. Stevens, J. Fan, H. M. R. Gardimalla, M. Yen and Y. Gao, *Org. Lett.*, 2005, **7**, 2085; A. Hu, G. T. Yee and W. Lin, *J. Am. Chem. Soc.*, 2005, **127**, 12486; M. Kotani, T. Koike, K. Yamaguchi and N. Mizuno, *Green Chem.*, 2006, **8**, 735.
- 2 Q.A. Pankhurst, J. Connolly, S. K. Jones and J. Dobson, *J. Phys. D: Appl. Phys.*, 2003, **36**, R167 and references therein; Z. M. Saiyed, S. D. Telang and C. N. Ramchand, *Biomagn. Res. Technol.*, 2003, **1**, 2; S. K. Sahoo and V. Labhasetwar, *Drug Discovery Today*, 2003, **8**, 1112.
- 3 A. P. Philipse, M. P. B. van Bruggen and C. Pathmamanoharan, *Langmuir*, 1994, **10**, 92.
- 4 Y. Lu, Y. Yin, B. T. Mayers and Y. Xia, *Nano Lett.*, 2002, **2**, 183.
- 5 I. Haller, *J. Am. Chem. Soc.*, 1978, **100**, 8050; C. M. Halliwell and A. E. G. Cass, *Anal. Chem.*, 2001, **73**, 2476; K. C. Vrancken, L. D. Coster, P. V. D. Voort, P. J. Grobet and E. F. Vansant, *J. Colloid Interface Sci.*, 1995, **170**, 71.
- 6 T. Kang, Y. Park, J. C. Park, Y. S. Cho and J. Yi, *Stud. Surf. Sci. Catal.*, 2003, **146**, 527; T. Kang, Y. Park and J. Yi, *Ind. Eng. Chem. Res.*, 2004, **43**, 1478.
- 7 C. M. Crudden, M. Sateesh and R. Lewis, *J. Am. Chem. Soc.*, 2005, **127**, 10045.
- 8 K. Yu, W. Sommer, J. M. Richardson, M. Weck and C. W. Jones, *Adv. Synth. Catal.*, 2005, **347**, 161; A. Biffis, M. Zecca and M. Basato, *Eur. J. Inorg. Chem.*, 2001, 1131.
- 9 P. S. Haddad, E. L. Duarte, M. S. Baptista, G. F. Goya, C. A. P. Leite and R. Itri, *Prog. Colloid Polym. Sci.*, 2004, **128**, 232.
- 10 L. M. Rossi, G. Machado, P. F. P. Fichtner, S. R. Teixeira and J. Dupont, *Catal. Lett.*, 2004, **92**, 149; J. A. Widegren and R. G. Finke, *J. Mol. Catal. A: Chem.*, 2003, **198**, 317.
- 11 J. Huang, T. Jiang, B. Han, H. Gao, Y. Chang, G. Zhao and W. Wu, *Chem. Commun.*, 2003, 1654; J. Huang, T. Jiang, H. Gao, B. Han, Z. Liu, W. Wu, Y. Chang and G. Zhao, *Angew. Chem.*,

- Int. Ed.*, 2004, **43**, 1397; M. Ooe, M. Murata, T. Mizugaki, K. Ebitani and K. Kaneda, *Nano Lett.*, 2002, **2**, 999.
- 12 See for example: L. M. Rossi, J. Dupont, G. Machado, P. F. P. Fichtner, C. Radtke, I. J. R. Baumvol and S. R. Teixeira, *J. Braz. Chem. Soc.*, 2004, **15**, 904; J. Dupont, G. S. Fonseca, A. P. Umpierre, P. F. P. Fichtner and S. R. Teixeira, *J. Am. Chem. Soc.*, 2002, **124**, 4228; C. W. Scheeren, G. Machado, J. Dupont, P. F. P. Fichtner and S. R. Teixeira, *Inorg. Chem.*, 2003, **42**, 4738; C. W. Scheeren, G. Machado, S. R. Teixeira, J. Morais, J. B. Domingos and J. Dupont, *J. Phys. Chem. B*, 2006, **110**, 13011; X. Mu, D. G. Evans and Y. Kou, *Catal. Lett.*, 2004, **97**, 151; J. Schulz, A. Roucoux and H. Patin, *Chem. Commun.*, 1999, 535; A. M. Doyle, S. K. Shaikhutdinov, S. D. Jackson and H.-J. Freund, *Angew. Chem., Int. Ed.*, 2003, **42**, 5240; J. D. Aiken, III and R. G. Finke, *J. Am. Chem. Soc.*, 1999, **121**, 8803.
- 13 G. Schmid, *Chem. Rev.*, 1992, **92**, 1709.
- 14 J. R. Carbajal, *Short Reference Guide of The Program Fullprof, version 2005*, <http://valmap.dfis.uill.es/fullprof/php/downloads.php>.
- 15 C. D. Wagner, W. M. Riggs, L. E. Davis and J. F. Moulder, in *Handbook of X-ray Photoelectron Spectroscopy*, ed. G. E. Muilenberg, Perkin-Elmer Corporation, Eden Prairie, MN, USA, 1978.



Looking for that **special** chemical biology research paper?

TRY this free news service:

Chemical Biology

- highlights of newsworthy and significant advances in chemical biology from across RSC journals
- free online access
- updated daily
- free access to the original research paper from every online article
- also available as a free print supplement in selected RSC journals.*

*A separately issued print subscription is also available.

Registered Charity Number: 207890

RSCPublishing

www.rsc.org/chembiology

18030681

A HCN-based reaction under microreactor conditions: industrially feasible and continuous synthesis of 3,4-diamino-1*H*-isochromen-1-ones

Davy R. J. Acke and Christian V. Stevens*

Received 18th October 2006, Accepted 12th January 2007

First published as an Advance Article on the web 26th January 2007

DOI: 10.1039/b615186h

Microreactor technology has been studied as a suitable process to produce chemicals *via* multicomponent reactions. In this study, efforts were made to produce 3,4-diamino-1*H*-isochromen-1-ones. Based on a known reaction procedure, using *in situ* generated HCN, a safe reaction setup was created to avoid the release of the hazardous gas during the process. The 3,4-diamino-1*H*-isochromen-1-ones were produced continuously in moderate to good yields.

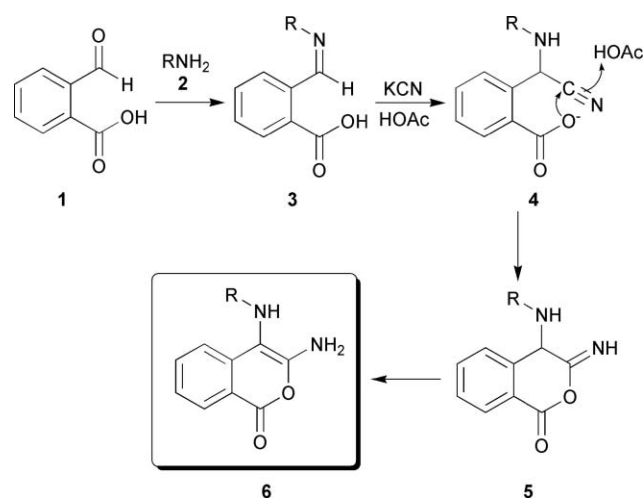
Introduction

The use of multicomponent reactions (MCRs) is an easy and interesting way to produce complex structures using simple starting materials.¹ Starting from the Strecker reaction, discovered in 1850, a wide range of different types of MCRs has been designed.² Some important examples are the Mannich reaction,³ the Biginelli reaction,⁴ the Ugi reaction⁵ and the Baylis–Hillman reaction.⁶ Another interesting MCR recently described the production of 3-amino-4-(arylamino)-1*H*-isochromen-1-ones (Scheme 1). This type of isocoumarin is of great interest due to the possibility of forming base pairs with guanine due to the ‘donor–acceptor’ similarity with cytosine.⁷ Unfortunately, the reaction proceeds *via* a modified Strecker reaction, in which the highly toxic hydrogen cyanide is needed. In order to avoid large quantities of HCN, the idea of using microreactor technology for production of this

isochromen-1-one was proposed. Microreactor systems are – in a strict and rather ‘old-fashioned’ way – defined as devices produced by micro engineering techniques. Nowadays the broader definition also contains scaled-down designs of existing reactors, modern reactor concepts, *e.g.* structured catalysts like foams, and even capillary-in-tube reactors.⁸ Important advantages are the high mass and heat transfer and the possibility of using toxic reagents in a safe way. During the past decade a lot of work has been done in this field of technology.⁹ In this study, the CYTOS[®] College System, a microreactor which is produced by CPC-Cellular Process Chemistry Systems GmbH, was used.¹⁰ Several reaction types such as exothermic reactions, conversions with unstable intermediates, toxic reactions,^{9e} Mizoroki–Heck reactions,^{9f} nitration reactions,^{9h} pigment production,^{9k} were already successfully performed using this microreactor technology. In the past, specialized microreactor systems were already assembled to synthesize HCN *via* the Andrussov process, an industrial process to produce large quantities of HCN by reacting methane and ammonia in the presence of oxygen.¹¹ To the best of our knowledge, this is the first study in a microreactor system in which HCN is produced reacting further in the microreactor.

Results and discussion

In our efforts to study the potential of microreactor technology for MCRs,¹² a micro-meso design¹³ is used. This device consists of a stacked plate microreactor (micro) and a residence time unit, which consists of an isolated tube to increase reaction time (RTU, meso). The microreactor itself has a mixing zone and a reaction zone. Pumping of the reagents through the system is pressure-driven. The MCR to form the 3-amino-4-(arylamino)-1*H*-isochromen-1-ones **6** consists of a Strecker reaction–intramolecular nucleophilic addition–tautomerization sequence. First, the cyanide anion is added to the imine **3**, followed by an attack of the carboxy group onto the nitrile to form an *O*-acyl imidate **5**. This compound tautomerizes towards the final structure **6**. The *in situ* generation of the hydrogen cyanide results from the addition of acetic acid to potassium cyanide.



Scheme 1 Formation of 3,4-diamino-1*H*-isochromen-1-ones **6** (R = aryl).

Research Group SynBioC, Department of Organic Chemistry, Faculty of Bioscience Engineering, Ghent University, Coupure links 653, B-9000 Ghent, Belgium. E-mail: Chris.Stevens@UGent.be; Fax: +32 9264 6243; Tel: +32 9264 5950

Table 1 Optimization of the production of 3-amino-4-(arylamino)-1*H*-isochromen-1-ones **6** under microreactor conditions^a

Entry	Residence time/min ^b	Concentration of 1/M ^c	Yield (%) ^d	Output/g h ⁻¹
1	118	0.2	Clogging ^e	—
2	118	0.15	Clogging	—
3	118	0.1	67	0.41
4	39.2	0.2	Clogging	—
5	39.2	0.15	43–66	1.17–1.80
6 ^f	29.3	0.2	49	2.37
7	19.6	0.2	46–54	3.34–3.92
8 ^g	5	0.2	48	0.58
9 ^g	0.83	0.2	51	3.70

^a General conditions: temperature: 50 °C; inlet A₁: 2-formylbenzoic acid and 2 equiv. acetic acid in methanol; inlet A₂: 1.2 equiv. potassium cyanide and 2 equiv. amine in methanol. ^b The residence time was calculated according to eqn (1). ^c Concentration of the reagents in the reactor. ^d After crystallization. ^e By 'clogging', the formation of crystals in the tubes and the subsequent blockage of the tubes is indicated. ^f Partial clogging occurred after the first sample. ^g The sample was taken at the end of the microreactor.

Optimization

The optimization of a reaction under microreactor conditions always contains a number of important steps: the order of mixing of the starting materials, the residence time (flow rate), the concentration of the reagents and the solvent choice are of major importance to get a good production of the desired compound. Table 1 summarizes the results of this optimization.

A primary experiment was based on the reaction conditions provided by Opatz and Ferenc (Table 1, entry 1).⁷ Some changes had to be made, however, to fit the microreactor setup:

(1) The reaction temperature was lowered from 65 to 50 °C, since temperatures approaching the boiling point of the solvent (less than 10 °C under the boiling point) provide irregular residence times due to partial evaporation of the solvent (in this case methanol).

(2) The concentration of the reagents in the microreactor was lowered by 50% due to the limited solubility of KCN (the maximum solubility of KCN in methanol at room temperature is approximately 0.48 M). Moreover, other solvents could not be used because of the low solubility of KCN.

(3) The maximum residence time of the system (approximately 2 h) was used instead of 3 h. For safety reasons and in order to generate HCN only *in situ*, the potassium cyanide and the acetic acid were pumped separately into the microreactor.

The reaction setup is given in Fig. 1. This experiment gave no good results because crystals of the end-product were formed in the tubing at the end of the reactor which led to clogging of the system.

Since the crystallization only occurred at the end of the tubing, it can be explained by a combination of a high product concentration and a saturation effect. Because the microreactor output was flushed with nitrogen for safety reasons (removal of traces of HCN), the solvent was partially removed at the end of the system due to evaporation. This initiated crystallization due to saturation and led after some time to crystals appearing everywhere in the end tubing.

In an attempt to solve this problem, the setup was changed by submerging the end tubing in the solvent with or without the use of an ultrasound bath to prevent nucleation in the tube. Both alternatives appeared to be insufficient, although putting the end tubing in the solvent meant that slower crystallization occurred. The use of ultrasound gave only smaller crystals: more nucleation and less growth, which seemed to be in accordance with the literature.¹⁴

A decrease to a concentration of 0.10 M of starting material was finally enough to prevent blocking of the system (Table 1, entry 3). In order to increase the amount of product produced in a certain time, a combination of residence time decrease and concentration increase was tested. In the case of 0.20 M of starting material, the residence time had to be lowered to one-sixth of the maximal residence time to prevent clogging (entry 7). A reduction to approximately 30 min gave no initial crystallization in the tubing, but after a longer run, partial blocking of the system was observed (entry 6). Final tuning of the reaction conditions to 0.15 M of starting material and a residence time of approximately 40 min gave a maximum yield of 66% (entry 5). Although some outputs (g h⁻¹) were higher in other cases, this optimal setup was chosen because of the higher yields.

Next to these results, a different setup was applied. Since no crystallization occurred after the microreactor, a HPLC pump was installed between the microreactor and the RTU by means of a T-junction (Fig. 1). Through this pump an immiscible perfluorated solvent, Fluorinert[®] FC-70, was introduced to the reaction flow. This method created plugs of the reaction mixture, which was mixed in the microreactor, separated from each other by the immiscible solvent, with lengths depending on the flow rates of the pumps. Based on the research of Ismagilov and coworkers,¹⁵ the idea was proposed that the

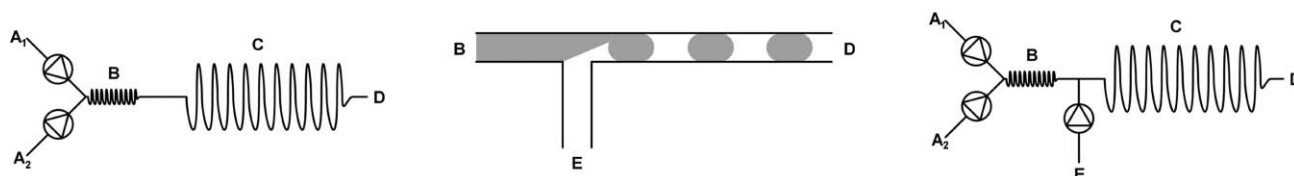


Fig. 1 Reaction setup: (left) normal setup; (middle) plug formation; (right) adjusted setup. A = input reagents, B = microreactor, C = residence time unit, D = output reaction mixture, E = input Fluorinert[®] FC-70.

Table 2 Production of 3-amino-4-(arylamino)-1*H*-isochromen-1-ones **6** under microfluidic plug flow conditions^a

Entry	Residence time/min ^b	Reaction mixture fraction (<i>rmf</i>) ^c	Yield (%) ^d	Output/g h ⁻¹
1	50	0.71	50	1.07
2	30	0.20	42	0.26
3	23	0.33	44	0.44

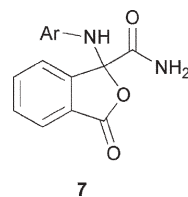
^a General conditions: temperature: 50 °C; inlet A₁: 0.4 M of 2-formylbenzoic acid and 0.8 M of acetic acid in methanol; inlet A₂: 0.48 M of potassium cyanide and 0.8 M of amine in methanol. ^b The residence time was calculated according to eqn (2). ^c The *rmf* was calculated according to eqn (3). ^d After crystallization.

immiscible solvent will drive the product further through the system, even if there was crystallization in the plugs itself. Table 2 shows the results of this setup. Although installation of the pump directly after the mixing zone of the microreactor is a better method to study the effect of the plug formation, this was practically impossible due to the specific construction of the microreactor. So it must be emphasized that already some reaction (but no crystallization) takes place before the plug formation.

The results show that the yields in this particular setup are lower than in the normal setup (Table 1, entry 5). However, it must be emphasized that, even at those high concentrations, no clogging was observed in the tubes. It was even possible to work at higher concentrations of reaction product and longer residence times without the problem of crystallization in the tubing system (Table 1, entry 4 and Table 2, entry 1). The immiscible solvent forms an oily layer between the wall of the microreactor and the plug.¹⁵ This prevents the crystals accumulating on the walls of the reactor. Fig. 1 shows the formation of plugs in the tubes. An additional advantage is that, owing to the immiscibility and, moreover, the rapid separation of the solvent, the quite expensive Fluorinert[®] FC-70 can be reused directly *via* a loop by simple separation from the reaction mixture. From an economical point of view, Table 2, entry 1 provides the best conditions since it has the highest yield and the lowest consumption of Fluorinert[®] FC-70 (highest *rmf*). The only disadvantage is the somewhat higher residence time which leads to a longer startup procedure.

Safety of the procedure

As mentioned in the Introduction, one of the important advantages of microreactor technology is the possibility of using in a safe way toxic reagents which cannot be used in a conventional reaction setup without considerable safety risks. Because of the small dimensions of the microreactor (2 mL), only minor amounts of the toxic reagent are formed. In this particular case, it was supposed that no hydrogen cyanide was released at the end of the reaction setup, in the case that equimolar (or lower) quantities of KCN were used. In order to test this, a hydrogen cyanide spot-test was used.¹⁶ Unfortunately, this test provided only qualitative results. In both the batch and the microreactor system, coloration of the reagent was detected which proved that HCN was released. A slower coloration was detected in the case of the microreactor setup.

**Fig. 2** Side product.

Degradation

The 3-amino-4-(arylamino)-1*H*-isochromen-1-one **6** appeared to be very unstable in solution. Several solvents (chloroform, DMSO, methanol, acetone) were tested and led to degradation after some days. DMSO gave degradation after one week towards the starting product and 3-oxo-1-(arylamino)-1,3-dihydroisobenzofuran-1-carboxamide **7** (Fig. 2).¹⁷ The other solvents gave complex mixtures of degradation products. This led to the fact that during the sample collection and evaporation of the solvent, a nitrogen atmosphere was necessary to prevent degradation of the end-product. Once the crystals were separated and dried, the 3-amino-4-(arylamino)-1*H*-isochromen-1-ones **6** are stable, even in open air.

Scope of the reaction

Finally, the optimized procedure was tested for different amines. When anilines were used, moderate to good yields were achieved (Table 3, entry 1–4). Allylamine was converted mostly to the Strecker product (37%), while 4-allylamino-3-iminoisochroman-1-one **5e** was only produced in 6% yield. Apparently, when non-aromatic amines are used the imino tautomer is more stable than the corresponding enamine tautomer. A production rate around 2 g/h was achieved for some adducts.

Comparing the yields of the batch procedure and the microreactor procedure show higher yields in most batch procedures. This is easy to explain, since in the batch procedure crystallization occurs in the round-bottom flask during the reaction, which promotes a shift towards the formation of the end-product. In the microreactor procedure, crystallization was avoided due to clogging problems. Nevertheless, scale-up of this reaction is more advantageous in the case of the microreactor procedure. The most important reason is that more severe precautions are needed due to the formation of

Table 3 Production of different 3-amino-4-(arylamino)-1*H*-isochromen-1-ones **6** using the CYTOS[®] College System^a

Entry	Amine 2	Product	Yield (%) ^b	Yield (%) ^c	Output/g h ⁻¹
1	Aniline	6a	66	82	1.80
2	3-Methoxyaniline	6b	75	88	2.28
3	3-Methylaniline	6c	69	60	1.98
4	<i>N</i> -Methylaniline	6d	49	64	1.41
5	Allylamine	5e	6 ^d	—	0.14

^a General conditions: residence time: 39.2 min; temperature: 50 °C; inlet A₁: 0.3 M of 2-formylbenzoic acid and 0.6 M of acetic acid in methanol; inlet A₂: 0.36 M of potassium cyanide and 0.6 M of amine in methanol. ^b After crystallization. ^c Ref. 7. ^d No crystallization occurred and the reaction mixture was subjected to column chromatography which gave product **5e**.

high concentrations of HCN in the scale-up of the batch reaction, while in the case of the microreactor procedure this is possible by simple numbering-up (*i.e.* the number of reactors is increased instead of the volume of the reactor) without changing the reaction conditions. Furthermore, the procedure is continuous, which guarantees a more constant quality of the end-product in comparison to different batch reactions.

Conclusions

A multicomponent reaction was studied to produce 3-amino-4-(arylamino)-1H-isochromen-1-ones *via in situ* generation of HCN. To the best of our knowledge, this is the first chemical reaction in a microreactor system in which HCN is generated and further reacted in the microreactor. Moderate to good yields were achieved. Also, an alternative and easy setup was developed to work at higher concentrations in case the reaction suffers from crystallization in the tubings at the end of the microreactor.

Experimental

General

The microreactor used in this study is a CYTOS[®] College System¹⁰ (Fig. 3). The CYTOS[®] College System microreactor consists of several stacked plates with microstructures in the sub-millimeter range (width approx. 100 μm). The volume of the microreactor itself is 2 mL ($V_{\text{microreactor}}$) and that of the RTU is 45 mL (V_{RTU}) so the total volume (V_{total}) of the system is 47 mL. The pumps were calibrated at the desired flow rate ($r_{\text{piston pumps}}$). The temperature was controlled using an external circuit (Huber Tango thermostat).

The reagents were used without prior purification. Fluorinert[®] FC-70 was purchased from Acros Organics. ¹H NMR spectra (300 MHz) and ¹³C NMR spectra (75 MHz) were recorded on a Jeol Eclipse FT 300 NMR spectrometer and peaks are relative to SiMe₄ (TMS). IR spectra were measured with a Perkin-Elmer Spectrum One FT-IR spectrophotometer. Low resolution mass spectra were recorded on an Agilent 1100 Series VL mass spectrometer (ES 70 eV).

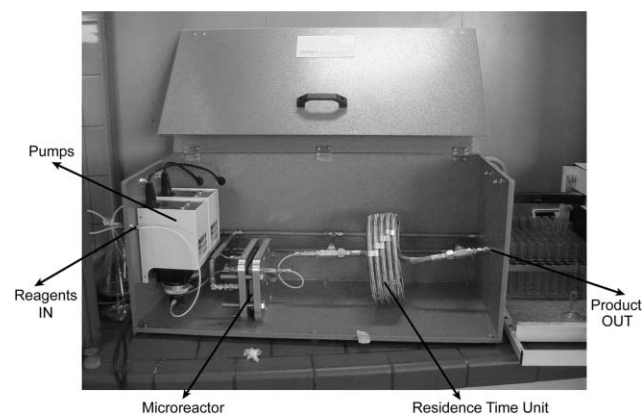


Fig. 3 CYTOS[®] College System.¹⁰

General procedure (Table 1, entry 1)

2-Formylbenzoic acid (4.2 g, 28 mmol) and acetic acid (3.36 g, 56 mmol) were dissolved in 70 mL of methanol in a measuring cylinder. The other measuring cylinder contained aniline (5.22 g, 56 mmol) and potassium cyanide (2.19 g, 33.6 mmol) dissolved in 70 mL of methanol. Both solutions were connected to the inlets of the device. Both pumps were adjusted to the same flow rate (r) and the flow rate was controlled by measuring the ingoing and outgoing volumes. The residence time (τ) was calculated by the formula:

$$\tau = \frac{V_{\text{total}}}{r_{\text{total}}} \quad (1)$$

At the outlet, the end-product was collected at steady state conditions, *i.e.* after 1.6τ . About 30 mL was collected for work up. The work up consisted of the removal of the solvent *via* evaporation under a N₂ atmosphere. The residual mixture was filtered and the crystals were washed with methanol and water. The crystals were dried with P₄O₁₀.

General procedure for the plug flow reactions (Table 2)

The same reaction mixtures were used as described above. A HPLC pump was connected between the microreactor and the RTU *via* a T-connection (see Fig. 1). A solution of Fluorinert[®] FC-70 was connected to the pump. The flow rates ($r_{\text{piston pumps}}$ and r_{HPLC}) were calculated by measuring the outgoing volume of reaction mixture and Fluorinert[®] FC-70. The residence time (τ) was calculated as follows:

$$\tau = \frac{V_{\text{microreactor}}}{r_{\text{piston pumps}}} + \frac{V_{\text{RTU}}}{r_{\text{piston pumps}} + r_{\text{HPLC}}} \quad (2)$$

The reaction mixture fraction (rmf) at the output was calculated as follows:

$$rmf = \frac{V_{\text{reaction mixture}}}{V_{\text{reaction mixture}} + V_{\text{Fluorinert}}} \quad (3)$$

Fluorinert[®] FC-70 was separated and the rest of the work up was identical to the procedure described above.

Spectral data

The spectral data of compounds **6a–d** were in accordance with the literature.⁷

4-Allylamino-3-iminoisochroman-1-one **5e**

Yield 6%. Mp: 200–201 °C. IR [ν_{max} (KBr)/cm⁻¹]: 3349, 3178 (2 × NH), 1689, 1675 (C=O and C=N). ¹H NMR: (δ /ppm, J/Hz, 300 MHz, DMSO) 3.59 (1 H, dd, $J = 15.7$ and 7.1 , NHCH_aH_b), 4.51–4.58 (1 H, pseudo-dd, $J = 15.7$ and 4.7 , NHCH_aH_b), 5.11 (1 H, s, NCH), 5.16 (1 H, pseudo-d, $J = 11.8$, CH=CH_aH_b), 5.20 (1 H, pseudo-d, $J = 5.2$, CH=CH_aH_b), 5.80–5.93 (1 H, m, CH=CH_aH_b), 7.50–7.72 (5 H, m, arom. H + C=NH), 8.05 (1 H, s, NH). ¹³C NMR (δ /ppm, 75 MHz, DMSO): 43.19 (NHCH₂), 62.35 (C-4), 117.67 (=CH₂), 122.39 (C-7), 122.83 (C-5), 128.60 (C-8), 131.38 (C-8a), 131.69 (C-6), 133.26 (=CH), 141.50 (C-4a), 167.55 (C=O), 168.48 (C=NH). m/z (70 eV, ES⁺): 217 (M + H⁺). White powder. R_f (CH₂Cl₂–MeOH 95 : 5): 0.21.

Acknowledgements

The authors wish to thank the National Fund for Research-Flanders and Ghent University for financial support (BOF) and CPC – Cellular Process Chemistry Systems GmbH for their collaboration.

References

- (a) R. V. A. Orru and M. de Greef, *Synthesis*, 2003, 1471–1499; (b) J. Sapi and J. Laronze, *Arkivoc*, 2004(vii), 208–222.
- J. Zhu and H. Bienaymé, *Multicomponent reactions*, Wiley-VCH, Weinheim, 2005.
- For some interesting reviews about the Mannich reaction, see: (a) M. Tramontini and L. Angiolini, *Tetrahedron*, 1990, **46**, 1791–1837; (b) M. Arend, B. Westermann and N. Risch, *Angew. Chem., Int. Ed.*, 1998, **37**, 1044–1070; (c) M. M. B. Marques, *Angew. Chem., Int. Ed.*, 2006, **45**, 348–352.
- For some interesting reviews about the Biginelli reaction, see: (a) C. O. Kappe, *Tetrahedron*, 1993, **49**, 6937–6963; (b) C. O. Kappe, in *Multicomponent reactions*, ed. J. Zhu and H. Bienaymé, Wiley-VCH, Weinheim, 2005, pp. 95–120.
- L. Banfi, A. Basso, G. Guanti and R. Riva, in *Multicomponent reactions*, ed. J. Zhu and H. Bienaymé, Wiley-VCH, Weinheim, 2005, pp. 1–32.
- For some interesting reviews about the Baylis–Hillman reaction, see: (a) D. Basavaiah, P. D. Rao and R. S. Hyma, *Tetrahedron*, 1996, **52**, 8001–8062; (b) D. Basavaiah, A. J. Rao and T. Satyanarayana, *Chem. Rev.*, 2003, **103**, 811–891.
- T. Opatz and D. Ferenc, *Eur. J. Org. Chem.*, 2005, 817–821.
- (a) L. Kiwi-Minsker and A. Renken, *Catal. Today*, 2005, **110**, 2–14; (b) M. W. Losey, M. A. Schmidt and K. F. Jensen, *Ind. Eng. Chem. Res.*, 2001, **40**, 2555–2562.
- (a) K. Geyer, J. D. C. Codée and P. H. Seeberger, *Chem.–Eur. J.*, 2006, **12**, 8434–8442; (b) T. Kawaguchi, H. Miyata, K. Ataka, K. Mae and J. Yoshida, *Angew. Chem., Int. Ed.*, 2005, **44**, 2413–2416; (c) A. Nagaki, M. Togai, S. Suga, N. Aoki, K. Mae and J. Yoshida, *J. Am. Chem. Soc.*, 2005, **127**, 11 666–11 675; (d) A. Iles, R. Fortt and A. J. de Mello, *Lab Chip*, 2005, **5**, 540–544; (e) X. Zhang, S. Stefanick and F. Villani, *Org. Process Res. Dev.*, 2004, **8**, 455–460; (f) S. Liu, T. Fukuyama, M. Sato and I. Ryu, *Org. Process Res. Dev.*, 2004, **8**, 477–481; (g) C. Wiles, P. Watts and S. J. Haswell, *Org. Process Res. Dev.*, 2004, **8**, 28–32; (h) G. Panke, T. Schwalbe, W. Stirner, S. Taghavi-Moghadam and G. Wille, *Synthesis*, 2003, 2827–2830; (i) S. J. Haswell and P. Watts, *Green Chem.*, 2003, **5**, 240–249; (j) G. Dummann, U. Quitmann, L. Gröschel, D. W. Agar, O. Wörz and K. Morgenschweis, *Catal. Today*, 2003, **79**, 433–439; (k) E. Dietz, J. Weber, D. Schnaitmann, C. Wille and L. Unverdorben, *US Pat.*, 6 582 508, 2003; (l) K. F. Jensen, *Chem. Eng. Sci.*, 2001, **56**, 293–303; (m) J. R. Burns and C. Ramshaw, *Lab Chip*, 2001, **1**, 10–15; (n) O. Wörz, K. P. Jäckel, T. Richter and A. Wolf, *Chem. Eng. Sci.*, 2001, **56**, 1029–1033; For some reviews, see: (o) G. N. Doku, W. Verboom, D. N. Reinhoudt and A. van den Berg, *Tetrahedron*, 2005, **61**, 2733–2742; (p) K. Jähnisch, V. Hessel, H. Löwe and M. Baerns, *Angew. Chem., Int. Ed.*, 2004, **43**, 406–446; (q) P. Watts and S. J. Haswell, *Drug Discovery Today*, 2003, **8**, 586–593; (r) P. D. I. Fletcher, S. J. Haswell, E. Pombo-Villar, B. H. Warrington, P. Watts, S. Y. F. Wong and X. Zhang, *Tetrahedron*, 2002, **58**, 4735–4757; (s) P. Watts and S. J. Haswell, *Chem. Soc. Rev.*, 2005, **34**, 235–246.
- CPC – Cellular Process Chemistry Systems GmbH: Heiligkreuzweg 90, D-55130 Mainz, Germany, www.cpc-net.com; T. Schwalbe, K. Golbig, M. Hohmann, P. Georg, A. Oberbeck, B. Dittmann, J. Stasna and S. Oberbeck (Cellular Process Chemistry Inc., USA), *Eur. Pat. Appl.*, 2001, EP 1 123 734, in *Chem. Abstr.*, 2001, **135**, 154468b.
- (a) V. Hessel, W. Ehrfeld, K. Golbig, C. Hofmann, S. Jungwirth, H. Löwe, T. Richter, M. Storz, A. Wolf, O. Wörz and J. Breyse, in *Microreaction Technology: Industrial Prospects, Proceedings of IMRET 3*, ed. W. Ehrfeld, Springer-Verlag, Berlin, 1999, pp. 151–164; (b) W. Ehrfeld, V. Hessel and H. Löwe, *Microreactors: New Technology for Modern Chemistry*, Wiley-VCH, Weinheim, 2000, pp. 217–227.
- (a) E. Van Meenen, K. Moonen, D. Acke and C. V. Stevens, *Arkivoc*, 2006, (i), 31–45; (b) D. R. J. Acke, R. V. A. Orru and C. V. Stevens, *QSAR Comb. Sci.*, 2006, **25**, 474–483; (c) D. R. J. Acke and C. V. Stevens, *Org. Process Res. Dev.*, 2006, **10**, 417–422.
- V. Hessel, *CERC3 Young Chemists' Workshop: Micro Reactor Technology*, Enschede, The Netherlands, March 16–18, 2006.
- L. J. McCausland and P. W. Cains, *Drug Delivery Systems Sci.*, 2002, **2**(2), 47–51.
- (a) I. Shestopalov, J. D. Tice and R. F. Ismagilov, *Lab Chip*, 2004, **4**, 316–321; (b) D. L. Chen, C. J. Gerdtts and R. F. Ismagilov, *J. Am. Chem. Soc.*, 2005, **127**, 9672–9673; (c) D. L. Chen, *CERC3 Young Chemists' Workshop: Micro Reactor Technology*, Enschede, The Netherlands, March 16–18, 2006.
- F. Feigl and V. Anger, *Analyst*, 1966, **91**, 282–284.
- T. Opatz and D. Ferenc, *Eur. J. Org. Chem.*, 2006, 121–126.

Water-soluble arene ruthenium catalysts containing sulfonated diamine ligands for asymmetric transfer hydrogenation of α -aryl ketones and imines in aqueous solution

Jérôme Canivet and Georg Süß-Fink*

Received 30th August 2006, Accepted 12th January 2007

First published as an Advance Article on the web 2nd February 2007

DOI: 10.1039/b612518b

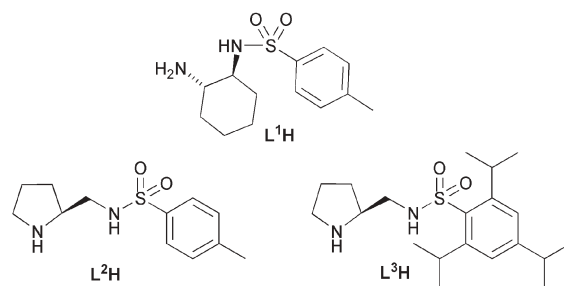
A new family of nine cationic organometallic aqua complexes of the type [(arene)Ru(RSO₂N(O)NH₂)(OH₂)]⁺ (**1–9**), containing chiral *N,N*-chelating ligands, has been synthesised and isolated as the tetrafluoroborate salts, which are water-soluble and stable to hydrolysis. The enantiopure complexes **1–9** catalyse the transfer hydrogenation of prochiral aryl ketones and imines in aqueous solution to give the corresponding alcohols and amines with good conversion and enantioselectivity. This method gives an environmentally friendly access, for instance, to isoquinoline alkaloids by asymmetric catalysis in water.

Introduction

Water-soluble organometallic complexes attract continuously growing interest for applications in catalysis, because of environmentally friendly processing, simple product separation and pH dependent selectivity in aqueous media. The chemistry of organometallic aqua ions was comprehensively reviewed by Koelle.¹ Related reviews deal with water-soluble organometallics complexed by hydrophilic ligands,² metal-mediated organic synthesis in water³ and catalysis by water-soluble organometallic complexes in biphasic systems.⁴ In particular, the transfer hydrogenation of ketones and imines in organic solvents is a powerful tool for asymmetric synthesis which was pioneered by Noyori,^{5–7} Morris,⁸ Bullock⁹ and Bäckvall.¹⁰ Several recent reports deal with asymmetric transfer hydrogenation of ketones with formate in aqueous media using active catalytic systems based on *N*-(*p*-toluenesulfonyl)-1,2-diphenylethylenediamine and derivatives,^{11–16} or on aromatic proline amides derivatives.¹⁷ These catalytic systems show good activities and enantioselectivities, but the catalysts are formed *in situ* from precursors and have not been isolated.

Recently we reported the synthesis of arene ruthenium chloro complexes, [(arene)Ru(L¹)Cl] (L¹H = (*R,R*)-*N*-(*p*-toluenesulfonyl)diaminocyclohexane), which catalyse the transfer hydrogenation of acetophenone in aqueous solution using formate as the hydrogen source, with a TOF of 43 h⁻¹ and enantiomeric excess of 93%.¹⁸ Moreover, the known 2-*S*-(*p*-toluenesulfonylamino)methylpyrrolidine (L²H) and 2-*S*-(2,4,6-triisopropyl-benzenesulfonylamino)methylpyrrolidine (L³H) ligands show, in combination with *p*-cymene ruthenium dichloro dimer, a slight activity and selectivity for the same reaction in isopropanol.¹⁹

Whereas the enantioselective transfer hydrogenation of C=O double bonds is well-known, the same reaction for the C=N



double bonds is much less studied. There are several reports on the enantioselective transfer hydrogenation of imines, particularly of derivatives of 3,4-dihydroisoquinoline, using catalytic systems based on *N*-(*p*-toluenesulfonyl)-1,2-diphenylethylenediamine and derivatives in combination with ruthenium or rhodium precursors in azeotropic formic acid–triethylamine to give the corresponding chiral amine, with TOFs between 20 and 30 h⁻¹ and more than 95% for enantiomeric excess.^{20–23} More recently, Wu *et al.* reported, for the same reaction, similar catalytic systems involving a surfactant in aqueous solution, with sodium formate as the hydrogen source, with enantiomeric excesses greater than 96%.²⁴

Herein, we report the synthesis of water-soluble arene ruthenium complexes containing enantiopure chiral mono-sulfonated diamine ligands, including the new ligand *S*-2-(*S*-camphor-10-sulfonylamino)methylpyrrolidine, and their catalytic potential for the asymmetric transfer hydrogenation of aromatic ketones and imines in aqueous solution using sodium formate as the hydrogen source.

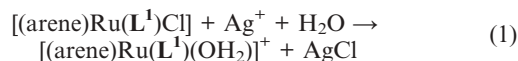
Results

Synthesis of cationic arene ruthenium complexes containing chiral sulfonated diamine ligands

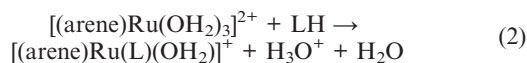
The arene ruthenium chloro complexes [(arene)Ru(L¹)Cl], containing a chiral bidentate ligand derived from L¹H = *N*-tosyl-*trans*-1,2-diaminocyclohexane, which have been

Institut de Chimie, Université de Neuchâtel, Case Postale 158, Neuchâtel, CH-2009, Switzerland. E-mail: georg.suess-fink@unine.ch; Fax: 0041 32 718 25 11; Tel: 0041 32 718 24 00

reported recently,¹⁸ react in aqueous solution with silver sulfate to give, with precipitation of silver chloride, the corresponding cationic aqua complexes $[(\text{arene})\text{Ru}(\text{L}^1)(\text{OH}_2)]^+$ (**1**: arene = C_6H_6 , **2**: arene = $p\text{-MeC}_6\text{H}_4^i\text{Pr}$, **3**: arene = C_6Me_6), which can be isolated from the filtered solution, upon addition of NaBF_4 , as the tetrafluoroborate salts (eqn (1)).



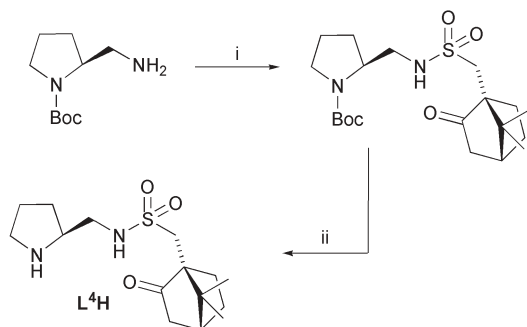
On the other hand, the L^2 and L^3 analogues $[(\text{arene})\text{Ru}(\text{L}^2)(\text{OH}_2)]^+$ (**4**: arene = C_6H_6 , **5**: arene = $p\text{-MeC}_6\text{H}_4^i\text{Pr}$, **6**: arene = C_6Me_6) and $[(\text{arene})\text{Ru}(\text{L}^3)(\text{OH}_2)]^+$ (**7**: arene = C_6Me_6) are accessible from the corresponding arene ruthenium triaqua complexes and L^2H and L^3H , according to eqn (2). All cationic aqua complexes can be isolated from the filtered solution, upon addition of NaBF_4 , as the stable tetrafluoroborate salts.



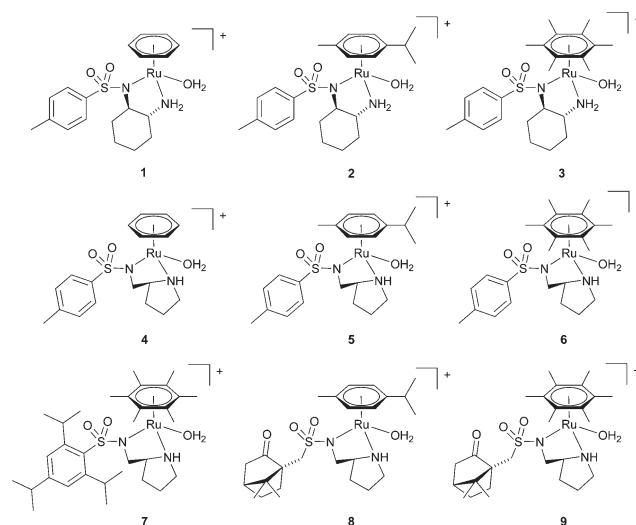
Moreover, we synthesised a new representative of the series of chiral (sulfonylamino)methylpyrrolidine ligands, which contains a second chiral centre in the sulfonyl moiety: Thus, 2-*S*-(*S*-camphor-10-sulfonylamino)methylpyrrolidine (L^4H) was obtained by reacting the *N*-Boc protected *S*-2-aminomethylpyrrolidine (Boc = *t*-butyl carbonate) with *S*-Camphor-10-sulfonyl chloride, followed by deprotection with trifluoroacetic acid. (Scheme 1)

The new enantiopure L^4H reacts in the same way (eqn (2)) as L^2H or L^3H with arene ruthenium triaqua complexes $[(\text{arene})\text{Ru}(\text{OH}_2)_3]^{2+}$ to give the cations $[(\text{arene})\text{Ru}(\text{L}^4)(\text{OH}_2)]^+$ (**8**: arene = $p\text{-MeC}_6\text{H}_4^i\text{Pr}$, **9**: arene = C_6Me_6), which precipitate from the aqueous solution as tetrafluoroborate salts upon saturation with NaBF_4 .

All compounds $[(\text{arene})\text{Ru}(\text{L})(\text{OH}_2)][\text{BF}_4]$ (containing cations **1–9**), are air-stable, orange-yellow and water-soluble powders, which have been fully characterised by ^1H and ^{13}C NMR spectroscopy, mass spectroscopy and elemental analysis (see Experimental). The systematic variation of the substituents in both the arene and the sulfonated diamine ligands allows us to study in detail the steric and electronic influence on the catalytic activities and selectivities of these complexes for transfer hydrogenation reactions.



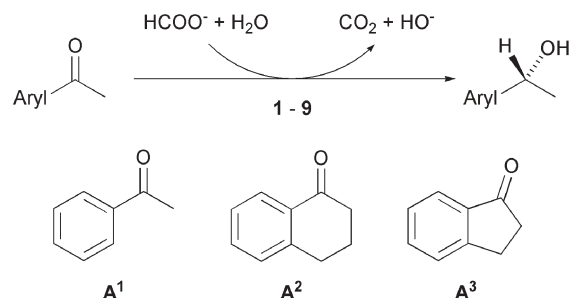
Scheme 1 (i) *S*-Camphor-10-sulfonyl chloride, Et_3N . (ii) CF_3COOH .



Enantioselective transfer hydrogenation of aryl ketones in water

The synthesis of chiral alcohols from the corresponding prochiral ketones by enantioselective transfer hydrogenation has a great potential, particularly if the reaction can be carried out in water using sodium formate as the hydrogen source.^{11,14,18,25–27} Recently we found the chloro complexes $[(\text{arene})\text{Ru}(\text{L}^1)\text{Cl}]$ were able to catalyse the transfer hydrogenation of acetophenone to give enantioselectively phenylethanol; in the case of arene = C_6Me_6 , the aqua complex $[(\text{arene})\text{Ru}(\text{L}^1)(\text{OH}_2)]^+$ (**3**) could be identified as a catalytically active species.¹⁸ As expected, all aqua complexes **1–9** are active catalysts for the enantioselective transfer hydrogenation of various prochiral aryl ketones (A^1 = acetophenone, A^2 = α -tetralone, A^3 = 1-indanone, see Scheme 2) to give the corresponding chiral aryl alcohols with enantioselectivities up to 94% (Table 1). All reactions are found to be quantitative (TON > 99) after 2 to 5 h.

As Table 1 reveals, the best results, as far as both catalytic activity and enantioselectivity are concerned, have been obtained with the aqua complex **3** as the catalyst, the turnover frequencies varying from 25 to 44 h^{-1} and the enantiomeric excess attaining 93 to 94% (entries 3, 12 and 20). For the hydrogenation of A^1 (entries 1–9), the diaminocyclohexane complexes **1** to **3** show a more than two times better enantioselectivity than the 2-methylaminopyrrolidine complexes **4** to **9**, which contain less rigid ligands. This difference



Scheme 2 Enantioselective transfer hydrogenation of aryl ketones A^1 , A^2 and A^3 catalysed by aqua complexes **1–9** in water.

Table 1 Enantioselective transfer hydrogenation of aryl ketones **A**¹, **A**² and **A**³ by aqua complexes **1–9** in water^a

Entry	Catalyst	Substrate	TOF/h ⁻¹ ^{b,c}	ee (%) ^b
1	1	A ¹	48	51
2	2	A ¹	45	83
3	3	A ¹	44	93
4	4	A ¹	34	25
5	5	A ¹	37	23
6	6	A ¹	43	39
7	7	A ¹	40	38
8	8	A ¹	39	44
9	9	A ¹	38	30
10	1	A ²	15	91
11	2	A ²	37	84
12	3	A ²	25	94
13	4	A ²	15	48
14	5	A ²	24	23
15	6	A ²	19	13
16	7	A ²	25	11
17	8	A ²	28	21
18	9	A ²	25	14
19	2	A ³	35	70
20	3	A ³	35	93
21	5	A ³	21	30
22	6	A ³	28	13

^a Conditions: H₂O (5 mL), A (1 mmol), ratio catalyst/substrate/formate = 1/100/500, 60 °C, pH = 9, 2 h. ^b Determined by chiral HPLC analysis. ^c Turnover frequencies determined after 30 minutes and expressed in mol of product/(mol of Ru × h).

increases with the backbone rigidity of the substrate, as found for **A**² (entries 12 and 15) and **A**³ (entries 20 and 22). As far as catalytic activity is concerned, all aqua complexes **1–9** show comparable TOF values for one given substrate. However, the catalytic activities differ substantially with changing substrate: the more rigid substrates **A**² and **A**³ are hydrogenated slower than the more flexible **A**¹. The substitution pattern of the chiral ligand L or an additional chiral centre in **1–9** has no significant influence on the catalytic activity.

The pH dependence of both, catalytic activity and enantioselectivity of the transfer hydrogenation reaction has been studied in the case of substrate **A**¹ and catalyst **6**. Fig. 1 shows the conversion and ee profiles in the pH range from 5 to 10. While enantioselectivity is almost independent of the pH, the highest activity was found for pH = 9.

Enantioselective transfer hydrogenation of aryl imines in water

The aqua complexes [(arene)Ru(L)(OH₂)]⁺ (**1–9**) are also found to catalyse the enantioselective transfer hydrogenation of aryl imines in aqueous solution, using sodium formate as the hydrogen source. This catalytic reaction, so far much less studied than the transfer hydrogenation of ketones, works with **1–9** for the prochiral substrates phenyl-*N*-(1-phenylethylidene) methanamine (**A**⁴), 1-methyl-6,7-dimethoxy-3,4-dihydroisoquinoline (**A**⁵) and 1-(5-chloro-2-nitrophenyl)-6,7-dimethoxy-3,4-dihydroisoquinoline (**A**⁶), see Scheme 3. This is particularly interesting in the case of **A**⁵, because the product *R*-salsolidine and its derivatives are valuable intermediates in the synthesis of alkaloid drugs showing antibacterial effects^{28,29} or being active in neurodisease treatment.³⁰

The results are compiled in Table 2. In all cases, the best results are obtained with the *p*-cymene and hexamethylbenzene

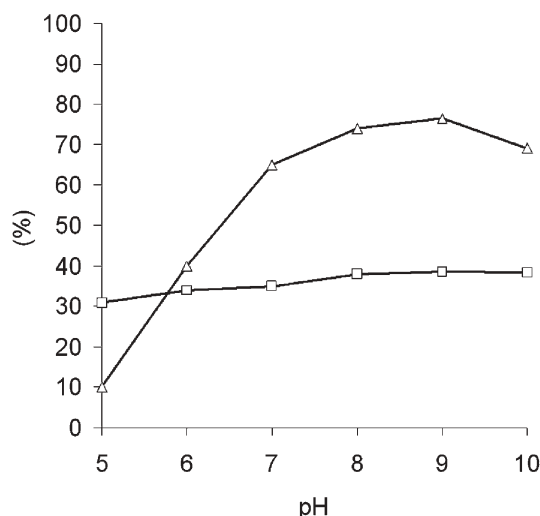


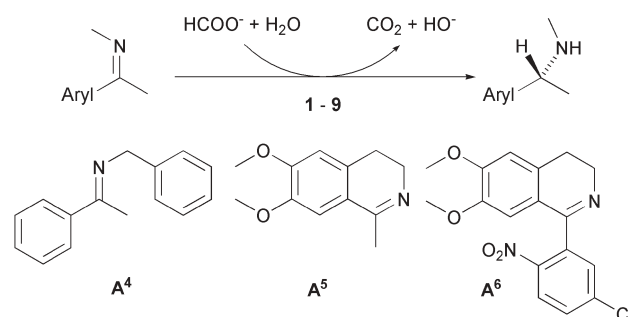
Fig. 1 pH-dependent profile of conversion (Δ) and enantiomeric excess (□) for the transfer hydrogenation of acetophenone **A**¹ (1 mmol) using **6** as catalyst and HCOONa as hydrogen donor in water (5 mL), at 60 °C, for 2 h, the catalyst/substrate/formate ratio being 1/100/500.

complexes containing the chiral ligand **L**¹ (**2** and **3**); while the differences in the catalytic activities are less pronounced, the enantioselectivities differ more markedly. All reactions are found to be quantitative (TON > 99) after 2 to 5 h.

The pH-dependence of catalytic activity and enantioselectivity, studied in the case of substrate **A**⁵ and catalyst **5**, in the pH range from 7 to 12 (Fig. 2), also shows an activity maximum at pH = 9, while the enantioselectivity is almost not influenced by the pH, in line with the findings for aryl ketones.

Discussion

In all catalytic reactions reported herein, the transfer hydrogenation of aryl ketones or of aryl imines in aqueous solution using sodium formate as hydrogen source, the catalytically active aqua complexes [(arene)Ru(L)(OH₂)]⁺ can be recovered unchanged after the catalytic run as tetrafluoroborate salts. Based on the observation of an intermediary hydrido complex in the case of the transfer hydrogenation of acetophenone catalysed by the non-chiral ortho-phenanthroline (phen) complex [(C₆Me₆)Ru(phen)(OH₂)]²⁺,³¹ and the X-ray-crystallographic characterisation of the bipyridine (bipy) analogue



Scheme 3 Enantioselective transfer hydrogenation of aryl imines **A**⁴, **A**⁵ and **A**⁶ catalysed by aqua complexes **1–9** in water.

Table 2 Enantioselective transfer hydrogenation of aryl imines **A**⁴, **A**⁵ and **A**⁶ by aqua complexes **1–9** in water^a

Entry	Catalyst	Substrate	TOF/h ⁻¹ ^{b,c}	ee (%) ^b
1	1	A ⁴	54	48
2	2	A ⁴	49	74
3	3	A ⁴	51	91
4	4	A ⁴	37	21
5	5	A ⁴	40	48
6	6	A ⁴	38	35
7	7	A ⁴	32	29
8	8	A ⁴	35	44
9	9	A ⁴	29	32
10	1	A ⁵	46	46
11	2	A ⁵	50	88
12	3	A ⁵	44	51
13	4	A ⁵	46	21
14	5	A ⁵	45	47
15	6	A ⁵	45	44
16	7	A ⁵	38	41
17	8	A ⁵	41	45
18	9	A ⁵	40	42
19	2	A ⁶	24	61
20	3	A ⁶	22	50
21	5	A ⁶	18	25
22	6	A ⁶	12	18

^a Conditions: H₂O (5 mL), A (1 mmol), ratio catalyst/substrate/formate = 1/100/500, 60 °C, pH = 9, 2 h. ^b Determined by chiral HPLC analysis. ^c Turnover frequencies determined after 30 minutes and expressed in mol of product/(mol of Ru × h).

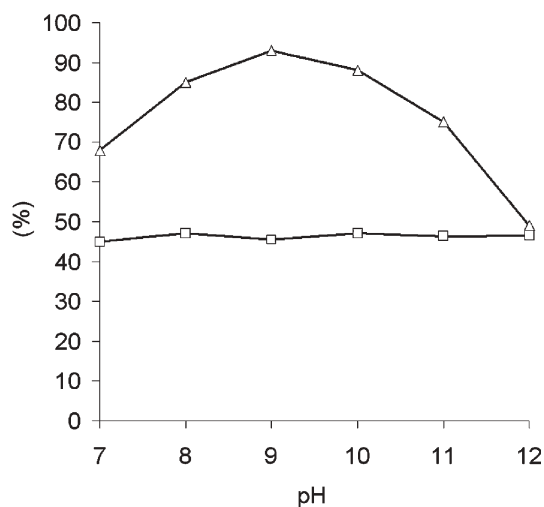
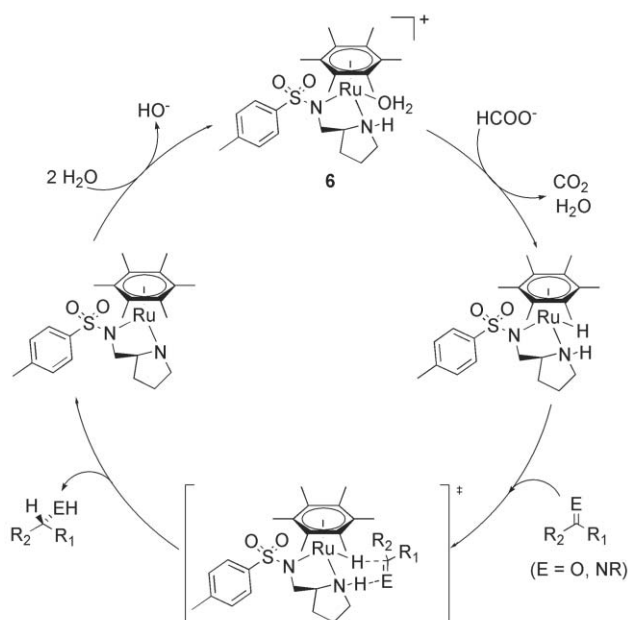


Fig. 2 pH-dependent profile of conversion (Δ) and enantiomeric excess (\square) for the transfer hydrogenation of acetophenone **A**⁵ (1 mmol) using **5** as catalyst and HCOONa as hydrogen donor in water (5 mL), at 60 °C, for 2 h, the catalyst/substrate/formate ratio being 1/100/500.

$[(C_6Me_6)Ru(bipy)H][CF_3SO_3]$,³² and based on the pioneering mechanistic work of Noyori, with $[(arene)Ru(TsNCHPh-CHPhNH_2)Cl]$,^{6,7,33,34} Morris,⁸ and Wills,³⁵ we propose the catalytic cycle outlined in Scheme 4 (for the example of complex **6**) as a mechanistic description of the catalytic action of the aqua complexes **1–9** in the transfer hydrogenation of aryl ketones and imines.

Interestingly, we observed that all prochiral aryl ketones and imines preferentially yield, with **1–9**, the *R* enantiomer of the corresponding chiral alcohols or amines, although the configuration of the chiral ligands is not the same: *R,R*-**L**¹ in

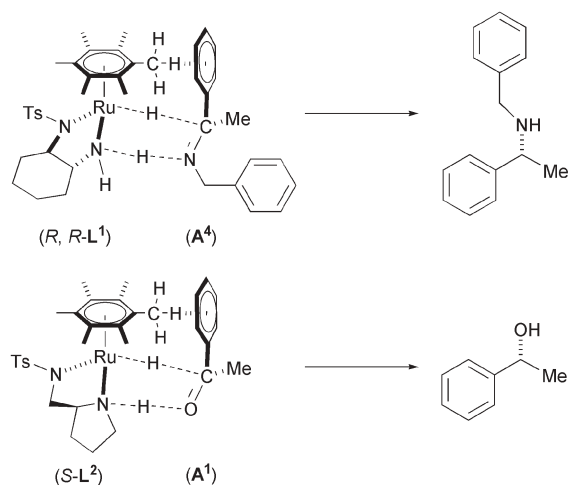


Scheme 4 Postulated catalytic cycle for the enantioselective transfer hydrogenation of imines using $[6]BF_4$ as catalyst and sodium formate as hydrogen source in aqueous solution.

1–3, *S*-**L**² in **4–6**, *S*-**L**³ in **7** and *S,S*-**L**⁴ in **8** and **9**. This can be rationalised in terms of CH/ π interactions³⁶ between the hydrogen atoms of the arene ligand of the ruthenium complex and the aryl substituent of the substrate in the hydrogen bridged transition state (see Scheme 4, bottom). In all cases, the chiral ligand *L* (*R*, *R*-**L**¹, *S*-**L**², *S*-**L**³, *S*, *S*-**L**⁴) orients the *Si* face of the prochiral carbon atom of the substrate towards the ruthenium centre (Scheme 5).

Conclusion

In conclusion, we report herein the synthesis of nine water-soluble chiral arene ruthenium aqua complexes containing



Scheme 5 CH/ π interaction postulated between the arene ligand of the ruthenium complexes and the aryl substituent of the prochiral substrate, exemplified for two different cases.

R,R-N-(*p*-toluenesulfonyl)diaminocyclohexane or *S*-2-(sulfonyl-amino)methylpyrrolidine derivatives as chelating ligands. All these complexes are found to effectively catalyse the transfer hydrogenation of α -aryl ketones and α -aryl imines in aqueous solution using formate as the hydrogen source, without any additional surfactant. These catalytic reactions involve CH/ π interactions between the arene ligand of the catalyst and the aryl substituent of the substrate, previously reported by Noyori.³⁶ Moreover, the transfer hydrogenation of 1-methyl-6,7-dimethoxy-3,4-dihydroisoquinoline (**A**⁵) to *R*-salsolidine with a TOF of 50 h⁻¹ and ee of 88% using water-soluble complexes give an environmentally friendly access to isoquinoline alkaloids by asymmetric catalysis in aqueous solution.

Experimental

General remarks

All manipulations were carried out in an inert atmosphere using standard Schlenk techniques and freshly distilled solvents saturated with nitrogen prior to use. The starting dimers [(arene)RuCl₂]³⁷ and the *N*-Boc-*S*-2-aminomethylpyrrolidine, the *S*-2-[*N*-(4-toluenesulfonyl)aminomethyl]pyrrolidine (**L**²H) and the *S*-2-[*N*-(2,4,6-triisopropylbenzylsulfonyl)aminomethyl]pyrrolidine (**L**³H) were prepared according to the published methods.¹⁹ The arene ruthenium chloro complexes, [(arene)Ru(L¹)Cl], were synthesised as previously reported.¹⁸ All other reagents were commercially available and were used without further purification. NMR spectra were recorded on a Bruker 400 MHz spectrometer. Electro-spray mass spectra were obtained in positive- or negative-ion mode with an LCQ Finnigan mass spectrometer. Microanalyses were carried out by the Laboratoire de Chimie Pharmaceutique, Université de Genève (Switzerland).

Synthesis of L⁴H

***S*-tert-butyl-2-(*S*-camphor-10-sulfonylamino)methylpyrrolidine-1-carboxylate.** To a solution of *S*-tert-butyl-2-aminomethylpyrrolidine-1-carboxylate (350 mg, 1.84 mmol) in pyridine (20 mL) was added 1.5 equivalents of the *S*-camphor-10-sulfonyl chloride (693 mg, 2.8 mmol) at 0 °C. After 6 hours, Et₂O (100 mL) was added and the organic layer was washed with HCl 10% (2 × 30 mL), saturated NaHCO₃ (2 × 30 mL) and saturated NaCl (30 mL). The resulting yellowish oil was purified on a silica gel column (pentane–ethylacetate = 3 : 1) to obtain the pure product as colourless oil. (Yield: 65%, 485 mg). ¹H NMR δ (400 MHz, CDCl₃, 21 °C): 0.85 (s, 3H), 1.02 (s, 3H), 1.21 (b, 1H), 1.43 (s, 9H), 1.82–2.13 (b, 9H), 2.84–2.91 (d, *J* = 15 Hz, 1H), 3.27–3.34 (b, 4H), 3.92 (b, 1H) ppm. ¹³C NMR δ (200 MHz, CDCl₃, 21 °C): 19.39 (CH₃), 19.93 (CH₃), 25.52 (CH₂), 26.94 (CH₂), 27.00 (CH₂), 27.55 ((CH₃)₃), 28.81 (CH₂), 31.58 (CH), 42.75 (C(CH₃)₂), 42.92 (CH₂CO), 46.15 (CH₂), 46.72 (CH₂), 49.80 (CH₂SO₂), 58.06 (CH), 59.29 (CCH₂), 79.88 (C(CH₃)₃), 170.65 (CO^{*t*}Bu), 217.05 (CO) ppm. *m/z* (ESI, negative ion) 413.6 [C₂₀H₃₃N₂O₅S⁻]. (Found: C, 57.88; H, 8.24; N, 6.71. C₂₀H₃₄N₂O₅S requires C, 57.94; H, 8.27; N, 6.76).

***S*-2-(*S*-camphor-10-sulfonylamino)methylpyrrolidine (L⁴H).**

To a solution of *S*-tert-butyl-2-(*S*-camphor-10-sulfonylamino)methylpyrrolidine-1-carboxylate (284 mg, 0.7 mmol) in dry CH₂Cl₂ were added 10 equivalents of trifluoroacetic acid (0.6 mL) at room temperature to give a dark yellowish solution. After 8 hours, the organic layer was washed with saturated NaHCO₃ (2 × 50 mL) and saturated NaCl (2 × 30 mL). After evaporation, the residue was purified on silica gel column (pentane–ethylacetate = 3 : 1) to give the desired product **L**⁴H as colourless oil. (Yield: 60%, 130 mg). ¹H NMR δ (400 MHz, CDCl₃, 21 °C) = 0.91 (s, 3H), 1.05 (s, 3H), 1.25 (b, 1H), 1.72–2.07 (b, 9H), 2.78–2.86 (d, *J* = 16 Hz, 1H), 3.29–3.32 (b, 4H), 3.91 (b, 1H) ppm. ¹³C NMR δ (200 MHz, CDCl₃, 21 °C) = 19.37 (CH₃), 19.93 (CH₃), 25.51 (CH₂), 26.94 (CH₂), 27.04 (CH₂), 28.81 (CH₂), 31.58 (CH), 42.75 (C(CH₃)₂), 42.88 (CH₂CO), 46.17 (CH₂), 46.70 (CH₂), 49.84 (CH₂SO₂), 58.01 (CH), 59.32 (CCH₂), 217.12 (CO) ppm. *m/z* (ESI, negative ion) 313.2 [C₁₅H₂₅N₂O₃S⁻]. (Found: C, 57.38; H, 8.38; N, 9.08. C₁₅H₂₆N₂O₃S requires C, 57.30; H, 8.33; N, 8.91).

Preparation of arene ruthenium aqua complexes 1–9

Method A for complexes 1 to 3. To a suspension of the appropriate chloro complex [(arene)Ru(L¹)Cl]¹⁸ (0.3 mmol) in deionised water was added 2 equivalents of silver sulfate (0.6 mmol, 187 mg). After stirring at room temperature in the dark for 2 hours, the resulting orange solution was filtered over celite. Then solid NaBF₄ was added until saturation of the solution, visible by the appearance of a yellow precipitate. Then the suspension was centrifuged, the solid was dissolved in 10 ml of dry acetonitrile and filtered over celite to eliminate the excess of NaBF₄. After evaporation of the solvent, the tetrafluoroborate salt was obtained as an orange-yellow powder in good yields.

[(C₆H₆)Ru(L¹)(OH₂)](BF₄) (1**)(BF₄).** (Yield: 70%, 116 mg). ¹H NMR δ (400 MHz, D₂O, 21 °C) = 0.94(m, CH₂), 1.23 (m, 2 CH₂), 1.44 (m, CH), 1.58 (m, CH₂), 1.86 (m, CH), 2.32 (s, *p*-(CH₃)C₆H₄SO₂), 5.81 (s, C₆H₆), 7.15 (d, *J* = 7.1 Hz, *p*-(CH₃)C₆H₄SO₂), 7.72 (d, *J* = 7.0 Hz, *p*-(CH₃)C₆H₄SO₂) ppm. ¹³C NMR δ (200 MHz, D₂O, 21 °C) = 21.9 (*p*-(CH₃)C₆H₄SO₂), 23.8 (CH₂), 25.2 (CH₂), 32.2 (CH₂), 32.7 (CH₂), 59.1 (CH), 60.5 (CH), 83.8 (C₆H₆), 127.8 (2 CH), 128.4 (2 CH), 138.1 (*p*-(CH₃)C₆H₄SO₂), 143.5 (*p*-(CH₃)C₆H₄SO₂) ppm. *m/z* (ESI, positive ion) 465.1 [C₁₉H₂₇N₂O₃RuS⁺]. (Found: C, 41.43; H, 5.08; N, 4.98. C₁₉H₂₇N₂O₃RuS requires C, 41.39; H, 4.94; N, 5.08).

[(*p*-MeC₆H₄^{*i*}Pr)Ru(L¹)(OH₂)](BF₄) (2**)(BF₄).** (Yield: 73%, 133 mg). ¹H NMR δ (400 MHz, D₂O, 21 °C) = 1.11 (m, CH₂), 1.22 (m, 2 CH₂), 1.30 (d, *J* = 7.2 Hz, (CH₃)₂CH), 1.55 (m, CH), 1.74 (m, CH₂), 2.08 (m, CH), 2.34 (s, *p*-(CH₃)C₆H₄SO₂), 2.92 (m, *J* = 7 Hz, (CH₃)₂CH), 5.62 (d, *J* = 6.2 Hz, C₆H₄), 5.78 (d, *J* = 6.3 Hz, C₆H₄), 7.21 (d, *J* = 8 Hz, *p*-(CH₃)C₆H₄SO₂), 7.75 (d, *J* = 8 Hz, *p*-(CH₃)C₆H₄SO₂) ppm. ¹³C NMR δ (200 MHz, D₂O, 21 °C) = 18.1 (CH₃), 21.6 (CH(CH₃)₂), 22.1 (*p*-(CH₃)C₆H₄SO₂), 24.2 (CH₂), 24.5 (CH₂), 31.8 (CH(CH₃)₂), 33.4 (CH₂), 34.1 (CH₂), 57.8 (CH), 60.5 (CH), 87.2 (C₆H₄), 104.5 (C₆H₄), 108.3 (C₆H₄), 126.5

(*p*-(CH₃)C₆H₄SO₂), 129.4 (*p*-(CH₃)C₆H₄SO₂), 138.8 (*p*-(CH₃)C₆H₄SO₂), 143.5 (*p*-(CH₃)C₆H₄SO₂) ppm. *m/z* (ESI, positive ion) 521.1 [C₂₃H₃₅N₂O₃RuS⁺]. (Found: C, 45.51; H, 5.98; N, 4.58. C₂₃H₃₅BF₄N₂O₃RuS requires C, 45.47; H, 5.81; N, 4.61).

[(C₆Me₆)Ru(L¹)(OH₂)](BF₄) ([3]BF₄). (Yield: 97%, 185 mg). ¹H NMR δ (400 MHz, D₂O, 21 °C) = 1.12 (m, 2 CH₂), 1.28 (m, CH₂), 1.31 (m, CH), 1.45 (m, CH₂), 1.82 (m, CH), 2.24 (s, C₆(CH₃)₆), 2.51 (s, CH₃), 7.34 (d, *J* = 7.3 Hz, C₆H₄), 7.84 (d, *J* = 7.6 Hz, C₆H₄). ¹³C NMR δ (200 MHz, D₂O, 21 °C) = 16.8 (C₆(CH₃)₆), 21.7 (*p*-(CH₃)C₆H₄SO₂), 24.3 (CH₂), 34.1 (CH₂), 34.8 (CH₂), 57.5 (CH), 59.3 (CH), 91.7 (C₆Me₆), 127.4 (*p*-(CH₃)C₆H₄SO₂), 127.8 (*p*-(CH₃)C₆H₄SO₂), 138.1 (*p*-(CH₃)C₆H₄SO₂), 142.8 (*p*-(CH₃)C₆H₄SO₂). *m/z* (ESI, positive ion) 549.2 [C₂₅H₃₉N₂O₃RuS⁺]. (Found: C, 47.41; H, 6.31; N, 4.32. C₂₅H₃₉BF₄N₂O₃RuS requires C, 47.25; H, 6.19; N, 4.41).

Method B for complexes 4 to 9. To a suspension of the appropriate dimer [(arene)RuCl₂]₂ (0.15 mmol) in deionised water was added 2 equivalents of silver sulfate (0.6 mmol, 187 mg). After stirring at room temperature in the dark for 2 hours, the resulting yellow solution was filtered and then added to 0.4 mmol of L²H, L³H or L⁴H under inert atmosphere. Then the solution was allowed to react at room temperature for 2 hours, during this time the solution darkened. Then solid NaBF₄ was added until saturation of the solution, which led to a yellow precipitate. Then the suspension was centrifuged, the solid was dissolved in 10 ml of dry acetonitrile, and filtered on celite to eliminate the excess of NaBF₄. After evaporation of the solvent, the tetrafluoroborate salt was obtained as an orange-yellow powder.

[(C₆H₆)Ru(L²)(OH₂)](BF₄) ([4]BF₄). (Yield: 60%, 97 mg). ¹H NMR δ (400 MHz, D₂O, 21 °C) = 1.32–1.45 (m, 1H), 1.51–1.62 (m, 2H), 2.27 (s, 3H), 2.62 (m, 2H), 2.88–2.91 (m, 1H), 3.14–3.21 (m, 1H), 5.62 (s, 6H), 7.21 (d, *J* = 8.1 Hz, 2H), 7.55 (d, *J* = 8.0 Hz, 2H) ppm. ¹³C NMR δ (200 MHz, D₂O, 21 °C) = 21.32 (CH₃), 25.42 (CH₂), 28.56 (CH₂), 46.11 (CH₂), 46.56 (CH₂), 58.21 (CH), 83.36 (C₆H₆), 127.18 (CH_{arom.}), 129.78 (CH_{arom.}), 137.06 (C_{arom.}), 143.21 (C_{arom.}) ppm. *m/z* (ESI, positive ion) 451 [C₁₈H₂₅N₂O₃RuS⁺]. (Found: C, 40.31; H, 4.73; N, 5.26. C₁₈H₂₅BF₄N₂O₃RuS requires C, 40.23; H, 4.69; N, 5.21).

[(*p*-MeC₆H₄^{*i*}Pr)Ru(L²)(OH₂)](BF₄) ([5]BF₄). (Yield: 58%, 107 mg). ¹H NMR δ (400 MHz, D₂O, 21 °C) = 1.12 (d, *J* = 6.8 Hz, 6H), 1.29–1.37 (m, 1H), 1.54–1.61 (m, 2H), 1.97 (s, 3H), 2.32 (s, 3H), 2.52 (m, 2H), 2.63 (m, 1H), 2.92–2.99 (m, 1H), 3.15–3.23 (m, 1H), 5.61 (d, *J* = 6.2 Hz, 2H), 5.78 (d, *J* = 6.2 Hz, 2H), 7.24 (d, *J* = 8.0 Hz, 2H), 7.55 (d, *J* = 8.1 Hz, 2H) ppm. ¹³C NMR δ (200 MHz, D₂O, 21 °C) = 19.04 (CH₃), 21.32 (CH₃), 22.44 ((CH₃)₂), 25.42 (CH₂), 27.38 (CH), 28.56 (CH₂), 46.11 (CH₂), 46.56 (CH₂), 58.21 (CH), 86.31 (CH_{arom.}), 88.28 (CH_{arom.}), 106.13 (C_{arom.}), 107.08 (C_{arom.}), 127.05 (CH_{arom.}), 129.85 (CH_{arom.}), 137.12 (C_{arom.}), 143.18 (C_{arom.}) ppm. *m/z* (ESI, positive ion) 507.1 [C₂₂H₃₃N₂O₃RuS⁺]. (Found: C, 44.45; H, 5.71; N, 4.57. C₂₂H₃₃BF₄N₂O₃RuS requires C, 44.53; H, 5.60; N, 4.72).

[(C₆Me₆)Ru(L²)(OH₂)](BF₄) ([6]BF₄). (Yield: 61%, 112 mg). ¹H NMR δ (400 MHz, D₂O, 21 °C) = 1.33–1.42 (m, 1H), 1.57–1.64 (m, 2H), 1.98 (s, 18H), 2.28 (s, 3H), 2.57 (dd, *J* = 5.1 Hz, *J* = 5.8 Hz, 2H), 2.91–2.96 (m, 1H), 3.17–3.28 (m, 1H), 7.26 (d, *J* = 8.2 Hz, 2H), 7.57 (d, *J* = 8.2 Hz, 2H) ppm. ¹³C NMR δ (200 MHz, D₂O, 21 °C) = 15.18 (C₆(CH₃)₆), 21.32 (CH₃), 25.42 (CH₂), 28.56 (CH₂), 46.11 (CH₂), 46.56 (CH₂), 58.21 (CH), 92.05 (C₆(CH₃)₆), 127.18 (CH_{arom.}), 129.78 (CH_{arom.}), 137.06 (C_{arom.}), 143.21 (C_{arom.}) ppm. *m/z* (ESI, positive ion) 535.2 [C₂₄H₃₇N₂O₃RuS⁺]. (Found: C, 46.41; H, 6.08; N, 4.48. C₂₄H₃₇BF₄N₂O₃RuS requires C, 46.38; H, 6.00; N, 4.51).

[(C₆Me₆)Ru(L³)(OH₂)](BF₄) ([7]BF₄). (Yield: 59%, 132 mg). ¹H NMR δ (400 MHz, D₂O, 21 °C) = 1.18 (s, 6H), 1.20 (s, 3H), 1.23 (s, 9H), 1.25 (m, 1H), 1.44 (m, 2H), 1.87 (s, 18H), 2.48 (m, 2H), 2.82 (m, 2H), 2.89 (m, 1H), 3.16–3.21 (m, 1H), 3.31 (m, 1H), 7.10 (s, 2H) ppm. ¹³C NMR δ (200 MHz, D₂O, 21 °C) = 15.03 (C₆(CH₃)₆), 23.31 (CH₃), 25.42 (CH₂), 25.78 (CH₃), 28.56 (CH₂), 29.56 (CH), 34.15 (CH), 46.11 (CH₂), 46.56 (CH₂), 58.21 (CH), 92.12 (C₆(CH₃)₆), 123.56 (CH_{arom.}), 134.25 (CH_{arom.}), 150.15 (C_{arom.}), 152.32 (C_{arom.}) ppm. *m/z* (ESI, positive ion) 647.3 [C₃₂H₅₃N₂O₃RuS⁺]. (Found: C, 52.21; H, 7.39; N, 3.78. C₃₂H₅₃BF₄N₂O₃RuS requires C, 52.38; H, 7.28; N, 3.82).

[(*p*-MeC₆H₄^{*i*}Pr)Ru(L⁴)(OH₂)](BF₄) ([8]BF₄). (Yield: 60%, 118 mg). ¹H NMR δ (400 MHz, D₂O, 21 °C) = 1.02 (s, 3H), 1.11 (s, 3H), 1.12 (d, *J* = 6.8 Hz, 6H), 1.21 (b, 1H), 1.67–1.99 (b, 9H), 1.97 (s, 3H), 2.63 (m, 1H), 2.71–2.79 (b, 1H), 3.26–3.30 (b, 4H), 3.84 (b, 1H), 5.61 (d, *J* = 6.2 Hz, 2H), 5.78 (d, *J* = 6.2 Hz, 2H) ppm. ¹³C NMR δ (200 MHz, D₂O, 21 °C) = 19.04 (CH₃), 19.28 (CH₃), 19.89 (CH₃), 22.44 ((CH₃)₂), 25.48 (CH₂), 27.01 (CH₂), 27.10 (CH₂), 27.38 (CH), 28.79 (CH₂), 31.62 (CH), 42.71 (C(CH₃)₂), 42.85 (CH₂CO), 46.12 (CH₂), 46.53 (CH₂), 49.88 (CH₂SO₂), 57.96 (CH), 59.27 (CCH₂), 86.31 (CH_{arom.}), 88.28 (CH_{arom.}), 106.13 (C_{arom.}), 107.08 (C_{arom.}), 217.03 (CO) ppm. *m/z* (ESI, positive ion) = 567.2 [C₂₅H₄₁N₂O₄RuS⁺]. (Found: C, 45.81; H, 6.40; N, 4.32. C₂₅H₄₁BF₄N₂O₄RuS requires C, 45.94; H, 6.32; N, 4.29).

[(C₆Me₆)Ru(L⁴)(OH₂)](BF₄) ([9]BF₄). (Yield: 62%, 122 mg). ¹H NMR δ (400 MHz, D₂O, 21 °C) = 1.02 (s, 3H), 1.11 (s, 3H), 1.21 (b, 1H), 1.67–1.99 (b, 9H), 2.01 (s, 18H), 2.71–2.79 (b, 1H), 3.26–3.30 (b, 4H), 3.84 (b, 1H) ppm. ¹³C NMR δ (200 MHz, D₂O, 21 °C) = 15.15 (C₆(CH₃)₆), 19.28 (CH₃), 19.89 (CH₃), 25.48 (CH₂), 27.01 (CH₂), 27.10 (CH₂), 28.79 (CH₂), 31.62 (CH), 42.71 (C(CH₃)₂), 42.85 (CH₂CO), 46.12 (CH₂), 46.53 (CH₂), 49.88 (CH₂SO₂), 57.96 (CH), 59.27 (CCH₂), 92.11 (C₆(CH₃)₆), 217.03 (CO) ppm. *m/z* (ESI, positive ion) 595.2 [C₂₇H₄₅N₂O₄RuS⁺]. (Found: C, 47.46; H, 6.54; N, 4.13. C₂₇H₄₅BF₄N₂O₄RuS requires C, 47.58; H, 6.65; N, 4.11).

Transfer hydrogenation catalysis

The transfer hydrogenation reactions of aryl ketones **A**¹ to **A**³ and aryl imines **A**⁴ to **A**⁶ (1 mmol), using **1** to **9** as tetrafluoroborate salts (10 μmol) as catalyst and HCOONa (5 mmol) as hydrogen source, were carried out in water (5 mL) under inert atmosphere. In a typical experiment, the solution

was heated for 2 hours at 60 °C, then the reaction was quenched by cooling to 0 °C. The organic products were extracted by Et₂O and identified after filtration through silica gel by HPLC on Chiracel OB-H capillary column for aryl ketones **A**¹ to **A**³ (hexane–isopropanol = 92 : 8, 0.7 mL min⁻¹, 215 nm) and on Chiracel OD-H capillary column for aryl imines **A**⁴ to **A**⁶ (hexane–isopropanol–diethylamine = 90 : 10 : 0.1, 1 mL min⁻¹, 230 nm). Conversion and enantioselectivity were determined by integration of the signals. The pH was monitored using a pH meter (Mettler Toledo InLab[®] 413) and adjusted using HNO₃ (for pH = 4 to 9) or NaOH (for pH = 10).

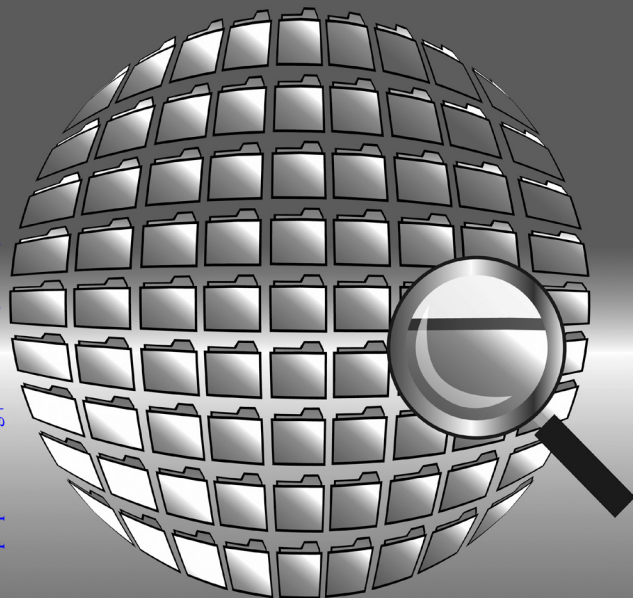
Acknowledgements

Financial support of this work by the Swiss National Science Foundation and a generous loan of ruthenium(III) chloride hydrate from the Johnson Matthey Research Centre are gratefully acknowledged.

References

- U. Koelle, *Coord. Chem. Rev.*, 1994, **135**, 623–650.
- M. Barton and J. D. Atwood, *J. Coord. Chem.*, 1991, **24**, 43–67.
- A. G. Samuelson, *Curr. Sci.*, 1992, **63**, 547–550.
- W. A. Herrmann and C. W. Kohlpaintner, *Angew. Chem., Int. Ed. Engl.*, 1993, **32**, 1524–1544.
- R. Noyori, *Angew. Chem., Int. Ed.*, 2002, **41**, 2008–2022.
- T. Ohkuma, N. Utsumi, K. Tsutsumi, K. Murata, C. Sandoval and R. Noyori, *J. Am. Chem. Soc.*, 2006, **128**, 8724–8725.
- T. Ikariya, K. Murata and R. Noyori, *Org. Biomol. Chem.*, 2006, **4**, 393–406.
- V. Rautenstrauch, X. Hoang-Cong, R. Churlaud, K. Abdur-Rashid and R. H. Morris, *Chem.–Eur. J.*, 2003, **9**, 4954–4967.
- R. M. Bullock, *Chem.–Eur. J.*, 2004, **10**, 2366–2374.
- J. S. M. Samec, J. E. Backvall, P. G. Andersson and P. Brandt, *Chem. Soc. Rev.*, 2006, **35**, 237–248.
- P. N. Liu, J. G. Deng, Y. Q. Tu and S. H. Wang, *Chem. Commun.*, 2004, 2070–2071.
- Y. P. Ma, H. Liu, L. Chen, X. Cui, J. Zhu and J. E. Deng, *Org. Lett.*, 2003, **5**, 2103–2106.
- F. Wang, H. Liu, L. F. Cun, J. Zhu, J. G. Deng and Y. Z. Jiang, *J. Org. Chem.*, 2005, **70**, 9424–9429.
- X. F. Wu, X. G. Li, F. King and J. L. Xiao, *Angew. Chem., Int. Ed.*, 2005, **44**, 3407–3411.
- J. Xiao, X. Wu, A. Zanotti-Gerosa and F. Hancock, *Chim. Oggi*, 2005, **23**, 50–55.
- X. F. Wu, X. G. Li, W. Hems, F. King and J. L. Xiao, *Org. Biomol. Chem.*, 2004, **2**, 1818–1821.
- H. Y. Rhyoo, H. J. Park and Y. K. Chung, *Chem. Commun.*, 2001, 2064–2065.
- J. Canivet, G. Labat, H. Stoeckli-Evans and G. Suss-Fink, *Eur. J. Inorg. Chem.*, 2005, 4493–4500.
- N. Dahlin, A. Bøgevig and H. Adolffsson, *Adv. Synth. Catal.*, 2004, **346**, 1101–1105.
- J. M. Mao and D. C. Baker, *Org. Lett.*, 1999, **1**, 841–843.
- N. Uematsu, A. Fujii, S. Hashiguchi, T. Ikariya and R. Noyori, *J. Am. Chem. Soc.*, 1996, **118**, 4916–4917.
- E. Vedejs, *J. Org. Chem.*, 2004, **69**, 5159–5167.
- D. G. Blackmond, M. Ropic and M. Stefinovic, *Org. Process Res. Dev.*, 2006, **10**, 457–463.
- J. S. Wu, F. Wang, Y. P. Ma, X. C. Cui, L. F. Cun, J. Zhu, J. G. Deng and B. L. Yu, *Chem. Commun.*, 2006, 1766–1768.
- X. F. Wu, D. Vinci, T. Ikariya and J. L. Xiao, *Chem. Commun.*, 2005, 4447–4449.
- X. G. Li, X. F. Wu, W. P. Chen, F. E. Hancock, F. King and J. L. Xiao, *Org. Lett.*, 2004, **6**, 3321–3324.
- H. Y. Rhyoo, H. J. Park, W. H. Suh and Y. K. Chung, *Tetrahedron Lett.*, 2002, **43**, 269–272.
- V. A. Zagorevsky, E. A. Bendikov, R. S. Mirzoyan, D. A. Zykov, V. V. Shavyrina, T. S. Ganshina and Z. D. Kirsanova, *Khim.-Farm. Zh.*, 1982, **16**, 815–817.
- P. C. Wyss, P. Gerber, P. G. Hartman, C. Hubschwerlen, H. Locher, H. P. Marty and M. Stahl, *J. Med. Chem.*, 2003, **46**, 2304–2312.
- M. Gao, D. Y. Kong, A. Clearfield and Q. H. Zheng, *Bioorg. Med. Chem. Lett.*, 2006, **16**, 2229–2233.
- J. Canivet, L. Karmazin-Brelot and G. Suss-Fink, *J. Organomet. Chem.*, 2005, **690**, 3202–3211.
- S. Ogo, K. Uehara, T. Abura, Y. Watanabe and S. Fukuzumi, *Organometallics*, 2004, **23**, 3047–3052.
- R. Noyori, M. Yamakawa and S. Hashiguchi, *J. Org. Chem.*, 2001, **66**, 7931–7944.
- C. A. Sandoval, T. Ohkuma, N. Utsumi, K. Tsutsumi, K. Murata and R. Noyori, *Chem. Asian J.*, 2006, **1-2**, 102–110.
- P. Peach, D. J. Cross, J. A. Kenny, I. Mann, I. Houson, L. Campbell, T. Walsgrove and M. Wills, *Tetrahedron*, 2006, **62**, 1864–1876.
- M. Yamakawa, I. Yamada and R. Noyori, *Angew. Chem., Int. Ed.*, 2001, **40**, 2818–2821.
- M. A. Bennett, T. N. Huang, T. W. Matheson and A. K. Smith, *Inorg. Synth.*, 1982, **21**, 74–78.

RSC Database and Current Awareness Products



- Abstracted from high quality sources
- Easy to use search functions
- Clearly displayed results
- Spanning the chemical sciences

for quick and easy searching

Graphical Databases

present search results in both text and graphical form. Titles include *Catalysts & Catalysed Reactions*, *Methods in Organic Synthesis* and *Natural Product Updates*.

Specialist Databases

review both academic and industrial literature on a wide range of hard to reach and unique information. Titles include *Chemical Hazards in Industry* and *Laboratory Hazards Bulletin*.

Analytical Abstracts

is the first stop for analytical scientists. Offering coverage on all areas of analytical and bioanalytical science. With a fresh new look, including improved search and results features, *Analytical Abstracts* offers an excellent online service.

Find out more at

GO GREEN !

Events at York focusing on the role of Green Chemistry in providing sustainable solutions for commercial products

For industry, academia, retail, government, NGOs, trade, media ...

An invaluable opportunity for networking and technology transfer.

June 27th: 1-day Master Class

Green Chemistry: Sustainable Development & Policy

Principles; Drivers including environmental policy and cross-sector legislation; socio-economic and environmental benefits; tools including green metrics and life cycle assessments; commercial opportunities including case studies.

June 28th: Green Chemistry & the Consumer Symposium

Measuring Green: Green performance indicators across the chemical product lifecycle

The GC&C annual symposia bring together representatives from the whole product supply chain to learn about Green Chemistry solutions for sustainable consumer products. This year's speakers Include:

GlaxoSmithKline, BASF, Ecover, Biffa, Resource Efficiency Network, B&Q plc, InterfaceFlor, GreenBlue



Summer 2007: Web-based CPD courses

Principles of Green & Sustainable Development; Greener Products

In-depth courses building on the June Master Class and covering the principles, tools and socio-economic and environmental benefits of Green Chemistry and its commercial potential. The programme will also address the drivers including legislation and the associated challenges and opportunities.

Who should attend?

- Organizations and individuals with an interest in green chemistry and sustainable chemical products. Courses require no technical background and are suitable for industry, retail, government, NGOs, media, academia and others.

The Venue

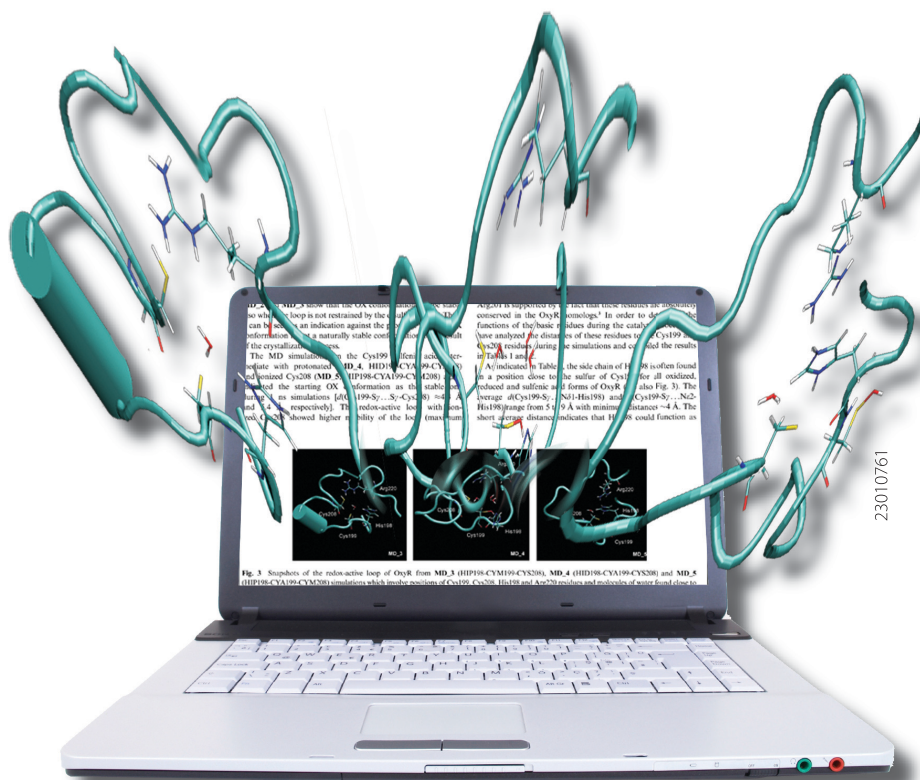
The Kings Manor in York - a group of York's most attractive medieval buildings that served the Tudors and Stuarts as a seat of government. (<http://www.york.ac.uk/admin/presspr/kmanor/>).

www.greenchemistry.net



THE UNIVERSITY of York

See Science Come Alive



23010761

Introducing Project Prospect

Scientists trawling through the thousands of research papers published every month must wish their computer could do the job for them.

This could soon be a reality thanks to **Project Prospect**, an initiative developed by RSC Publishing together with academic partners.

Readers can click on named compounds and scientific concepts in an electronic journal article to download structures, understand topics, or link through to electronic databases. Powerful functionality instantly helps researchers to find, understand and share (bio)chemical knowledge with each other quicker than ever before. See the science in journal articles *come alive*: visit the **Project Prospect** website for FAQs, examples, contact information and latest news.

Features include

IUPAC Gold Book terms linked

Hyperlinked compound information in text

Ontology terms linked to definitions and related papers

RSS feeds with ontology terms and compound structures

Benefits

Completely free service

At a glance HTML view with additional features accessed by toolbox

Downloadable compound structures

Printer friendly

RSC Publishing

www.projectprospect.org

Registered Charity Number 207890